UNIVERSITY OF SOUTHAMPTON

FACULTY OF MEDICINE

Clinical and Experimental Sciences

Impact of the Major Histocompatibility Complex class I peptide repertoire on Natural Killer cell function

by

Berenice Mbiribindi Nvunabandi

Thesis for the degree of Doctor of Philosophy

December 2016

UNIVERSITY OF SOUTHAMPTON

ABSTRACT

FACULTY OF MEDICINE

Clinical and Experimental Sciences

Transfer Thesis for the degree of Doctor of Philosophy

IMPACT OF THE MAJOR HISTOCOMPATIBILITY COMPLEX CLASS I PEPTIDE REPERTOIRE ON NATURAL KILLER CELL FUNCTION

Berenice Mbiribindi Nvunabandi

Background: Natural Killer (NK) cell activation requires the integration of inhibitory and activating signalling. Inhibitory signals are determined by members of the KIR family, which have MHC class I ligands. Peptide antagonism of MHC class I provides an alternative mechanism for loss of inhibition of KIR2DL2/3-positive NK cells. This occurs when a weak KIR binding peptide disrupts the inhibitory signalling of a strong binding peptide. Peptide antagonism has been defined only for HLA-C*0102, endogenously expressed in TAP-deficient cells, using a peptide variant of VAPWNSLSL (VAPWNS**DA**L and VAPWNS**DY**L), therefore it may be a unique property of HLA-C*0102 or more general finding.

Hypothesis: We hypothesize that small changes in MHC-I peptide repertoire can impact on NK cell activation and that additional peptides can antagonise inhibitory KIR can be discovered.

Results: 721.221 cells were transfected with HLA-C*0304 and ICP47 used for peptide loading and as target cells in CD107a assays. We studied previously described position 8 (P8) derivatives and also generated novel P7 derivatives of the endogenously processed peptide GAVDPLLAL. In contrast to our observations for HLA-C*0102, arginine at P7 triggered stronger inhibition than phenylalanine. L7D did not inhibit KIR2DL2/3-positive NK cells. However it did antagonise inhibition by L7R in CD107a assays. I used peptide elution and HPLC analysis to demonstrate that peptide antagonism was not related to displacement of L7R or L7F by LD7. In a study

of the immunopeptidome of Hepatitis C virus expressing cells expressing HLA-C*0102 were generated to study its peptide repertoire and to identify potential NK activating or inhibitory peptides. I identified that the peptide repertoire of HLA-C was preferentially altered in comparison to HLA-A. To improve our methods for studying the influence of peptides on NK cell, I developed a Granzyme B assay based on HPLC technology. This showed that it is possible to perform a functional assay using NK lines with low backgrounds, however it was not robust enough to detect small differences in peptides.

Conlcusions: Peptide antagonism is a generalizable phenomenon and it appears that HLA-C alleles has become specialised to NK cells.

Contents

List of tables

List of figures

List of accompanying materials

DECLARATION OF AUTHORSHIP

I, **Berenice Mbiribindi Nvunabandi**

declare that this thesis and the work presented in it are my own and has been generated by me as the result of my own original research.

IMPACT OF THE MAJOR HISTOCOMPATIBILITY COMPLEX CLASS I PEPTIDE REPERTOIRE ON NATURAL KILLER CELL FUNCTION .....

.....

I confirm that:

1. This work was done wholly or mainly while in candidature for a research degree at this University;
2. Where any part of this thesis has previously been submitted for a degree or any other qualification at this University or any other institution, this has been clearly stated;
3. Where I have consulted the published work of others, this is always clearly attributed;
4. Where I have quoted from the work of others, the source is always given. With the exception of such quotations, this thesis is entirely my own work;
5. I have acknowledged all main sources of help;
6. Where the thesis is based on work done by myself jointly with others, I have made clear exactly what was done by others and what I have contributed myself;
7. [Delete as appropriate] None of this work has been published before submission [or] Parts of this work have been published as: [please list references below]:

Signed: .....

Date:

Acknowledgements

I would like to express all my gratitude to my supervisor Salim who gave me confidence and assigned me to a rewarding role with this project. I learnt a lot thanks to him and, the most important aspect is that now I am reinforced in my career choices, which for me is a real achievement. All of these being tremendously beneficial for my professional but also personal development. Thank you to Chris McCormick for his help and support in my debuts.

To my academic mentor David Wilson, thank you for our discussions and your guidance… and coffees.

Warm thanks to all the "NK group" members (past and present). Special thanks to Theresa Hydes, Li Zhuang, and my lovely Hara Kranidioti. Thank you for listening to me and of course thank you for all the laughs and tea chats which especially disturbed Li's and Theresa's work... Thank you Pauline Rettman for feeding me with Croissants when needed and Becky Fulton for always showing me the bright side of all situations. I would like to thank all "Level E" members (past and present) because each of you always find a bit of time to help me when I needed it, talk to me and advised me.

To my housemates of the Cawte Castle: to Adam Hield, Ciaran Mullan, Rob MacKenzie and Ruairi McNicholas. Thanks you guys for making my last year of the PhD so fun, enjoyable and exciting. I definitely learnt a lot around you. Thanks to the Croppies (Ciaran, Clare, John, Helen, Hanna, Alan and Sam) for introducing me to the Irish Music and for the entertainment!

For those who are far from the lab and from the bench but close to my heart: to my parents Françoise and Romain who gave me a great support (each of them in their own way). To my sisters: To Amarilys, Patricia, Divine, Cécile Oliveira, Christianah Ogundele, Cléa Rekhou, Elizabeth Sadiq, Elodie Gustave, Shamin Li, and Sity Soilihi.

To Bastien Riera, my first best friend in Southampton who gave me an amazing support since my first day here. To my friend Nam Nguyen with who I always have fun when I am back home in Paris. This acknowledgement would not be complete without mentioning my dear friend Garrett Heidebrink who I genuinely love.

To all of you who always encourage me, support me, listen to me, advise me, and who I deeply love.

Lastly I would to mention that my research would not have been complete without blood donors of the Southampton General Hospital and that is why I would like to address my gratitude to them as well.

A vous tous, un grand MERCI !

Definitions and Abbreviations

AICL	Activation-induced C-type lectin
ACN	Acetonitrile
ADCC	Antibody Dependant Cell mediated Cytotoxicity
BSA	Bovine Serum Albumin
C18	18 Carbon atoms to form the stationary phase of a column
C3P	Caspase 3 Peptide
CD	Cluster of Differentiation
CMV	Cytomegalovirus
CRACC	CD2 like receptor activating cytotoxic cells
DNAM-1	DNAX accessory molecule-1
FACS	Fluorescence Activated Cell Sorting
FBS	Fœtal Bovine Serum
GFP	Green Fluorescence Protein
GH1	human Growth Hormone 1
GzmB	Granzyme B
HCC	Hepatocellular Carcinoma
HCV	Hepatitis C Virus
HLA	Human Leucocyte Antigen
HPLC	High Performance Liquid Chromatography
huGzmB	human Granzyme B
huIL	human Interleukin
ICP47	Infected Cell Protein 47 (from Herpes simplex virus)
IFN	Interferon
Ig	Immunoglobulin
IL	Interleukin
ITAM	Immunoreceptor Tyrosine-based Activation Motif
ITIM	Immunoreceptor Tyrosine-based inhibition Motif
JAK3	Janus Kinase-3
KIR	killer cell immunologbulin-like receptor
LAMP-1	Lysosomal-Associated Membrane Protein 1
LAIR-1	Leucocyte-associated immunoglobulin receptor 1

LCMV	lymphocytic choriomeningitis Virus
LCR	Leukocyte Receptor Cluster
LDH	Lactate Dehydrogenase
mAb	monoclonal Antibody
MCMV	Mouse Cytomegalovirus
MFI	Mean Fluorescence Intensity
MHC-I	Major Histocompatibility Complex Class I
MHV	mouse Hepatitis virus
MICA/B	Major Histocompatibility Complex class-I related chain A/B
NCR	Natural Cytotoxicity Receptor
NK	Natural Killer
NKG2	Natural Killer Group 2
NKL	Natural Killer cells Line
NKp	Natural Killer cell protein
NO	Nitric Oxide
P7	position 7 (amino acid position in a peptide sequence)
P8	position 8 (amino acid position in a peptide sequence)
PBMC	Peripheral Blood Mononuclear Cell
PBS	Phosphate Buffered Saline
PCR-SSP	Polymerase Chain Reaction – Sequence Specific Primer
RPMI	Roswell Park Memorial Institute Medium
S.O.C	Super Optimal broth with Catabolite repression
TAP	Transporter Associated with Antigen Presentation
TFA	Trifluoroacetic Acid
TNF	Tumour Necrosis Factor
TRAIL	TNF Related Apoptosis Inducing Ligand
TRAILR	TNF Related Apoptosis Inducing Ligand Receptor
UHPLC	Ultra High Performance Liquid Chromatography
ULBP1/2/3/4	UL16 binding protein 1/2/3/4.

1. Introduction

1.1 Natural Killer cells

1.1.1 General description

Natural Killer (NK) cells were described and functionally identified by several groups in the early 1970s. They were first described in the mouse as a unique subset of lymphocytes with a natural ability to kill mouse Moloney leukemia cells (1,2). There has been significant progress in our understanding of NK cell biology and function over the last twenty years. Consistent with their roles in immune defence and surveillance, NK cells are widely distributed in the body throughout lymphoid and non-lymphoid tissues. The tissue with the highest frequency of NK cells among its lymphocytes is the uterus, the lung, followed by the liver, the peripheral blood, the spleen, the bone marrow, the lymph nodes, and the thymus. Evidence suggests that NK cell functions are strongly influenced by the tissue microenvironment (3).

1.1.2 NK cells development: transcription factors and lineage commitment

The proportion of NK cells in the peripheral blood is high at birth (around 20% on average) but drops to its lowest amount between 5 and 9 months of age (around 5% on average) after which the cell proportion climbs steadily until late adolescence (4). It has been shown that the percentage of NK cells in the peripheral blood varies with age (4,5). Interestingly, NK cells are relatively infrequent in the lymphatic fluid and in lymph nodes but upon stimulation and when they are needed, they rapidly home to, and accumulate in, the draining lymph nodes (6). NK cells develop from a common lymphoid progenitor resident in the bone marrow (BM) but diverge from other lymphocyte lineages fairly early in development. They require expression of transcription factors such as c-KIT, FLT-3; cytokines such as IL-15; and acquire specific cell surface markers as they progress through their developmental stages (7). It is currently not known whether there is a defined selection process analogous to thymic selection of T cells. A valuable and unique setting for assessing this particular question has been hematopoietic stem cell transplantation (HSCT) (8), where the

requirements and effects of specific receptor ligand matches and interactions have demonstrated a possible process of NK cell selection. Recent studies, showed that NK cells have to pass checkpoints during development in order to be fully functional in the peripheral blood (**Figure 1-1**) (9).

Moreover, insight into human NK cell biology was gained from studying patients with severe combined immunodeficiencies. For instance, mutations of the common gamma chain, which is required for the function of IL-2, IL-4, IL-7, IL-9, IL-15 and IL-21, causes failure of both T and NK cell development. Similarly, mutations of Janus kinase-3 (JAK3) utilized by the gamma chain results in failure of T and NK cell development. In contrast, it was demonstrated that humans with an IL-7Ra mutation are T cell deficient, but NK cell replete (10), demonstrating that IL-7 is not necessary for NK cell development. Some mutations of the gamma chain prevent T cell development but allow NK cell development (11). For example, the A156V gamma chain mutation results in an inhibition of IL-4 and IL-7 function but has no effect on IL-15 response. This result suggested that IL-15 is necessary for human NK cell development (12), a conclusion anticipated by using IL-15α knockout mice (13). The importance of IL-15 was further illustrated by the description of a patient with absent expression of IL-2/15Rβ chain who had a complete absence of NK cells (14). Once NK cells have developed within the bone marrow, they exit and circulate in the peripheral blood where they consist of 5 to 20% of peripheral blood lymphocytes.

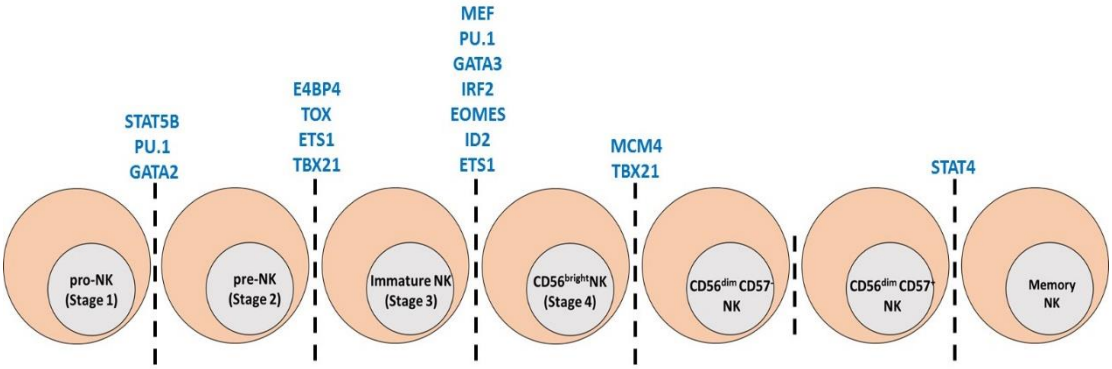

Figure 1-1: checkpoints in human NK cell development. During their development, NK cells travel through the body and progress through checkpoints that are controlled by transcription factors. Throughout this process, the expression of developmental markers, cytokine receptors, natural cytotoxicity receptors are all dynamically regulated which result in substantial heterogeneity within the NK cell population.

1.1.3 NK cells development: the journey from the bone marrow to the periphery

Understanding of the maturational stages of NK cell development offers a fundamental framework to facilitate in depth prospective studies of the regulation of this process. Indeed, a large area of investigation in this field has been devoted to the elucidation and understanding of the immune-phenotypes of human and mouse NK cell developmental intermediates (NKDIs) that represent distinct maturational stages (**Figure 1-2**). As the field is rapidly progressing, to date, there is as yet no formal consensus as to how theses NKDIs should be defined. In a recent review, Yu *et al.* used terminology based on contemporary publications and reviews published by leaders in the field to refer to human and mouse NKDIs (15).

Remarkable progress has been made in the field of NK cell development. For instance, research in mice and humans over the past decade have provided well-defined models of the cellular stages of NK cell development in these species. The observation that NKDIs circulate through peripheral blood and are normal cellular constituents of multiple extra medullary tissues, strongly supports the idea that NK cells can, and likely do, develop outside of the bone marrow. Nonetheless, many fundamental questions still remain to be answered.

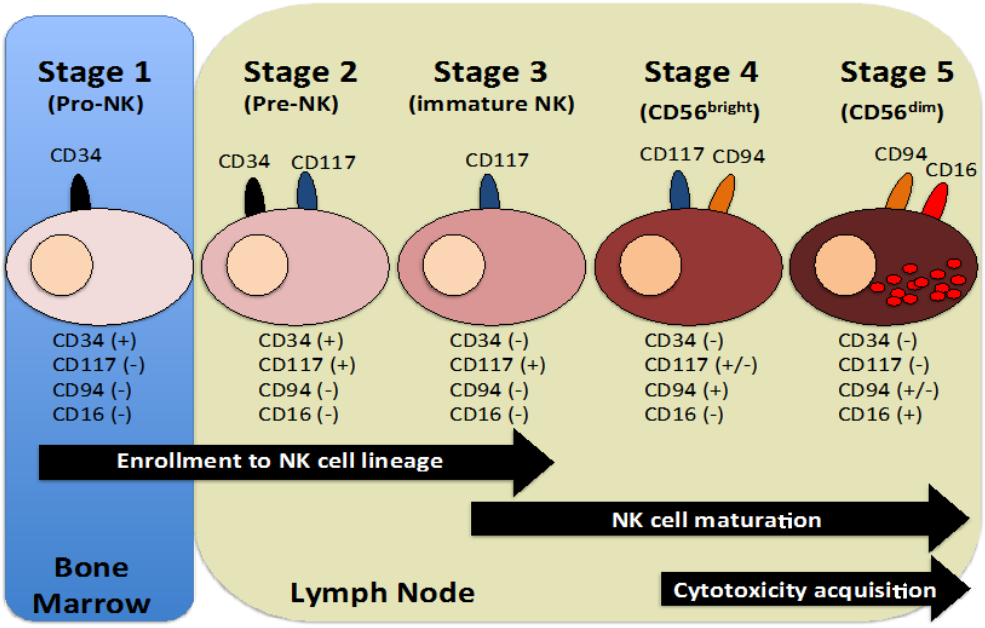

Figure 1-2: Schematic representation of the cellular intermediates of human NK cell development. Human NK cell development from stage 1 pro-NK in the bone marrow to mature stage 5 $CD56^{dim}$ NK cells is represented as a linear pathway from left to right. Shown for each developmental stage is the expression of each surface antigen useful to characterize populations of NK developmental intermediates. Expression is labelled as '+' (expression), '–' (no expression).

1.2 NK cell education

1.2.1 Chronic exposure of NK cells to activating ligands make them tolerant.

Mouse models have shown that despite a constant exposure to activating ligands, NK cells are tolerant and do not cause autoimmunity. For instance, studies on activating NKG2D ligands (the Rae-1 family) described how the expression of the ligand is constitutive in the embryo but then silenced before birth and finally less or not expressed in healthy adult mice tissues. Furthermore, immunocompetent adult mice reject transplanted tumours expressing NKG2D ligands and eliminate virus-infected cells in which NKG2D ligands are up-regulated (16–20).

NK cells efficiently reject adoptively transferred syngeneic hematopoietic cells from mice constitutively expressing a *Raet1* transgene, which encodes a ligand for NKG2D. These observations indicate that NK cells have the ability to recognize and attack

otherwise normal, healthy cells if they express ligands that can be recognised by NKG2D (21,22). Interestingly and in contrast with the first observations, NK cells in *Rae-1* transgenic mice (i.e. mice that already express NKG2D ligands) do not attack Rae- 1-bearing tissues and are unable to reject transplanted tumours expressing NKG2D ligands. These findings demonstrated that when NK cells are developing in the constant presence of NKG2D ligands, they are able to tolerate cells which express these ligands. This is due to both the downregulation of the NKG2D receptor on the surface of NK cells as well as hyporesponsiveness to NKG2D signalling (17). Additionally, investigations using NK cells from transgenic mice which constitutively express Rae-1 have demonstrated that activating receptors other than NKG2D may also be impaired, depending on the particular ligand expressed as well as its distribution and its abundance (21–24). Lastly, In vitro co-culture of mouse NK cells in presence of tumour cells expressing NKG2D ligands can also desensitize other activating receptors on the NK cells (25).

Another example of NK cells becoming tolerant after continuous exposure to activating ligand is Ly49D. The mouse activating Ly49D receptor recognizes H-2Dd, and NK cells from mice lacking that ligand are able to kill H-2Dd-bearing (26,27) targets via Ly49D. Conversely, NK cells from H-2Dd-expressing mice are capable of killing H-2Dd expressing target cells via Ly49D, which shows how NK cells with this self-reactive activating receptor are functionally tolerant when the NK cells develop in the presence of the ligand. Although the molecular mechanisms of this tolerance or "receptor anergy" are still unclear, it has been proposed that it is the results of the co-expression of the H-2Dd-reactive inhibitory receptors Ly49A and Ly49G2 (28). In human, there is no direct evidence that NK cells expressing activating KIR receptors with the ability to recognize self-HLA-C ligands cause autoimmunity in individuals. But, a genetic association between activating KIR receptor and certain autoimmune diseases has been reported, but these findings might relate to T cell lymphocytes as they can also express activating KIR (29). However, Fauriat et al have described the first mechanism for human NK cell education by an activating KIR where KIR2DS1 positive NK cells were tolerant in HLA-C group 2 positive individuals. They suggested that the education of NK cells through activating KIR receptors is a mechanism to secure tolerance that complements education via inhibitory KIR receptors (30).

In the mouse model, a mouse cytomegalovirus (MCMV)-encoded glycoprotein, m157 is recognized by both Ly49H and Ly49I receptors which are respectively activating

and inhibitory. In MCMV-resistant mice, this viral protein engages the activating receptor (Ly49H) and confers host protection. As these activating and inhibitory receptors are highly homologous, it has been suggested that one evolved from the other in response to selective pressure imposed by the pathogen. (31,32). Thus, it has been implied that the gene encoding Ly49H resulted from the duplication of the gene encoding Ly49I and conversion to an activating receptor by swapping the ITIM-bearing cytoplasmic and transmembrane domains for a transmembrane domain with a charged residue and a truncated cytoplasmic tail. Even if Ly49H is advantageous for controlling MCMV infection, its precursor might have potentially been autoreactive due to its specificity for MHC class I. Hence it is thought that further selecting events eliminated this self-reactivity, whilst retaining MCMV specificity.

In the literature, it has been described that wild-type mice which possess Ly49H expressing NK cells respond efficiently when they face MCMV-infected cells whereas ubiquitous transgenic or retroviral expression of m157 in transgenic mice makes the Ly49H-expressing NK cells non-responsive to Ly49H stimulation. This phenomenon is caused, in part, by down-modulation of the Ly49H receptor on the NK cells encountering m157 during development, but also by hyporesponsiveness of the receptor signalling. It is still unclear whether or not chronic stimulation through Ly49H affects signalling through other activating receptors is or not dependent on the amount of ligand expressed or the anatomical location of the expressed ligand. Experiments involving adoptive transfer of NK cells from non-m157-expressing hosts into the transgenic animal can induce NK cell anergy. This indicates that anergy can be induced in mature NK cells. m157 did not need to be expressed by the developing NK cells themselves as a *trans* expression of m157 is sufficient to impair functions of Ly49H receptor (26,27). Taken together, these studies show that NK cells, similar to T cells, reach a state of tolerance when they are chronically exposed to endogenous, as well as foreign ligands recognized by their activating receptors. The mechanisms explaining this receptor proximal tolerance and whole cell anergy are not yet defined, described and understood.

1.2.2 Inhibitory receptor repertoire selectivity of NK cells receptors

The inhibitory receptors, KIR (in human) and Ly49 (in mouse), recognize polymorphic MHC-I ligands. Amongst the total NK cell population, the inhibitory receptors are

diversely expressed on overlapping subsets of NK cells. Additionally, the inhibitory KIR and Ly49 receptors themselves are highly polymorphic and have different affinities for their MHC-I ligands (33–35). These characteristics, as well as the fact that the NK receptors and their MHC-I ligands are not genetically related, result in a situation where some NK cells in the host do not express an inhibitory receptor for any self-MHC-I protein. Undeniably, it is now well established that in some individuals a substantial proportion of NK cells fail to express inhibitory receptors reactive with the polymorphic MHC-I molecules that they have inherited (36,37). Nevertheless, these individuals do not show evidence of autoimmune attack by their NK cells. This observation raises the question of how NK cells lacking self-MHC- I inhibitory receptors achieve tolerance.

The considerable receptor diversity within the NK cell population is the result of the possession of multiple genes encoding the receptors: for instance, some strains of rodents possess 20 or more *Ly49* genes and some humans possess 15 *KIR* genes. Expression of these receptors appears stochastic and NK cells can express many KIR or Ly49 receptors that are unable to bind to self-MHC-I complexes in the host. Consequently, the existence of an MHC-I ligand is not compulsory for NK cells to stably express a given Ly49 or KIR on a substantial subset of cells. In addition, there is no preferential expansion or deletion of NK cells expressing an activating KIR or Ly49 receptor that is able to bind MHC-I in a host possessing a reactive MHC-I allele. Consequently and contrasting the T lymphocytes development, there is no evidence for either strong positive or negative selection of NK cells with respect to the activating KIR or Ly49 receptors. Nevertheless, the presence of self-ligands recognizing the inhibitory NK receptors does influence the development of NK cells. Indeed, the frequency of NK cells expressing multiple inhibitory receptors can be approximately predicted by multiplying the frequency of NK cells expressing each inhibitory receptor: the “product rule” (38,39). However in MHC class I-deficient mouse models which express two or more inhibitory receptors, co-expression of receptors happens less frequently than it would be anticipated in MHC-I sufficient mouse models. In fact, the frequency of NK cells expressing MHC-I reactive inhibitory receptors is higher in MHC-I deficient animals than in MHC-I sufficient animal models (40,41). Thus, it seems that there is a selective or educational event that restricts the expression of two or more inhibitory receptors for self-MHC-I on a given NK cell. Reports have already shown that the expression of peptide:MHC-I complexes on both hematopoietic and somatic cells influences the development of the inhibitory Ly49

repertoire (42,43). Furthermore, transgenic expression of an inhibitory Ly49 receptor limits the expression of endogenous Ly49 receptors in vivo which suggests that engagement with self-MHC class I prevents subsequent expression of new inhibitory receptors during development (44). This underlines the existence of a mechanism that ensures that NK cells do not express too many inhibitory receptors for self-MHC class I (38,44,45). However a mechanism for this has not been described yet. Similarly, human NK cell interactions with self-HLA class I ligands shape the inhibitory KIR repertoire in an individual (37,46,47). Recently, Boudreau *et al.* showed the roles of cell-extrinsic HLA in increasing NK cell reactivity, and cell-intrinsic HLA in maintaining NK cell education via HLA-KIR interaction. NK cell reactivity increased or decreased, respectively, when HLA was acquired from neighbouring cells or was silenced in educated cells. They, therefore concluded that, both cell-intrinsic and -extrinsic HLA cooperate to maintain and adjust NK cell education (48).

1.2.3 Self-MHC Class I and Inhibitory receptors recognition is involved in NK Cell Education

Valiante *et al.* showed that all human NK cell clones from two individuals express at least one inhibitory receptor that recognize a self-MHC-I protein and their observation suggested that there is likely to be a selective process shaping the NK cell repertoire to maintain tolerance to host cells (49). Nevertheless, as mentioned earlier in this chapter, recent *in vivo* studies have reported a significant number of mature NK cells in humans and mice and these NK cells do not express any inhibitory receptors for MHC- I or only express receptors that can recognize non-self MHC class I (36,37). Moreover, mice missing cell surface expression of MHC- I due to genetic silencing of β2-microglobulin, TAP-1, and/or MHC-I heavy chains H-2K and H-2D have ordinary numbers of mature NK cells and do not display obvious NK cell mediated autoimmunity. NK cells which have developed in the absence of MHC- I are not capable of killing MHC-I deficient tumour cell lines *in vitro* and fail to reject MHC-I deficient bone marrow in vivo (50,51). In MHC-I sufficient humans or mice, the subset of NK cells lacking inhibitory receptors for self-MHC-I are hyporesponsive to *in vitro* stimulation through several activating receptors and fail to reject MHC-I deficient bone marrow *in vivo* (36,52,53). Consequently, expression of inhibitory receptors that recognise self-MHC-I enhances the responsiveness of NK cells.

Although studies have shown that uneducated NK cells tended to be less responsive compared to educated NK cells (less cytotoxicity and cytokine production), several reports have revealed that uneducated NK cells can become activated. In certain circumstances these cells can perform better than educated cells. For instance, uneducated but not educated NK cells eliminate MHC class I expressing cancer cells and they also promote better mouse survival and viral clearance of MCMV (54,55). Furthermore, these cells are able to respond to activating stimuli. They have been described to be activated through activating receptor such as Fc receptor CD16 (56). Mechanistically, it seems that the deficiency in term of activating signaling is the main cause of the hyporesponsivness uneducated NK cells (57,58). It now clear that very early signaling events appear to be disrupted in these cells. Nevertheless questions remain to be addressed regarding the extent of these disrupted signaling pathways.

1.2.4 Mechanisms leading to hyporesponsive NK cells: licensing or disarming?

The ability of NK cells to attack normal cells expressing MHC-I when inhibitory receptors are blocked is one of the strongest pieces of evidence that self-MHC-I expressing cells have ligands that can activate NK cells. In 2006, Raulet *et al.* predicted that NK cells that lack inhibitory receptors for self MHC receive stimulatory signals that are not counterbalanced by inhibitory signals from MHC-specific inhibitory receptors (59). This process could be expected to result in persistent stimulation of these NK cells during their differentiation process. It is well established that persisting stimulation of T cells or B cells can lead to induction of anergy, a quasi-stable hyporesponsive state (60,61). Following the same idea, Raulet *et al.* assumed that as a response to persistent stimulation, developing NK cells that lack inhibitory receptors for self MHC adopt a hyporesponsive state comparable to anergy of T cells or B cells.

The MHC-expressing cell types that interact with NK cells and set the tolerance and responsiveness of NK cells remain largely unknown. Ten years ago, Kim *et al.* observed that NK cells that express Ly49C in C57BL/6 (B6) mice respond better to stimulation via the NKR-P1 stimulatory receptor compared to those which lack Ly49C and were hypo-functional (53). It was still unclear why the Ly49C-negative NK cells were functionally deficient as many mouse NK cells that lack Ly49C express either

Ly49I or CD94/NKG2A or both receptors that bind to MHC molecules in B6 mice. One proposition to explain the underlying mechanism was that engagement of the inhibitory receptors specific for self MHC molecules induces the cells to undergo a maturation step which was called “licensing”. This process was described as the step that gives functionality to NK cells with inhibitory receptors for self MHC (53). In fact, the strength of the inhibitory interactions between the receptors and their ligands determines the overall functional reactivity of the NK cell when faced with targets that lack the corresponding HLA class I ligand.

Other models, in contrast, suggest that this mechanism can be an active mechanism that “disarms” NK cells that can be potentially autoreactive. In the “arm/disarm model”, continuous stimulation disarms NK cells and all the NK cells that developed in a mixture of normal cells and MHC class I deficient cells would receive such stimulation from the class I-deficient cells and would adopt the hyporesponsive state. In the “licencing” model, it would be predictable that in such mixture, the MHC positive cells would dominantly license the NK cells.

Results obtained in two different systems indicate that hyporesponsiveness, rather than responsiveness, is dominant in a mixture of MHC-I positive and negative cells (62,63). These studies support the disarming model rather than the licensing model: persistent stimulation of NK cells by self-cells that lack inhibitory MHC ligands disarms the NK cells, by inducing the cells to transition to the hyporesponsive state.

The plasticity of NK cell responsiveness has been well recognized as NK cells have the capacity to tune their activity in changing conditions. However, such plasticity could be maladaptive under conditions of infection, where it leads to desensitization of NK cells that would otherwise serve a protective role. These hypotheses suggest that infections may generate conditions that change NK cell responsiveness, preventing or reversing hyporesponsiveness. For instance, it was reported that hyporesponsive NK cells in B6 mice (i.e. those that the lack inhibitory receptors Ly49C, Ly49I and NKG2A) respond as powerfully as other NK cells in terms of IFNγ production when the mice are infected with Listeria monocytogenes (36). Listeria causes major inflammation in infected mice, and it was thought that the potent responses of otherwise hyporesponsive NK cells could be due at least in part to the cytokines produced in the course of the infection. Furthermore, several studies have shown that hyporesponsive NK cells from MHC I-deficient mice killed efficiently after following culture in IL-2 for several days (64).

Moreover, it has been demonstrated that viral infections can strongly influence the responsiveness of NK cells. Studies involving hematopoietic mouse chimeras, with mixed bone marrow cells, showed that a state of tolerance to MHC-deficient cells established in resting conditions, could be reversed when infected with mouse Cytomegalovirus (MCMV) (65). In another study, the same group showed that during MCMV infection in wild type B6 mice, the $Ly49C^{-}Ly49I^{-}$NK cells, which exhibit low responsiveness in steady state conditions, expand preferentially and provide better protection than $Ly49C^{+}Ly49I^{+}$NK cells (66). Similar preferential expansions of $Ly49C^{-}Ly49I^{-}$NK cells were observed in other infections such as lymphocytic choriomeningitis Virus (LCMV), vaccinia as well as mouse Hepatitis virus (MHV) infections (67). These observations were explained by the fact that the initial NK cell hyporesponsiveness can be reversed by the cytokines produced during the infection. Then, following this process, preferential expansion of NK cell which lack inhibitory receptors for self MHC but inhibition of expansion of $Ly49C^{+}Ly49I^{+}$NK cells. Overall, the available data demonstrate that responsiveness is both plastic and contextual.

Changes in steady state MHC expression can lead to gain or loss of responsiveness, but the inflammation which is often associated with infections act to sustain a higher state of responsiveness, allowing initially hyporesponsive NK cells to provide protective activity, and to do so without being subject to inhibition by self MHC I molecules (68).

1.3 NK cells in health and disease

1.3.1 NK cells in cancer

It is now well established that NK cells act on cells during disease either through their receptors or following cytokine stimulation. The influence of NK cells has now been confirmed in various disease conditions. Indeed, as mentioned earlier, one of the major functions of NK cells is immune-surveillance of our body and its integrity. Numerous in vitro investigations on human cells, and also in vivo studies that involved mice and rats demonstrate that NK cells recognize tumour cells as targets. It is well established that NK cells control tumour growth and metastasis in vivo. For instance, tumour immune-surveillance role of NK cells has also been implicated in controlling the growth of B cell lymphomas that spontaneously arise in mice deficient

in both perforin and β2-microglobulin (69). Furthermore, an epidemiologic survey of eleven years follow-up shows a link between low NK cells activity in peripheral blood and increased cancer risk in adults (70).

Down-regulation of MHC-I on tumour cells is the classical way by which NK cells are known to recognise and attack tumour cells. But, up-regulation of NKG2D ligands on tumour cells can also make them susceptible to NK cells attack. In most cases, cancer cells engage the NK cells activating receptors which then triggers its natural kill response.

An important role is played by cytokines and chemokines which act in conjunction with NK cells to tackle various diseased conditions. In the case of cancer, IL-12 and IL-18 are NK activating cytokines which have a role during late NK cell differentiation and which have been demonstrated to synergistically enhance cytotoxicity against tumour cells. These cytokines also induce IFN-γ production by NK cells. IFN-γ on the other hand induces type I immune response and directly acts on cancer cells.

Dendritic Cell (DCs) are known to cross- talk with NK cells through production of cytokines such as IL-12 and IL-18 as well as through cell–cell interactions which promote NK cell activity against tumours. Furthermore, in patients with gastro-intestinal, colon and prostate cancers, a high level of regulatory T cells (Treg) which has been associated with a reduced number of NK cells alongside and reduced levels of functionality (71–73). An in vitro study has shown that Treg cells from hepatocellular carcinoma patients inhibit NK cell killing ability. However, it is known that during pregnancy, NK cells, along with Treg cells, contribute towards the creation of a tolerant environment for the foetus, which may be important in preventing complications of pregnancy.

1.3.2 NK cells in pregnancy

Maternal uterine NK (uNK) cells have a role in reproduction by interacting with fetal trophoblasts that invade the uterus and change small spiral arteries into voluminous channels that will be involved and essential for fetal growth. Studies have shown that Inadequate trophoblast invasion causes several common disorders of pregnancy such as fetal growth restriction, recurrent miscarriage and preeclampsia (74). Despite the

laws of classical transplantation immunology, the fetus is considered to be an allograft that can paradoxically survives graft and lead to a successful pregnancy. It is known that there is no direct interaction between the mother and the embryo, only with the extra-embryonic placenta as it implants in the host uterus. Mouse models and genetic correlation in human studies support the fact that interaction between the trophoblast and uNK cell is crucial for the achievement of uterus remodeling, optimal depth of invasion and successful pregnancy (75–80). Furthermore, there is a key role of interactions between uNK cell KIRs and HLA class I ligands of the trophoblast with a major role of HLA-C as trophoblast expresses maternal and paternal HLA-C (group 2 or HLA-C2), but not HLA-A or HLA-B. To date, evidence lead to HLA-C2 and the reactivity of uNK cells expressing KIR2DS2/L1 as key players.

1.3.3 NK cells in infection

Regulations of NK cells during Herpesviridae infections have been documented in patients lacking NK cells and evidence of NK activation during this viral infection (81,82). Interactions between viruses and NK cells has been reported to be involved in innate immune evasion and allow viral latency such as EBV (Epstein-Barr virus), CMV (Cytomegalovirus) or KSHV (83–85). For instance, KSHV (Kaposi's sarcoma virus) similarly to CMV encode proteins which down-regulate MHC-I and MICA/B.

The protective influence of NK cells has also been studied in various cases of infections by flaviviruses, such as chikungunya and dengue virus. Their role in viral hepatitis, influenza virus and HIV-1 infection is also well documented in several studies (86–90). Comparably, their role in defending against respiratory infection by bacteria or viruses such as respiratory syncytial viruses (RSV), and influenza has been highly described in animal studies mostly using murine model (91–93). Furthermore NK cells are assumed to be a major determinant of the development of viral-associated asthma. In most studied cases, the role of NK cells is found to be either disease controlling or disease enhancing. On one hand, it was shown that NK cells contribute towards the progress of T cell mediated allergic airway response during the allergen specific sensitization phase in asthma (94,95). On the other hand, existing evidence also suggests that NK cells are involved in resolving acute allergic airway inflammation (96). The peripheral blood of asthmatic patients shows augmented NK cell activity which declines upon antigen challenge. These

observations suggest that NK cells migrate from the peripheral blood towards lungs and lymphoid organs (96,97). NK cells interact with various other immune cells both in healthy conditions as well as during pathological circumstances. In healthy and asthmatic lungs, NK cells form synapses with lung resident dendritic cells and macrophages. These associations lead to generation of NK derived cytokines and effector molecules involved in local immunity as well as in the regulation of allergic disease severity (98).

Several members of the NK cell receptor families contribute towards the defense against viral infections. Infection of mouse or human cells with flaviviruses is known to up-regulate MHC-I class expression at the cell surface of on infected cells as demonstrated in WNV infection. This mechanism therefore leads to evasion from NK cell mediated killing. During HIV-1 infection, it has been reported that there is a remarkable increase in inhibitory receptors and a decrease in the number of activating receptors like NKp30, NKp46 on NK cells. Unfortunately, no specific NK cell receptors have been identified that recognize HIV-1 infected cells but a recent study showed that KIR3S1 recognising HLA-F induce primary NK cells to degranulate as well as to produce antiviral cytokines such as IFNγ, TNFα and MIP-1β (99,100). In vivo investigations have shown that NK cell receptor KIR3DS1 and its ligand HLA-B Bw4-801 are associated in the inhibition of HIV-1 replication and the killing of target cells by NK cells (88,90). This results in a decrease in activity of NK cells during HIV-1 infection. The malfunction of NK cell during HIV-1 infection may be due to viral proteins. Indeed, HIV-1 gp41, gp120, Nef and Tat have been shown to induce a down-regulation of NK cell activity by various mechanisms (101,102).

In response to certain viral infections, type 1 interferons (IFN-α/β) are produced which then enhance the cytotoxicity mediated by NK cell, leading to the killing of the viral infected cells. In addition to this, many key pathways related to antiviral functions are activated by IFN–γ. IL-21, is another cytokine that binds to the common γ–chain (shared with IL-2, IL-4, IL-7, IL-9, and IL-15). This cytokine has been demonstrated to be involved in the onset of the most cytotoxic $CD56^{dim}CD16^{+}$ NK cell subset and to enhance its cytotoxicity. Tumour Necrosis Factor -α (TNF-α) is another factor produced by NK cells and which is known to mediate antiviral and immunoregulatory effects.

Crosstalk between NK cells and DCs may be disrupted during HIV-1 infection, although this mechanism is not completely worked out. In fact, a recent report showed that it is possible for NK cell mediated lysis of virally infected cells to be a source of apoptotic bodies for uptake of DCs, which may promote DCs maturation and at the same time allow viral antigen presentation to T cells (103).

1.3.4 NK cells in autoimmune diseases

In human autoimmune diseases, alterations have been observed in circulating blood NK cells in terms of frequency and activity. Indeed, many instances of autoimmune disease, a reduction in number of NK cells along with decreased cytotoxic function has been observed. Reports demonstrated that NK cells are involved in the control of autoimmune disease conditions. Indeed, in vivo studies using animal model which develop experimental auto-immune encephalomyelitis (EAE), a mouse model of human multiple sclerosis (MS) showed increased severity and mortality when NK cells are depleted prior to disease induction. EAE animals showed a characteristic phenotype with a cellular infiltration, central nervous system (CNS) inflammation, and demyelination. Additionally, clinical trials on MS patients suggest low activity of NK cells and frequency in the peripheral blood.

The cytotoxicity of NK cells can exacerbate an autoimmune disease. In fact, auto-reactive NK cells can induce the destruction of cells in a targeted organ. For instance, in Type 1 diabetes (T1D), NK cells have been found in pancreatic islets only during infection or inflammation, which is not the case in healthy and non-diseased conditions (104). Involvement of NK cells in this pathology is furtherer reinforced by preclinical data that suggest that NK cells are involved in the development of T1D. Some studies on T1D patients show that NK cells are either decreased in number or their function is impaired (105–107). Evidence of NK cell activating receptor involvement is also known in T1D. Gur *et al.* recently demonstrated that in both mice and humans, NKp46 binds to an unknown ligand on pancreatic cells which leads to the killing of the latter due to the degranulation of NK cells (104,105). The study established that NKp46 was one of the essential receptor for the development of T1D. It is well documented that in humans, this ligand is expressed constitutively in both the young and in adults. However the fact that not all humans become diabetic in spite of having the ligand that makes β cells subject to NK cell attack is due to the

fact that NK cells are usually absent in the healthy pancreas. In another study, patients with long-standing T1D showed a remarkably low expression of NK cell activating receptors such as NKp30 and NKp46 receptors in their blood in comparison to those of the control group. Besides, the expression of NKG2D, an NK cell inhibitory receptor, was found to be reduced relative to the healthy control group, irrespective of disease duration. Additionally, long-standing patients also displayed reduced perforin mRNA expression (108). Consistent with these results, a decreased lysis activity by the NK cells was observed by Lorini *et al.* in patients with long-standing diabetes. Generally, the decline in term of NK cell activity in diabetic patients is thought to be a consequence of the disease rather than a cause.

Tissue resident NK cells may also have disease promoting functions. In Rheumatoid Arthritis (RA), Laszlo *et al.* reported a decade ago that patients with RA have NK cell accumulations in their synovial fluid (109). Furthermore, the NK cell subset was $CD56^{bright}$ and secretes more IFNγ compared with peripheral NK cells from the same patients. However, in Systemic Lupus Erythematosus (SLE), patients show a variable and moderate reduction of NK cell frequency along with reduced numbers of $CD4^{+}CD25^{+}$ Treg cells. The function of NK cells is down-regulated in these patients and there is a change from the $CD56^{dim}$ (more cytotoxic) population to the $CD56^{bright}$ (less cytotoxic) subset (110). This is supported by the fact that NK cells in these patients have a reduced cytotoxic effect. Additionally, this deficiency of NK cells is linked with clinical conditions such as nephritis and thrombocytopenia during SLE. The abnormality in NK cell number and function could therefore play a key role during inflammation. This shows how NK cells could play a protective or disease controlling role to prevent SLE.

Changing the cytokine and cellular profile of the microenvironment can influence the development of specific NK subtypes which may lead to conversion from a pro-inflammatory to an anti-inflammatory NK sub- type. In general, chemokines produced by NK cells such as MIP-1α are capable of promoting inflammatory response but, in some cases, they can produce IL-10 and favour an anti-inflammatory response. IL-10 contributes to the inhibition of DCs which reduces the effect of antigen presentation by Antigen Presenting Cells (APCs) and diminishes T cell proliferation (111). DCs and T cells are normally observed to be accumulated at the site of immunization, and they produce cytokines which are involved in the pathogenesis. Furthermore, NK cells

produce IFN-γ, TNF-α, GM-CSF and MIP-1 upon stimulation with IgE, and also demonstrate cytotoxicity against IgE coated target cells via FcγRIII (112).

Macrophages are another important immune system component during cancer. They are known to increase the anti-tumour as well as anti-infection activity of NK cells through their crosstalk (73,113,114). Along with macrophages, Tregs which are part of the adaptive immune system, are also known to interact with NK cells and mostly control their activity during various disease conditions. In autoimmune disease conditions, Treg cells have been seen to suppress NK cells via IL-21 mediation (115).

1.4 Therapeutic applications of NK cells

NK cells play a crucial role in attacking tumour cells and are considered a promising tool for cancer therapy. Over the past two decades, clinical treatments have ranged from IL-2 administration to activate the endogenous NK cells to adoptively transfer IL-2 activated NK cells (116). Therapy using autologous NK cell has been used as the treatment of renal cell carcinoma, malignant glioma, or metastatic breast cancer. Nevertheless, it was soon noticed that autologous adoptive NK cell therapy may have certain drawbacks and thus may not be as efficient as predicted. The downside of this strategy is mostly attributed to the inhibition of NK cells by self-MHC I molecules expressed on the tumour cells. This has led clinical teams to the use of allogeneic NK cell therapy in trials. In a pioneering study, Ruggeri *et al*... elegantly showed that alloreactive NK cells which were given to patients with Acute Myelogenous Leukemia (AML) could prevent relapse, graft rejection, and protect them against Graft-Vs-Host Disease (GvHD) (117). Later, adoptive cellular transfer of allogeneic NK cells from haploidentical donors was also attempted for treatment of renal cell carcinoma, metastatic melanoma, refractory Hodgkin's disease, and refractory AML (118). This procedure was also found to be useful against several solid tumours such as ovarian, renal, colon, gastric cancers, and neuroblastoma (119,120). The trials concluded that NK cell transfer was successful, safe, and efficient. Similar trials were also conducted recently in patients with recurrent metastatic breast and ovarian cancer (121). The allogeneic NK cells have the advantage of being derived from healthy donors and therefore have more cytotoxic activity. Furthermore, unlike T cells, NK cells do not induce GvHD.

As discussed in the previous sections, the role of NK cells has been established not only in cancer but also in various other disease situations. Therefore, adoptive NK cell therapy can thus be explored for diseases such as asthma, multiple sclerosis, diabetes or arthritis. The effectiveness of NK cells in controlling HIV-1 infection has already been demonstrated in in vitro and in vivo experiments (87,89). NK cell therapy can be a strategy to treat patients who are refractory to standard highly active antiretroviral therapy (HAART). Besides the option of using NK cells for adoptive transfers, understanding the role of NK cells and their receptors can open up other strategies to treat diseases. For example, during the developmental stages of T1D, the activation of NK cells can be prevented by blocking activating receptors such as NKp46. This can be done by using specific antibodies against activating receptor. Similarly, in RA where the role of NK cells is either protective or disease-enhancing, therapy can be considered accordingly. Another strategy that involves NK cells will be to block the inhibitory receptor like NKG2A. This approach will then help to induce NK cells stimulation and thus control the disease. In situation where NK cells enhance the disease, the blocking, for instance of RANKL (receptor activator of NFKB ligand) and M-CSF (macrophage colony-stimulating factor), which are elements that mediate osteoclastogenesis and bone destruction, have been shown to help (122–124) .

For therapeutic purposes, allogeneic NK cells can be obtained from umbilical cord blood (UCB), adult donor lymphapheresis products, or even from NK cell lines such as NK-92. Recent reports have shown successful in vitro derivation of functional NK cells from human embryonic stem cell (hESC) and induced pluripotent stem cell (iPSC) (125–127). Indeed, hESC and iPSC-derived NK cells have demonstrated potent anti-tumourigenic and anti HIV activity, and present a similar phenotype as peripheral NK cells. Moreover, these derived NK cells are considered better than UCB-derived NK cells since they have higher levels of KIR expression which make them more potent. Pluripotent cell-derived NK cells can therefore be an unlimited source for the adoptive transfer of NK cells to treat a range of diseases. However, the safety of hESC and iPSC-derived NK cells in terms of potential tumourigenicity as well as ethical boundaries needs to be determined before they can be used in clinic.

The use and application of NK cells as immunotherapeutic agent necessitates several technical developments. Indeed, NK cells need to be isolated and expanded in sufficient numbers for them to act as effector cells. Moreover, NK cell activity needs to be enhanced for better efficacy. Expansion of NK cells has been attempted using

cytokines such as IL-2 and IL-15 (128,129). In fact, these two cytokines can also help to increase the viability of the NK cells. Furthermore, IL-2 is also thought to potentiate the cytotoxic ability of NK cells. In vitro studies where NK cells are in co-culture with accessory cells such as irradiated Epstein Barr Virus (EBV) transformed lymphoblastoid cells, HFWT (a Wilm's tumour derived cell line) or K562 have been reported to enhance NK cell proliferation (130,131). Furthermore, activation of NK cells can be achieved by various genetic engineering techniques to increase activating signals and also to down-regulate inhibitory signals (132,133). Similarly, the specificity of NK cells can be increased through genetic modification approaches such as the use of chimeric antigen receptors known as CARs (134–136).

1.4.1 NK cells in Liver disease

NK cells are the most abundant immune cells in the liver and they have one of the most important role as a way of defence against infections, in particular viral infection (137). For instance, NK cells contribute to antiviral defence through direct cytotoxicity of virally infected cells and by the production of cytokines that are involved in the prevention of viral replication. Nevertheless, many viruses have developed strategies to escape recognition by cells of the adaptive immune system. Indeed, infected cells often down-modulate HLA molecules from the cell surface to block antigen presentation to CD8 or CD4 T cells. These infected cells, however, will not engage the inhibitory receptors on NK cells, making them inclined to NK cell lysis. Viruses, on the other hand, have evolved a number of specific approaches to evade NK cell recognition and killing (83). These involve expression of HLA-like molecules that can ligate KIR molecules, inducing NK cell inhibition (138,139).

NK cells execute their biological activity by a triad of functions which are: cytotoxicity, cytokine secretion and co-stimulation. In humans, they appear to have an important role in viral infection, cancer immunity, transplantation, pregnancy as well as autoimmunity. Focusing on liver diseases, the evidence accumulated from the last two decades suggests that NK cells not only have beneficial effects in inhibiting viral hepatitis, liver fibrosis, and carcinogenesis in the liver but also contribute to hepatocellular damage. Although these findings have significantly enhanced our understanding of liver disease pathogenesis and treatments, further studies are still

required to clarify the multiple functions of NK cells and translate these findings into clinical practice and therapies.

1.4.2 NK cells as therapeutic targets for the treatment of liver disease

NK cells accumulate within the liver and compared to other organs, have higher levels of cytotoxicity and cytokine production, which can be beneficial in inhibiting viral infection, tumour cell growth, and liver fibrosis but can also enhance hepatocellular damage. It is well established that chronic liver diseases are associated with a decreased number of NK cells and impaired NK cell cytotoxicity and cytokine production. As mentioned above, NK cells play an important role in inhibiting viral hepatitis, liver fibrosis, and hepatocellular carcinoma. These functions suggest that the activation of NK cells can potentially be used as therapeutic strategy for the treatment of these liver disorders. For instance, it has been shown that IFN-α, one of the most potent NK cell activators, has been widely used to treat viral hepatitis and has also been shown to suppress liver fibrosis and tumour formation. These anti-viral, anti-fibrotic, and anti-tumour effects of IFN-α therapy are likely mediated, at least in part, via the activation of NK cells. Other NK cell activators, like IL-12 as well as IL-18, have been demonstrated to successfully inhibit liver carcinogenesis in animal models (140,141). In addition, the stimulation of NK cells has been used to enhance NK cell antibody-dependent cell-mediated cytotoxicity (ADCC) against tumour cells and has been tested for the treatment of various types of cancers such as lymphoma (142,143). Furthermore, blockade of NK cell inhibitory receptors is another way to augment NK cytotoxicity against tumour cells. For example, antibodies that block KIR are currently being tested for the potential treatment of haematological cancers in Phase II clinical trials (144,145). Therefore, the activation of NK cells by cytokines, the targeting of NK cells to enhance ADCC, and the release of NK cell from inhibition via the blockade of inhibitory receptors all have therapeutic potential for the treatment of HCC. Lastly, feasibility and safety of the adoptive transfer of activated NK cells extracted from cadaveric donor liver graft perfusate for liver transplant recipients with HCC are currently under investigation in Phase I clinical trials (www.clinicaltrials.gov NCT01147380).

1.5 The molecular specificity of NK cell receptors

NK cells express a large number of different receptors that contribute to the regulation of effector function (**Figure 1-3**). Opposing signals from activating and inhibitory receptors provide an appropriate balance in NK cell activation or inhibition. A large set of activating NK cell receptors is expressed by most peripheral blood NK cells and they have the ability to recognize a diverse array of molecular structures (146). Furthermore, they utilize a variety of signalling pathways. By contrast, expression of any given MHC class I specific inhibitory receptor is restricted to subsets of NK cells. Inhibition occurs through recruitment of tyrosine phosphatases to immunoreceptor tyrosine-based inhibition motifs (ITIM) in the cytoplasmic tail of inhibitory receptors. Taken together, the specificity of activating and inhibitory receptors offers NK cells several strategies to discriminate healthy cells from those in distress. More recently, ligands to orphan receptors have been identified, and advances made in understanding how interplay between different receptors is involved in the specificity of NK cells responses.

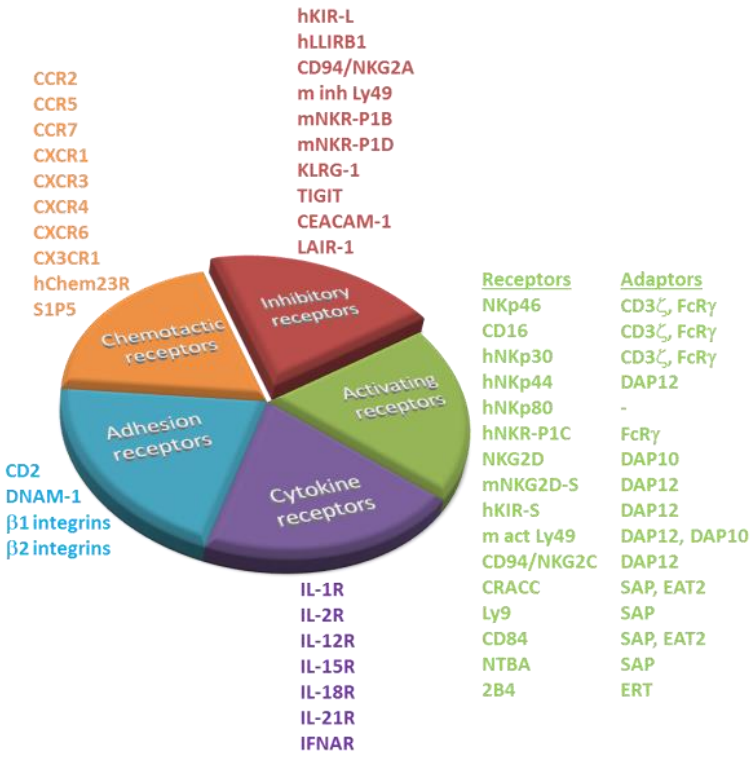

Figure 1-3: NK cell receptors expression. NK cells have a highly diverse expression of receptors that can be classified as: activating and inhibitory receptors; chemotactic receptors; adhesion receptors; and cytokine receptors. Adapted from Vivier *et al.*(146)

1.5.1 Receptor-mediated NK cell responses

Unlike T cells and B cells, NK cells do not require antigen specificity in order to respond. But, they express a large series of receptors that have either activating or inhibitory function. The balance between activating and inhibitory signals determine whether an NK cell becomes activated or inhibited. This recognition system does have some level of flexibility and in contrast with T and B cells, this flexibility is not achieved through the rearrangement of genes coding for the receptors. Instead, NK cell recognition receptor families have achieved plasticity through rapid genetic evolution (mainly KIR receptors) and reported promiscuity of ligand binding (147). To contribute to the first line of defence, NK cells are always ready to attack abnormal cells. Having in mind that their ability to respond immediately may present a danger to healthy cells in the event of inappropriate NK cell activation, it is logical to assume that the process of NK cell activation is tightly regulated. Part of this regulation is intrinsic in the type of receptors that NK cells use to identify and react towards target cells. Two suggested hypotheses of NK cell activation are the 'missing self ' and 'induced self ' theories (148,149). The 'missing self' hypothesis suggested that NK cells attack target cells that show reduced or abnormal level of surface expression of major histocompatibility complex (MHC). This corresponds to a situation where the cells are missing expression of self-molecules, which are usually expressed on healthy tissue. Therefore, when MHC class I molecules are expressed on cells, activation of NK cells is prevented. However, reports have undoubtedly revealed that NK cell activation may be determined, not only by lack of MHC class I expression, but also by the expression of ligands for NK cell-activating receptors (16,18,150). In the original 'missing self' model, the presence of activating receptors was implicit, nevertheless, Karre *et al*. suggested that activating receptors recognized ubiquitous ligands, and that inhibitory signals were determinant of a functional response (151). On the other hand, the 'induced self' model of NK cell activation is therefore not entirely exclusive from the missing self-model and describes the recognition of cellular stress ligands, induced upon malignant transformation or viral invasion. For instance, MHC class I chain-related gene MICA/MICB are ligands for the NKG2D-activating receptor and the expression of these molecules is induced under situations of cellular stress, such as viral infection. This circumstance then triggers NK cells activation through the induced expression of stress-related proteins (152).

1.5.2 NK cell recognition and response receptors

NK cell inhibitory and activating receptors are a complex group of receptors that use opposing signalling motifs to stimulate or inhibit activation. On one hand, inhibitory receptors signal through intracellular immunoreceptor tyrosine-based inhibitory motifs (ITIMs), located in the cytoplasmic tail of these receptors. During inhibitory signalling, Src homology 2 domain containing phosphatases (SHP1 or 2) are recruited after phosphorylation of a tyrosine residue (153). The way inhibitory signals interfere with activating signals is still unclear, but it is proposed that ITIM-mediated signalling results in both dephosphorylation and specific phosphorylation of intracellular components. A recent report demonstrated the implication of the β-arrestin 2 in the inhibition of NK cell activation, via the recruitment of SHP1 and 2 (154). An additional report showed that that a common point of NK cell activation signalling could be targeted, in which a SHP1 phosphorylation site (Vav1) is dephosphorylated during inhibitory signalling (155). This report suggested that inhibitory signalling can prevent not only NK cell-mediated cytotoxicity, but also interfere with adhesion of NK cells to target cells. In contrast, Long and Peterson have described mechanisms involving the specific phosphorylation of a tyrosine adapter, Crk, as a result of ITIM engagement (156). Therefore, it is now clear that whilst ITIM signalling prevents intracellular phosphorylation, it is likely to involve more complex signalling than initially thought. It is now clear that the more we can learn about the inhibitory signals used by NK cells, the better we can manipulate these signals in order to optimize NK cell-based therapies.

On the other hand, some activating receptors such as the NKG2C/CD94 heterodimer, signal through immune-receptor tyrosine-based activating motifs (ITAMs), although these are not contained in the receptors' cytoplasmic tails but rather in associated molecules. Following phosphorylation of a tyrosine residue in the tail, the Src homology 2 domain containing kinases (Syk or ZAP70) are recruited, which induce a signal cascade. The signalling will then lead to degranulation and transcription of cytokine and chemokine genes (153). Additional investigation has shown a requirement for PKC-y in sustained ITAM signalling, which results in NK cell activation, and suggest that ITAM-mediated activation of NK cells does not require co-stimulatory signals (155,157). However, it was reported several times that stimulation of a unique activating receptor was not enough to stimulate cytotoxicity and cytokine secretion, but stimulation of more than one receptor is required for NK

cells to be functional (158). Hence the question of why NK cells require co-stimulation for activation still requires invstigation.

Other activating receptors, including NKG2D, use an alternative signalling mechanisms, such as through the adaptor molecules either DAP-10 or DAP-12. DAP-12 signals through an ITAM motif (as described above), whereas DAP-10 binds either to Grb2 or P85 and signals through phosphatidylinositol-3 kinase and other alternative signalling pathways (159–161). Although the subsequent signalling events are yet not well characterized, it is clear that the outcomes of DAP-10 and DAP-12 signalling differ, as DAP-12 signalling results in cytokine secretion and cytotoxicity and DAP-10 signalling results in cytotoxicity (162,163).

A third activation/inhibition signalling pathway is possible in NK cells, and results from stimulation of the CD244 (2B4) receptor. Indeed, this receptors cytoplasmic tail contains an immunoreceptor tyrosine-based switch motif, which recruits Src homology 2 domain containing adapter proteins SAP or ERT (164). Recruitment of SAP induces activation of NK cell function, where recruitment of ERT prevents NK cell from being activated. It is still unclear why NK cells have several different activating pathways. Nevertheless, it has been shown that activating signals can be overridden with signalling of an ITIM-containing receptor (155,165).

It is agreed that receptor family classification more easily defines the recognition receptors on NK cells than the functional categories of “inhibitory” or “activating”. This is due to the fact that some receptor families contain both activating and inhibitory receptors, as described earlier for 2B4 and this is also the case for the family of KIR receptors. The reasons for these phenomena is not entirely clear, although it is hypothesized to increase the ability of NK cells to distinguish normal, healthy cells from infected or malignant cells, thereby stopping unsuitable NK cell activation.

1.5.3 Activating receptors

The low-affinity receptor for IgG, CD16, mediates antibody- dependent cellular cytotoxicity (ADCC) and signals through adaptors containing cytoplasmic immunoreceptor tyrosine-based activation motifs (ITAM). As a result of investigations into the mechanism of action for different therapeutic antibodies, such as rituximab

(anti-CD20) and Herceptin (anti-erbB2), which have been used successfully in the clinic, have led to an increasing understanding of NK cell-mediated ADCC. Multiple receptors, which activate antibody-independent, natural cytotoxicity are also associated with ITAM-containing signalling adaptors. These receptors include NKp30, NKp44, and NKp46, which are referred to as natural cytotoxicity receptors (NCR) (166). The nature of the ligands for natural cytotoxicity receptors (NCRs) is still unclear. Although NKp46 has been reported to bind viral hemaglutinin on infected cells (167), cellular ligands have not been identified. NKp46 contributes to enhanced killing of mitotic cells by NK cells which suggests a role of NK cells in controlling expansion of rapidly dividing cells (168). NKp30 mediates killing of immature dendritic cells by NK cells (169). Surprisingly, an intracellular protein implicated in the induction of apoptosis after DNA damage or endoplasmic reticulum stress, called HLA-B associated transcript 3 or BAT3, was described as a ligand of NKp30 (170). The process underlying mechanism as to how BAT3 protein becomes exposed at the cell surface is still unknown. In 2013, Matta *et al.* described B7-H6 as a ligand. Additionally, immunostaining of various tumour cells with soluble forms of NKp30 and NKp44 resulted in intracellular staining which suggested that translocation from the inside to the surface of cells may be a common theme among ligands of NCRs (171). Alongside this notion, it has been shown that the human cytomegalovirus (human CMV) tegument protein pp65, which is not expressed at the surface of infected cells, has also been identified as a ligand for NKp30 (172). Nevertheless, binding of pp65 results in the inhibition of NK cell cytotoxicity induced by NKp30, which seemed to characterize one of the many evasion manoeuvres developed by human CMV to counter detection by NK cells.

The NK cell activation receptor NKG2D is associated with the adaptor protein DAP10, which has a tyrosine motif completely distinct from the ITAM motif. NKG2D binds a number of different ligands, including Major Histocompatibility Complex class-I related chain A/B (MICA/B) and UL16 binding protein (ULBP) 1/2/3/4. Expression of these ligands is up-regulated on infected, stressed, and transformed cells (173). The DNA damage response induces expression of NKG2D ligands (174). Detection of tumour cells by NKG2D can be prevented by soluble NKG2D ligands, which are released from the cell surface after cleavage by a protease called ERp5 (175). Furthermore, soluble ligands provoke internalization of NKG2D from the cell surface. The importance of NKG2D as a mechanism of defence against tumours has already been reported (176) as well as its role in autoimmunity (177,178). Many of the other

NK cell activation receptors signal through motifs in their own cytoplasmic tail, and through pathways that are still in the process of being characterized. DNAX accessory molecule-1 (DNAM-1) binds nectins CD112 and CD155, which are components of cellular junctions. On NK cells, it has been reported that DNAM-1 may facilitate surveillance of damaged endothelium and transformed cells (179,180) demonstrating its involvement in cancer.

2B4, CD2 like receptor activating cytotoxic cells (CRACC), and CD2 bind ligands that are predominantly expressed on hematopoietic cells. The structures of CRACC homophilic interactions and 2B4 in complex with CD48 were solved. It has been reported that at the membrane, spacing required for homophilic CRACC and 2B4-CD48 interactions, respectively, is similar to the space required for KIR–MHC class I interactions (181,182). Therefore, activating receptors such as 2B4 and CRACC could potentially intermix with inhibitory KIR at the NK cell immune synapse, facilitating dynamic assessment of activation thresholds.

NKP80 is another NK cell activation receptor with unknown signalling properties. The cellular ligand of NKP80 was identified as being Activation-induced C-type lectin (AICL). The NKP80 and AICL genes are closely linked in the NK cell gene complex on chromosome 12. Expression of AICL is confined to granulocytes and macrophages, and is up-regulated by inflammatory stimuli (183). As a result, NKP80–AICL interactions may be important for NK cell myeloid cell crosstalk during immune reactions.

Finally, over 30 different KIR haplotypes with discrete gene content have been characterized to date by sequencing genomic clones and haplotype segregation analysis in families. One of the haplotypes that is present in all populations is conventionally named the ‘A haplotype’ and consists of nine genes (3DL3, 2DL3, 2DP1, 2DL1, 3DP1, 2DL4, 3DL1, 2DS4 and 3DL2). The haplotype A mainly encodes inhibitory receptors. The remaining haplotypes are collectively referred to as ‘group B haplotypes’, which have variable gene content comprising several genes (2DS1, 2DS2, 2DS3, 2DS5, 2DL2, 2DL5, and 3DS1) that are not part of the A haplotype, and thus B haplotypes encode more activating KIR compared with the A haplotype that encodes a single activating receptor, KIR2DS4 (184). Activating KIR receptors may have HLA molecule as ligands.

1.5.4 Inhibitory receptors

NK cell reactivity is controlled by inhibitory receptors with specificity for different MHC class I alleles (**Figure 1-4**). Receptors such as KIR in humans and Ly49 in mice allow NK cells to sense cells with reduced expression of MHC class I, thus complementing T cell mediated immunity. Furthermore, the clonal distribution of MHC class I specific inhibitory receptors on individual NK cells, and the repertoire of receptors specific for different MHC class I allotypes, can give rise to NK cell alloreactivity. However, this alloreactivity may be exploited in clinical immunotherapy in order to reduce graft-versus-host-disease while providing beneficial graft-versus-leukaemia effects.

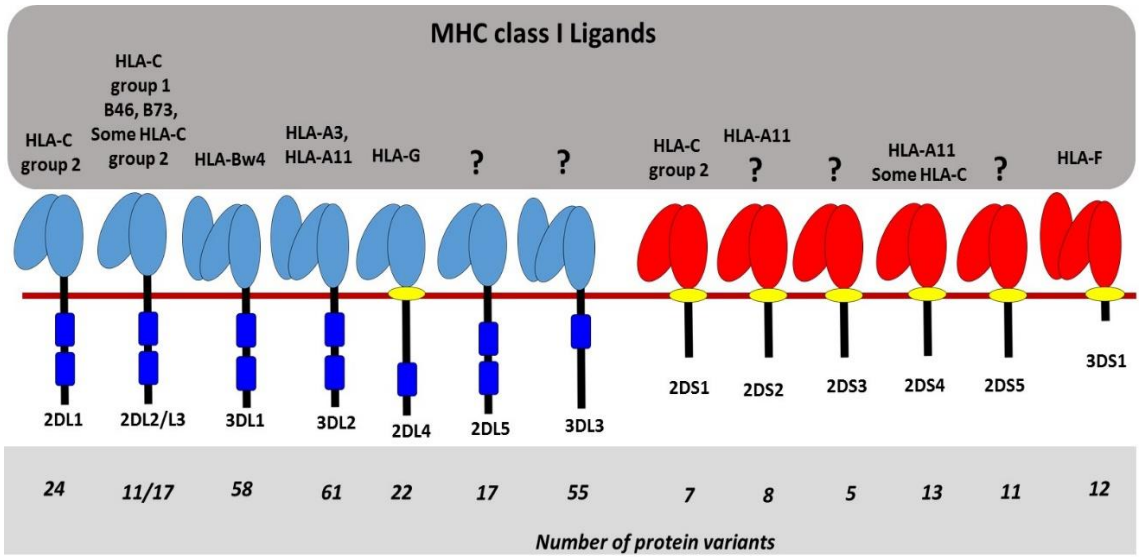

Figure 1-4: KIR receptors and their ligands. Fourteen distinct KIR receptors have been described in humans. Six different KIR receptors are activating types and the remaining KIR are inhibitory types. The inhibitory KIR receptors bind to distinct HLA class I allotypes and the ligands for most activating KIR receptors are unknown. This data was extracted from the IPD-KIR database (http://www.ebi.ac.uk/ipd/kir/stats.html; Release 2.4.0; April 2011) that provides a centralized repository for human KIR sequences.

Besides receptors for classical MHC class I molecules, NK cells may indirectly assess MHC class I expression on target cells by interaction between another inhibitory receptor which is CD94/NKG2A heterodimer. Its ligand HLA-E is a non-classical MHC class I molecule that presents MHC class I leader peptides. Additionally, the crystal structure of CD94/NKG2A, in combination with mutagenesis studies, has

demonstrated a model for the CD94/NKG2A–HLA-E complex. According to this the model, the CD94 chain has a more dominant role in interaction with HLA-E than NKG2A (185). The binding of an inhibitory receptor to MHC class-I is usually considered sufficient for inhibition.

Numerous other inhibitory receptors, which bind to non- MHC class-I ligands, have been identified and characterized. For instance, the lectin-like receptor KLRG1 which binds cadherins, in both humans and mice could serve as a system to detect potentially metastatic epithelial tumours that downregulate cadherin expression (186,187). Another one is the Leucocyte-associated immunoglobulin receptor 1 (LAIR-1) which is an inhibitory receptor that binds to collagen and is widely expressed on immune cells like NK cells as well as T and B cells (188). LAIR-1 mainly prevents the lysis of cells considered as "self". Some members of the Siglec family of receptors, which bind sialyl groups with various specificities, also carry ITIMs in their cytoplasmic tail. Additional inhibitory receptors have been described, such as IRp60, for which a ligand has not been identified yet. The biological reasons for this array of inhibitory receptor–ligand systems still require investigation. It is possible that differential expression of ligands for inhibitory receptors facilitates detection by NK cells of various types of cells, each of which may rely on a few specific ligands to inhibit NK cells.

1.6 Killer Immunoglobulin like Receptors: KIR

1.6.1 Structural and diversity of KIR receptors

KIR are encoded by a compact cluster of genes that constitute part of the leucocyte receptor complex also called LRC and situated on chromosome 19q13.4 (189,190). More than one hundred mRNA and DNA sequences represent the human KIR family in gene data banks. KIR receptors were classified according to three criteria: number of extracellular Ig-like domains, cytoplasmic tail length, and sequence similarity. These criteria helped to classify the encoded KIR proteins into 13 groups. A specific nomenclature is used to describe these groups: KIR3DL1–2, KIR3DS1, KIR2DL1–5, and KIR2DS1–5. The number of Ig-like domains is given by 2D for 2 domains or 3D for 3 domains; the length of the cytoplasmic tails is given as "L" for long or "S" for

short; and different KIR with similar overall organization but sequence divergence of >2% are generally numbered in series (**Figure 1-5**).

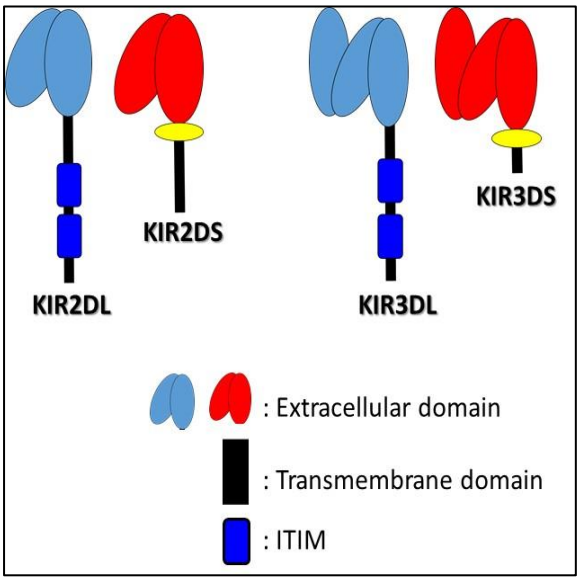

Figure 1-5: Human KIR receptors molecules. KIR receptors in humans that include either two (2D) or three (3D) extracellular immunoglobulin-like domains and either a long (L) or short (S) cytoplasmic tail. In general, the specificity for HLA C alleles is conferred by the amino acids present at positions 77 and 80. Those HLA-C molecules with Asn 77/Lys 80 (HLA Cw2/4/5/6/) bind to KIR2D1, whereas those with Ser 77/Asn80 (HLA Cw1/3/7/8) bind to KIR2D2 and KIR2D3.

The inhibitory KIR have long cytoplasmic tails containing pairs of immune tyrosine-based inhibitory motifs (ITIMs). On the another hand, KIR with short cytoplasmic tails are activating receptors and associate with adaptor molecules such as DAP12 which signal via a positively charged Lysine (K) residue in their transmembrane domain (159). In humans, KIR3DL1 and KIR3DL2 represent a more evolutionary ancient KIR from which 2D KIR can be derived.

The majority of human KIR have two extracellular Ig-like domains. These are of two distinct types: type 1 KIR2D having domains homologous to D1 and D2 of KIR3DL, and type 2 KIR2D having domains homologous to D0 and D2 of KIR3D. Genes encoding type 1 KIR2D are similar in organization to those encoding KIR3D and contain a region homologous to exon 3 encoding the D0 domain of KIR3D (78.7–79.8% sequence identity with *3DL1* and 79.8–81.2% with *3DL2*) (191,192). This region known as "pseudo-exon 3," is spliced out of the RNA transcript even when it maintains the correct reading frame and has correct splicing sites, as is the case in half of the genes encoding type 1 KIR2D. The one feature that distinguishes exons 3 from the pseudoexons 3 is that they are longer by one codon. If the three nucleotides missing from pseudoexons are part of an exonic splicing enhancer necessary for inclusion of exon 3 in mature mRNA, then their absence maybe an explanation for the lack of expression of type 1 *KIR2D* pseudoexons (192). 2DL4 and 2DL5 receptors represent

type 2 KIR2D. In comparison to genes encoding KIR3D, the *2DL4* and *2DL5* genes have a deletion of more than 2kb that includes exon 4 encoding the D1 domain. KIR cytoplasmic tails can have different lengths, despite that exons encoding them have similar lengths and sequences. This is made possible because of the single-nucleotide substitutions which produce stop codons at diverse positions within the exonic sequence (193). Another important component of KIR variation involves variation in gene content within the KIR haplotypes itself (189).

1.6.2 Structural basis of KIR-HLA recognition

The structural heterogeneity of KIR and their specificity for polymorphic determinants of HLA class I molecules were established from studies of NK cell cytotoxicity. In these reports the susceptibility of allogeneic targets, and, later on, HLA class I- deficient cell lines transfected with single HLA class I alleles, were tested against NK cell clones and KIR-transfected cells (49,194-197). Furthermore, chimeric molecules containing the extracellular portion of KIR and the activating cytoplasmic tails of the FcεRIγ-chain or CD3ζ were used to overcome the technical difficulty of studying inhibitory signals (198,199). Further improvements in the understanding of KIR-HLA interaction and recognition were achieved by generating soluble forms of the receptor or its ligand. Firstly, fusion proteins containing the extracellular fragment of KIR and the Fc of human IgG1 were used in flow cytometry to assess different HLA class I molecules expression on cells (197,200,201). Then, native gel electrophoresis experiments revealed the basic 1:1 stoichiometry of KIR-HLA complexes. Direct interaction between recombinant KIR and HLA molecules demonstrated this aspect of KIR and HLA interaction. The usage of recombinant proteins also helped to study the specificity of KIR-HLA binding and the influence of other molecules (e.g., bivalent cations, antigenic peptides) on KIR binding (53,202-204). More sensitive techniques such as surface plasmon resonance (SPR) methodology have permitted quantitative assessment of KIR-HLA interactions (205-208). SPR was also used to study the kinetics and thermodynamics of the binding between KIR molecules and their ligands. This methodology helped to clarify the specificity and peptide-dependence during the KIR-HLA interaction.

On one hand, the affinity of KIR for HLA-C in particular are comparable to the range shown by TCR for specific peptide-MHC complexes. On the other hand, the kinetics

of KIR-HLA-C binding and detachment (on and off rate) are much faster compared to the TCR. As a result, NK cell surveillance of MHC class I expression on a succession of potential target cells may be facilitated by this fast on and off rate. Three dimensional structures of HLA-C being recognized by inhibitory KIR were identified by X-ray diffraction studies of crystallized 2DL2-C*03 (**Figure 1-6**) and 2DL1- C*04 complexes (207,209), as well as 2DL1/2/3 alone (210–212). In several aspects of their three-dimensional structure KIR2DL1/2/3 are similar to hemopoietic receptors. Most importantly, an acute angle between the D1 and D2 domains creates an elbow that constitutes the interface with HLA-C. This angle ranges from 55± to 84± degrees, depending on the KIR and the method used to interpret raw data. Two loops of D1, three of D2, and the loop connecting the two Ig-like domains contribute to the interaction. All six loops bear negatively charged glutamate or aspartate residues that face a positively charged surface on HLA-C. The C-terminal end of the alpha-1 domain helix (α1), the N-terminal end of the alpha-2 domain helix (α2) are the parts of the HLA-C surface that become buried by interaction with KIR2DL1/2 as well as the C-terminal residues of the peptide. The shape complementarity of KIR-HLA-C surfaces, as assessed by the median shape correlation statistics value, is similar or greater than those of antigen-antibody or MHC-TCR complexes (209).

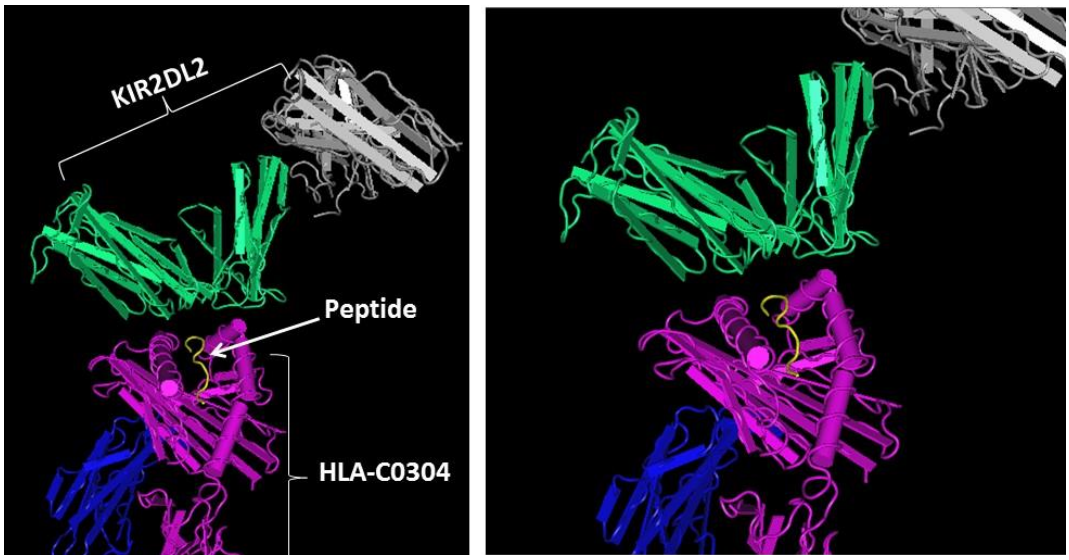

Figure 1-6: KIR2DL2 receptor recognising HLA-C*0304 complexed with its GAVDPLLAL peptide. HLAC*0304 molecule (β2m in bleu and the heavy chain in purple) is presenting its peptide from Importin α2 (in yellow). The complex is recognised by KIR2DL2 receptor (KIR A in green and KIR B in grey). We can distinguish Domain 1 (D1) and 2 (D2) of the KIR A as they are in contact with the class I: peptide complex. This structure was uploaded from the NCBI and visualised using Cn3D program. The structure is based on data from Snyder *et al.* (210) and Boyington *et al.* (207).

In addition to interactions with the α1 and α2 domains of HLA class I, the co-crystal structures demonstrated how KIR also make direct contacts with the HLA-bound peptide, consistent with the peptide-specific differences observed in biochemical and functional studies. All the different KIR–HLA class I combinations examined to date have shown some degree of peptide selectivity (213–216). It has been well reported how KIR binding and function are particularly sensitive to the residue at position 8 (P8), with the neighbouring position 7 (P7) contributing an additional, but weaker effect (207,214). These findings are compatible with the footprints of bound KIR2DL1 and KIR2DL2 on the HLA-C*04:01 and HLA-C*03:04 molecules, respectively, that show interaction with residues P7 and P8 of the HLA-C bound peptide (207,209). During the interaction between KIR2DL2 and HLA-C1, glutamine 71 of KIR forms a hydrogen bond with the amide nitrogen of the alanine at P8 of the peptide. Additionally, KIR residues (lysine44, serine184, and asparagine 187), which are in close proximity to the peptide bound by HLA-C, provide an additional restriction regarding the size of the residue at P8 in the peptides that permit KIR binding. This limitation favours small residues such as Alanine (A) and Serine (S), whilst not favouring large side chains (207,209). The crystal structure of KIR2DS2 revealed a displacement of Glutamine 71 that is predicted to prevent hydrogen bonding with the main chain nitrogen of peptide residue 8. This is likely leads to the poor C1 binding observed for KIR2DS2 (217). Moreover, peptide HLA combinations that bind KIR weakly appear to function as peptide antagonists, by competing with strongly binding peptides for complex formation with HLA-C and inducing KIR disruption and leading to NK cell activation (218,219).

1.6.3 HLA-C Recognition by inhibitory HLA-C specific KIR

To date, much of the research in understanding KIR-HLA interaction has been concentrated on inhibitory KIR that recognize HLA-C. As stated above, the specific recognition of HLA-C alleles with either Lysine or Asparagine in position 80 by 2DL1 and 2DL2-3 respectively, has been confirmed by studies involving recombinant receptors and their ligands. Site-directed mutagenesis experiments and crystallographic analysis have clarified how KIR2D recognize HLA-C allotypes. Allospecificity is mostly determined by dimorphisms of KIR-residue 44 (2DL1Met44/2DL2-3Lys44) and amino acid 80 of HLA-C (Lys/Asn) which establish

direct interactions with each other (207,209,220–222). All other KIR-contact amino acids of HLA-C*03 and HLA-C*04 are completely conserved amongst HLA-C allotypes. However, the binding of 2DL2 to C*03 and 2DL1 to C*04 are based on largely different interactions, which result in Lys80 of C*04 being accommodated by a cavity in 2DL1 that is not seen in 2DL2 (207,209). HLA-C residue 77, for which the Ser/Asn dimorphism is in strong linkage disequilibrium with that of residue 80, does not contribute directly to KIR recognition, as shown by the results of mutagenesis experiments (222). In contrast, the suggested influence of two additional HLA-C dimorphisms (Ala/Thr73 and Ala/Asp90) in the strength of binding to 2DL1/2/3 remains unclear despite the crystallographic data (223). Furthermore, HLA-C*1503, one of few natural alleles encoding the Ala73-Ala90 combination is recognized by both 2DL1-Fc and 2DL2-Fc constructs (221,223).

Although HLA-C and HLA-Bw6 have the same amino acid sequence at positions 77–80, HLA-C ligands KIR recognizing HLA-CAsn80 does not cross-react with Bw6-positive HLA-B allotypes, (221). Thus, the locus-specificity of 2DL2 and -L3 is determined, at least partly, by amino acid Val76 of HLA-C (Glu in HLA-B) because these KIR recognize B*4601, an exceptional HLA-B allotype carrying Val76.

1.6.4 The role of the peptide: peptide presentation

Human MHC class I molecules (**Figure 1-7**) are encoded by a series of genes which are highly polymorphic. These polymorphisms result in differential susceptibilities to infection and autoimmune diseases which result from the high diversity of peptides that can bind to MHC class I in different individuals. Moreover, MHC class I polymorphisms make it very difficult to have a perfect tissue match between an unrelated donor and a recipient.

On the surface of a cell, the MHC class I peptide repertoire provides a readout of the expression level of up to 10,000 peptides. Cytotoxic T lymphocytes and NK cells then decode this wide range of peptide. The cell surface peptide repertoire allows them to monitor the events inside the cell and detect infection and cell transformation (224,225).

The off rate of the peptide:MHC class I complexes from the cell surface allow the internalization of the heavy chain. This phenomenon that occurs in the endosome

can give place to the MHC class-II presentation pathway. Indeed, some of the MHC class I molecules can be recycled and present endosomal peptides as a part of a process so-called cross-presentation.

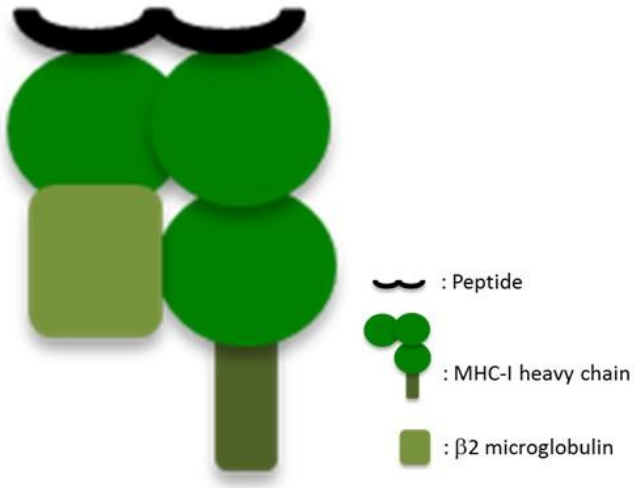

Figure 1-7: Complete Major Histocompatibility Class I complex molecule. MHC-I protein consists of a heavy α chain which comprises α1 and α2 domains in contact with the peptide, a α3 immunoglobulin domain, a transmembrane domain with a cytoplasmic tail. The second chain is the β2 microglubilin that stabilises the whole complex.

Peptide: MHC class I complexes are built in the endoplasmic reticulum (ER) and consist of two types of chain: a polymorphic heavy chain, the monomorphic β2-microglobulin chain and a short peptide. Initially, the heavy chain is stabilized by the chaperone calnexin, prior to coupling with the β2-microglobulin and then with a peptide (**Figure 1-8**). In absence of peptides, MHC-I molecules are stabilised by chaperone proteins: calreticulin (Erp57), protein disulfide isomerase (PDI) and tapasin. The complex of TAP, tapasin, MHC-I, ERp57 and calreticulin is called the peptide-loading complex. During the peptide loading process, tapasin interacts with the transport protein TAP (transporter associated with antigen presentation) which translocates peptides from the cytoplasm into the ER. Prior to entering the ER, peptides are derived from the degradation of proteins, which can come from a viral as well as a self-origin. The proteasome machinery is mainly involved in the degradation of proteins leading to peptides that are then translocated into the ER by means of TAP. TAP translocates peptides of 8 –16 amino acids length but if additional trimming is required in the ER before binding, an ER aminopeptidase associated with

antigen processing (ERAAP) can further trim the peptide. A peptide pool from defective ribosomal products (DRiPs) comes from 30–70% of proteins that are immediately degraded after synthesis because of defective transcription or translation (226). This pathway allows viral peptides to be presented rapidly (227). For instance, during influenza infection, infected cells can be recognized by cytotoxic lymphocytes only approximately 1.5 hours post-infection.

Peptide:MHC class I complexes leave the ER for presentation at the cell surface only when peptides bind to MHC class I molecules and the chaperones are released from the complete complex. MHC class I molecules return to the cytosol when the peptide dissociate from the complex. In other cases, some MHC class I molecules never bind peptides and they are also degraded by the ER-associated protein degradation (ERAD) system. Finally, it is important to note that there are different proteasomes that produce peptides for MHC-I presentation: the 26S proteasome which is expressed by most cells; the immunoproteasome which is expressed by several immune cells; and the thymic-specific proteasome expressed by thymic epithelial cells.

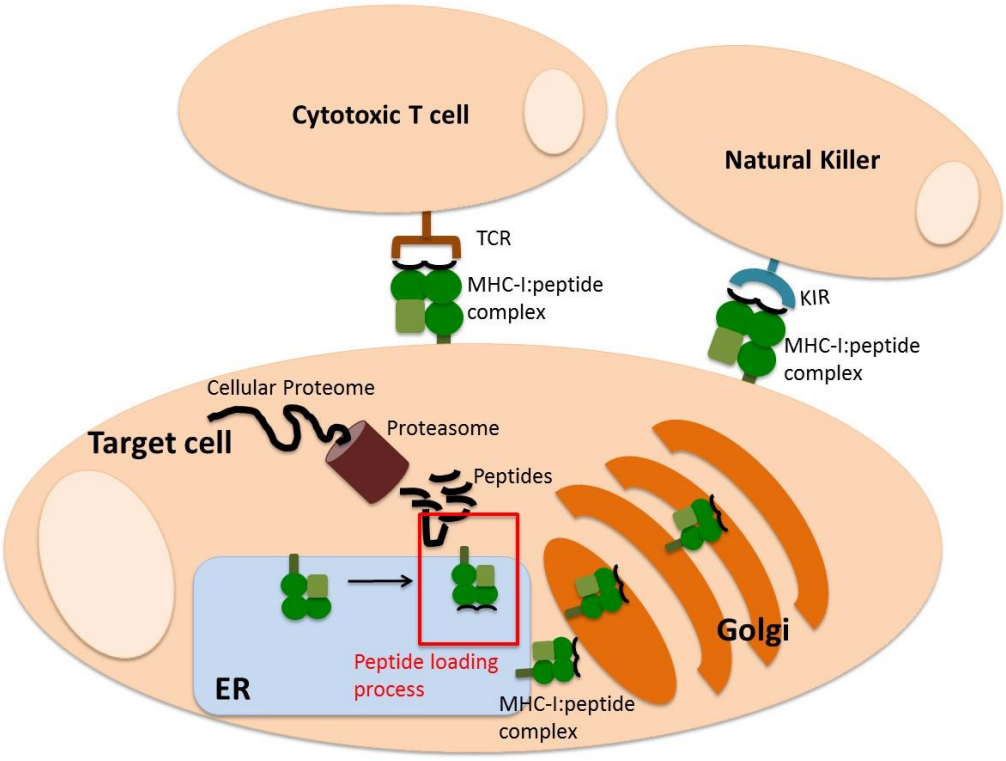

Figure 1-8: Schematic of MHC-I peptide presentation to cytotoxic lymphocytes. Proteins are degraded by the proteasome in the cytoplasm which produce peptides. Peptides then enter the ER in order to be loaded on class I molecules using the peptide loading complex. Peptides stabilise the MHC-I complexes which can then reach the cell surface and present the peptide to cytotoxic lymphocytes such as NK or T cells.

1.6.5 The role of the peptide: KIR recognition

It is clearly established now that KIR recognition is indeed influenced by the peptide bound to HLA (**Figure 1-9**). Conversely, there is no truly peptide-specific recognition, since KIR can bind to the same HLA molecule carrying different peptides (114,214,228). Exogenous peptide presentation experiments using synthetic peptides, have demonstrated that P8 in nonamers is most critical for recognition of HLA-B and HLA-C (207,214,228–231). In the 2DL2:HLA-C*03 complex, the spatial structure for the formation of the ligand-receptor complex limits the peptide repertoire to amino acids with small side chains at position P8 (207). In contrast, in the 2DL1:Cw4 interface context, P8 residue is not in contact with the KIR and the electronegative surface of 2DL1 seems to not allow peptides with acidic residues in that position (209). Reports showed that peptides can influence KIR interaction with different HLA-C molecules (207,209,232). This may contribute to the variable recognition of allotypes sharing the same nominal specificity according to the residue at position 80 and in the meantime show that peptides can be either permissive or non-permissive to KIR recognition of HLA molecule (221). Despite the lack of peptide specificity in the KIR:HLA interaction, it is still relevant to investigate how peptides can influence NK cell recognition of abnormal cells. The basal set of peptides presented by healthy cells may contain a proportion of permissive peptides regulated just above the threshold that allowed inhibition of NK cells. Therefore, we can assume that subtle changes in that pool might then trigger NK cell activation. This could be a relevant mechanism for HLA-C molecules which are expressed at a very low level compare to HLA-A and B and are therefore closer to the threshold necessary for NK-cell inhibition (233,234).

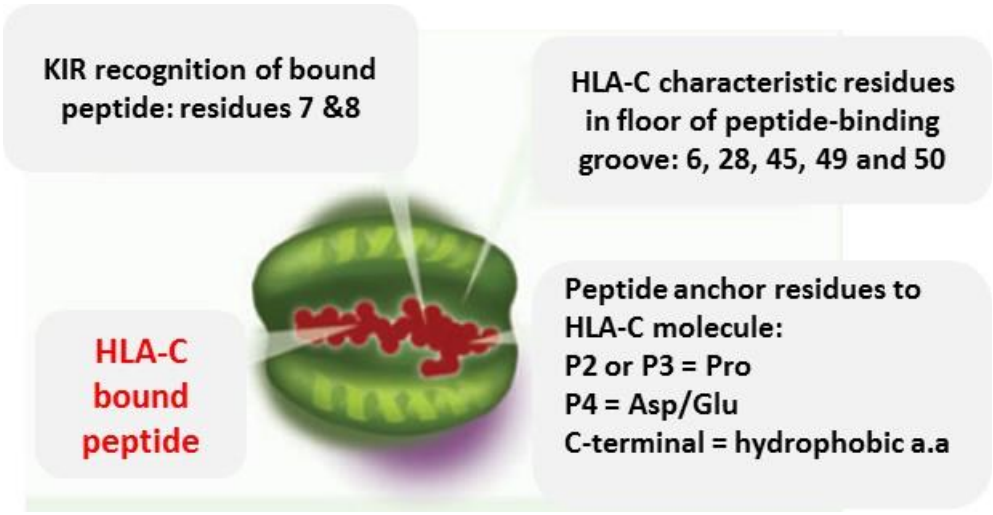

Figure 1-9: Peptide binding to HLA-C grove. Residues important for binding of peptide (red) to HLA-C molecule (green) and for killer immunoglobulin receptor (KIR) recognition are highlighted. Figure adapted from Blais *et al.*, 2011 (323)

1.6.6 NK cells inhibitory receptors and peptide selectivity

Key experiments performed in the mid-1990s have shown that the KIR are extremely sensitive to the peptide bound by MHC class I. This was originally demonstrated for KIR3DL1 and HLA-B*2705, and then for KIR2DL1 (213,214,230). Subsequent studies have extended these findings to other inhibitory KIR such as KIR2DL2, KIR2DL3, and KIR3DL2 (114,206,207,215,228,235). Furthermore, findings from these functional experiments were reinforced by co-crystal structures of KIR and their MHC class I ligands. The co-crystal of KIR2DL2 and HLA-C*03 with the GAVDPLLAL peptide demonstrated that specific residues of KIR directly contact P7 and P8 residues of the bound peptide (207). But, in the crystal structure of KIR2DL1 with HLA-Cw4, direct contacts between KIR and MHC class I peptide were not observed (209). Yet, P8 is solvent accessible and changes in this residue do lead to alterations in NK cell function, implying secondary effects of MHC class I peptide on KIR2DL1:HLA-C binding.

The second big family of NK inhibitory receptor is the C-type lectin-like receptor NKG2A which forms a heterodimer with a related family member CD94 to recognize the non-classical MHC class I molecule HLA-E (236–240). It is well established that HLA-E binds leader peptides derived from other HLA molecules (HLA-A, -B, –C as well

as -G) (241). Furthermore, studies shown that inhibitory signalling by CD94:NKG2A is also critically dependent on the type of peptide presented by HLA-E, and a hierarchy of HLA-E-bound peptides with different inhibitory properties for NKG2A-positive NK cells has been established (242,243). Co- crystallization of HLA-E and the HLA-G leader peptide VMAPRTLFL highlighted the peptide dependence of CD94:NKG2A (244,245). These studies showed that binding of CD94:NKG2A is determined by the non-signalling CD94 moiety, and also that P5, P6, and P8 residues have contacts with CD94 while only P8 interact with NKG2A. The importance of these specific residues has been confirmed in surface plasmon resonance (SPR) studies (246). Therefore, both inhibitory KIR and NKG2A are peptide selective. Furthermore, despite the rapid evolution of the KIR alongside that of classical MHC class I, this peptide dependence is a feature that has been retained across divergent KIR lineages (247).

1.6.7 Antagonism of NK cells inhibition through inhibitory receptors

In 2010, our group used a reductionist model system to investigate the functional consequences of KIR peptide selectivity. We identified peptides that bind to and stabilize the cell-surface expression of HLA-C*0102, but do not support a high affinity KIR/HLA interaction (218). We used VAPWNSLSL peptide and its derivatives. VAPWNSLSL is a peptide derived from TIMP1 (Tissue Metalloproteinase Inhibitor 1) eluted from an HLA-C*0102 transfectant of the MHC class I deficient 721.221 cell line (248). HLA-C*0102 belongs to HLA-C1 group specificity and is well known to engage with inhibitory receptors KIR2DL2 and KIR2DL3. Peptide derivatives differed only at the KIR-binding residues of P7 and P8 (218). By using KIR-fusion constructs in assay we were able to identify peptide derivatives that induced significant binding to KIR2DL2 and KIR2DL3. This allowed to established strong, weak, and null KIR binders, and this binding reactivity correlated with their ability to inhibit NK cells. To assess the effect of peptide repertoire changes on NK cell activation, the strongest inhibitory peptide VAPWNS*F*AL (VAP-FA), and the non-inhibitory peptide VAPWNS*D*AL (VAP-DA) were studied in detail. In this study, it was found that the non-inhibitory peptide VAP-DA modulated the inhibition of KIR2DL2/3-positive NK cells. This phenomenon was called “peptide antagonism” in order to indicate that peptides that have no effect on NK cell function when used in isolation, can efficiently reduce the inhibition due to inhibitory peptides. Thus, peptide antagonism can be listed among the different manner that get NK cells to be activated (**Figure 1-10**).

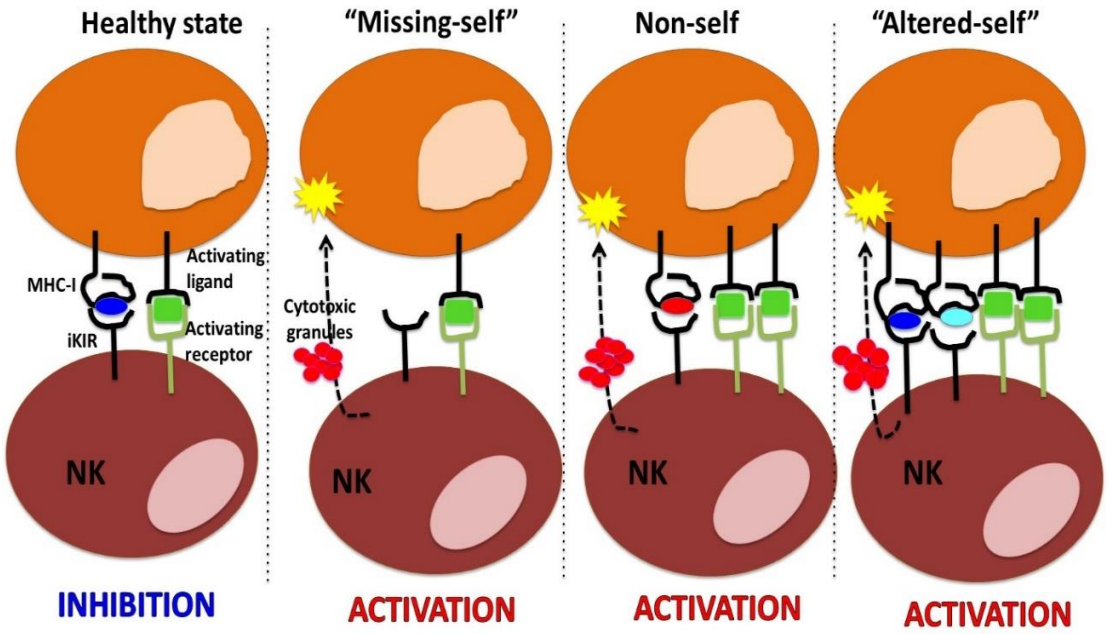

Figure 1-10: Different mechanism leading to NK cell activation. Target cells at a healthy state inhibit NK cell as the balance between inhibitory and activating signals is in favour of the inhibitory signalling. When target cells become abnormal, they trigger NK cell activation as the activating signalling overcome the inhibitory one. This happen in the following situations: down regulation of MHC-I molecule (missing self), increased expression of foreign activating ligand (non-self) or expression of endogenous altered peptide (Altered-self).

We also demonstrated that this effect is more prevalent for KIR2DL3 than for KIR2DL2, presumably due to the stronger inhibitory interaction of the later with C1 (249). Such sensitivity to peptide interactions could enable NK cells to sense subtle changes in the peptide repertoire that can occur during viral infections or during cancer. Further investigation demonstrated that the antagonist peptide VAP-DA which did not bind KIR in the fusion construct assay disrupted KIR clustering and therefore induce a release of NK cells from their inhibition (219). In principle this would be a more sensitive sensing mechanism than the large-scale alterations of HLA expression on target cells that cause self-HLA class I to be missing (250).

The precise molecular mechanism of antagonism is not clear at present but it appears that intracellular signalling events are likely to be important. Mechanisms governing the phenomenon of "peptide antagonism" require additional investigation.

Finally, all studies carried about the peptide selectivity of KIR2DL2/3 and CD94:NKG2A have so far given novel insights into the functions of these receptors. Additionally, "altered self-recognition" need to be considered as much as induced self- and missing self- recognition for NK cells expressing these receptors. Testing of these models *in vivo* is now required to establish the significance of these observations for disease.

1.6.8 Considerations for viral infections

NK cells may be sensitive to changes in the peptide repertoire presented by MHC class I as both inhibitory receptor families (KIR and CD94:NKG2A) are peptide selective receptors. Consequently, we can assume that the content of peptide presentation can be a key for changing NK cell reactivity.

The MHC class I peptidome is a complex mixture of host peptides. The MHC class I repertoire on the cell surface is the result of several processes: cellular protein degradation; access of peptides to nascent MHC class I molecules; and the multi-step process of peptide loading. Viral infection or cell transformation can alter the cell peptidome at many levels, including switching off host protein synthesis, turning on viral peptide synthesis, interfering with MHC class I peptide loading, and changing the recycling of MHC class I, leading to cell-surface down-regulation (251).

Peptides presented by MHC class I are derived from the degradation of mature proteins or "retirees." Still, recent data suggest that an extensive fraction of MHC class I peptide derives from defective protein synthesis also called "DRiPs" (defective ribosomal products) (252,253). DRiPs may additionally be derived from alternative open- reading frames, and the presentation of these "cryptic" epitopes may make understanding the peptide repertoire more difficult (254). For instance, as the HCV genome is 9.3 kb long which means that there is a substantial probability of mutation. This feature actually favours viral escape mutation, but may also lead to the synthesis of DRiPs. Favouring the DRiPs model, viral epitopes for CTL have been shown to be produced from newly synthesized peptides, rather than from mature proteins, confirming the potential of this mechanism for altering the host peptide repertoire (255). Also, the effectiveness of presentation of an epitope may depend on the source of the mRNA (viral or cellular) and there may also be compartmentalization in the subcellular localization of peptides for class I presentation (256,257).

Thus, generating a peptide repertoire in the context of a viral infection is a complex procedure that is not readily predictable. Quantitation of viral epitopes stands as a key factor, as although both NKG2A and KIR-positive NK cells are sensitive to changes in peptide repertoire, the relative level of these changes will likely be important. Additionally, it has been shown that KIR2DL2 can be a driving force on HIV sequence (258) and the selection of a strong inhibitory peptide may skew the balance in the favour of inhibition which is a means of evasion of the immune response by the virus. Nevertheless, accurate quantitation is required to determine whether this is only due to the generation of viral peptides or a combination of host and viral peptides. Indeed, the wide range of peptide specificity of KIR involves that host peptides would be as effective as viral peptides in modifying NK cell reactivity. Interference with host protein synthesis by virus infection may enhance the formation of DRiPs that could then lead to a large change in peptide repertoire content (259,260). The way a virus can affect a peptide repertoire is complex. To date, this process requires much more detailed investigation before it can be possible to draw a link with how they can impact inhibitory receptor signalling by NK cells.

A number of key points remain to be resolved with respect to peptide antagonism. At present, this phenomenon has only been demonstrated for one receptor:ligand system, and whether this extends to other KIR, or even KIR2DL2/3 with other group 1 HLA-C ligands needs to be examined. The physiological relevance of the antagonism phenomenon during viral infections, and especially how it affects the balance between inhibition and activation of an NK cell in physiological and pathological situations still needs to be understood. A study on HIV peptides has shown that the majority of peptides is non-KIR binders and could be considered antagonistic or null peptides (261). In this work of 217 HIV-derived peptides tested, 11 were identified that bound HLA-C*0102, and only one of these bound KIR2DL2.

1.7 Specificity of Activating KIR2D receptors

KIR2DS1 and -2 binding to HLA-C has been clearly shown to be weaker than to their inhibitory counterparts 2DL1/2/3 (201,221,235). Nevertheless, binding specificity of KIR2DS1 for Lys80 HLA-C and KIR2DS2 for Asn80 HLAC allotypes could be reproduced in flow cytometry assays using Fc constructs of 2DS1 and a 2DS2Y45F mutant with enhanced affinity (201,221). All 2DL1 residues that contact C*0401 are conserved in

2DS1, but the non-conservative substitution of Lys for Thr70 seems to define the lower affinity of the latter receptor (201). Similarly, only a phenylalanine to tyrosine change distinguishes the interacting loops of 2DL2 from those of 2DS2, but swapping this residue enhances the affinity of 2DS2 for HLA-CAsn80 allotypes (201,221,235).

Among the other human KIR2D with activating character, 2DS3 and 2DS5 are similar to 2DL1 at residues implicated in HLA-C recognition, whereas 2DS4 is more similar to 2DL2. The actual specificities of 2DS3 and 2DS5 have yet to be investigated, and as their extracellular domains bear one or more substitutions in the loops implicated in HLA-C recognition, reliable prediction of their specificity is not possible. As for 2DS4, some reports show recognition of certain, but not all, HLA-C allotypes, while other studies failed to demonstrate interaction with any HLA-A, -B or -C allotypes (221,232,235,262–265). Identifying peptide ligands for KIR2DS receptors still remain an actual challenge. But further investigations will help to understand the KIR:HLA interactions as well as on the specificity and function of these KIR.

1.8 NK cell activation

NK cells directly kill targeted cells through a number of mechanisms:
(i) by releasing cytoplasmic granules containing perforin and granzymes which leads to cell apoptosis by caspase-dependent and -independent pathways (**Figure 1-11**). Cytotoxic granules are orientated in the direction of the target cell soon after NK-target cell interaction. These granules are then released into the intercellular space in a calcium-dependent manner. Granzymes can penetrate into the cell via pores made into the cell membrane by perforin. These processes lead to target cell apoptosis (266,267);
(ii) by death receptor-mediated apoptosis. Some of the NK population express tumour-necrosis factor (TNF) family members, such as FasL or TNF-related apoptosis-inducing ligand (TRAIL), which can prompt tumour-cell apoptosis by interacting with their respective receptors, Fas and TRAIL receptor (TRAILR), expressed on tumour cells. TNF-α which is produced by activated NK cells can also induce tumour-cell apoptosis (268–273);
(iii) by secreting various effector molecules, such as IFN-γ, that encourage anti-tumour functions in various ways, such as restricting tumour angiogenesis and stimulating adaptive immunity. Cytokine activation or exposure to tumour cells is also associated

with nitric oxide (NO) production, where NK cells kill target cell by NO signalling (274–277);

(iv) through antibody-dependent cellular cytotoxicity (ADCC) by expressing CD16 molecule which is involved in the killing of tumour cells. The anti-tumour activity of NK cells can be further boosted by cytokines such as IL-2, IL-12, IL-18, IL-15 or those that induce IFN production (278–282).

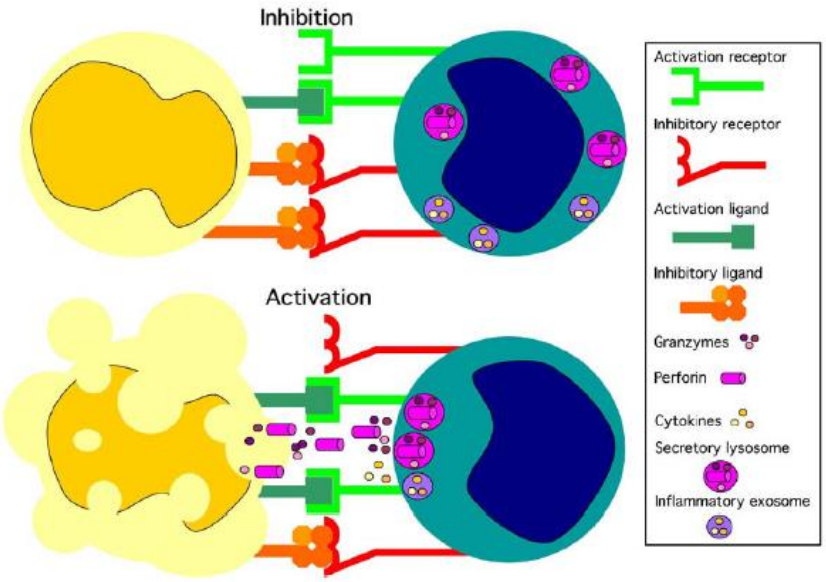

Figure 1-11: Schematic for NK cell inhibition and activation. In inhibition, both activating as well as inhibitory receptors can be ligated, but the inhibitory receptor interaction dominates. In the inhibitory interaction, the balance favours the ligation of the inhibitory receptors and the secretory lysosomes containing Perforin and Granzymes, as well as the exosomes containing cytokines remain evenly distributed within the cytoplasm. In the activating interaction, a preponderance of activating receptors dominates over inhibitory receptor signalling. This results in a reorganization of the cell surface molecules and cytoskeleton leading to the polarization of the secretory bodies to the contact site (also known as the immunological synapse). Once polarized, the granules can be released to exert their cytotoxic effect. From Orange and Ballas, (324).

1.9 Hypothesis, aims and Experimental plan

Viral infection and tumourigenesis lead to changes in MHC-I peptide repertoire and these changes affect NK cell activation. My project aims to understand how the MHC-I peptide repertoire modulation can affect NK cells function and their activation by focusing on the HLA-C ligands and especially the HLA-C group 1 (HLA-C1).

Understanding how peptide repertoire influences NK cells function may be important for interpreting their role in the immune response to viral infections and tumourigenesis. On the other hand, studying the MHC-I peptide repertoire could identify interesting peptides which modulate NK cell function and lead to peptide vaccine candidates.

1.9.1 Aim 1: Demonstrate that peptide antagonism is not restricted to only one HLA-C allele

Natural Killer (NK) cells activation requires the integration of inhibitory and activating signalling. Inhibitory signals are determined by members of the killer cell immunoglobulin-like receptor (KIR) family, which have MHC class I for ligands. Therefore down-regulation of MHC I during viral infection or tumourigenesis induces NK cells activation. However we have shown that peptide antagonism of MHC class I provides an alternative mechanism for activation for KIR2DL3-positive NK cells. This occurs when a weak KIR binding peptide disrupts the inhibitory signalling of a strong binding peptide.

Peptide antagonism has been defined only for HLA-C*0102, endogenously expressed in TAP-deficient cells, using a peptide variant of VAPWNSLSL (VAPWNS**DA**L and VAPWNS**DY**L) (218,219). To determine whether this phenomenon is a unique property of HLA-C*0102, we studied HLA-C*0304. HLA-C*0304 as HLA-C*0102 belongs to the HLA-C1and has for inhibitory receptor KIR2DL2/L3. We aimed to identify an antagonist peptide for HLA-C*0304. Our objective is to show that this peptide is a weak NK cell inhibitor and releases NK cell from inhibition despite the presence of a peptide that strongly inhibits NK cells. Additionally, we would like to demonstrate that the identified peptide disrupts the KIR receptor clustering in presence of the strong NK cell inhibitory peptide.

1.9.2 Aim 2: Design of a novel method for peptide high throughput screen

In our hands, assessment of NK cell activation using NK lines demonstrated high background when using traditional functional assays such as degranulation assay (CD107a) or LDH assay. Now, we aim to develop a novel assay, the Granzyme B assay,

which is based on the HPLC technology and which will help to evaluate a wide range of peptide in term of NK cell activation.

The principle of this experiment is to analyse the cleavage of the Caspase 3 (C3P) designed peptide in the presence of GzmB. The cleavage of this peptide only occurs when NK cells produce the Granzyme B enzyme during the co-culture between NK lines and target cells (beforehand loaded with different peptides). The objectives for this assay are: feasibility, sensitivity and usage for high-thought put experiments.

1.9.3 Aim 3: Identifying viral induced changes in peptide repertoire and assessing how this may affect NK cell reactivity

Peptidome analysis of a cell line under different conditions can inform us as to how having HLA-C or HLA-C plus a replicon system which mimics a viral infection can impact on the baseline peptidome.

HuH-7 is a well differentiated hepatocyte derived cellular carcinoma cell line that was initially taken from a liver tumour in a 57-year-old Japanese male back in 1982. These cells are an immortal cell line of epithelial-like tumorigenic cells which usually grow in 2D monolayers. They will be used as a study model to determine the impact of HLA-C expression and subsequently the combination of HLA-C and a replicating viral construct on the peptidome

2. Materials and Methods

2.1 Peptides

Synthetic peptides were purchased from Peptide Protein Research (Hampshire, UK) and GL Biochem (Shanghai, China). High Performance Liquid Chromatography (HPLC) and Mass Spectrometry (MS) confirmed their identities and the purity was greater than 95%. One peptide series had an amino acid substitution at position 8 (P8) (GAVDPLL**X**L): GAVDPLL**A**L (LA), GAVDPLL8**S**L (L8S), GAVDPLL8**Y**L (L8Y) and GAVDPLL8**V**L (L8V) and GAVDPLL8**K**L (L8K) and the second series with an amino acid substitution at position 7 (P7) (GAVDPL**X**AL): GAVDPL7**F**AL (L7F), GAVDPL7**D**AL (L7D) and GAVDPL7**R**AL (L7R).

The YYGI**ETDSG**VDDYY (Caspase 3 peptide, C3P) peptide was purchased from GL Biochem (Shanghai, China). HPLC and MS were use to confirm identity and the purity was greater than 95%.

Selected peptides from the immunopeptidome analysis [VFLPKDVAL (VFL), FLVNHDFSPL (FLV), VVPPFLQPEV (VVP), FFMPGFAPL (FFM), SSPITLQAL (SSP), YVHDAPVRSL (YVH), RLPPLLSPL (RLP), FLITQLKML (FLI) and MAPARLFAL (MAP)] were ordered from GL Biochem manufactured to the same specifications as above.

2.2 Cells lines, PBMC and cell culture

We used the following target cells, 721.221, 721.221:C*0304 and 721.221:C*0304-ICP47 which are B cell derivatives (283). 721.221:C*03-ICP47 cells are 721.221 cells transduced with HLA-C*0304 and transfected with ICP47, a Herpes simplex protein that blocks TAP.

PBMC from healthy donors were used as source of NK cells (effector cells) during degranulation assays. Cells were all cultured in R10 medium (RPMI 1640 medium supplemented with 1% penicillin/streptomycin (Invitrogen) and 10% FBS (HyClone) and for 721.221C*03-ICP47 cells the medium was supplemented with 500μg/ml of Hygromycin (HygroGold, Invivogen, Toulouse, France).

We used NKL lines that were transfected with KIR2DL2 receptor (NKL-2DL2). Cells were cultured in R10 medium supplemented with 100IU/ml of IL-2. Prior to use in Granzyme B assays, NKL-2DL2 and target cells were washed and re-suspended in AIM-V+AlbuMAX (AIM-V) (BSA) 1X medium (Gibco Life Technologies, Paisley, UK) medium before co-culture.

All cells were maintained in culture at 37°C, 5%CO_2 and in humidified atmosphere.

2.3 ICP47 gene transfection in 721.221:C*0304 cells

721.221:C*0304 cells were transfected with the pcDNA3.1(+) plasmid containing the ICP47 gene and were then selected with 500μg/ml of Hygromycin. pcDNA3.1(+) is a 5428bp plasmid which carries the CMV promoter, SV40 origin or replication and a Hygromycin resistance gene (**Figure 2-1**).

For the transfection, we used jetPrime transfection kit (Polyplus Transfection). In a six well plate, we seeded 5x10^5cell/well. Two ratios of DNA to transfection reagent were tested (2:1 and 3:1). Untransfected cells were used as negative controls. 200μl of jetPrime buffer were mixed with the DNA and incubated for 10min at room temperature. Then, the mix was added onto the cells and cells were incubated for four hours at 37°C, 5%CO_2 in a humidified atmosphere. After the incubation, the medium was changed and after 24 hours cells were put under selected using 500μg/ml of hygromycin for 30 days before obtaining outgrowth of 721.221:C*0304:ICP47 transfected cells. After cell expansion, grown cells were tested for MHC-I and HLA-C expression using the DT9 antibody. The staining procedure was the same as described below.

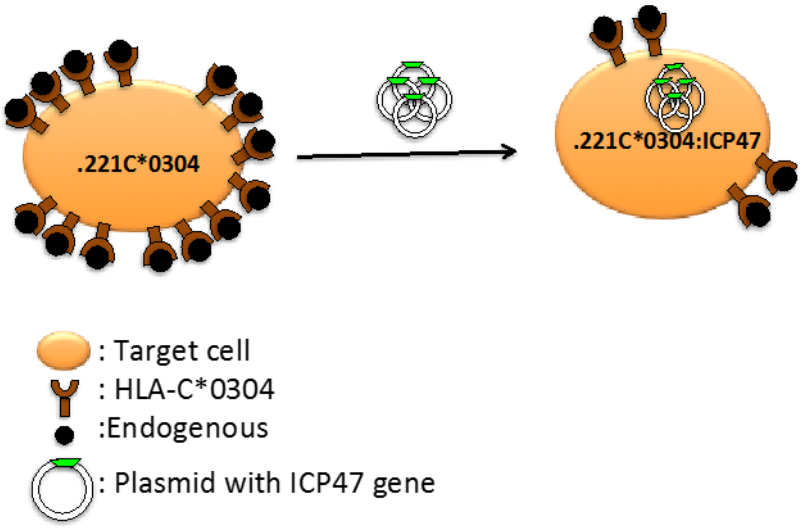

Figure 2-1: Schematic describing the establishment of the new study model for HLA-C*0304 peptides presentation. 721.221 cells expressing HLA-C*0304 were transfected with plasmid construct containing ICP47 gene. Successful transfection induces down regulation of HLA-C*0304.

2.4 Peptide stabilization assay

$2x10^5$ 721.221C*0304-ICP47 cells were incubated overnight at 26°C, 5%CO_2 and humidified atmosphere in R10 alone or in R10 medium containing 0-100µM of the specified peptide. Stabilization was assessed with DT9 antibody which is binds HLA-C but can also recognize HLA-E (284).

After incubation with the peptides, cells were washed twice with 200µl of FACS wash buffer (PBS 1X + 1%BSA + 0.1%NaN_3) and re-suspended in 100 µl of FACS blocking buffer (PBS 1X + 1%BSA + 0.1%Na_2N_3 + 10%human AB serum) then incubated for 30min at 4°C. The primary antibody, DT9, was produced and purified in-house from the hybridoma cells. DT9 was diluted at 1/10 before to be used. Then cells were incubated at 4°C with these antibodies for 1hr followed by 30min of incubation with a polyclonal goat anti-mouse antibody conjugated with PE diluted at 1/50 (Abcam, UK). All antibody incubations were done in 50µl final volume. After final washes, cells were re-suspended in fixing buffer [1x PBS+ 1%PFA (Santa Cruz, USA)] and staining analysed on a BD Accuri C6 Flow Cytometer with BD CFlow Software (BD Biosciences, Oxford, UK).

2.5 Measurement of the decay of cell surface HLA-C molecules

$6x10^5$ 721.221-ICP47 cells were incubated overnight with 100μM of peptide (P7 and P8 GAV peptide variants) in a 48 well plate in 600μl final at 26°C. The next day, aliquots of $1x10^5$ cells were harvested and washed once with 200μl of R10 then resuspended in 100μl RPMI 1640 supplemented with 10% FCS and containing 1X brefeldin A (5μg/ml) (Biolegend, San Diego, USA) at 37°C. Cells were incubated at 0, 0.5, 1, 2, 4 and 6 h with brefeldin A treatment. Surface expression of HLA-C was quantified by indirect immunofluorescent staining using a saturating concentration of the conformation-dependent HLA-C specific monoclonal antibody DT9 followed by fluorescent-labelled goat anti mouse IgG and analysis by flow cytometry. 10,000 events gated in live cells were acquired.

2.6 Degranulation Assays

PBMCs, isolated using Hypaque-Ficoll density centrifugation, were stimulated overnight with 1ng/ml recombinant HuIL-15 (R&D Systems, Abingdon, UK). The 721.221C*0304-ICP47 cells were loaded with peptide at 26°C overnight and resuspended, with the PBMCs at an E:T ratio of 5:1, in fresh R10 medium containing peptides and CD107a-eFluor 660 mAb (eBioscience, Hatfield, UK). Cells were incubated at 26°C for 4hrs, with 6 μg/ml GolgiStop (BD Biosciences, Oxford, UK) added after 1hr of the incubation. Cells were stained with CD3-PerCP (BioLegend UK, Cambridge, UK), CD56-PE, and CD158b-FITC (anti-KIR2DL2/3 and 2DS2; BD Biosciences, Oxford, UK) and then analysed as describe below.

To assess the effect of changing peptide repertoire on NK cell activation, we proceeded to degranulation assays (285). This technique is based on the detection of Lysosomal-Associated Membrane Protein-1 (LAMP-1: CD107a). Peptide loaded cells were co-cultured in presence of PBMC for 1hr in presence of anti- LAMP-1 antibody (CD107a) (**Figure 2-2**). After 1hr of incubation, Golgi Stop (Monensin) was added and cells where incubated for 4hrs hours at 26°C. After a total of 5hrs of incubation cells were washed, blocked and stained with: an anti-CD3 to identify T cells, with an anti-CD56 to identify and select NK cells ($CD3^-/CD56^+$ population) and with an anti-CD158b to distinguish KIR-positive from KIR-negative populations among NK cells. In

all our CD107a assays, we included controls for activation and inhibition by using 721.221 and 721.221:C*0304 target cells rspectively.

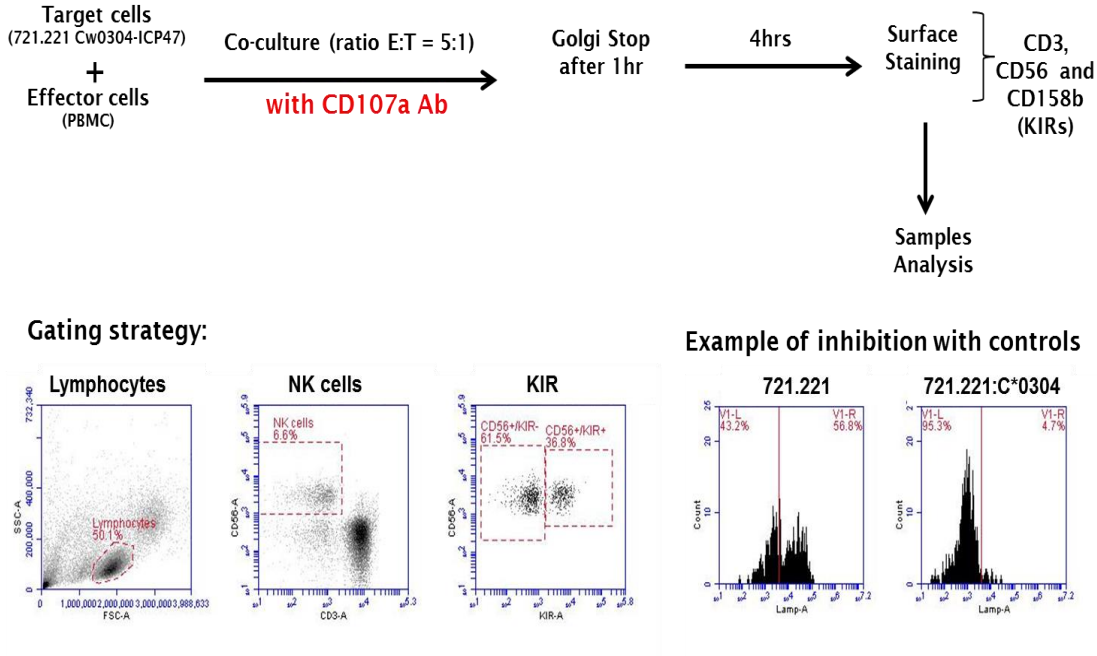

Figure 2-2: Degranulation Assay with Lamp detection and gating strategies. Target cells were cultured with PBMC and then stained for Lamp-1 but also CD3, CD56, and CD158b. Lamp expression is analyzed among CD158b positive cells. 721.221 (activation) and 721.221:C*03 (inhibition) were used as controls.

2.7 Peptide elution from MHC class I and HPLC analysis

Peptide elution from class I molecules was performed using the mild acid elution method also called "the Storkus method" (286). In order to obtain enough material and to be able to detect loaded peptide, $2.5x10^6$ 721.221C*0304-ICP47 cells were used. After an overnight of incubation with 20μM of peptide, cells were harvested and washed three times with 500μl of sterile PBS 1X (*300xg* for 5min at 4°C). Cell pellets were re-suspended in approximately 250μl citrate-phosphate buffer (0.131M Citric Acid + 0.066M Sodium Phosphate Dibasic, pH 3.3), gently mixed and incubated for 1min at room temperature, before being centrifuged at maximum speed of 16,000g to eliminate any trace of cells debris in the supernatants. The clear supernatant was retained, diluted 1:2 with the loading buffer and run through the uHPLC. Excess supernatant was stored at -80°C for future analysis.

Eluted peptides were separated by a one dimension set up Reversed Phase-HPLC (RP-HPLC) on a Dionex system equipped (Hemel Hempstead, UK) with a reversed phase C18 trapping and analytical columns using an acetonitrile gradient in 0.05% TFA. Loading buffer (98%H_2O + 2% ACN + 0.05% TFA), solvent A (100%H_2O + 0.05% TFA) and solvent B (20%H_2O + 80% ACN + 0.05% TFA) were used for the UHPLC analysis and peptides detection. H_2O, Acetonitrile (ACN) and Trifluoroacetic acid (TFA) were all HPLC grade and from Fisher Scientific (Loughborough, UK).

Eluates, diluted in loading buffer, were chromatographically analysed on a Dionex UltiMate 3000 RSLC nanoflow LC system equipped with a Dionex Acclaim PepMap 100 C18 (5mm length x 300μm internal diameter; 5μm particle size, 100Å) trap column to concentrate analytes, and a Dionex Acclaim PepMap RSLC C18 (15cm length x 75μm internal diameter; 2μm particle size, 100Å) analytical column for sample separation.

6.6μl of each sample diluted at 1/2 in the loading buffer and 1-5μl of standard (0.2μM-1μM) diluted on in the loading buffer, were loaded by injection loop (20μl sample loop) onto the trap column at a 350nl/min flow rate. After trapping the flow was redirected by means of a 10-port switching valve and the flow-through from the trap column directed onto the analytical column at 15μl/min.

The columns were subjected to a gradient of 96:4 – 40:60 (solvent A:solvent B for 30mins and from 40:60 – 10:90 A:B (5mins) at 15μl/min. This was then held for 5mins before a reverse gradient to 96:4 A:B (10min) was applied. Columns were then re-equilibrated in (Solvent A) for 15mins (total run time of 53 minutes). Peptides were detected by a UV detector set at a wavelength of 214nm.

2.8 PBMC DNA extraction

PBMC were thawed, washed with PBS 1X and counted (10^7 cells were used for the DNA extraction). Cells were resuspended in 200ml of 1X PBS 20μl of Proteinase K (Promega, UK) were aliquoted into the bottom of a 1.5 ml microcentrifuge tube (eppendorf tube) and 200μl of cell suspension were added to the tubes followed by an addition of 200μl of buffer AL and briefly vortexed. Samples were incubated for 10 minutes at 56°C. After a brief centrifugation, 200μl of 100% ethanol were added in the tubes followed by a brief vortex and spun again.

The mixture was carefully applied to the QIAamp Mini spin column (in a 2 ml collection tube) without wetting the rim. Tubes were centrifuge at 6000x*g* (8000 rpm)

for 1 minute. The QIAamp Mini spin columns were placed in a clean 2 ml collection tube and the tubes containing the filtrate were discarded. Carefully, 500μl of Buffer AW1 were added without wetting the rim and tubes were centrifuge at 6000x*g* (8000 rpm) for 1 minute. The QIAamp Mini spin columns were placed in a clean 2 ml collection tubes and the collection tubes containing the filtrate were discarded.
Then, 500μl of Buffer AW2 were added without wetting the rim and tubes were centrifuge at maximum speed (20 000x*g,* 14000 rpm) for 3 minutes followed by a second centrifugation at full speed for 1 minute.
The QIAamp Mini spin columns were placed in a clean 1.5 ml microcentrifuge tube, and the collection tubes containing the filtrate were discarded. 200 μl of Buffer AE were added and tubes were incubated at room temperature for 1 minute, and then centrifuge at 6000x*g* (8000 rpm) for 1 minute. A second elution step with a further 200μl Buffer AE was preceded in order to increase the yields by up to 15%. DNA was quantified using NanoDrop and then stored at -20°C for long term storage.

2.9 KIR genotyping

DNA extraction for PCR typing was prepared from PBMCs (n=8 donors) using the QIAamp Blood Kit according to manufacturer's instructions (QIAGEN, UK) as described above. KIR genotyping was performed by sequence specific primer PCR (PCR-SSP) (287) using the Tetrad 2 Engine Cycler (MJ Research, USA) as a thermocycler.
For KIR2DL2 the primers were, forward: 5'-ACTTCCTTCTGCACAGAGAA-3' (Fa538) and reverse: 5'-GCCCTGCAGAGAACCTACA-3' (Rt854), amplifying a 1868bp fragment. For KIR2DL3 the primers were, forward 5'-ACAGAGAAGGGAAGTTTAAG-3' (Fg550) and reverse: 5'- CCCTGCAGAGAACCTACG-3' (Rcon854), amplifying a 1858bp fragment. For KIR2DS2 the primers were, forward 5'- TGCACAGAGAGGGGAAGTA-3' (Fa546) and reverse: 5'-CACGCTCTCTCCTGCCAA-3' (Rt767), amplifying a 1775bp fragment. The GH1 gene was used as a internal control using the following primers: forward 5'- CTTCCCAACCATTCCCTTA-3' and reverse: 5'-CGGATTTCTGTTGTGTTTC-3' which gave a 424bp product (287). Amplification was performed in a 25 μl reaction, using the primers at a concentration of 1μM (specific) or 0.5μM (internal positive control), dNTP mix (Promega, UK) at a concentration of 200 μM, 5U/ml Go Taq Hot Start Polymerase (Promega, UK) and 200ng DNA under the following conditions: initial denaturation at 95°C for 2 min; followed by 10 cycles at 94°C for 20s, 65°C for 10s and 72°C for 1min30s; then 20 cycles at 94°C for 20s, 61°C for 20s and 72°C for

1min30s; and then a final extension at 72˚C for 5 min. Each experiment also included a negative control (H_2O). Amplification products were analysed on a 1.2% Agarose gel using a Nancy-520 DNA gel stain (Sigma Aldrich, UK).

2.10 Confocal microscopy

721.221:C*0403-ICP47 Cells were cultured with 100μM final concentration of peptide overnight at 26°C, and then incubated at a 1:1 ratio with NKL-2DL3 GFP for 10 min at 37°C. Conjugates were fixed 2% PFA for 30 min at 37°C and imaged by resonance scanning confocal microscopy with laser lines of 488nm and a 63x1.2 numerical aperture glycerol immersion objective (TCS SP8, Leica). Images were acquired with Leica Application Suite X (Leica) and analyzed with ImageJ (National Institutes of Health) software. The increase in fluorescence intensity at the immune synapse was calculated as a ratio of the average fluorescence intensity along NKL-2DL3 GFP - 721.221:C*0403-ICP47 interface, compared with the average fluorescence intensity along the NKL-2DL3 GFP plasma membrane not in contact with another cell, with both values corrected for background fluorescence, as measured within an empty region of the image.

2.11 KIR binding assay

2.11.1 Affinity of P7 peptide variants for KIR

$2x10^5$ 721.221:C*0403-ICP47 cells were incubated in the presence or absence of 100μM peptide overnight at 26°C. rhKIR2DL2-Fc chimera (R&D systems, Abingdon, UK) was conjugated with protein A Alexa Fluor 488 (Invitrogen, Paisley, UK) at a ratio of 12:1 KIR: protein A (12 KIR: 1 protein A) overnight at 4°C. The following day peptide loaded cells were stained with 50μg/ml of KIR chimera for 1hr at room temperature. Samples were washed twice with PBS and bound fusion proteins detected by flow cytometry, fluorescence of 10,000 cells gated by forward and side scatter was analyzed using BD Accuri C6 Flow Cytometer with BD CFlow Software (BD Biosciences, Oxford, UK).

2.11.2 KIR binding and peptide titration

$2x10^5$ 721.221C*0304-ICP47 cells were incubated overnight at 26°C, 5%CO_2 and humidified atmosphere in R10 alone or in R10 medium containing 0-100μM of L7R, L7F and L7D peptides. Staining was done as described above (**section 1.11.1**).

2.11.3 KIR binding, HLA-C and Degranulation Assay

$5x10^5$ 721.221:C*0403-ICP47 cells were incubated in the presence of L7R peptide from 0 to 100μM or with a combination of L7D and L7R overnight at 26°C. rhKIR2DL2-Fc chimera (R&D systems, Abingdon, UK) was conjugated with protein A Alexa Fluor 488 (Invitrogen, Paisley, UK) at a molecular ratio of 12:1 KIR: protein A (12 KIR: 1 protein A) overnight at 4°C. The following day, some of the peptide loaded cells were used in degranulation assay and some were stained with 50μg/ml of KIR-protein A^{A488} for 1hr at room temperature. KIR stained samples were washed twice with PBS and bound fusion proteins detected by flow cytometry. In parallel, target cells were also stained with DT9 to ensure HLA-C stabilization at the cell surface. Fluorescence of 10,000 cells gated by forward and side scatter was analyzed using BD Accuri C6 Flow Cytometer with BD CFlow Software for both KIR2DL2 and DT9 stainings (BD Biosciences, Oxford, UK).

2.12 Minigenes for endogenous peptide presentation

2.12.1 Minigene preparation

For these experiments, we used minigene constructs which consists of the endoplasmic reticulum signal sequence followed by the peptide sequence of interest and a stop codon at the end, as described in **Figure 2-3**. The ER signal sequence (MRYMILGLLALAAVCSA) is derived from the human adenovirus C serotype 6 virus

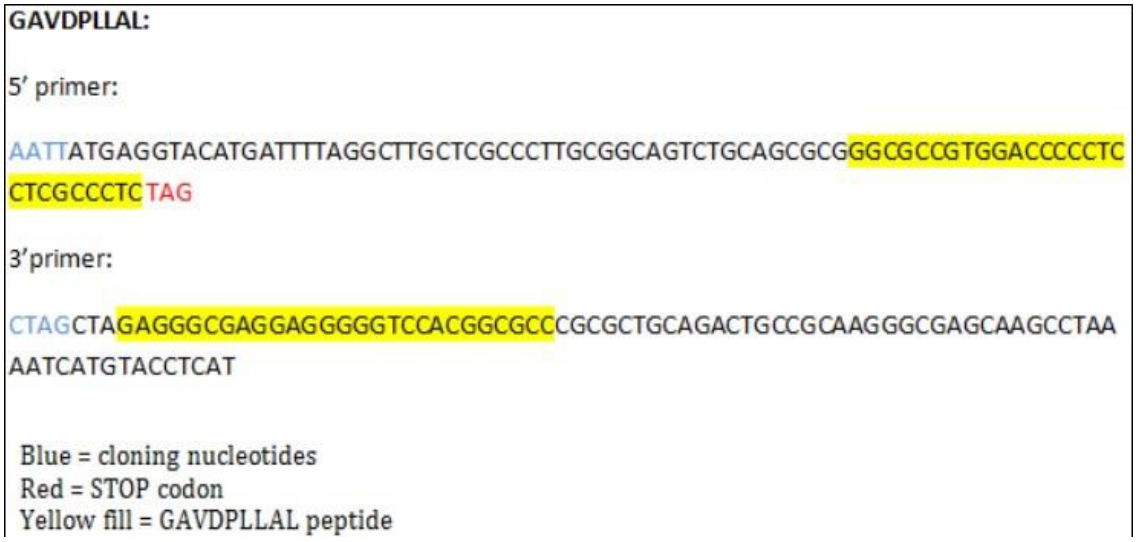

Figure 2-3: **Primers design**. 5' primer and 3' primer were designed to contain a cloning nucleotide in bleu, the peptide of interest sequence in yellow and a stop codon in red. These two primers will then constitute the minigene to insert in the plasmid vector.

Primers were designed by Dannielle Wellington (University of Southampton, UK) and dissolved at 1mM in H_2O. These were phosphorylated using T4 phospho-kinase in the following way. T4 Polynucleotide Kinase (New England Biolabs) and 10ug primer (10ul of 1mM stock) were diluted in dH_2O in T4 buffer (New England Biolabs, Hitchin, UK). Mixes were incubated for 1 hour at 37°C. Then 5' and 3' primers were added and floated on top of boiling water in a beaker until the water cooled (~3-4 hours).
DNA vector pcDNA6 (Life Technologies, Paisley, UK) was double digested with EcoRI (New England Biolabs, Hitchin, UK) and HindIII (New England Biolabs, Hitchin, UK) followed by gel extraction and purification. Minigenes were ligated into pcDNA6 overnight afterwards transformed into competent bacteria One Shot TOP10 Chemically Competent *E.Coli* (Thermo Fisher, Loughborough, UK).

2.12.2 Minigenes transformation into competent cells

S.O.C (Super Optimal broth with Catabolite repression) solution was pre-warmed at 37°C degree then aliquoted out, 250ul for each reaction. Aliquot of 50µl of chemically competent *E.coli* bacteria (Thermo Fischer, Loughborough, UK) were thawed on ice. Then ligation reaction mixture (5µl) was put straight into the competent cells by gentle tapping. Vials were placed on ice for 30 minutes, then placed 30 seconds in the water bath at 42°C for to Heat shock the *E.coli*. vials were placed back on ice for 2 minutes.

Pre-warmed S.O.C solution was added into the *E.Coli* containing vials then the latter were placed on the heat block at 37°C for 1 hour under shaking (250 rpm). 50µl of the transformed mixture were plated onto LB agar under ampicillin selection. Agar plates were placed at 37°C degree overnight. The next day, colonies were picked for further colony PCR and growth in liquid agar the next day.

2.12.3 Extraction of plasmids containing minigenes

Plasmids were extracted by Maxiprep (QIAGEN, UK). Bacterial cultures were harvested by centrifugation at 6000xg (8000rpm) for 15 minutes at 4°C. The supernatants were decanted and the entire remaining medium was removed. Bacteria were re-suspended in Buffer P1 (50mM Tris-Cl, pH 8, 10mM EDTA, 100µg/ml RNase A) then Buffer P2 was added (200mM NaOH, 1%SDS) and incubated at RT for 5min (until the suspension turned bleu). During this incubation, the QIAfilter cartridge were prepared. After incubation, Buffer P3 (3M Potassium Acetate, pH 5.5) was added and the suspension became colourless. The lysates were then poured into the filter cartridge and followed by 10 min of incubation at RT. In the meantime, QIAGEN-tip column were equilibrated by applying buffer QBT (750mM NaCl, 50mM MOPS, pH 7). Lysates were then filtered into the equilibrated column. Columns were washed twice with Buffer QC (1M NaCl, 50mM MOPS, pH 7) then the DNA were eluted using Buffer QF (1.25M NaCl, 50mM Tris-Cl, pH 8.5). DNA were precipitated by adding 70% ethanol and by spinning down at 15000xg for 10min. The supernatants were final carefully decanted and the pellets were air-dry in order to avoid DNA degradation. Finally, the DNA were dissolved in the TE buffer, pH 8 (10MmM Tris-Cl, pH 8, 1mM EDTA). DNA was quantified using the NanoDrop. Purified plasmids were stored at -20°C for long-term storage.

2.13 Transfection of minigenes constructs into 721.221:C*0304 cells by electroporation

Cells were counted and concentrated at $2x10^6$ cells/ml then $2x10^6$ cells were aliquoted for each transfection. After spinning cell suspension, supernatant were completely removed from each aliquot and cells were resuspended in 100µl Solution V mixed with Nucleofector Solution.

7.5µg of total DNA were used (5µg plasmid DNA containing L7R, L7D minigenes mixed with 2.5µg plasmid DNA containing GFP tag). Cells were added to the cuvette. Afterwards, the cuvette was put in the electroporator machine (Amaxa, Lonza) and program A-24 was run. Electroporated cells were removed quickly from cuvette and add to 1ml pre-warmed media in a 12-well dish. This procedure was repeated for each transfection (**Figure 2-4**).

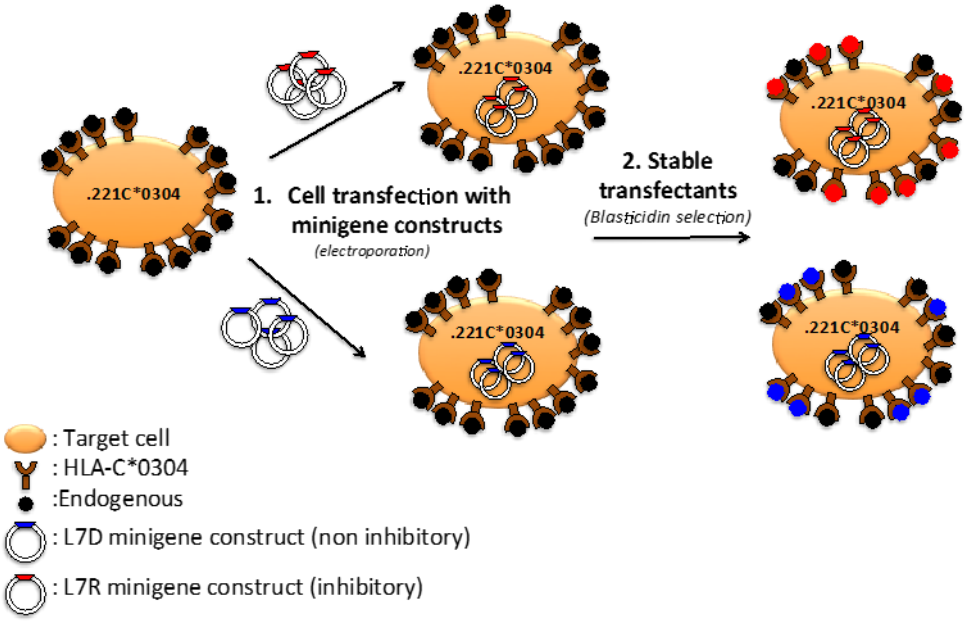

Figure 2-4: Schematic describing the minigene strategy. 721.221 cells expressing HLA-C*0304 were electroporated with one of two different minigene constructs (step 1): one construct encodes for the inhibitory peptide (in red) and the second construct encode for the non-inhibitory peptide (bleu). 24-48hrs after electroporation, cells were put under Blasticidin selection (10µg/ml) in order to generate stable transfected cells which will present the peptide on their surface (step 2).

2.14 Cytotoxicity Assay using Propidium iodide (PI)

NKL-2DL3 cells expressing GFP (effectors) and minigene-transfected 721.221:C*0304 cells (targets) were counted and then seeded in a 96 U-bottom well plate in 100μl final volume. Effector and target cells were co-incubated for 5hrs at 37°C, 5%CO_2 and at different ratios (10:1, 5:1, 2:1 and 1:1). After incubation 5ml of Propidium Iodide (Pi, eBioscience, Hatfield, UK) was added and cells were incubated for 30 minutes at 4°C and then samples were analysed and 10,000 events of GFP-negative cells were acquired.

2.15 Granzyme B Assay optimisation

Previous work in our group had shown that functional assays such as Lactate Dehydrogenase (LDH) or CD107a did not permit the detection of NK cell activation using peptide pulsed targets and NKL lines at 26°C. We therefore wished to develop a novel assay that was efficient and sensitive. Furthermore, we anticipated that such an assay could be used to screen high number of peptide variants in order to uncover peptides variants that can potentially activate NK cells either through activating or inhibitory receptors.

2.15.1 Determining the optimal wavelength for Caspase 3 Peptide (C3P) detection

We designed a Caspase 3 Peptide (C3P): YYGI**ETDSG**VDDYY (GL Biochem Ltd, Shanghai, China) which carries a Granzyme B cleavage site (in bold) and surrounded with Tyrosines (Y) for a specific detection through the UHPLC. Serial quantities of the peptide (from 3.9 to 2000μM) were tested using four different wavelengths (270, 275, 280 and 295nm). Analysis was performed in a one dimensional set up with the same nano-uHPLC system as described above.

C3P stock was first diluted in AIM-V medium then in the loading buffer (98%H_2O + 2% ACN + 0.05% TFA) at final concentrations of 3.9μM and 125μM. 1, 2, 3, 4 and 5μl of each sample (3.9-2000μM) was loaded by injection loop (20μl sample loop) onto the trap column at a 350nl/min flow rate. After trapping the flow was redirected by means of a 10-port switching valve and the flow-through from the trap column directed onto

the analytical column at 15μl/min. The columns were subjected to a gradient of 96:4 – 40:60 solvent A:solvent B for 23mins and from 40:60 – 10:90 A:B (5mins) at 15μl/min. This was then held for 5mins before a reverse gradient to 96:4 A:B (10min) was applied. Columns were then re-equilibrated in (A) for 15mins (total run time of 43 minutes).

2.15.2 Determining the optimal conditions for Caspase 3 Peptide digestion by the recombinant human Granzyme B (rhGzmB)

200-800μM final concentration of C3P was diluted in AIM-V medium in a final volume of 50 or 200μl in presence of various concentration of recombinant Human Granzyme B enzyme (rhGzmB) from Enzo Life Sciences (Exeter, UK). We initially tested ten different concentrations from 5U/μl to $9.7x10^{-11}$U/μl and then eight further concentrations from 10U/μl to 0.078U/μl. C3P and enzyme were incubated at 37˚C, 5%CO_2 and humidified atmosphere for 1hr, 4hrs, 8hrs, 24hrs, 48hrs and 72hrs for the preliminary experiments. The final experiment required incubation of C3P and enzyme for 24hs, 48hrs, 72hrs and 95hrs.
Samples were diluted at 1/4 in the loading buffer prior injection. UHPLC configurations were the same as described in section 8.1. The program only contained a single wavelength of 275nm and 6μl of diluted sample was injected into the system for analysis. The auto-sampler was kept at 4˚C in order to prevent enzyme activity as well as further C3P degradation.

2.15.3 Testing the cell culture supernatants

NKL-2DL2 and 721.221 or 721.221:C*0304 cells were washed in AIM-V medium, counted and re-suspended in AIM-V medium at $4x10^6$ cells/ml. $5x10^5$ NKL-2DL2 cells were co-cultured with or without $5x10^5$ of 721.221 or 721.221:C*0304 in the absence of IL-2 in 250μl final volume. Cells were incubated for 5hrs at 26˚C, 5%CO_2. After co-culture, cell suspensions were harvested and centrifuged at low speed (200Xg) for 5min at room temperature in order to remove dead cells and avoid contamination with intracellular proteins and cell debris. Supernatants were harvested (~200μl) and centrifuged again at higher speed (800Xg) to avoid cell debris contamination in samples. 2μl of C3P and 150μl of supernatant were incubated for 24hs, 48hrs, 72hrs

and 95hrs at 37˚C, 5%CO_2 and humidified atmosphere. Samples were diluted at 1/4 in the loading buffer prior injection for analysis. UHPLC configurations were the same as described in section 8.1. The program only contained a single wavelength of 275nm and 6µl of diluted sample were injected into the system for analysis. The auto-sampler was kept at 4˚C in order to prevent enzyme activity as well as further C3P degradation.

2.16 Testing cell culture supernatants by comparing HPLC GzmB assay to Granzyme B activity-assay (QuickZyme Biosciences)

721.221:C*0403-ICP47 Cells were cultured with 100µM final concentration of peptide overnight at 26°C, then incubated at a E:T 2:1 ratio with NKL-2DL2 for 5hrs at 26°C. After incubation, supernatants were harvested as described (**in section 1.15.3**). Half was reserved for HPLC analysis and the other half underwent GzmB activity assay using Quizyme Bioscience kit.

At the beginning of the assay, the microtiter plate (Costar EIA/RIA Stripplate flat bottom and High binding type I) was coated with 2 µg/ml anti-Granzyme B diluted in coating solution (NaAc buffer pH 5.5) then incubated overnight at 4°C in a humidified chamber. The next day, wells were emptied and washed four times with PBS/Tween (0.01 M Phosphate buffer pH 7.5 containing 0.05% (v/v) Tween 20). A Granzyme B standard (stock at 1µg/ml) curve was prepared using the following concentration: 1.25 - 0.625 0.31 - 0.15 - 0.08 - 0.04 – 0.02 – 0.01 – 0.05 - 0ng/ml. Standards and samples were diluted in Granzyme B assay buffer (0.2 M HEPES/ NaOH pH 7.5, 1 mM EDTA 0.05% v/v Triton-X-100) and 100µl were distributed per well. The plate was incubated for 1hr at room temperature with shaking. After incubation, wells were emptied and washed four times with PBS/Tween. Then 100µl of the detection reagent (detection enzyme diluted in Granzyme B assay buffer mixed with chromogenic substrate) were added to each well. The plate was shaken for 20 seconds and absorbance was measured at 405nm at t = 0. Then the plate was covered and incubated at 37°C, 5% CO_2 in a humidified atmosphere. After 4hrs and the following day, a graph of the absorbance at 405nm versus the Granzyme B concentration was made using of values acquired at 4 (suitable for a high standard line) and 24 hours

(suitable for a low standard line). A best-fit linearized curve through the points on the graph was drew. Using this standard curve, the A405 values of the test samples were calculated to ng/ml Granzyme B and from the sample volume used in the assay we determined the Granzyme B concentrations.

HPLC analysis was carried out the same way as described **in section 1.15.3.** Results obtained from both methods were compared.

2.17 Cells culture of Huh7 cell lines and bioinformatics analysis of Huh7 cell lines immunopeptidome

2.17.1 Cells preparation and peptide elution

$3x10^9$ cells of each cell lines were grown with selection with Puromycin (Sigma-Aldrich, Dorset, UK) and/or Blasicidin (Invitrogen, Paisley, UK) and cells were harvested using Versene (Invitrogen, Paisley, UK) and Trypsine (Invitrogen, Paisley, UK) before MHC-I peptide elution. Before and during expansion, cell lines were tested for HLA-C*0102 expression by Flow Cytometry by detecting GFP signal and for Replicon expression processed by Dr Mumtaz Naiyer (University of Southampton, UK) by measuring the luciferase activity (Promega, UK).

2.17.2 Bioinformatic tools

Several Bioinformatic programs and tools used were available online. NetMHCpan 3.0 is a server that predicts binding of peptides to any MHC molecule of known sequence using artificial neural networks (ANNs). The method is trained on more than 180,000 quantitative binding data covering 172 MHC molecules from human (HLA-A, B, C, E), mouse (H-2) as well as cattle (BoLA), primates (Patr, Mamu, Gogo) and swine (SLA). The Gibbs clustering algorithm attempts to group the input peptide data into a number of clusters where each cluster identify the optimal local sequence alignment based on the optimization of the fitness of the system in terms of Kullback-Leibler distance (KLD) sum of the alignments (288). The KLD allows measuring the information gain of an observed amino acid distribution compared to a back- ground distribution (the frequency of each amino acid in random protein sequences). A given

alignment can be represented by a log- odds (LO) weight matrix, which summarizes the amino acid preferences for each column of the alignment. In our analysis, we graphically represent LO matrices using the sequence logo visualization tool Seq2Logo (289). Furthermore, we used the Clustal Omega tool which is a multiple sequence alignment program which generate alignments between two or more sequences. And finally, UnitProt (Universal Protein resource) which is a freely accessible database of protein sequence and functional information of where many entries are being derived from genome sequencing projects. This database contains a large amount of information about the biological function of proteins derived from the research literature.

HeatMap is a graphical illustration of data that represent individual values contained in a matrix where they are represented as colours. Heat maps where produced by Dr Akul Singhania (Southampton University, UK)

Expression:
Heatmap depicts the expression levels of 3,099 peptides obtained from identified and quantified across the three samples group using Data Independent Acquisition (DIA) method. Hierarchical clustering was performed using Pearson correlation metric to calculate distances and clustered using Ward's linkage. Expression values of peptides are depicted as log2 and scaled across each row to indicate the number of standard deviations above (red) or below (blue) the mean, denoted as row Z-score.
Fold change:
Fold changes were calculated comparing difference of expression between Huh7 and Huh7C*0102, between Huh7 and Rep:C*0102 and between Huh7C*0102 and Rep:C*0102. Hierarchical clustering was performed using the Pearson correlation metric to calculate distances and clustered using Ward's linkage.

2.18 HLA-C*0102 peptide stabilisation and BFA decay Assays

$2x10^5$ 721.147 cells were incubated overnight at 26°C, 5%CO_2 and humidified atmosphere in R10 alone or in R10 medium containing 0-100μM of the specified peptide. Stabilization was assessed with DT9 antibody which is specific to HLA-C but can also recognize HLA-E. Stabilization assay was carried as described above (**Section 2.4**).

$6x10^5$ 721.221-ICP47 cells were pulsed with 100μM of peptide in a 48 well plate, 600μl final volume and incubate at 26°C. The following day, the assay was carried out as described above (**Section 2.5)**.

2.19 Total HLA I, HLA-C and HLA-A*11 staining

Huh7, Huh7:C*0102 and Rep:C*0102 cells were harvested and stained for total HLA I (W6.32), HLA-C (DT9) and HLA-A*11 (4i93). Cells were incubated at 4°C with these antibodies for 1hr followed by 30min of incubation with a polyclonal goat anti-mouse antibody conjugated with PE diluted at 1/6000 (Abcam, UK).

2.20 Co-culture with Huh7 cells and its derivatives

$60x10^4$ Huh7 cells and its derivatives were trypsinised and plated 24hrs before the co-culture with primary NK cells. Degranulation assays were conducted as described above (**section 2.6**).

2.21 Statistical Analysis

All graphs and statistical analyses were performed using GraphPad Prism, version 6 (GraphPad Software). The one-way analysis of variance (ANOVA) is used to establish whether there are significant differences between the means of two or more independent (unrelated) groups. The two-way ANOVA compares the mean differences between groups that have been split on two independent variables (called factors). The primary use of a two-way ANOVA is to appreciate if there is an interaction between the two independent variables on the dependent variable. The interaction term in a two-way ANOVA informs you whether the effect of one of your independent variables on the dependent variable is the same for all values of your other independent variable (and vice versa).

Student's t test was used to assess whether the means of two groups are statistically different from each other. This analysis is appropriate whenever you want to compare the means of two groups.

3. Peptide antagonism of NK cells by HLA-C*0304 binding peptide

3.1 A new model for HLA-C peptide antagonism

To study peptide antagonism at HLA-C*0304, I selected a primary series of HLA-C*0304 endogenous peptide GAVDPLL**A**L (LA) from the importin subunit apha-1 and its derivatives carrying a modified amino acid at position 8 (P8): [GAVDPLL8**S**L (L8S) GAVDPLL8**Y**L (L8Y), GAVDPLL8**K**L (L8K), GAVDPLL8**V**L (L8V) and GAVDPLL8**Y**L (L8Y)]. These had affinities for KIR2DL2 that had been previously measured by Boyington and colleagues (207) (**Table 3-1**).

Peptide Variants	Kd (μM)
GAVDPLLAL (LA)	9.5
GAVDPLL8SL (L8S)	42.3
GAVDPLL8VL (L8V)	525
GAVDPLL8YL (L8Y)	>600
GAVDPLL8KL (L8K)	>600

Table 3-1: Peptide variants induce differential binding of KIR2DL2 to HLA-C*03. Measurement of the KIR2DL2 affintiiy for the peptide:HLA-C*0304 complex by surface plasmon resononace, from Boyington et al (207).

3.2 ICP47 induces down regulation of HLA-C*0304 to generate a target cell that can be exogenously loaded with peptide

Exogenous peptide presentation uses TAP (Transporter associated with Antigen Processing) deficient cells. In order to bypass and avoid endogenous peptide presentation I generated a cell line that could be exogenously loaded with peptide. For this I used a TAP sufficient cell line which expressed HLA-C*0304 and blocked TAP function by expressing ICP47 protein. ICP47 (Infected Cell Protein 47) is a protein expressed by Herpes simplex virus that induces down regulation of the MHC-I expression. This strategy prevents transportation of antigenic peptides into the endoplasmic reticulum (290,291). As endogenous peptides cannot be loaded onto

MHC-I, the MHC class I molecule is only present on the cell surface at low levels (292), but its expression can be stabilised by addition of exogenous peptide.

C*0304 cells were transfected with ICP47 gene (a gift from Dr Edd James). Cells that were successfully transfected with the plasmid survived in 500μg/ml of Hygromycin selection. After selection, cells were tested for HLA-C expression using DT9 (**Figure 3-1**). Down-regulation of HLA-C (DT9) showed that ICP47 transfection had been successful (**Figure 3-1 B**). Compared to C*0304 cells (MFI=9,103.95), C*0304-ICP47 cells (MFI=3,285.19) showed a decrease in expression after transfection implying that the transfection has been successful. I thus obtained a new cell line expression HLA-C*0304 and used this for exogenous peptide loading.

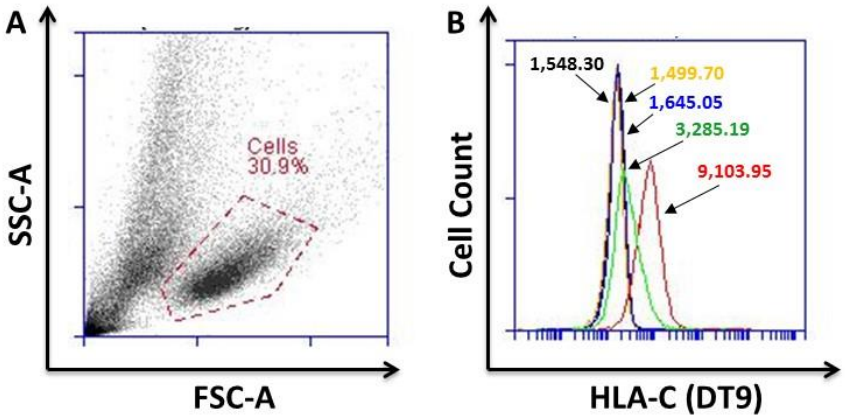

Figure 3-1: HLA-C (DT9) expression before and after transfection with ICP47 plasmid. (A) Cells were identified on the dot plot according to their size (FSC-A) and granulation (SSC-A). (B) Histogram plots showing DT9 staining on 721.221 (blue), C*0304 (red) and C*0304-ICP47 (green) with Unstained (black) as controls. Numbers in bracket correspond to the MFIs.

3.3 Peptides with position 8 (P8) variation stabilize HLA-C expression on the cell surface

Before using these peptides variants in functional assays, I tested their ability to stabilize HLA-C expression at the cell surface. Increasing concentrations of peptides from 0 to 100μM were loaded onto C*0304-ICP47 cells. Peptide loaded cells were stained for HLA-C (DT9).

An increase in HLA-C expression correlated with increasing peptide concentration (**Figure 3-2**). The level of expression reached a plateau at around 25μM peptide. I

concluded that this series of peptides stabilised HLA-C*0304 at 25μM of peptide concentration and so this concentration was used for functional assays. All peptides variants stabilised HLA-C to similar level.

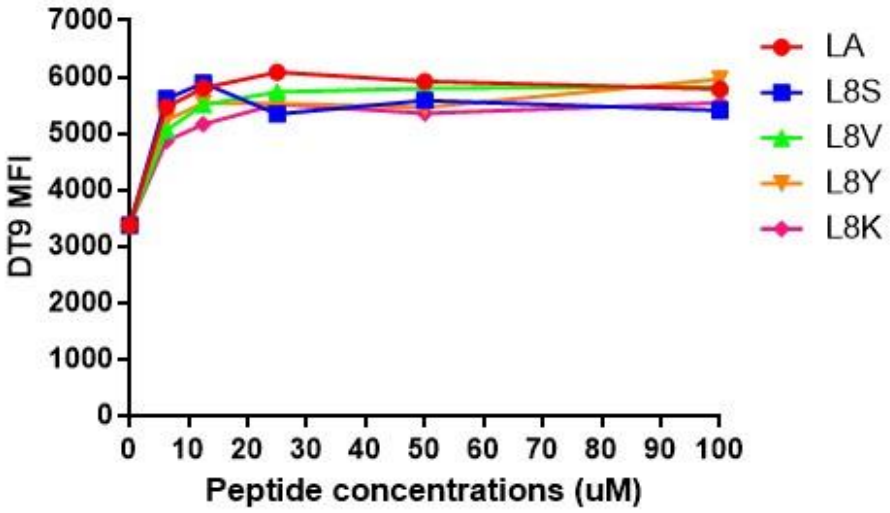

Figure 3-2: Series of peptides having amino acid substitution at position 8 (P8) stabilize HLA-C expression on the surface of C*0304-ICP47 cells. DT9 staining of 721.221 Cw0304-ICP47 after peptides loading with various and increasing concentrations of peptide having modification at P8 (LA, L8S, L8V, L8Y and L8K).

Zappacosta et al have reported that the L8K peptide has a shorter half life compared to the endogenous LA peptide (114). I verified this aspect of the peptides using a Brefeldin A assay in order to evaluate peptide stability and off-rate from HLA-C (**Figure 3-3**). Cells were loaded with saturating concentration of peptide (100μM) overnight at 26°C. The following day, cells were treated with brefeldin A and placed at 37°C then stained for HLA-C at different time points (from t=0 to 6hrs). Almost all peptides have the same off-rate with the exception of L8K, having a half-time of around four hours except for L8K which had a half time around one hour (**Figure 3-3**) . This observation correlates with report from Zapacosta et al where they described that L8K half life ($t_{1/2}$) of dissociation of the β2m from HLA-C*0304 was about 0.3hr compared to the endogenous AL peptide which was 9.8hrs (114).

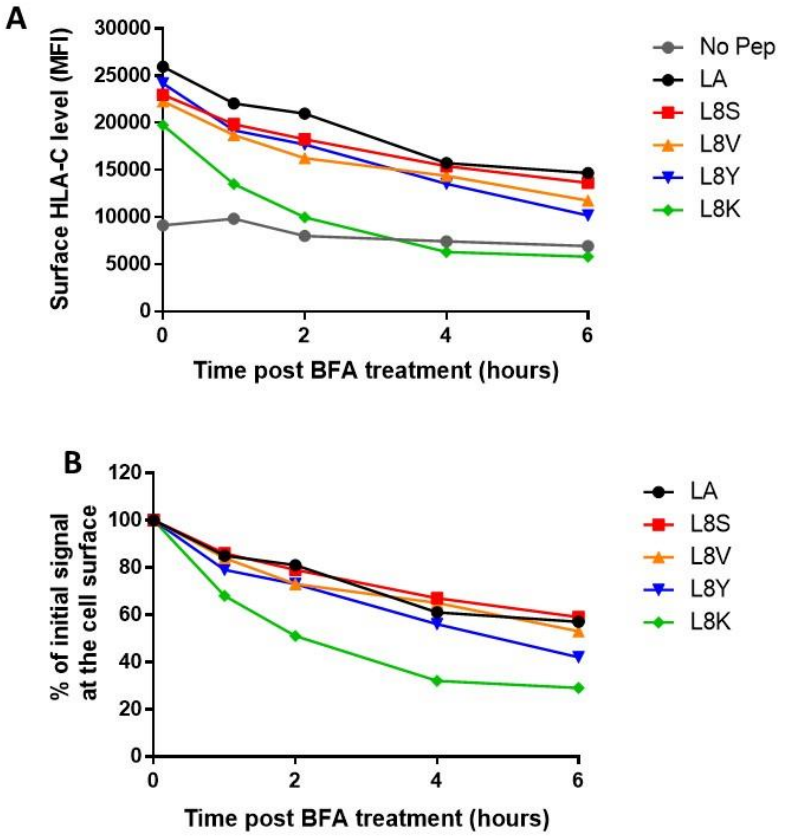

Figure 3-3: Decay of cell surface HLA-C staining on the surface of C*0304-ICP47 cells after peptide loading. Cells were treated with brefeldin A, aliquots harvested after 0, 0.5, 1, 2, 4 and 6hrs then stained with HLA-C antibody (DT9). (A) Level of HLA-C at the surface as determined by DT9 staining. (B) Same data as in panel A where MFI values were normalized to the initial HLA-C surface level (MFI at t=0hr). Similar rates of decay were observed in two separate experiments.

3.4 Absence of antagonism with low affinity position 8 (P8) peptide variants

Peptide antagonism describes a mechanism by which NK cells can be released from inhibition in the absence of MHC class I down- regulation. This phenomenon involves a strong inhibitory and a non-inhibitory peptide which both stabilise MHC-I expression at the surface and where the presence of the inhibitory peptide does not prevent NK cell activation. As observed after the stabilisation assay, with the exception of L8K, GAV P8 modified peptides bound HLA-C to a similar level.

Analysis of the degranulation is described **Figure 3-4 A-E**. Selection of the lymphocytes (according to their FCS and SSC) followed by identification of NK cells ($CD56^+/CD3^-$) allowed the discrimination of CD158b positive and negative population (**Figure 3-4 A**). Positive (721.221) and negative (721.221:C*0304) controls were used to for each donors (**Figure 3-4 B**). **Figure 3-4 C-E** depict analysis of CD107a expression avec co-culture with peptide loaded target cells. Using these peptides in a degranulation assay, I observed a hierarchy in inhibition which correlated with reported peptide affinity for KIR2DL2 (**Figure 3-5 A**). Indeed, LA and L8S which are peptides with a high affinity induced a statistically significant strong inhibition (<50%) whereas L8V, L8Y and L8K which were low affinity peptides did not inhibit NK cells (>90% activation vs no peptide). Although low affinity peptides did not inhibit KIR2DL2/$L3^+$ NK cells, there was no release of NK cells from the inhibition due to high KIR affinity peptides (LA or L8S) in the presence of low KIR affinity peptides (L8Y or L8K), which could have indicated peptide antagonism. Nevertheless, some reversal (15%) was observed with L8V peptide in combination with LA or L8S when compared to the inhibition produced by the single peptide, which was much less than the anticipated levels for a peptide antagonist. Thus, overall none of the peptides acted convincingly as antagonists and, L8Y and L8K behaved as null peptides. Effects observed were specific to KIR2DL2/$L3^+$ NK cells as there were no differences in term of degranulation within KIR2DL2/$L3^-$ NK cells (**Figure 3-5 B**).

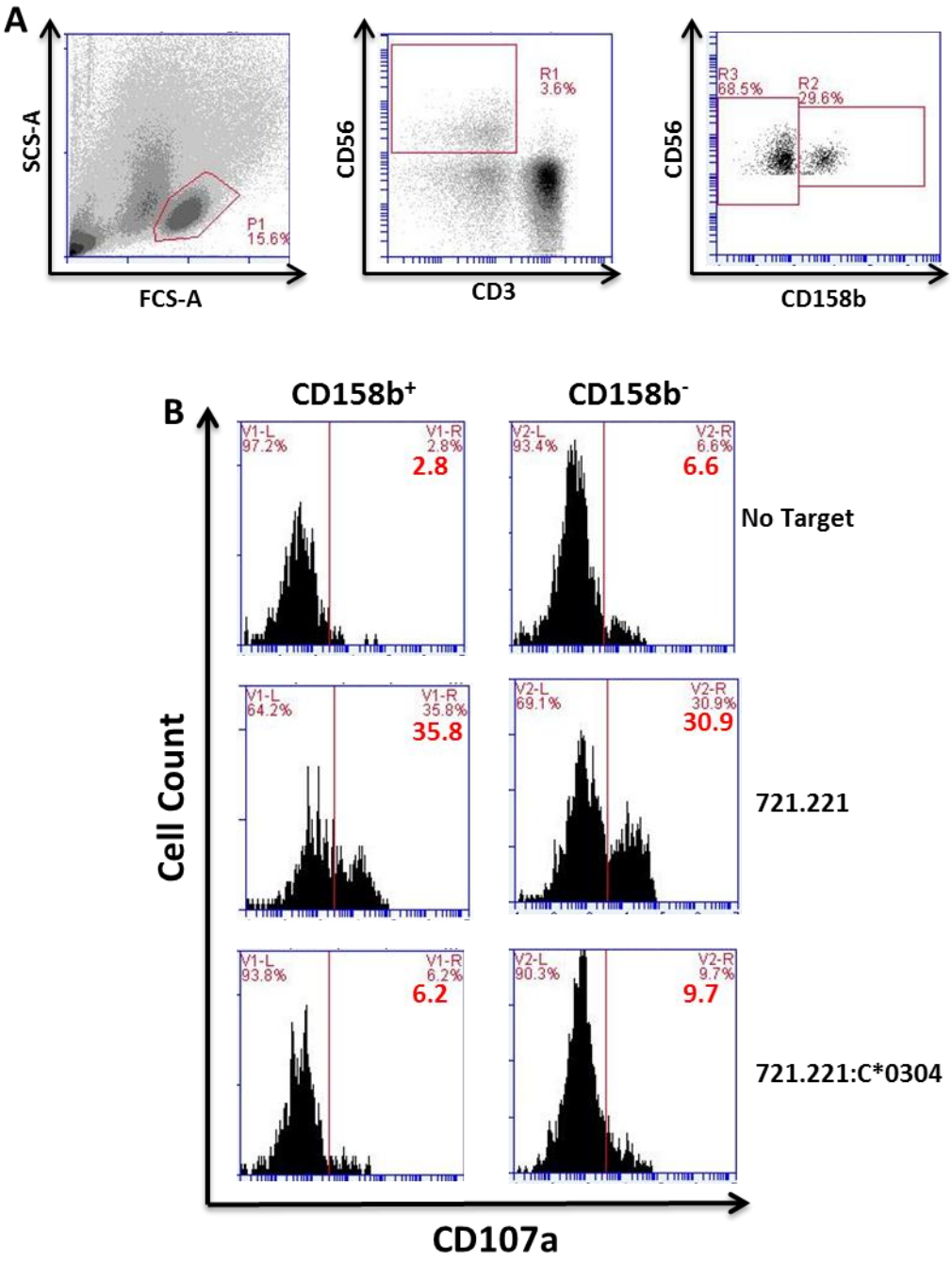
A
SCS-A
FCS-A
P1
15.6%
CD56
CD3
R1
3.6%
CD56
CD158b
R3
68.5%
R2
29.6%
B
CD158b+
CD158b-
Cell Count
CD107a
V1-L
97.2%
V1-R
2.8%
2.8
V2-L
93.4%
V2-R
6.6%
6.6
No Target
V1-L
64.2%
V1-R
35.8%
35.8
V2-L
69.1%
V2-R
30.9%
30.9
721.221
V1-L
93.8%
V1-R
6.2%
6.2
V2-L
90.3%
V2-R
9.7%
9.7
721.221:C*0304

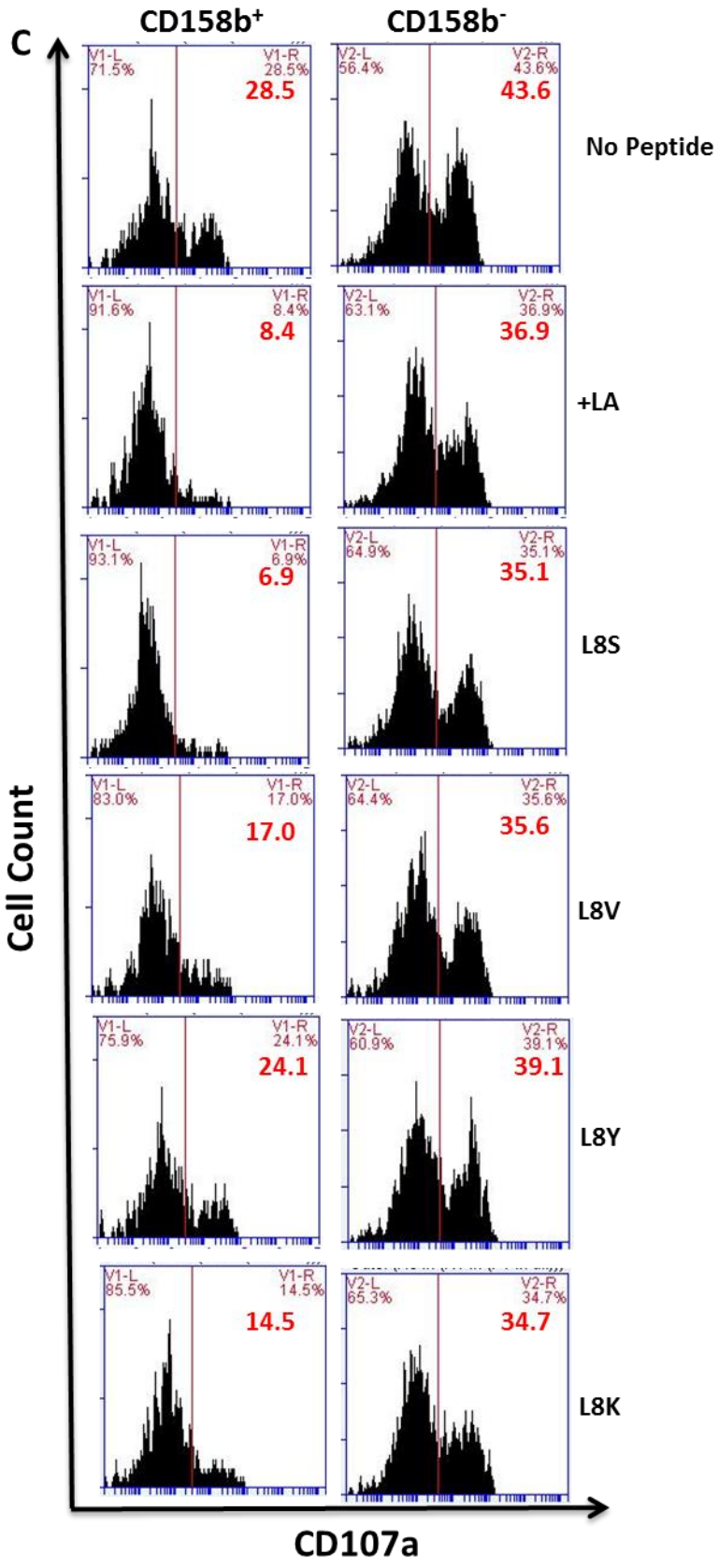
C
CD158b+
CD158b-
No Peptide
+LA
L8S
L8V
L8Y
L8K
Cell Count
CD107a
28.5
43.6
8.4
36.9
6.9
35.1
17.0
35.6
24.1
39.1
14.5
34.7

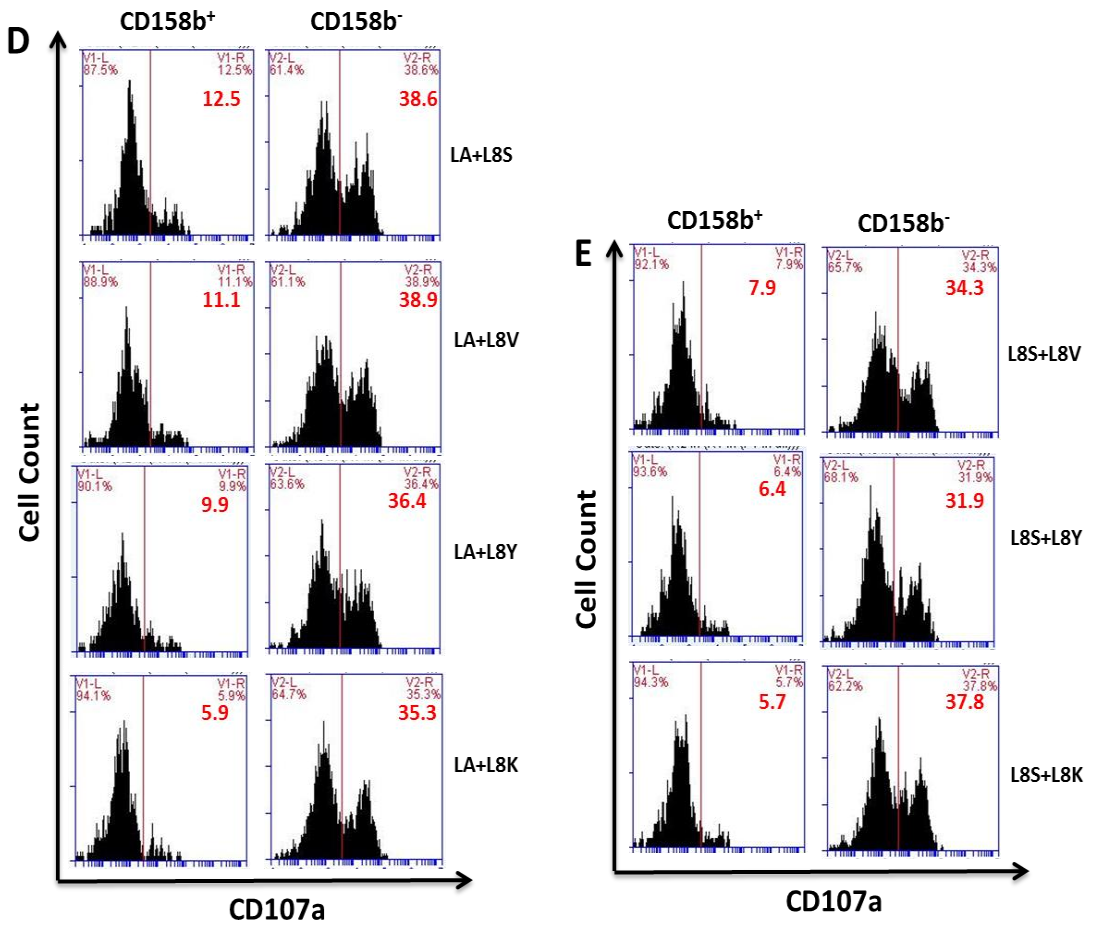

Figure 3-4: NK cell degranulation using P8 peptides variants. (A) Gating strategy of lymphocytes, NK cells and CD158b expressing cells. (B) Controls used to assess the integrity of the CD107a assay. (C) CD107a expression of NK cells after co-culture with cells loaded or not with a single peptide. (D) CD107a expression of NK cells after co-culture with cells loaded with a combination of LA peptide with P8 non-KIR binder peptides. (E) CD107a expression of NK cells after co-culture with cells loaded with a combination of L8S peptide with P8 non-KIR binder peptides.

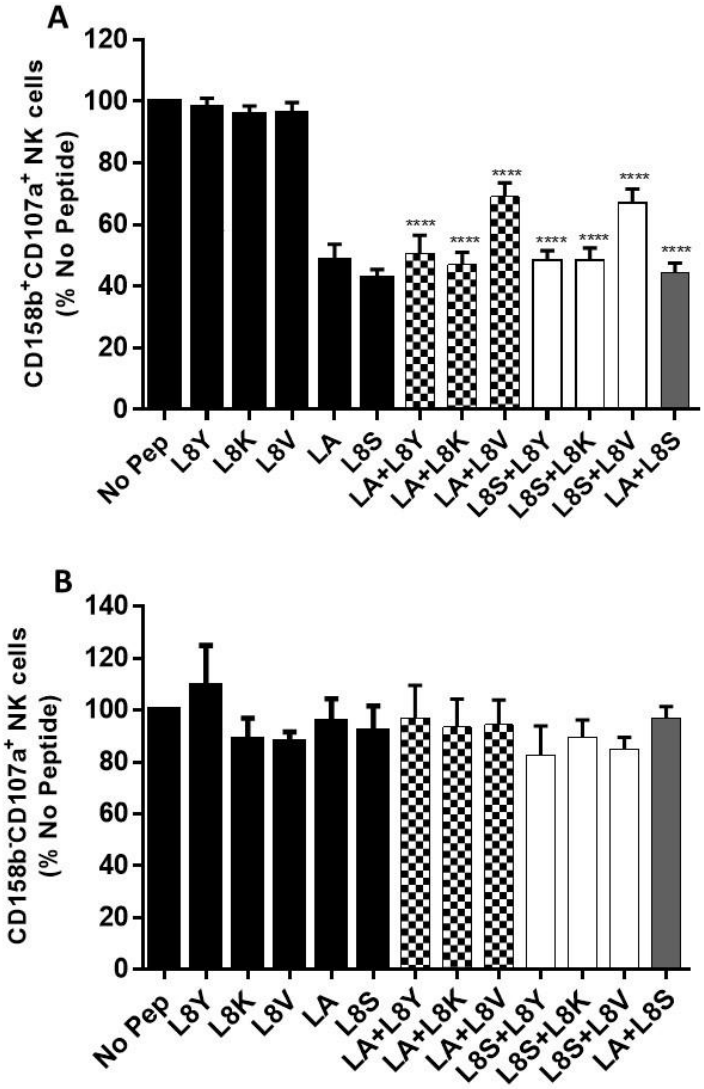

Figure 3-5: Comparison of NK cell inhibition using the series of peptide variants with P8 substitution. (A) Degranulation assays of KIR2DL2/L3^{+} cells. Peptides with lower affinity for KIR: L8V, L8Y and L8K were mixed or not with KIR strong binding peptides (LA and L8S). All values have been normalised to "No Peptide". Black bars represent individual peptides, grey bar represents high affinity peptides mixed together, black and white bars represent LA peptide mixed with low affinity peptides and white bars represent L8S peptide mixed with low affinity peptides. Red dashed line shows the maximum inhibition and the grey dashed line the maximum activation. Representation of n=8 experiments. *****p<0.0001* (Two way Anova) which compares each condition to "No peptide". (B) Degranulation assays of KIR2DL2/L3^{-} cells shown as a control for the KIR2DL2/L3^{+} cells.

3.5 VAP-LY is a null peptide for KIR2DL3 expressing NK cells at HLA-C*0102.

In the context of HLA-C*0304, I observed that P8 modifications of the endogenous peptide sequence did not induce antagonism. Therefore I wanted to verify if this can also be applied to HLA-C*0102 P8 peptide variants (**Figure 3-6**). HLA-C*0102 endogenous peptide VAPWNSLSL has for origin Metalloproteinase inhibitor 1.

As observed in **Figure 3-5**, the endogenous peptide (VAPWNSLSL or LS) produced inhibition as well as the VAPWNSFAL (FA) peptide variant. VAPWNSDAL (DA), VAPWNSLYL (LY) had no effect on activation compared to no peptide. When I pulsed cells with the strong inhibitory peptide (LS or FA) in combination with the known non-inhibitory peptide (DA) and a new non-inhibitory peptide (LY), I have observed that DA induced a release of NK cells from their inhibition despite the addition of FA. However, the presence of LY and LS did not produce the same effect. LY is a P8 modified peptide from the endogenous sequence was not antagonistic as I observed for L8Y for HLA-C*0304. Thus, P8 variants do not appear to be antagonistic.

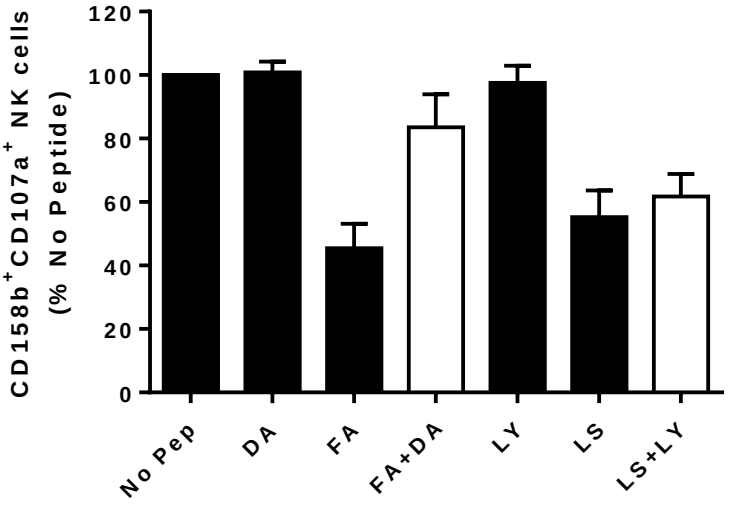

Figure 3-6: Comparison of NK cell inhibition using the series of HLA-C*0102 peptide variants with P8 substitution. Degranulation assays of KIR2DL2/L3^{+} cells. Inhibitory peptides (LS and FA) were mixed or not with non-inhibitory peptide (DA and LY). All values have been normalised to "No Peptide". Black bars represent individual peptides, white bars represent endogenous peptide (LS or FA) mixed with non-inhibitory peptides (DA or LY). Representation of n=5 experiments.

3.6 GAVDPLLAL position 7 (P7) variants stabilize HLA-C expression on the cell surface

As amino acids at P8 and P7 of the peptide are critical for KIR binding, I designed a second series of peptides with a modification at P7. These variants at P7 have been previously shown to be antagonistic for the combination of HLA-C*0102 and KIR2DL2/L3 (218). In the HLA-C*0102 study, peptide screening of HLA-C*0102 binding peptide and their affinity for KIR2DL3 revealed three classes of peptides: weak binding VAPWNS**DA**L (VAP-DA), intermediate binding VAPWNS**RA**L (VAP-RA) and strong binding VAPWNS**FA**L (VAP-FA). I therefore synthesized the following peptide series: GAVDPL7**R**AL (L7R), GAVDPL7**F**AL (L7F) and GAVDPL7**D**AL (L7D).

I first tested the binding of this new peptide series in a peptide stabilization assay using increasing concentrations of peptides from 0 to 20μM loaded onto C*0304-ICP47 cells. As observed with the first series of peptides, our results showed an increase in HLA-C expression, as determined by DT9 that correlated with the increase of peptide in concentrations until the level of expression of HLA-C molecule reached saturation (**Figure 3-7 A**). I then determined the K_d and the B_{max} for each peptide using a Scatchard analysis. All new variants of GAVDPLLAL peptides stabilized HLA-C on the cell surface with similar affinities. This second series showed a saturation of HLA-C at a peptide concentration of 12.5μM (**Figure 3-7 B-D**). These concentrations were used to inform CD107a assays.

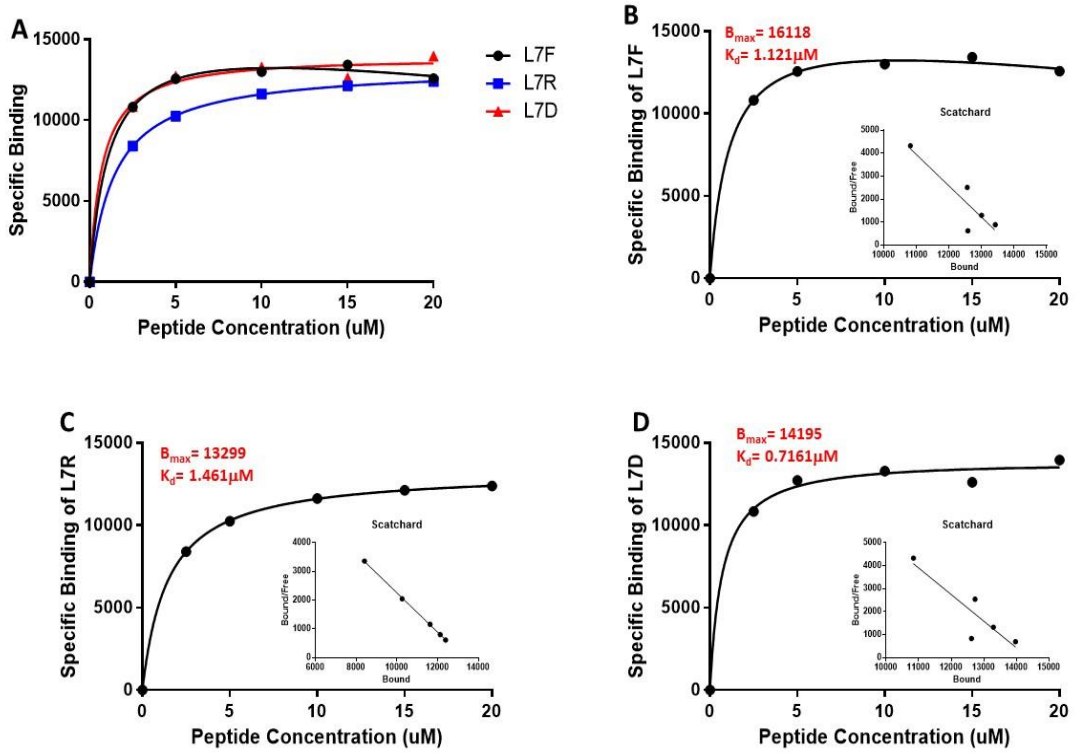

Figure 3-7: Peptide stabilisation and Scatchard analysis: affinity of GAV derived peptides for HLA-C*0304. Scatchard plots derived from stabilisation of the HLA-C*0304 and analysis by flow cytometry using DT9 antibody. (A) HLA-C stabilisation with all peptides, (B) GAVDPL7FAL (L7F), (C) GAVDPL7RAL (L7R), (D) GAVDPL7DAL (L7D). A regression line was derived using the formula $Y=B_{max}*X/(Kd+X)$ for each peptide using GraphPad Prism 6 software. K_d is the dissociation constant and B_{max} is the maximal binding.

Following the peptide stabilisation assay, I proceeded to a Brefeldin A decay assay in order to evalutae P7 variant peptides off-rate and their stability in the HLA-C peptide groove. This assay showed that all peptides have similar off-rates with a half life ($t_{1/2}$) around four hours (**Figure 3-8 A-B**).

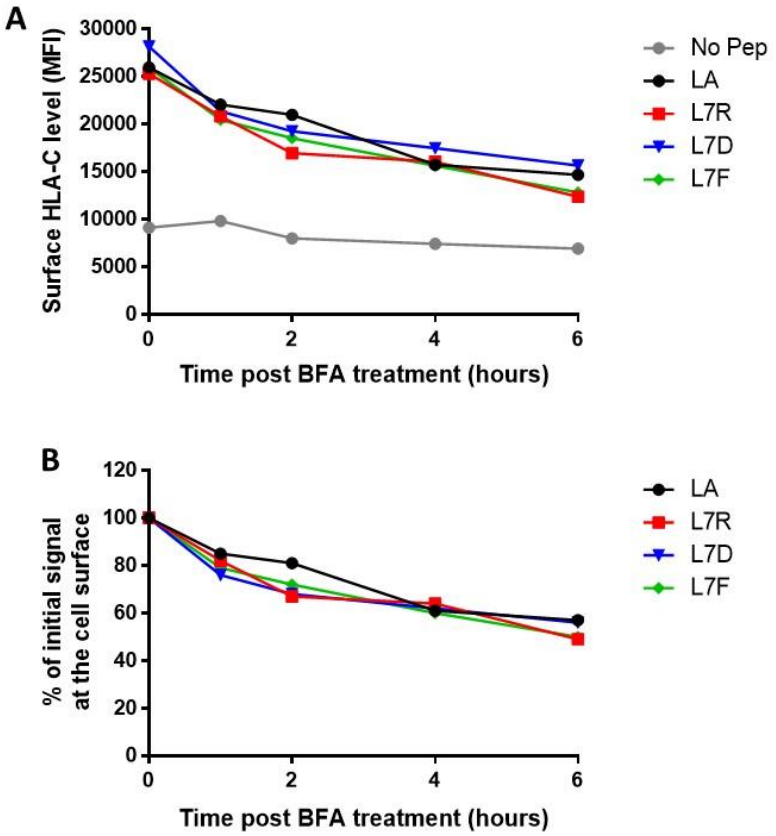

Figure 3-8: Decay of cell surface HLA-C staining on the surface of C*0304-ICP47 cells after peptide loading. Cells were loaded overnight with peptide, treated with brefeldin A, aliquots harvested after 0, 0.5, 1, 2, 4 and 6hrs, and then stained DT9. (A) Level of HLA-C at the surface as determined by DT9 staining. (B) Same data as in panel A where MFI values were normalized to the initial HLA-C surface level (MFI at t=0hr). Similar rates of decay were observed in two separate experiments.

3.7 P7 peptide variants with similar HLA-C affinity have different KIR binding

To test the affinity of the new series of peptide, I used a KI2RDL2-Fc fusion construct. This demonstrated that although the peptides have similar affinity for HLA-C, peptide variants have different affinities for KIR (**Figure 3-9 A-D**). Indeed, L7R peptide had the highest B_{max} value (203,591) which corresponds to the maximal binding and the lowest K_d value (0.8103μM). L7F had an intermediate medium B_{max} (150,479) and K_d (0.9375μM) whereas L7D had the lowest B_{max} (77,614) and the higher K_d (4.361μM). This data suggest that L7R will be strongly inhibitory, L7F weak inhibitory and L7D non inhibitory in an NK cell functional assay.

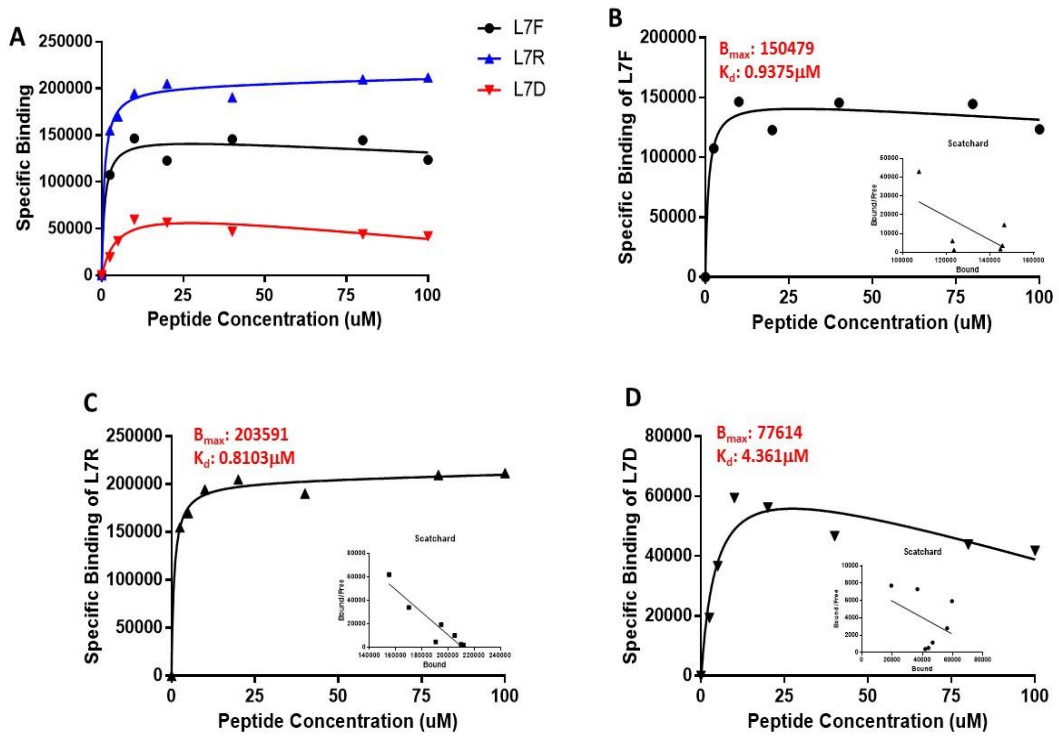

Figure 3-9: Peptide stabilisation and Scatchard analysis: affinity of GAV derived peptides for KIR2DL2. Scatchard plots made from stabilisation of the HLA-C*0304 and analysis by flow cytometry using DT9 antibody. (A) GAVDPLRAL (L7R, (B) GAVDPLFAL (L7F), (C) GAVDPLDAL (L7D) and (D) KIR2DL2 binding for all peptides. Regression line was derived using the formula $Y=B_{max}*X/(Kd+X)$ for each peptide using GraphPad Prism 6 software. K_d is the dissociation constant and B_{max} is the maximal binding.

All data from HLA-C stabilisation and KIR-Fc binding assay are summarised in **Table 3-2**. The table describes the binding of each peptide for their MHC ligand and the affinity of the MHC-I:peptide complexes to their KIR receptor.

	HLA-C		KIR2DL2	
	Bmax	Kd (µM)	Bmax	Kd (µM)
L7F	16,118	1.121	150,479	0.9375
L7R	13,229	1.461	203,591	0.8103
L7D	14,195	0.7161	77,614	4.361

Table 3-2: Summary of peptide stabilisation and KIR binding assays. HLA-C stabilization and KIR2DL2 binding data after single peptide pulse on C*0304-ICP47 cells.

3.8 L7D is a peptide antagonist

Figure 3-10 A-B depict analysis of CD107a expression after co-culture with peptide loaded target cells among CD158B expressing or not expressing NK cells.

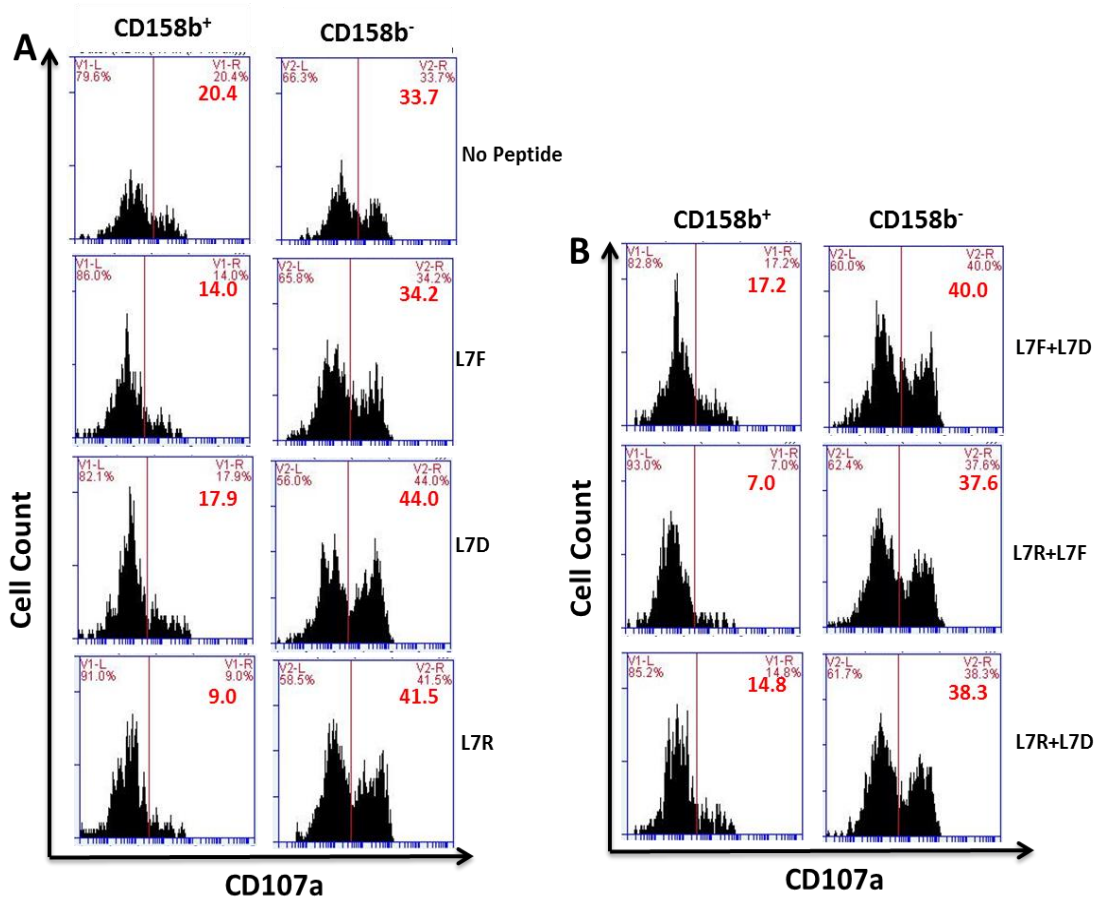

Figure 3-10: NK cell degranulation assay using P7 peptides variants. (A) CD107a expression of NK cells after co-culture with cells loaded or not with a single peptide. (B) CD107a expression of NK cells after co-culture with cells loaded with a combination of peptide.

I next tested the effect of these peptides on NK cells, singly or in combination. The initial results from the functional assays suggested a classification of L7R as a KIR strong inhibitor, L7F as an intermediate inhibitor and L7D is a weak KIR inhibitor (**Figure 3-9 A**). The difference in terms of inhibition between L7R and L7F was statistically significant ($p<0.001$). This contrasts with observations for VAPWNSLSL in which R at position 7 (P7) was an intermediate NK cell inhibitor and F at P7 a strong NK cells inhibitor. The degranulation assays were repeated with eight different donors

and showed that L7D reversed the inhibition driven by the strong and weak inhibitory peptides, and is thus a peptide antagonist for KIR2DL2/3 in this context. An increase in CD107a over were observed in presence of L7R+L7D when compared to L7R alone ($p<0.001$). Furthermore, the peptide effect was specific to KIR2DL2/L3$^+$ NK cells as there were no effect with the negative counterpart (**Figure 3-9 B**). In future experiments I focused on L7R (strong agonist peptide) and L7D peptides (non-inhibitory/antagonist peptide).

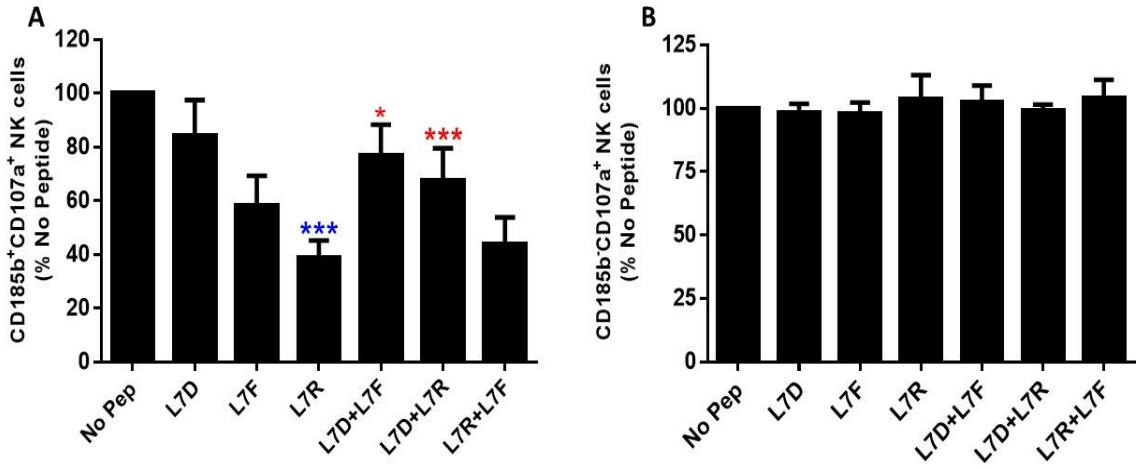

Figure 3-11: Inhibition and antagonism of NK cells by P7 peptide GAV variants. (A) Degranulation of KIR2DL2/L3$^+$ cells. Peptide hierarchy in term of inhibition and antagonism of NK inhibition by L7D peptide. All values have been normalised to "No Peptide". Representation of n=8 experiments using 6 different donors. Data are expressed as mean percentage +/-SEM. All values have been normalised to "No Peptide". **p<0.05, ** p<0.01 and *** p<0.001 (Two way Anova).* Red stars are for comparison between *L7F* and *L7F+L7D* or *L7R* and *L7R+L7D* and bleu stars compare *L7R* to *L7F.* (B) Degranulation of KIR2DL2/L3$^-$ cells where all values have been normalised to "No Peptide".

As previously noted for the antagonist peptide described by Fadda et al, small quantities of the antagonist peptide are sufficient to induce reversal of NK cells from inhibition (218). I performed peptide titration experiments where the concentration of L7R or L7F varied from 12.5 to 0μM whilst the L7D concentration was increased from 0 to 12.5μM as stated in **Table 3-3**.

Single Peptide (μM)	Peptide Mix (μM)	
L7R	L7R	L7D
0	0	12.5
2.5	2.5	10
5	5	7.5
6.25	6.25	6.25
7.5	7.5	5
10	10	2.5
12.5	12.5	0

Table 3-3: Peptide Concentrations used for the peptide titration experiment. Summary of conditions used for the peptide titration experiments.

Results showed that for all peptide concentrations, there was a release of NK cells from the inhibition due to L7R peptide. Moreover, I observed that a small concentration of L7R (2.5μM) was enough to reduce NK cell inhibition by 50%. Regression analysis have demonstrated that the L7R: L7RD peptide mix gave a linear change in activation (r^2=0.70), whereas the inhibition due to changing in L7R concentrations only fitted a one phase decay curve (R^2=0.87) (**Figure 3-12**). Consequently, the change in inhibition induced by changing the concentration of L7R has a distinct kinetic from that induced by changing the ratio between L7R and L7D, as reported by Fadda et al for HLA-C*0102 (218). The degranulation assays were repeated using six different donors. These results confirm that L7D is a weak KIR binding peptide that antagonises the inhibition driven by L7R. Thus I have demonstrated that peptide antagonism can be extended to a second HLA-C allele, HLA-C*0304 and is not a unique property of HLA-C*0102.

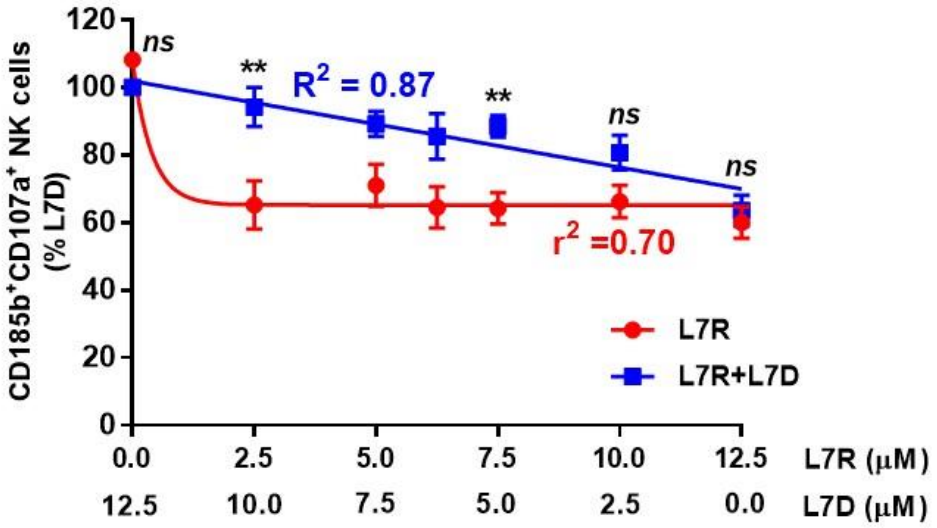

Figure 3-12: The ratio of strong to weak KIR binding highlights the antagonism effect of DA on strong inhibitory peptide. Degranulation of KIR2DL2/2DL3+ cells in response to 721.221C*0304-ICP47 cells alone or incubated with a single peptide or with a combination of L7D and L7R at 2.5 to 12.5mM. Peptide mixes consisted of different ratio of L7R and L7D from 0-100% L7R and 0-100% L7D. Data were normalised to the value observed with 100% L7D. Data are expressed as mean percentage +/- SEM. **p=0.0089 (two- way ANOVA). Results are representative of 4 independent experiments with 6 different donors.

3.9 Donor KIR genotype influences inhibitory peptide reactivity

As the KIR2DL2/L3/S2 genotype can influence peptide mediated inhibition, we characterized the donors in more detail by defining their KIR2DL2/2DL3/2DS2 genotype by PCR (**Figure 3-13**). Interestingly, two donors out of sixteen who only carry KIR2DL3, carried KIRDS2 as well. Usually it is reported that KIRDS2 gene is mainly linked to KIR2DL2.

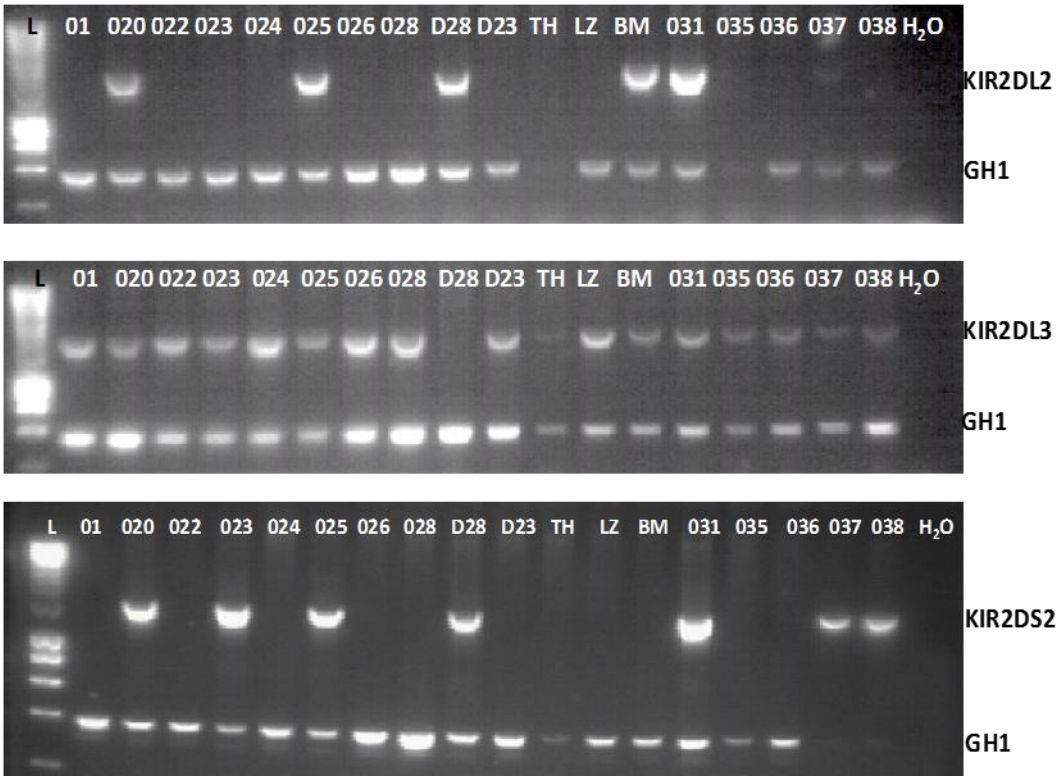

Figure 3-13: Genotyping of KIR2DL2/2DL3/2DS2 by PCR with sequence specific primers (PCR-SSP). Representative PCR results showing the ~1868 bp (KIR2DL2), the ~1858 bp (KIR2DL3) and the ~1775 bp (KIR2DS2) fragment that were amplified. All reactions were performed under identical conditions. Size marker 1Kb (Bioline, UK).

As I have observed donor variability in term of activation, I decided to segregate the KIR2DL3 homozygous donors from KIR2DL2/L3 heterozygous donors. I observed that an efficient inhibition from the strong inhibitory peptide when I compared KIR2DL3 homozygous donors which had 70% of inhibition (**Figure 3-14 A**) while KIR2DL2/L3 heterozygous donors displayed less inhibition (>40%) (**Figure 3-14 B**). This observation can be related by the fact that heterozygous donors have a more activating KIR repertoire compared to homozygous donors.

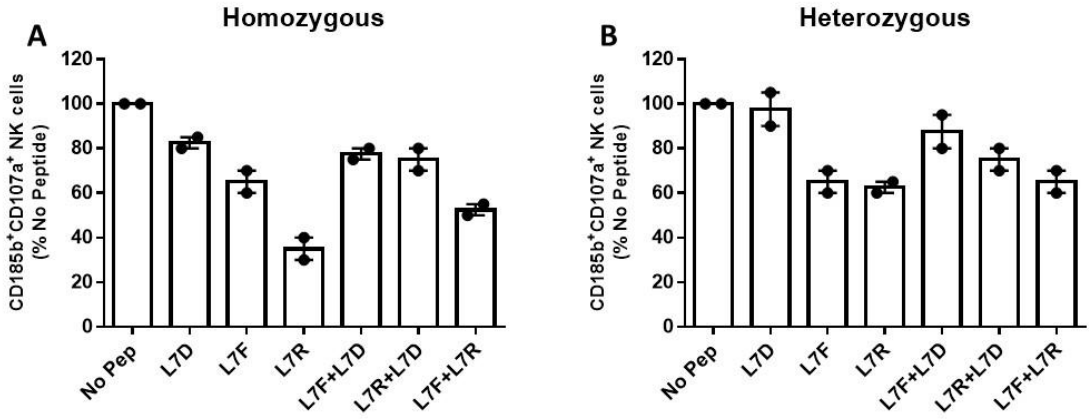

Figure 3-14: Comparison of KIR2DL3 homozygous and KIR2DL2/L3 heterozygous donors in term of KIR expression regarding NK cells inhibition using a series of peptide variants with P7 substitution. Degranulation of KIR2DL2/L3$^+$ cells from KIR2DL3 homozygous donor (A) and KIR2DL2/L3 heterozygous donor (B). All values have been normalised to "No Peptide". Representation of n=2 experiment for each genotype.

3.10 Reversal of inhibition is not due to peptide displacement

To investigate the mechanism of peptide antagonism phenomenon, I decided to assess three parameters at the same time. While using peptide-pulsed cells for degranulation, I also looked at HLA-C expression as well as the KIR binding. KIR-Fc binding strategy is explained in **Figure 3-15** where after peptides pulse (singly or in combination) I used our tetramerized KIR-Fc which consists of Protein A-A488 bound to a KIR2DL2 fusion construct. As observed in our previous experiments, target cells loaded with the strong inhibitory peptide (in red) gave a strong KIR binding signal while cells loaded with the non-inhibitory peptide (in blue) did not induce any KIR binding (KIR binding was comparable to the binding in absence of peptide condition). I have investigated the KIR binding in the presence of both peptides.

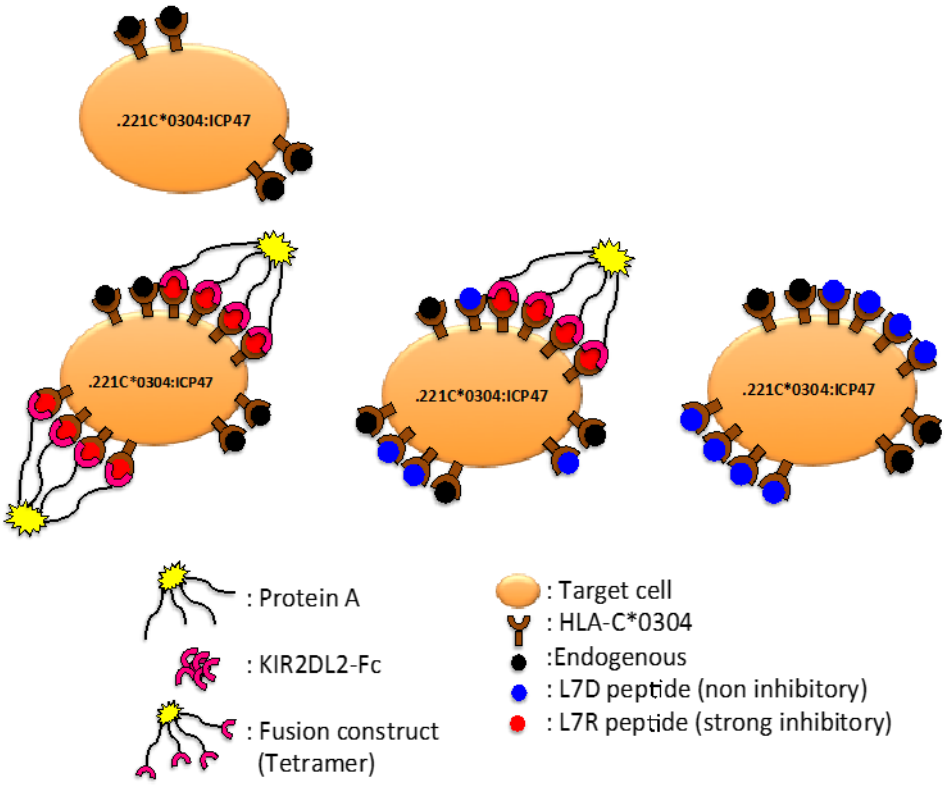

Figure 3-15: Schematic of KIR2DL2-Fc binding in presence of L7R (strong inhibitory), L7D (non-inhibitory) or both. 721.221Cw0304-ICP47 cells were loaded with a single peptide (L7R in red and L7D in blue) or a combination L7R + L7D.

To assess the effect of KIR binding during antagonism, I carried out an experiment that measures three parameters simultaneously: CD107a expression of NK cells after co-culture with peptides loaded target cells, HLA-C expression and KIR binding after peptide loading.

My first results showed that the KIR binding changes when I changed the peptide repertoire but the class I expression did not (**Figure 3-16 A-G**). After selecting the target cells and controlling the KIR binding (**Figure 3-16 A**) using 721.221 (negative control, no binding) and 721.221 C*0304 (positive control, over 90% of binding), I tested KIR-Fc binding when we pulsed cells with increasing concentrations of L7R (**Figure 3-16 B**) or with different ratios of L7R:L7D peptides (**Figure 3-16 B**). I observed an increase of KIR binding with increasing concentration of L7R peptide **Figure 3-16 G** (red bars). When I mixed the antagonistic peptide with the strong inhibitory peptide, I noticed that the KIR-Fc binding diminished as soon as I started

the addition (**Figure 3-16 C**). This means that the presented antagonist peptide abrogate the binding to KIR despite the presence of the strong inhibitory peptide. MFIs are summarised **Figure 3-16 G** (bleu bars).

As I also stained target cells with DT9 in order to verify HLA-C expression (**Figure 3-16 D-F**), I have found that singly (L7R) or in combination (L7R+L7D), HLA-C expression was not affected and tended to be steady in overall among all conditions tested (**Figure 3-16 G**). Earlier in the project I have already reported that singly or in combination, GAV peptide series do not disrupt HLA-C stabilization at the cell surface.

Taken together, these results implied that there may be displacement occurring during these assays or that small amounts of non-binding peptide are able to disrupt the binding of the multimeric KIR-Fc complex.

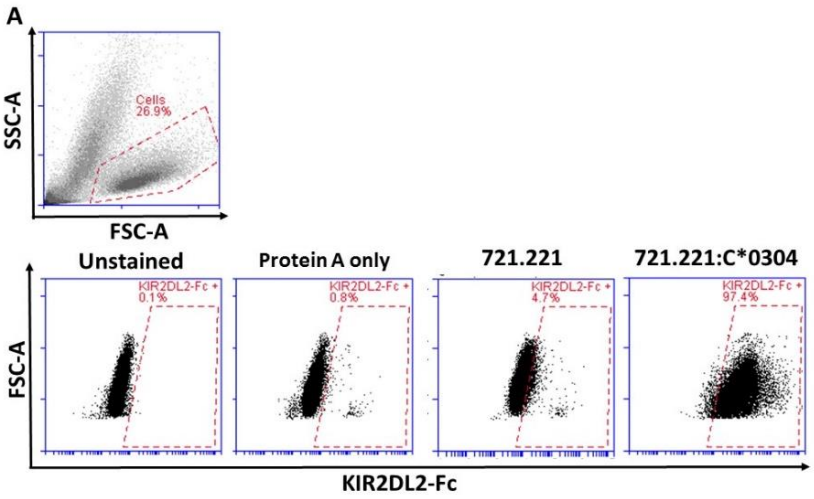
A
SSC-A
Cells
26.9%
FSC-A
Unstained
Protein A only
721.221
721.221:C*0304
KIR2DL2-Fc +
0.1%
0.8%
4.7%
97.4%
FSC-A
KIR2DL2-Fc

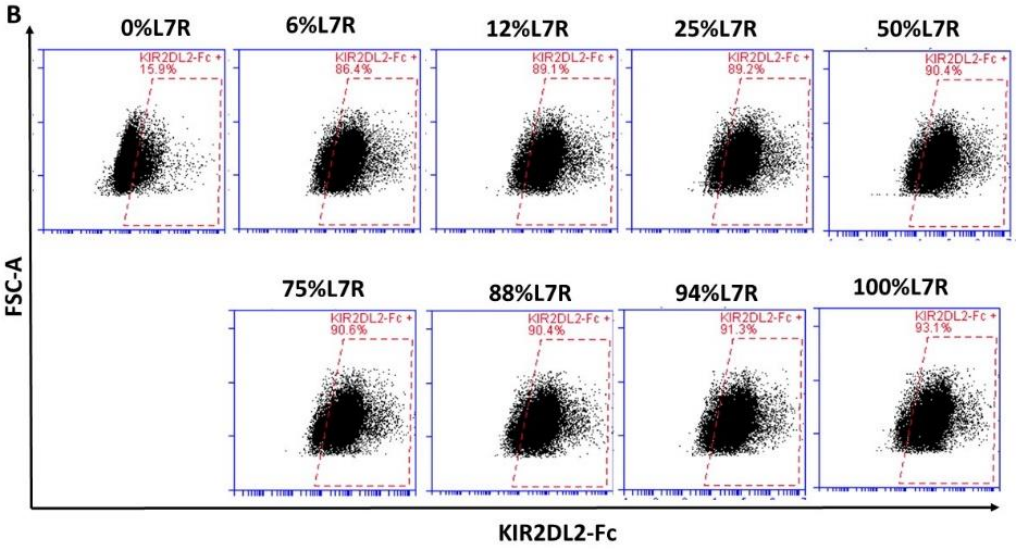
B
0%L7R
6%L7R
12%L7R
25%L7R
50%L7R
15.9%
86.4%
89.1%
89.2%
90.4%
75%L7R
88%L7R
94%L7R
100%L7R
90.6%
90.4%
91.3%
93.1%
FSC-A
KIR2DL2-Fc

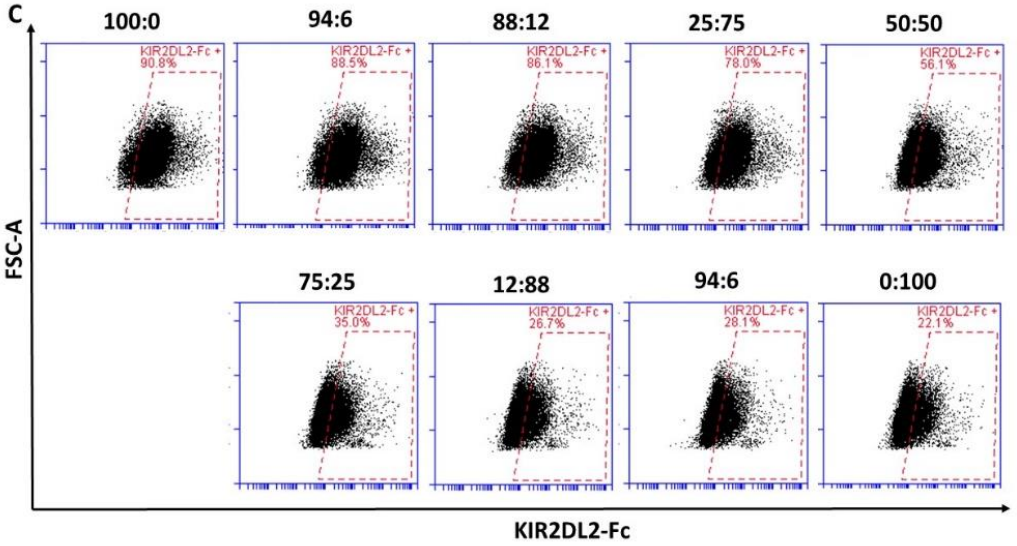
C
100:0
94:6
88:12
25:75
50:50
90.8%
88.5%
86.1%
78.0%
56.1%
75:25
12:88
94:6
0:100
35.0%
26.7%
28.1%
22.1%
FSC-A
KIR2DL2-Fc

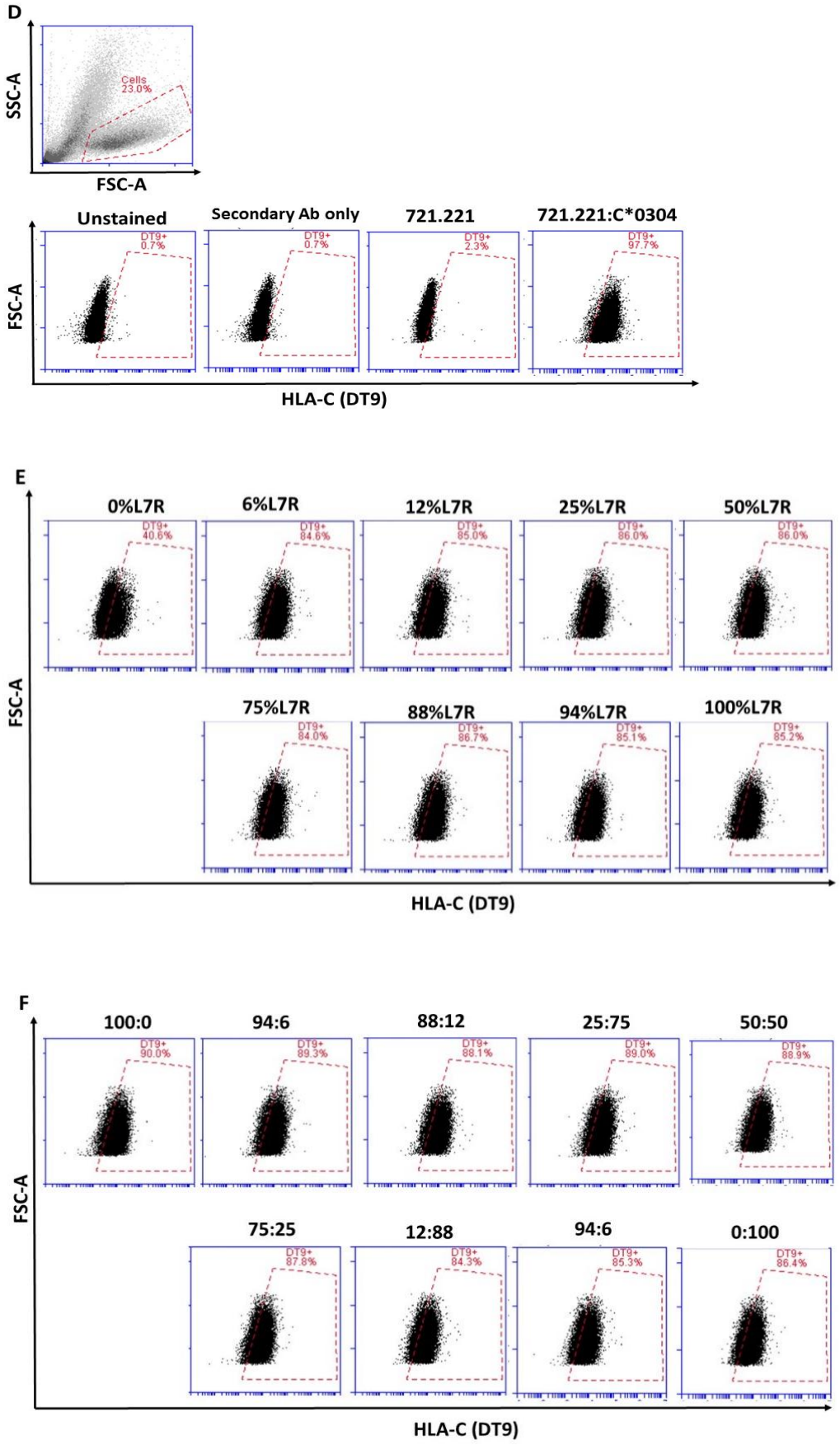
D
SSC-A
FSC-A
Cells
23.0%
Unstained
Secondary Ab only
721.221
721.221:C*0304
DT9+
0.7%
DT9+
0.7%
DT9+
2.3%
DT9+
97.7%
FSC-A
HLA-C (DT9)
E
0%L7R
6%L7R
12%L7R
25%L7R
50%L7R
DT9+
40.6%
DT9+
84.6%
DT9+
85.0%
DT9+
86.0%
DT9+
86.0%
75%L7R
88%L7R
94%L7R
100%L7R
DT9+
84.0%
DT9+
86.7%
DT9+
85.1%
DT9+
85.2%
FSC-A
HLA-C (DT9)
F
100:0
94:6
88:12
25:75
50:50
DT9+
90.0%
DT9+
89.3%
DT9+
88.1%
DT9+
89.0%
DT9+
88.9%
75:25
12:88
94:6
0:100
DT9+
87.8%
DT9+
84.3%
DT9+
85.3%
DT9+
86.4%
FSC-A
HLA-C (DT9)

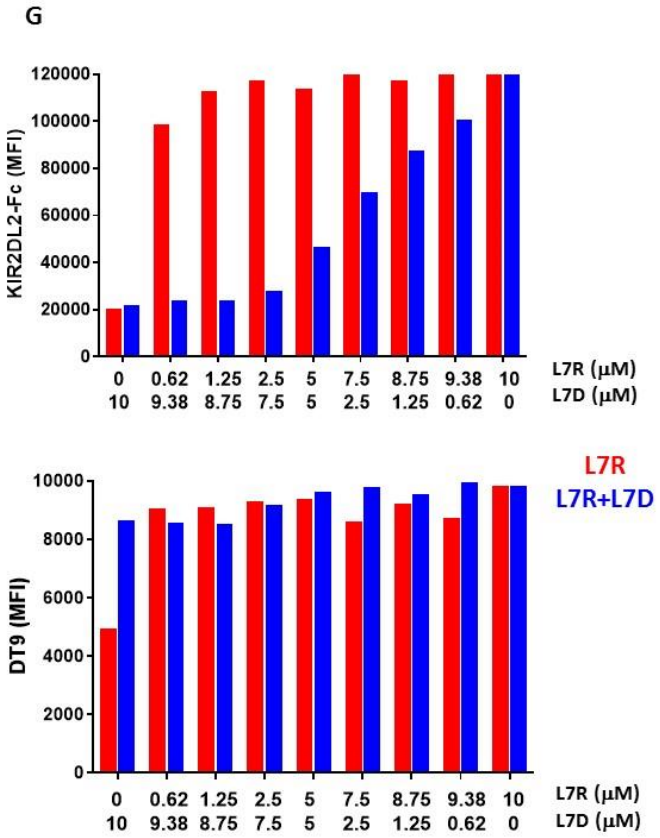

Figure 3-16: HLA-C staining associated with KIR2DL2-Fc binding. (A) Gating strategy and staining control for KIR2DL2-Fc binding. 721.221 cells were used as negative control and 721.221-C*0304 cells were used as positive control. (B) KIR2DL2-Fc binding on 721.221-C*0304-ICP47 cells pulsed with increasing concentration of L7R peptide (from 0.62 to 10µM). (C) KIR2DL2-Fc binding on cells pulsed with mixes between L7R and L7D at different L7R:L7D ratios at 10µM final concentration for each condition. (D) Gating strategy and staining control for HLA-C staining using DT9. 721.221 cells were used as negative control and 721.221 cells were used as positive control. (E) HLA-C staining on cells pulsed with increasing concentration of L7R peptide (from 0.62 to 10µM). (F) HLA-C staining on cells pulsed with mixes between L7R and L7D at different L7R:L7D ratios at 10µM final concentration for each condition. (G) Summary of MFI values from each condition tested.

As the degranulation of NK cells was measured simultaneously with the KIR-Fc binding and the HLA-C staining, I compared the degranulation to the KIR-Fc binding to assess the implication of the KIR binding in the release of NK cell from their inhibition in presence of the antagonistic peptide (**Figure 3-17**). **Figure 3-17 A** shows that at 10µM of L7R peptide we had 100% of KIR-Fc binding and nearly 40% of NK cell inhibition. Moreover, the decrease of L7R concentration used was associated with a decrease in KIR-Fc binding and with an increase of NK cell degranulation. When there

was no peptide, the KIR-Fc binding was at its lowest and the NK degranulation was at its maximum. Then when I looked into the different mixes (**Figure 3-17 B**) I noticed that at 10μM of L7D peptide, the degranulation was at its maximum (100%) and the KIR-Fc binding at its lowest (<15%). Decreasing the concentration of L7D in the ratio between L7R:L7D induced an increase of KIR-Fc binding and an increase of NK cells inhibition (up to almost 40%). At 50:50, I observed >35% of KIR binding with >60% of killing.

To sum up, I clearly show here that the release of NK cells from their inhibition in the presence of the antagonist peptide, is not due to the loss of HLA-C expression but is due to a loss of KIR binding hence the degranulation of the NK cells. This experiments have illustrated when there is less L7R then there is less degranulation which may involve peptide displacement.

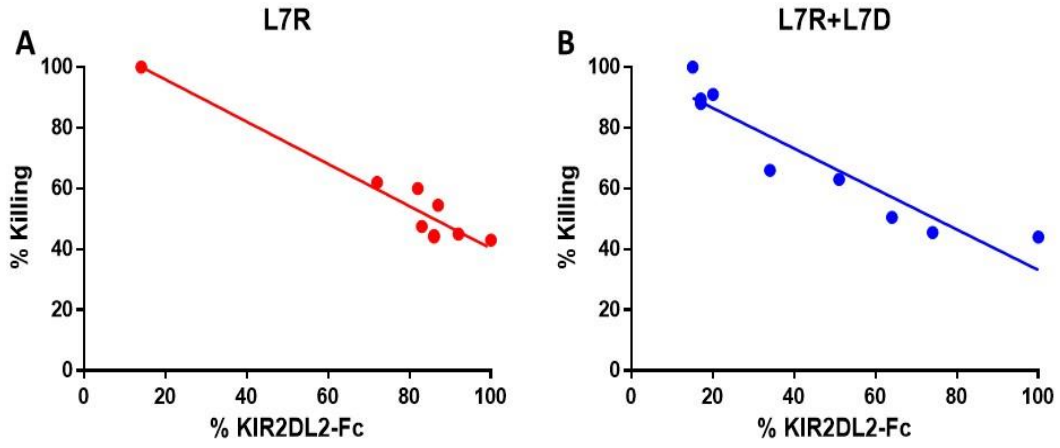

Figure 3-17: Correlation between NK cell degranulation and KIR2DL2 binding. Degranulation of KIR2DL2/2DL3+ cells in response to 721.221C*0304-ICP47 cells alone or incubated with a single L7R peptide from 0 to 10mM (A) or with a combination of L7D and L7R at 100%L7R:0%L7D to 0%L7R:100%L7D ratios (B). Peptide mixes consisted of different ratio of L7R and L7D from 0%L7R to 100%L7D. Data were normalised to the value observed with 100% L7D (mix conditions) and normalised to No peptide (single peptide pulse). Target cells were stained with KIR2DL2-Fc conjugated with Protein A Alexa Fluor488 at a molar ratio of 12:1 and a correlation between NK cells degranulation (killing) and level of KIR2DL2 binding was made. We used the maximum KIR binding obtained at 100%L7R as our 100% KIR binding. Representative figure of two experiments.

To test whether the antagonism effect observed was due to a preferential presentation of the L7D peptide resulting in a displacement of L7R, I analysed surface eluted peptides by HPLC (**Figure 3-18)**. $2.5x10^6$ cells were pulsed overnight with 20μM final concentration of peptide. Cells were collected, an aliquot reserved for HLA-C staining and peptides were eluted from the remainder of the sample using citrate buffer (**Figure 3-18**). I used synthetic peptides diluted in 1X PBS at a concentration of 0.2μM as a positive control.

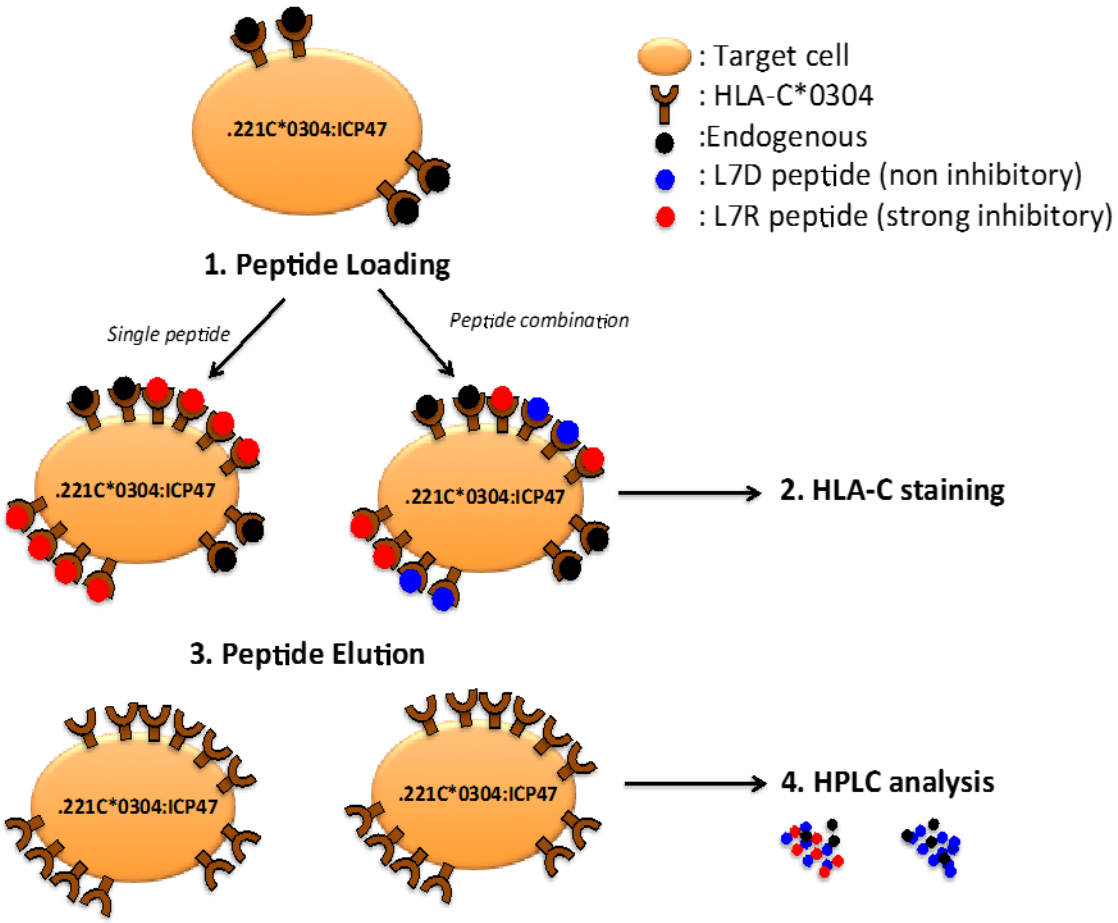

Figure 3-18: Peptide elution and HPLC analysis steps. 721.221Cw0304-ICP47 cells were loaded with a single peptide or a combination of L7F + L7D or L7R + L7D (step 1). Peptide stabilisation was assessed by staining for HLA-C (step 2). Eluted peptides were analysed via HPLC (step 3) under a gradient from 4% to 60% solvent B (organic solvent composed of 80%ACN+20%H_2O+0.05%TFA).

DT9 staining showed an effective stabilization of HLA-C expression on the cell surface after 16 hours (overnight incubation) of peptide loading (**Figure 3-19 A**). MFI

values more than doubled from 8,000 in absence of peptide up to 17,000 to 18,000 after peptide loading indicating an adequate stabilization. MFI values (8,824 in absence of peptide against around 17,000 in presence of peptide) were almost similar when cells were pulsed with a single peptide or with two peptides combined with all conditions having a final peptide concentration of 20μM. HPLC results confirmed that loaded peptides were presented at the cell surface (**Figure 3-19 B**). When L7R+L7D or L7F+L7D were mixed, both peptides were detectable after acid elution as indicated by the arrows. Furthermore the peak height showed that peptides in combination were similarly loaded onto HLA-C. This experiment demonstrated that peptide antagonism was not due to displacement of the strong inhibitory peptide but was due to the presence of the weak KIR binding peptide.

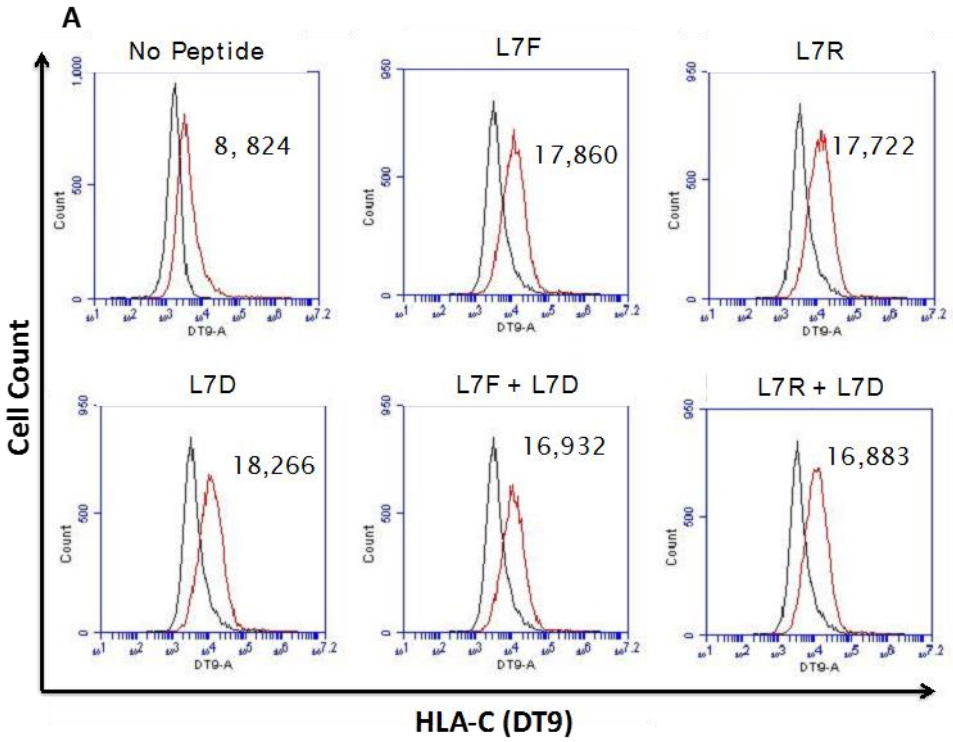

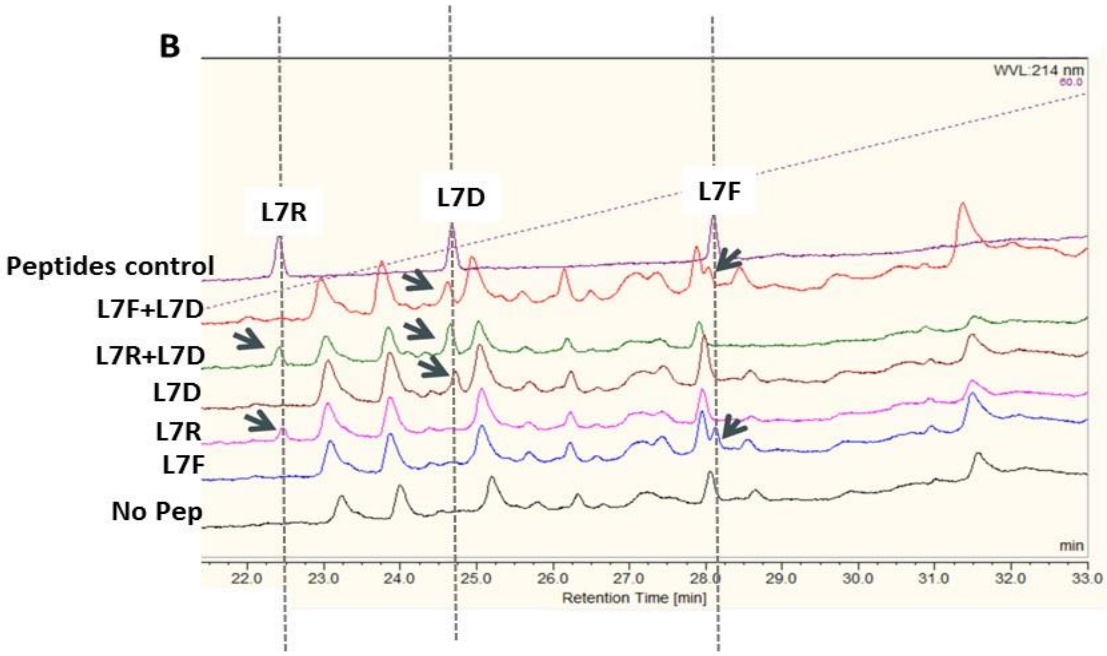

Figure 3-19: HLA-C expression of peptides pulsed 721.221C*0304-ICP47 cells after stabilization and prior peptide elution and HPLC analysis of eluates form mild acid elution of presented peptides completed with HLA-C staining. (A) 721.221Cw0304-ICP47 cells were loaded with single peptides or a combination of L7F + L7D or L7R + L7D. Cells were stained for DT9 to determine HLA-C stable expression before mild acid elution. The "no peptide" condition is compared to unstained cells; all other conditions are compared to the "no peptide" condition. Numbers indicate MFI of DT9 staining. (B) Eluted peptides were analysed via HPLC under a gradient from 4% to 60% solvent B (organic solvent containing 80% ACN).

3.11 L7D disrupt KIR clustering at the immunological synapse

Previous work has shown that an antagonist peptide disrupts KIR clustering at the immune synapse. As effector cells I used the NKL2DL3 cell line which had been transfected with GFP-KIR. These effectors were co-incubated with 721.221C*0304-ICP47 cells that had been pulsed with 200μM of peptide.

For each condition between 20 and 30 conjugates were analysed. The fold increase in fluorescence intensity at the interface between the NKL2DL3-GFP effector cells and peptide pulsed target cells was compared to a noncontact area of the NKL2DL3-GFP cell membrane. L7R induced clustering of KIR while L7D disrupted the clustering due to L7R (**Figure 3-20 A and B**). As seen in **Figure 3-20 C**, the percentage of conjugates with aggregation of KIR2DL3 was higher in the target cells pulsed with L7R (≥80%)

compared to target cell pulsed with L7D (≤40%) or a combination of L7R and L7D (≤40%). This differences in GFP fold increase between L7R and L7R+L7D synapses ($p<0.0001$) were statically significant as well as percentage of conjugate presenting a GFP fold increase superior to 2.5 ($p<0.01$).

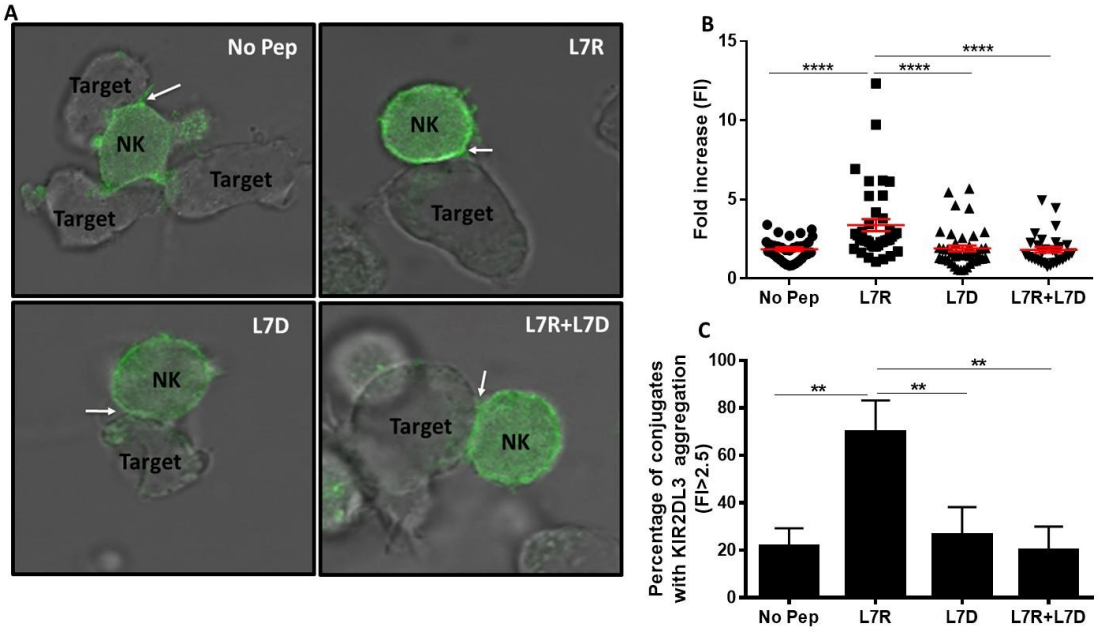

Figure 3-20: Clustering of KIR2DL3 at the surface between target and effector cells due to L7R. (A) KIRDL3 clustering at the interface between 721.221C*0304-ICP47 target cells loaded with 12.5μM of indicated peptides and NKL2DL3-GFP cells. Unpulsed target cells condition (No Peptide) was used as control. Arrows indicate the interface between target and effector cells. (B) The fold increase in GFP fluorescence intensity at the interface between target and effector cells was compared with a noncontact area of the NKL2DL3 GFP cell membrane. (C) The percentage of conjugates with aggregation of KIR2DL3 in each sample was analysed. A total of 145 conjugates were analysed. L7R was compared to other condition using a one way Anova **** $p<0.0001$, ** $p<0.01$.

3.12 Endogenous presentation of L7R (agonist) and L7D (antagonist) peptides

To investigate the possibility that an antagonistic peptide can be endogenously presented and reverse inhibition, I generated minigenes that encode an antagonistic peptide and introduced it into a cell that inhibited NK cells.

I generated two constructs in pcDNA6: one expressing L7D and one expressing L7R. pcDNA6 (**Figure 3-21 A**) was digested by two restriction enzymes: HindIII and EcoR1 within the multi cloning site (MCS) in order to remove *HLA-B*2705* gene.

Undigested and double digested DNA vector were run on 2% DNA gel (**Figure 3-21 B**) and showed an effective double digestion of the vector with the upper band corresponding to the vector and the lower band corresponding to HLA-*B*2705* gene. Digested vector was then gel purified and used for ligation. After ligation, the plasmid obtained was transformed into bacteria, extracted and sequenced in order to confirm the presence of the minigene coding for the peptide of interest.

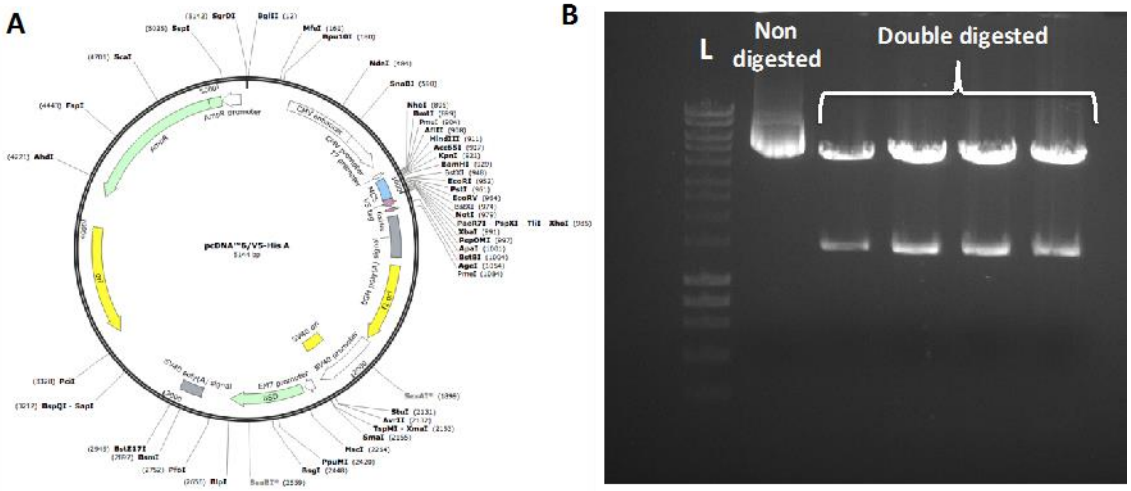

Figure 3-21: pcDNA6 map and agarose gel of pcDNA6 digestion by restriction enzymes. (A) pcDNA6 vector map. (B) DNA gel after vector digestion.

I simultaneously electroporated target cells with the plasmid containing the minigenes (pcDNA6+/- L7D or L7R) in combination with a plasmid containing a GFP reporter gene (pmaxGFP® vector). This strategy aimed to help to perform cytotoxicity assays at 48 hours after transient transfection using the GFP as a marker for minigene expressing cells in order to segregate target cells from effector cells.

Minigene constructs were then electroporated in 721.221C*0304 cells. 24hrs after electroporation, 22 to 36% of cells express GFP which indicating a good transfection efficiency (**Figure 3-22 A**). Then the viability as of electroporated cells and GFP expression were monitored from 24h up to seven days (**Figure 3-22 B**). Results showed that electroporated cells recovery ranged from 20% to 50% but GFP expression tended to decrease with time (from 30% to less than 2%). These preliminary results demonstrated that electroporated cells with two plasmids can be used as transient transfectants for functional assays, between 24 and 72hrs post electroporation. In initial cytotoxicity assays, double transfected cells tended to lose the GFP plasmid after encountering effector which have made data analysis and interpretation difficult. I therefore proceeded to make stable transfectants.

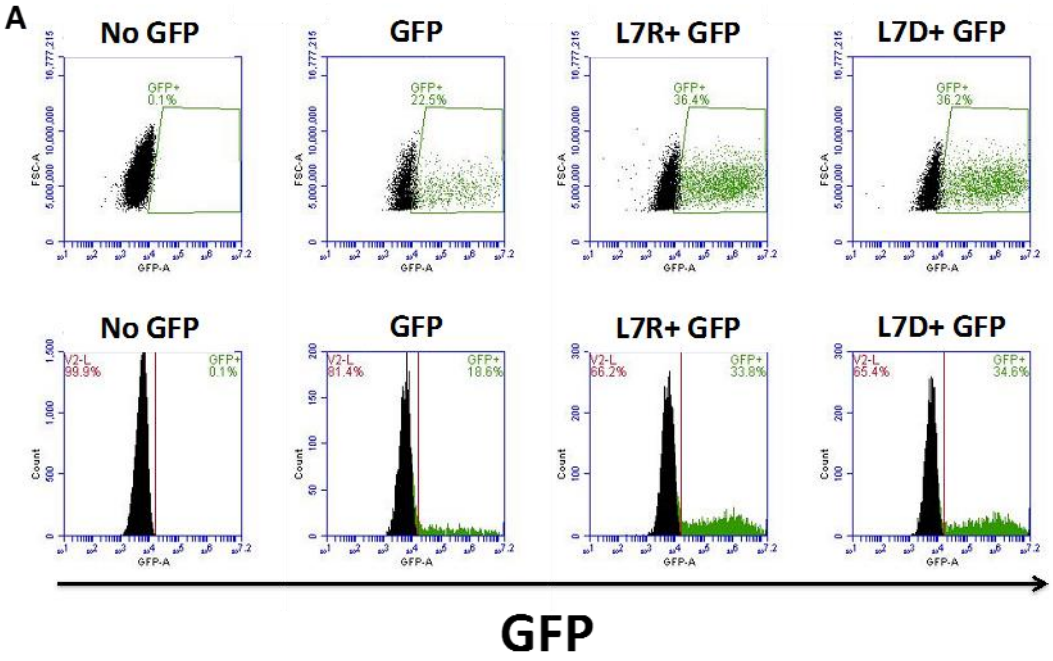

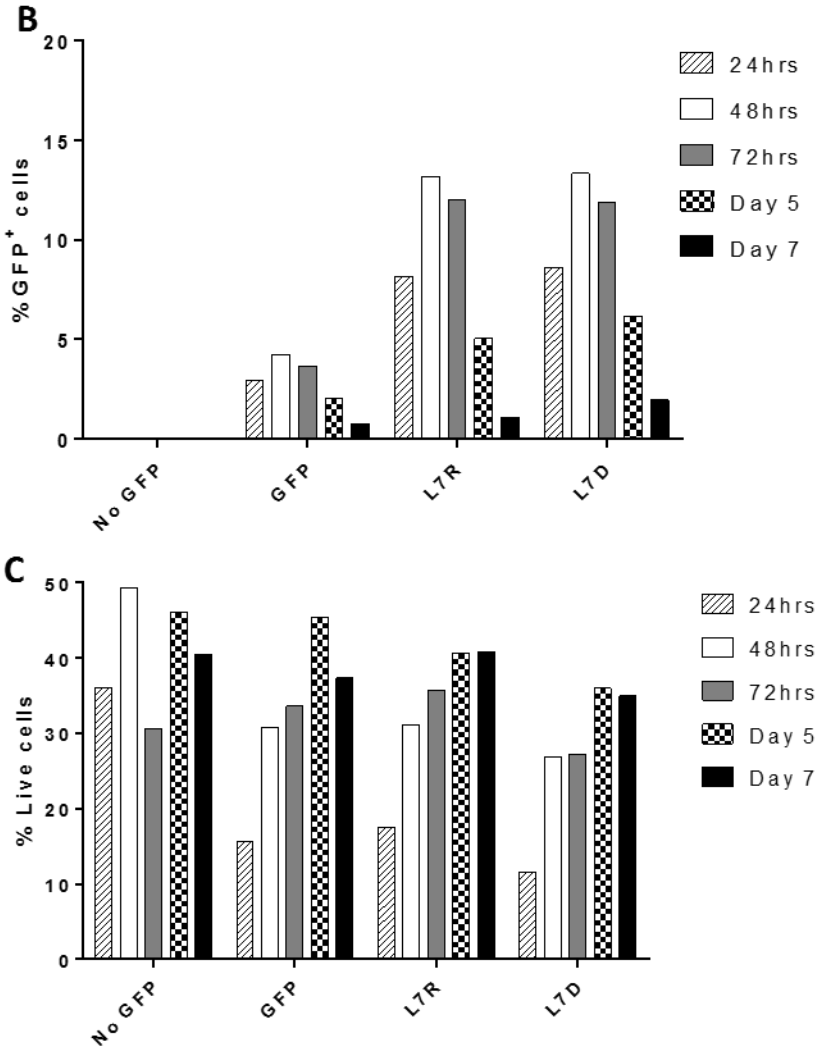

Figure 3-22: GFP expression and cell viability monitoring after electroporation. 721.221C*0304 cells were electroporated with a total of 10μg of DNA. 7.5μg of pcDNA6 containing the minigene and 2.5μg of plasmid containing GFP gene. From 24hrs up to seven days after electroporation, 10 000 cell analysed by flow cytometry. (A-B) Results are shown in dot plots regarding GFP expression and sum up in bar chart. (C) Cell viability was also was also monitored at the same time for the same period of time.

3.13 Endogenously presented L7D (antagonist) peptide induces antagonism

In order to generate stable transfectants, I electroporated C*0304 with a total of 50μg of DNA and selected using blasticidin. Untransfected cells were used as a control to monitor the efficiency of the selection (**Figure 3-23**). After D0 (24hrs after

electroporation), transfected cells expanded while un-transfected cells did not expand under selection. After four days (D4) post selection, transfected cells had expanded while marked cell death was observed in the un-transfected culture.

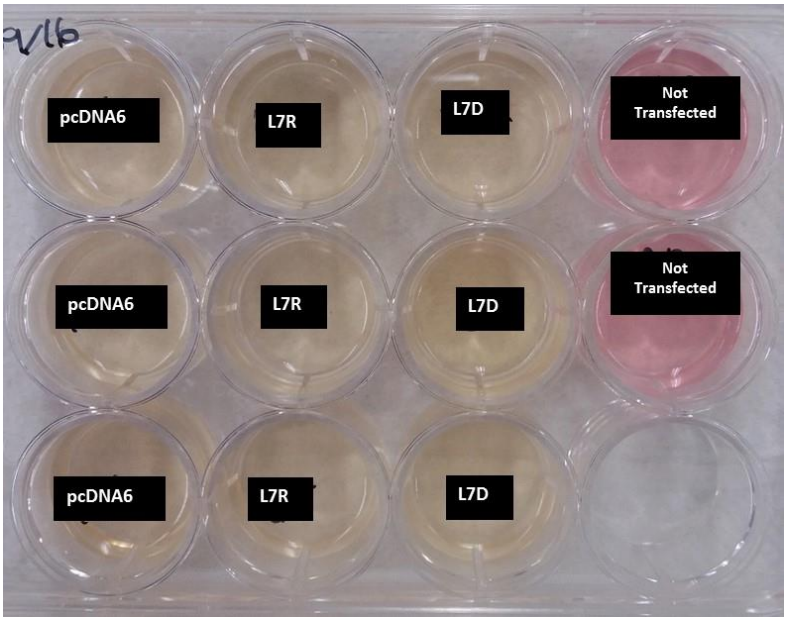

Figure 3-23: C*0304 cells transfection with minigenes constructs using electroporation method. $3x10^6$ cells per well were used for the transfection by electroporation. 50μg of each DNA (pcDNA 6, L7R and L7D) were used and 24hrs after transfection cells were selected with Blasticidin for over two weeks before use as targets.

I tested minigenes expressing targets cells in CD107a assays focusing on $CD3^-CD56^+CD158b^+$ ($KIR2DL2/L3^+$) and $CD3^-CD56^+CD158b^-$ ($KIR2DL2/L3^-$) NK cells. Cells containing the empty vector (pcDNA), as well as cells containing L7R (pcDNA_L7R) have an inhibitory peptide repertoire while cells containing pcDNA6_L7D were predicted to have a less inhibitory peptide repertoire.

Figure 3-24 A shows the gating strategy used to analyse the effect of each target cells. 721.221 and 721.221C*0304 were respectively used as positive and negative controls for the degranulation. 721.221 cells did induce degranulation of $KIR2DL2/L3^+$ NK cells and 721.221C*0304 did inhibit it. **Figure 3-24 B** shows the effect of minigenes induced peptide repertoire on NK cell reactivity of one representative donor.

Using the minigenes, analysis of the degranulation among the KIR2DL2/L3$^-$ NK cells have revealed no significant differences in term of degranulation. The CD107a was repeated in eleven different donors. In overall, the effect of the minigenes on NK cells reactivity were not statistically significant despite the slight reversal observed among few donors (**Figure 3-24 C-D**). Possibly the levels of expression of the minigenes was not sufficient to affect the peptide repertoire. Alternatively, using these target cells could be used to test a more homogenous population of NK cells could help to understand the effect of this constructs.

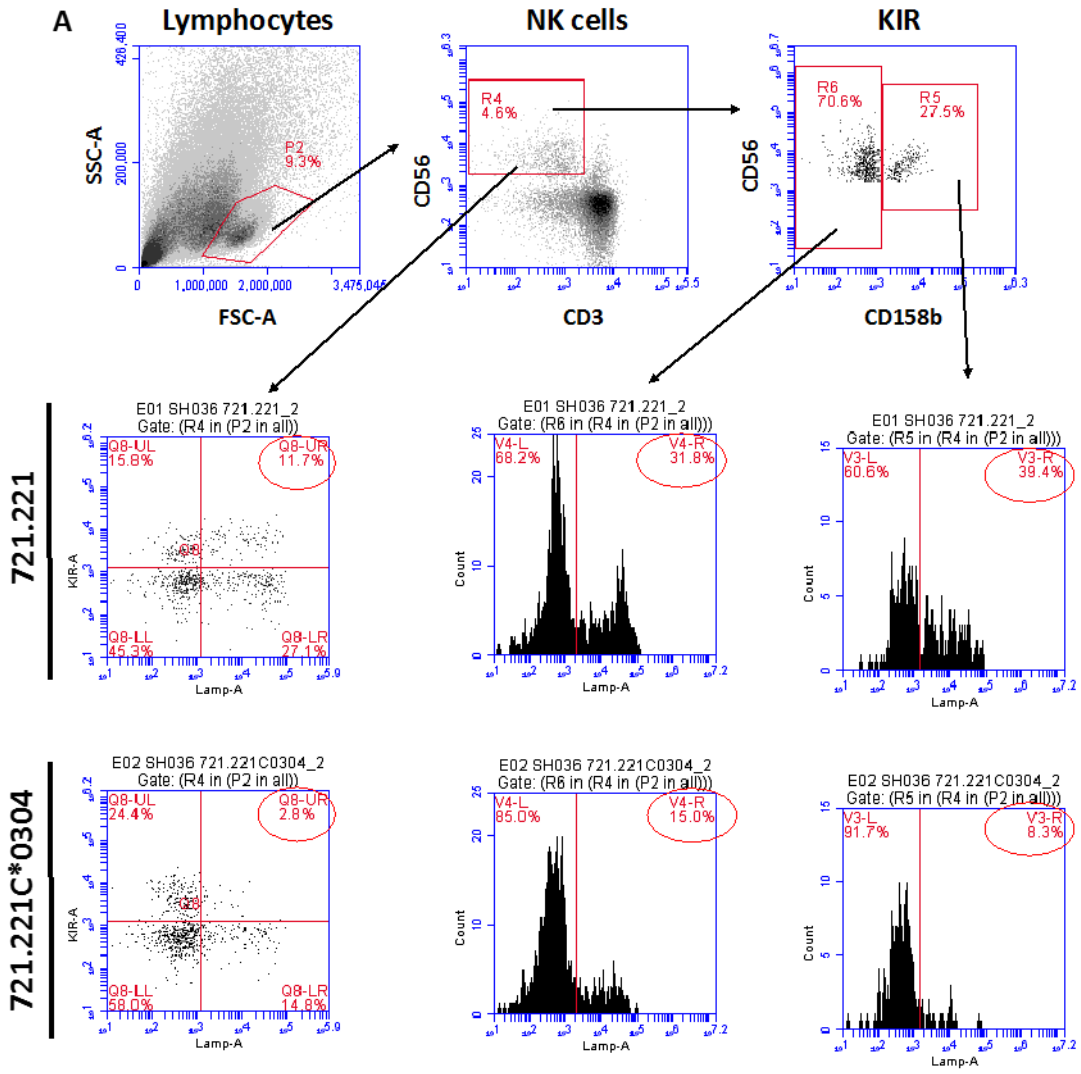

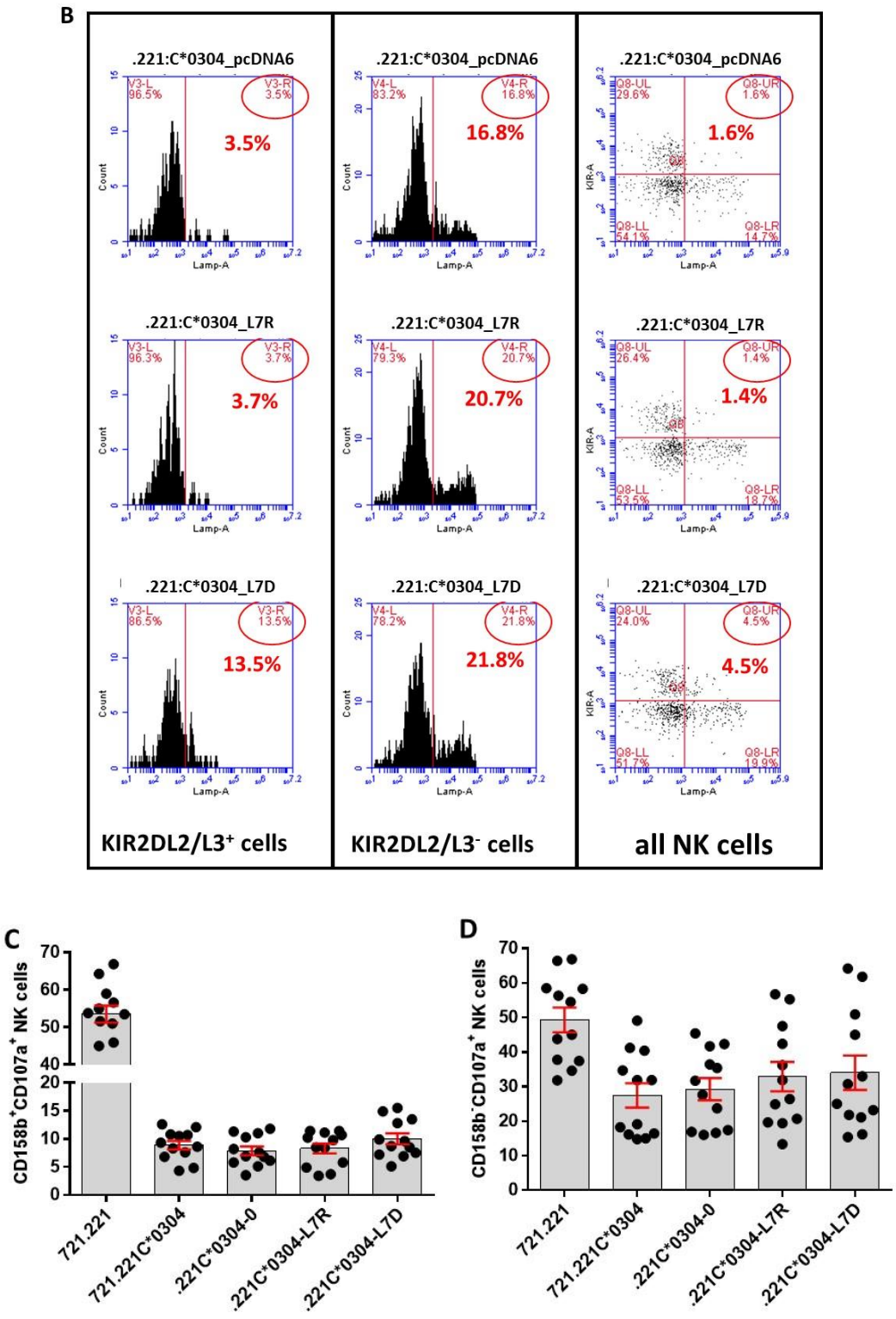

Figure 3-24: CD107a of NK cells using endogenously presented peptides. (A) Gating strategy for the degranulation analysis. 721.221 and C*0304 are used as negative and positive controls respectively. (B) Representative experiment of degranulation from NK cells after co-culture with minigenes transfected cells. Analysis of KIR positive and KIR negative populations. (C) and (D) Summary of NK cell degranulation within $CD158b^{+}$ and $CD158b^{-}$ population, n=12 donors.

As CD107a did not help to clearly evaluate the effect of our different minigenes constructs on NK cells reactivity, I tried an alternative strategy using the NKL-2DL3 cells and as effectors in a flow cytometry based cytotoxicity assay (figure). Effector to target (E:T) ratios of up to 30:1 were used.

I calculated the percentage of cytotoxicity (**Figures 3-25 D**) with the following formula:

[(Control – Test)/Control] x 100 = % of Cytotoxicity

Control = $GFP^{-}Pi^{-}$ cells / total GFP^{-} cells → in Control samples

Test = $GFP^{-}Pi^{-}$ cells / total GFP^{-} cells → in Test samples

In overall, cytotoxicity towards target cells transfected with L7D minigene construct (C*0304_L7D) was higher compared to cytotoxicity towards target cells transfected with L7R minigene (C*0304_L7R) or the empty vector (C*0304_pcDNA6).

To summarize, difference observed between the different constructs raise the question of the efficiency of endogenous presentation using the minigene strategy.

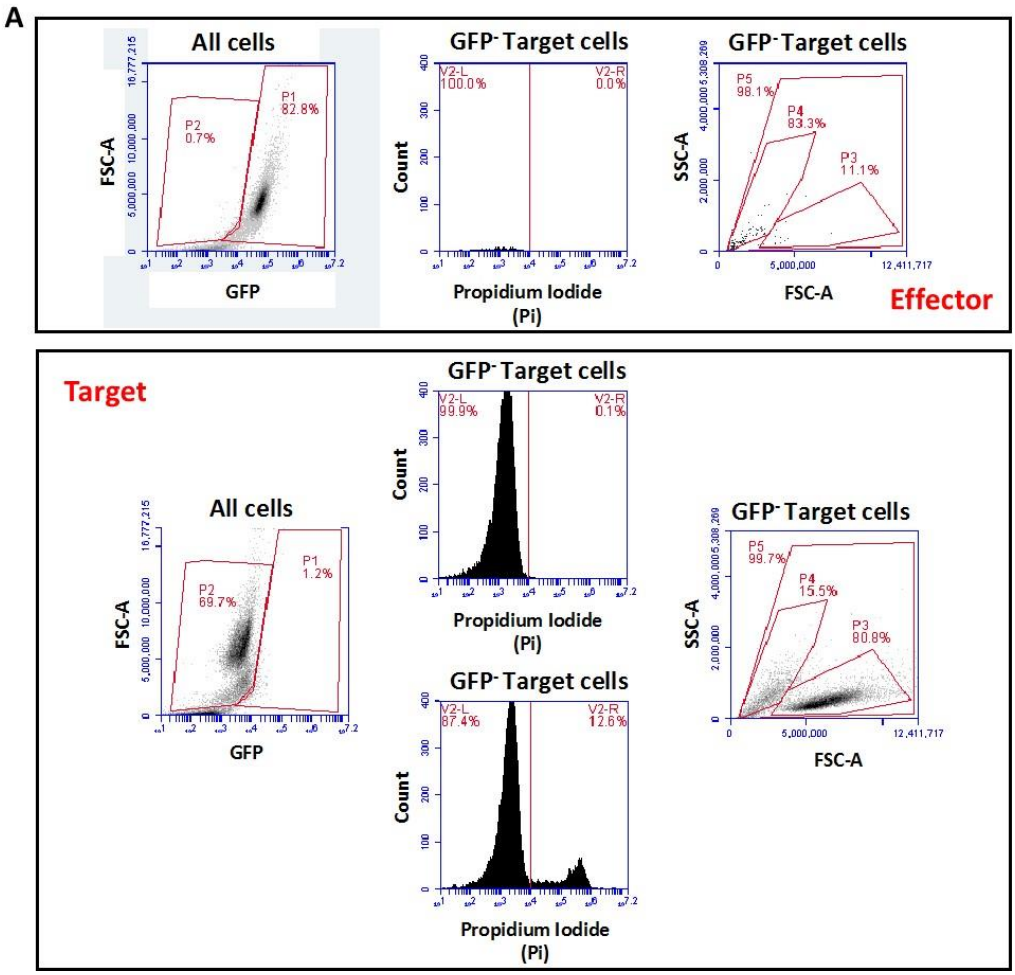
A
All cells
FSC-A
GFP
P1
82.8%
P2
0.7%
GFP- Target cells
Count
Propidium Iodide
(Pi)
V2-L
100.0%
V2-R
0.0%
GFP- Target cells
SSC-A
FSC-A
P5
98.1%
P4
83.3%
P3
11.1%
Effector
Target
All cells
FSC-A
GFP
P1
1.2%
P2
69.7%
GFP- Target cells
Count
Propidium Iodide
(Pi)
V2-L
99.9%
V2-R
0.1%
GFP- Target cells
SSC-A
FSC-A
P5
99.7%
P4
15.5%
P3
80.8%
GFP- Target cells
Count
Propidium Iodide
(Pi)
V2-L
87.4%
V2-R
12.6%

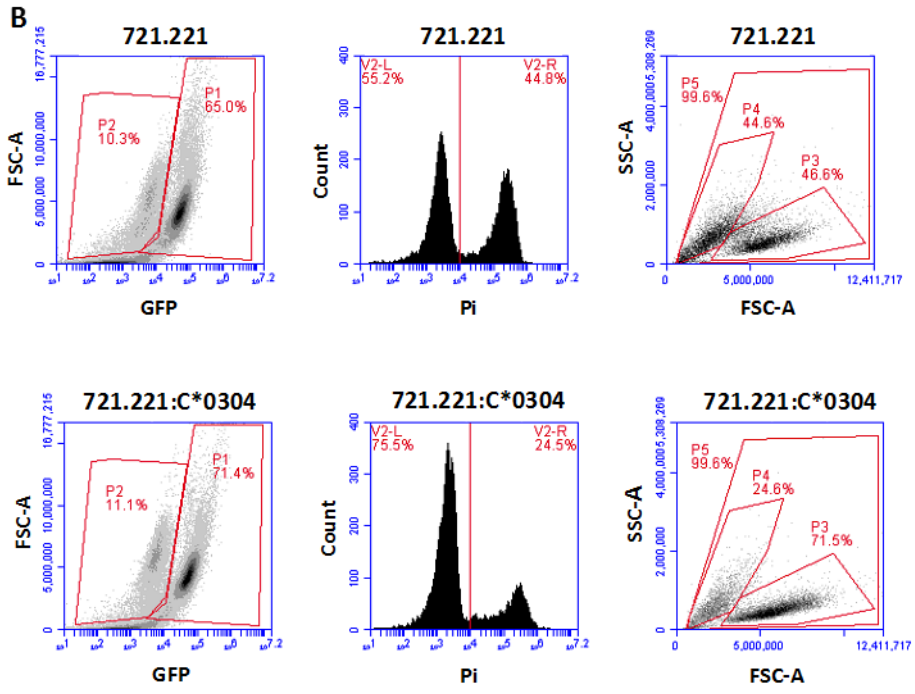
B
721.221
FSC-A
GFP
P1
65.0%
P2
10.3%
721.221
Count
Pi
V2-L
55.2%
V2-R
44.8%
721.221
SSC-A
FSC-A
P5
99.6%
P4
44.6%
P3
46.6%
721.221:C*0304
FSC-A
GFP
P1
71.4%
P2
11.1%
721.221:C*0304
Count
Pi
V2-L
75.5%
V2-R
24.5%
721.221:C*0304
SSC-A
FSC-A
P5
99.6%
P4
24.6%
P3
71.5%

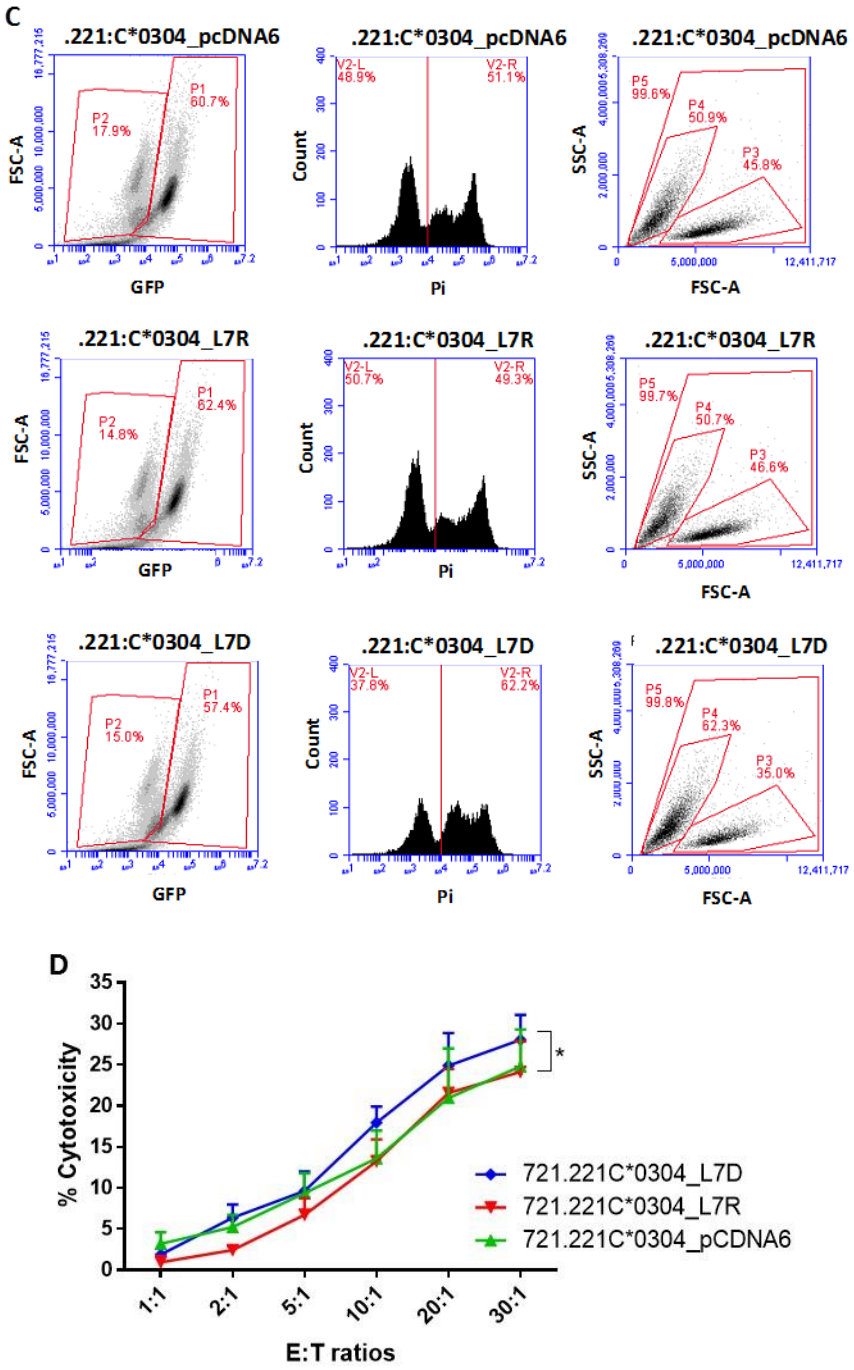

Figure 3-25: Killing of minigenes transfected target cells by NKL2DL3. (A) Gating strategy for the identification of effector and target cells among the mixture according to the GFP expression effector cells. (B) 721.221 and C*0304 are used as negative and positive controls respectively. (C) Representative experiment of the killing of target cells at E:T = 10:1 by NKL2DL3 cells after co-culture. Analysis of Pi staining and proportion of live and dead cells within the target cell population. (D) Percentage of cytotoxicity. *p=0.0117 using one way Anova (n=3).

3.14 Discussion

Peptide antagonism of MHC class I provides an alternative mechanism for releasing KIR2DL2/3-positive NK cell from inhibition. In fact, this mechanism is based on the release of NK cells from inhibition through inhibitory receptors. This occurs when a weak KIR binding peptide disrupts the inhibitory signalling of a strong binding peptide. Peptide antagonism has only been defined for HLA-C*0102, an allele that is endogenously expressed in TAP-deficient cells, using the peptide variants of VAPWNSLSL: VAPWNS**DA**L and VAPWNS**DY**L. I studied HLA-C*0304 to determine whether this phenomenon can be generalizable to other group 1 HLA-C alleles.

721.221 cells were transduced with HLA-C*0304 and transfected with ICP47 used for peptide loading and as target cells in CD107a assays. I studied previously described position 8 (P8) derivatives of the endogenously processed peptide GAVDPLLAL with a defined range of affinities for KIR2DL2 (9.5 to >600μM). All variants stabilised HLA-C*0304 equally and presented an inhibition hierarchy which correlated with their affinity for KIR. However, no antagonism was observed using combinations of peptides with high and low KIR affinities. Additionally, using HLA-C*0102 peptides derivatives having a modification at P8, I was able to show that we can also identify null peptide in VAP-LY.
As position 7 (P7) of the peptide sequence is known to impact the KIR binding, a new series of P7 derivatives, L7R, L7F and L7D were made. Although these peptides variants did stabilise HLA-C expression at the cell surface, KIR-Fc binding assay have shown that they had different affinities for KIR. Here I used KIR2DL2-Fc construct, as it was available to us. KIR2DL3-Fc construct could have been used as well. But it doesn't make a difference as KIR2DL2 and KIR2DL3 both recognise HLA-C*0304. However it has been several time reported that KIRD2L2 binds strongly to HLA-C: peptide complex compared to KIR2DL3 (293).

In contrast to our observations for HLA-C*0102, arginine at P7 triggered stronger inhibition than phenylalanine. L7D did not inhibit KIR2DL2/3-positive NK cells, but did antagonise inhibition by L7R in CD107a assays. Moreover, peptide elution and HPLC analysis have helped to demonstrate that peptide antagonism was not related to displacement of L7R or L7F by L7D. Additionally inhibitory KIR clustering analysis have shown that L7R induced receptor clustering at the immunological synapse while L7D disrupted the clustering. These results have together helped to confirm data

obtained in the functional assay by underlining the involvement of the receptor organisation at the synapse during the processes of inhibition.

The effect of L7D was further studied by combining the KIR binding with the degranulation assay. Mixture of L7R and L7D released NK cell from the inhibition as known and this phenomenon was associated with the loss of the KIR-Fc binding. This results have revealed that L7D peptide may be involved in the peptides distribution at the cell surface which then impaired the binding of the fusion construct. I have demonstrated that the release of NK cells from their inhibition in the presence of the antagonist peptide, is not due to the loss of HLA-C expression but is due to a loss of KIR binding hence the degranulation of the NKs. Indeed, after peptide loading, the strong KIR binder peptide have induced a strong binging of the fusion construct. When L7D was introduced, the binding of the fusion construct was prevented. L7D itself was not recognised by the fusion construct (due to the substitution by an aspartic acid, D at position 7). Mechanistically, it seemed that L7D has changed the cell surface organisation or distribution of the strong KIR binder peptide leading to the loss of the fusion construct binding. Alternative assays involving confocal or live microscopy can help to understand how the antagonistic peptide change the peptide rearrangement at the synapse. Furthermore these techniques will help to visualise and understand NK reactivity when it encounter target cells presenting an antagonistic peptide.

Preliminary experiments using minigenes constructs did not reflect endogenous effect of the antagonistic peptide. Differences between cells containing or not the antagonistic were not significant. Therefore, enhancing and adjusting the level of integration of plasmid containing the antagonistic peptide could improve these preliminary data.

Overall, I have shown here that peptide antagonism is not restricted to one HLA-C allele, but is likely to be a more generalizable phenomenon for KIR2DL2/3 and P7 residue appears more important than P8 in defining an antagonist peptide.

4. A Granzyme B assay: a novel functional assay to measure NK cells activation

The aim of the granzyme B (GzmB) assay was to be able to screen a high number of peptide variants in order to uncover variants that can potentially activate NK cells either through activating or inhibitory receptors. Functional assays such as lactate dehydrogenase (LDH) or CD107a have not allowed us to assess NKL cell activation, as the NKL cell line does not respond at 26˚C as well as at 37˚C.

4.1 Principle of Granzyme B Assay, an HPLC based assay

As described in **Figure 4-1**, selected peptide variants are loaded onto targets cells at 26°C overnight and then co-cultured with NKL cells at 26°C. Supernatants are harvested and tested for Granzyme B (GzmB) production using a peptide that can be cleaved by the GzmB presents in the medium. The Caspase 3 peptide (C3P) with the following full sequence YYGI**ETDSG**VDDYY carries a GzmB cleavage sequence which is between the indicated Aspartic Acid (D) and Serine (S) residues (underlined residues). In the presence of GzmB enzyme, this peptide is cleaved into two distinct products (YYGI**ETD** and **SG**VDDYY) that can be detected at different retention times compared to the original peptide itself. Therefore, C3P degradation can be assessed by HPLC.

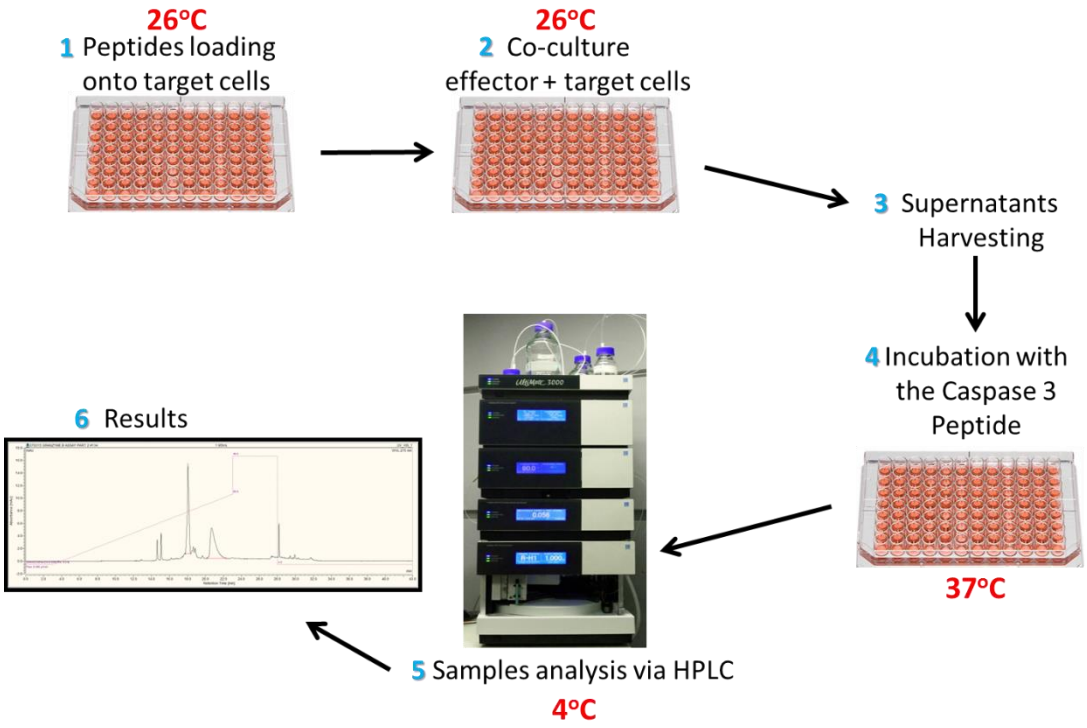

Figure 4-1: Worflow and principle of the Granzyme B Assay. Peptides are loaded onto target cells then both target and effector cells (NK lines) are cultured at 26°C for 5hrs. Supernatants from the co-culture are incubated with the Caspase 3 Peptide (C3P) at 37°C. HPLC analysis is carried at 4°C to prevent further peptide degradation during the analysis.

4.2 Definition of the wavelength for peptide product detection

The first step for the development of this assay was to test the detection of the C3P by the HPLC system. To evaluate this, we tested five different wavelengths (250, 260, 270, 280 and 290nm) using three different quantities of C3P: 3, 10 and 100pmol (**Figure 4-2**). These preliminary results informed us that the peptide can be detected with our system at a wavelength comprised between 270 and 280nm.

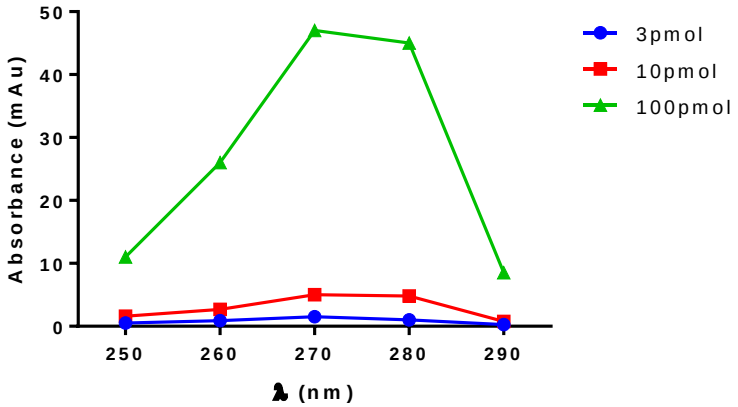

Figure 4-2: Absorbance of C3P quantities at 5 different wavelengths (250, 260, 270, 280 and 290nm). Representation of absorbance in milliAbsorbance unit (mAU) obtained according to Caspase 3 Peptide (C3P) quantities and wavelengths under a gradient from 4% to 60% solvent B (organic solvent)

Then we ran different concentrations from 3.9pmol to 2000pmol of the C3P using four different wavelengths simultaneously (270, 275, 280 and 290nm). This showed that we can detect amounts ranging from 3.9pmol to 2000pmol (**Figure 4-3 and Figure 4-4**). Secondly, 275nm is the optimal wavelength for detection of this peptide. Indeed, for all concentrations tested, 275nm gave us the optimal detection of the peptide compared to 270, 280 and 290nm.

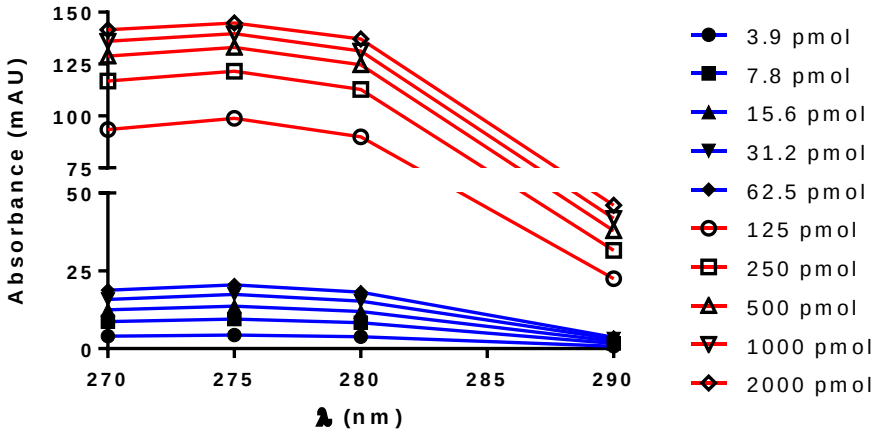

Figure 4-3: Absorbance of C3P quantities at four different wavelengths. Representation of absorbance in miliAbsorbance unit (mAU) obtained according to Caspase 3 Peptide (C3P) quantities and wavelengths tested under a gradient from 4% to 60% solvent B (organic solvent).

Chromatograms of peak profiles at 275nm (**Figure 4-4**), allowed us to define peak shapes for all quantities tested. **Figure 4-4** is an example of the peak profiles at 275nm. We observed that the more peptide we injected, the wider the peak was (500, 1000 and 2000pmol) and the opposite was observed for lower quantities. Furthermore retention time was consistently found to be between 17.5 and 18min and were consistent between injections (**Figure 4-4**).

This experiment showed that 275nm gave the optimal reading and therefore was used for future experiments. Finally, we decided to use quantities of C3P between 150 and 500pmol in the assay as chromatograms showed a better profile with theses quantities.

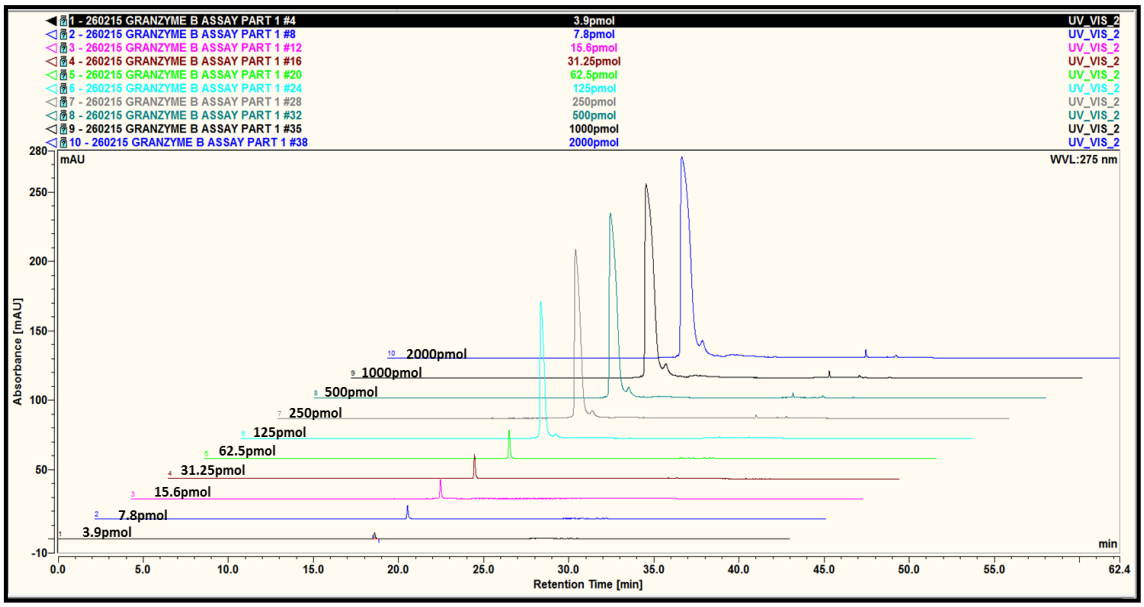

Figure 4-4: HPLC profiles of samples at a wavelength of 275nm. Assessment of various quantities of Caspase 3 Peptide at λ=275nm under a gradient from 4% to 60% solvent B (organic solvent).

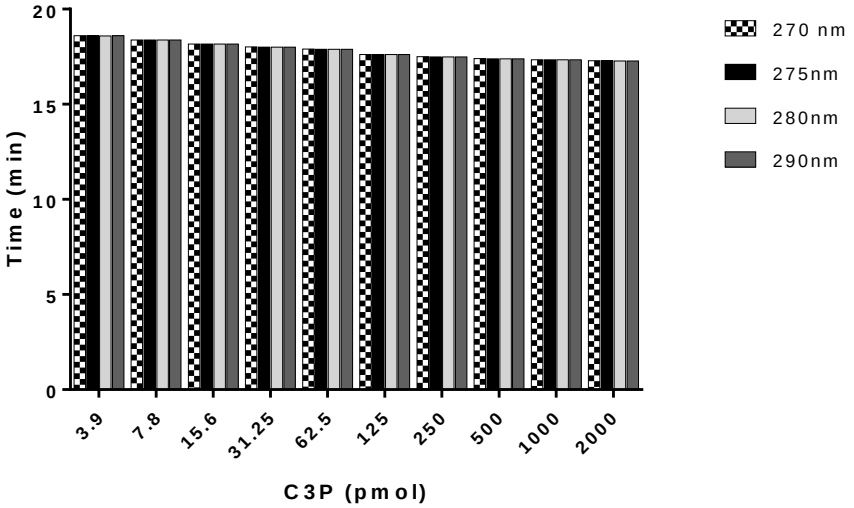

Figure 4-5: Retention times in minute of different quantities of C3P injected and tested at 4 different wavelengths (270, 275, 280 and 290nm). Representation of various quantities of C3P showing the reproducibility of sample injections.

4.3 Recombinant human Granzyme B (rhGzmB) induces C3 degradation

After testing UHPLC settings and C3P quantities, we investigated whether our designed peptide could be cleaved by a recombinant human Granzyme (rhGzmB) enzyme. This second experiment was also an opportunity to test different enzyme activities as well as C3P digestion efficiency within a certain period of time. We started by testing dilutions of the enzyme (rhGzmB) concentrations from $9.7x10^{-11}$ to 5U/µl and we evaluated C3P digestion efficiency from 1hr to 72hrs. This experiment showed that there is a limit of rhGzmB concentration at 0.25U/µl for peptide digestion (**Figure 4-6**). **Figure 4-6A** and **Figure 4-6B** show peak profiles of each sample after 72hrs of incubation. First, we observed that at higher concentration of enzyme, the signal from C3P decreased (**Figure 4-6A**) while the products from the digestion appeared (**Figure 4-6B**). To visualize products from C3P digestion, we zoomed in on the chromatogram by focusing in on the retention time of C3P products. Thus, **Figure 4-6B** consists of a zoom (from 400 to 960 seconds) of the chromatogram presented in **Figure 4-6A**. Finally, we also noticed that at each injection a peptide from the medium was also eluted around 28min (shown by an arrow in **Figure 4-6A**). This small peptide contained in the medium can be used as a standard. This peptide helped us to ensure that for each condition tested, the same amount of sample has been loaded. Here,

we observed that the peak height of this standard peptide is always the same for all samples tested. We assumed that the decrease in peak height of the C3P is exclusively due to its digestion by the rhGzmB and not due to a mistake during the loading. We considered this standard peptide as a "loading control".

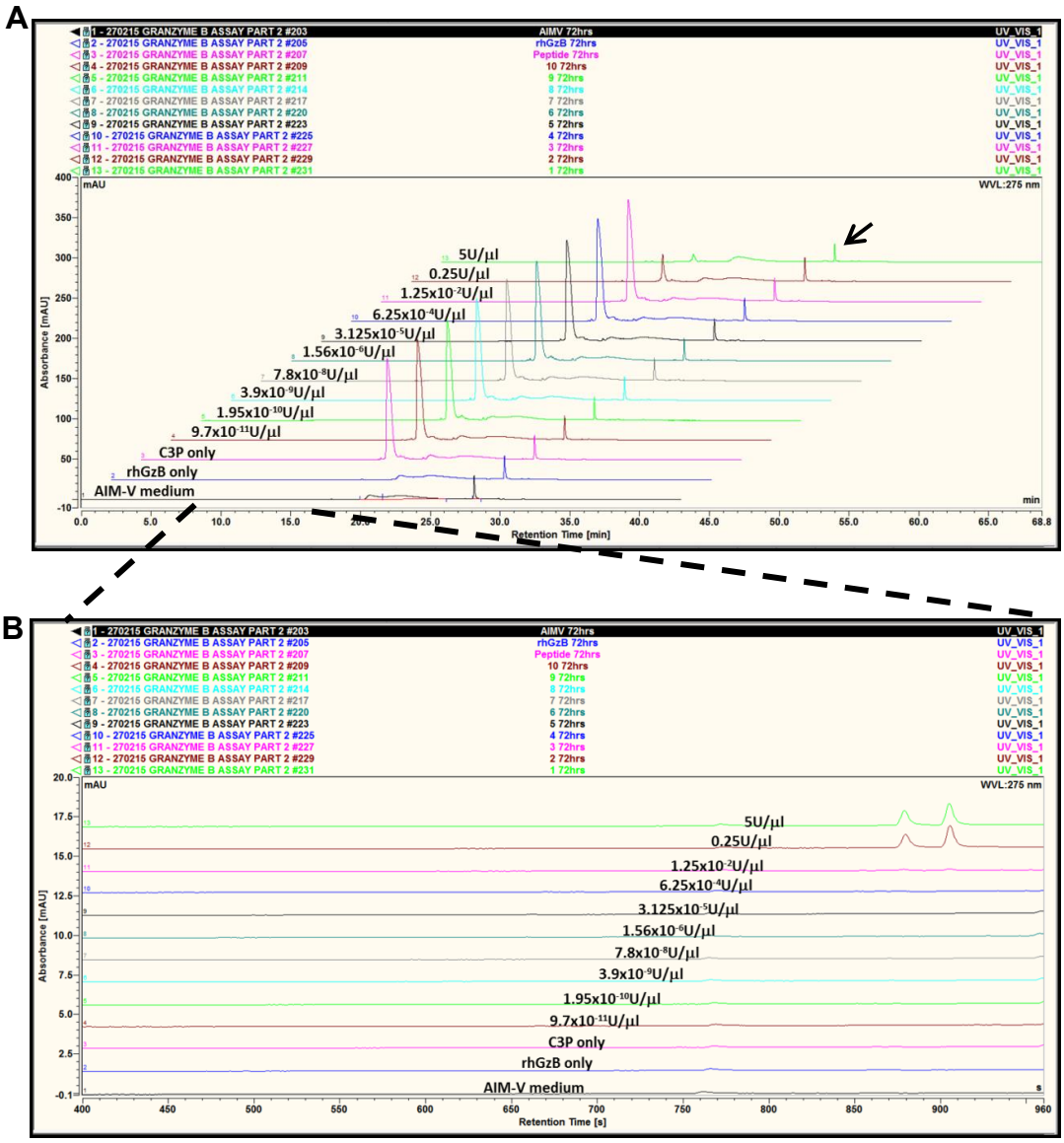

Figure 4-6: HPLC profiles of C3P after 72hrs of digestion using rhGzmB (A) and Zoom of HPLC profiles for products visualization (B). Assessment of C3P digestion under various rhGzmB concentrations (from $9.5x10^{-11}$/µl to 5U/µl). Reading at λ=275nm under a gradient from 4% to 60% solvent B (organic solvent) for 30min. Arrow indicates the "standard peptide" naturally presents in the AIM-V medium and which allowed us to verify that the same amount of sample have loaded into the HPLC from one condition to another (A). Second chromatogram (B) is the portion from 400 to 960seconds (6 to 15.8min) of the original profile and help to clearly visualize the products of the digestion.

Figure 4-7 summarises absorbance read out of the C3P peaks height after digestion by the rhGzmB, depending on the enzyme concentrations (from $9.7x10^{-11}$ to 5U/µl) and the time of incubation (from 1 to 72hrs).

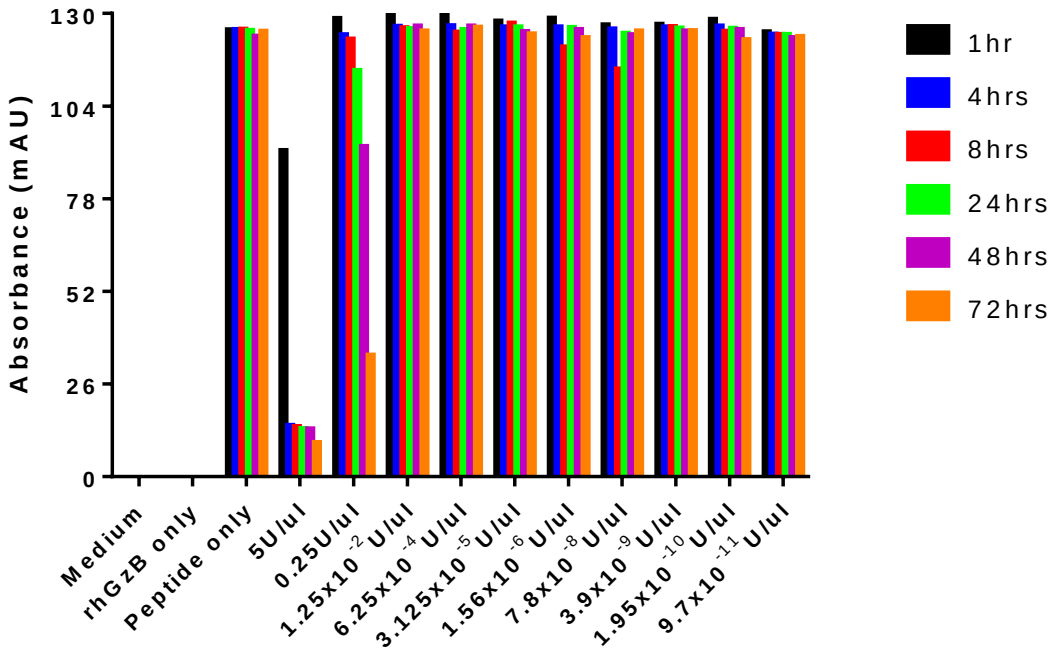

Figure 4-7: Absorbance of C3P after digestion using rhGzmB. Representation of absorbance in miliAbsorbance unit (mAU) of C3P obtained under a gradient from 4% to 60% solvent B (organic solvent) after incubation with rhGzmB for peptide digestion. Peptide digestion was assessed for 1, 4, 8, 24, 48, and 72 hr.

We next evaluated C3P digestion over a longer period of time (up to 95hrs) and we refined the assay to study a smaller window of enzyme concentrations (from 0.078U/µl up to 10U/µl). Consistent with our previous results, we observed that C3P cleavage was time dependant for enzyme concentrations lower than 10U/µl but happened after 24hrs of incubation with 10U/µl and tended to be steady after 48, 72 and 95hrs of incubation *(***Figure 4-8***)*. Chromatograms show how C3P peak is reduced (**Figure 4-8A**) and how the products of the digestion appear (**Figure 4-8B**). Here we chose to represent results obtained after 95hrs of incubation only because we can see the maximum effect of the rhGzmB on the C3P.

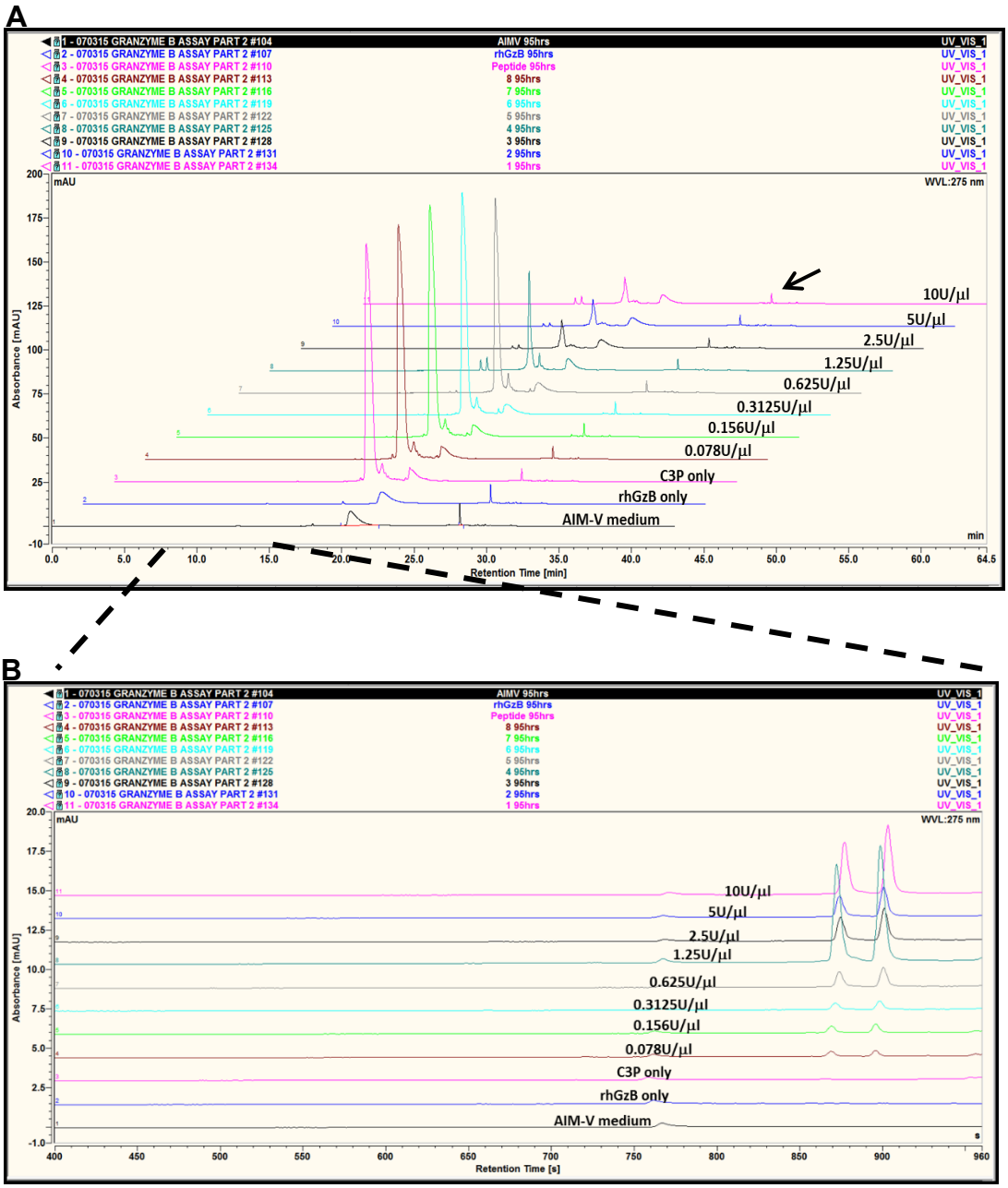

Figure 4-8: HPLC profiles of C3P after 95hrs of digestion using rhGzmB (A) and Zoom of HPLC profiles for products visualization (B). Assessment of C3P digestion under various rhGzmB concentrations (from 0.078U/µl to 10U/µl). Reading at λ=275nm under a gradient from 4% to 60% solvent B (organic solvent) for 30min. Arrow indicates the "standard peptide" naturally presents in the AIM-V medium and which allowed us to verify that the same amount of sample have loaded into the HPLC from one condition to another (A). Second chromatogram (B) is the portion from 400 to 960 seconds (6 to 15.8min) of the original profile and help to visualize the products of the digestion clearly.

As we have done for the previous experiment, we summarized all the data in order to show how the time and the enzyme concentration affect C3P digestion (**Figure 4-9**).

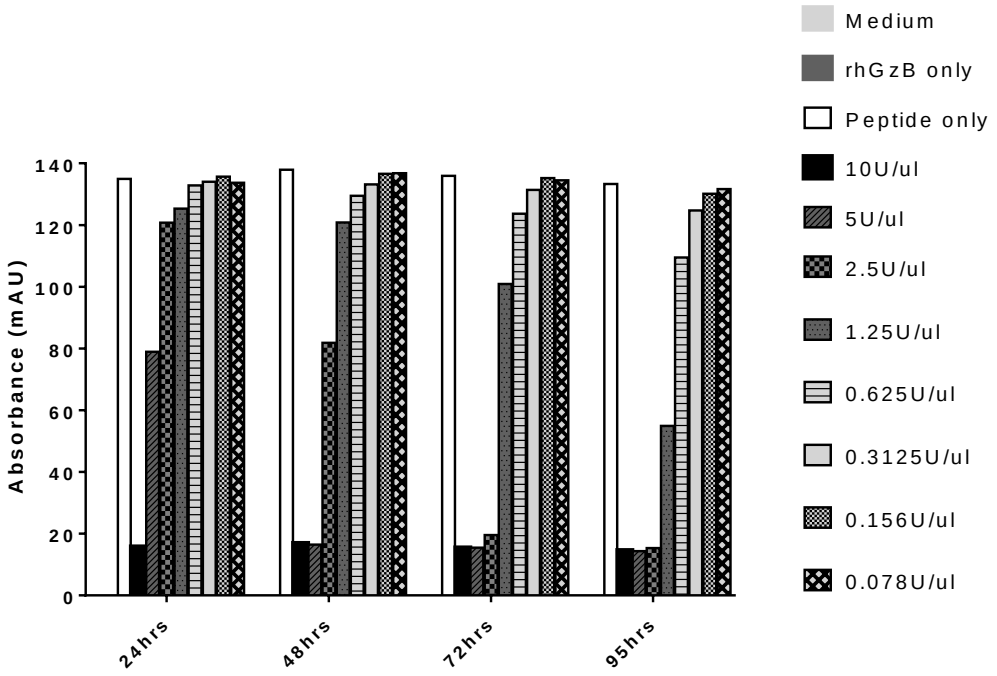

Figure 4-9: Absorbance of C3P after digestion using rhGzmB. Varying quantities of C3P were incubated with rhGzmB and analysed by HPLC under an organic gradient from 4% to 60% solvent B (organic solvent) after incubation with rhGzmB for peptide digestion. Peptide digestion was assessed for 24, 48, 72 and 95hrs.

4.4 Analysis of granzyme B (GzmB) produced after target and effector cell co-culture

To test whether we can detect GzmB produced by NK lines we co-incubated the C3P with supernatants from cell co-cultures. We used supernatants coming from co-culture between KIR2DL2 expressing NKL lines and the class I-negative 721.221 or HLA-C*0304 transduced 721.221C*03 cells. In these experiments we hypothesized that 721.221 should trigger NKL activation whilst 721.221C*03 should prevent NK activation due to the presence of HLA molecules on the cell surface and engagement of inhibitory KIR. Cells lines were stained for surface expression of molecules on interest before to be used following experiments which require effector and target cells.

As expected 721.221 cells did not express HLA-C while 721.221:C*0304 did (**Figure 4-10 A**). Effector cells expressed KIR molecules at their surface (**Figure 4-10 B-C**).

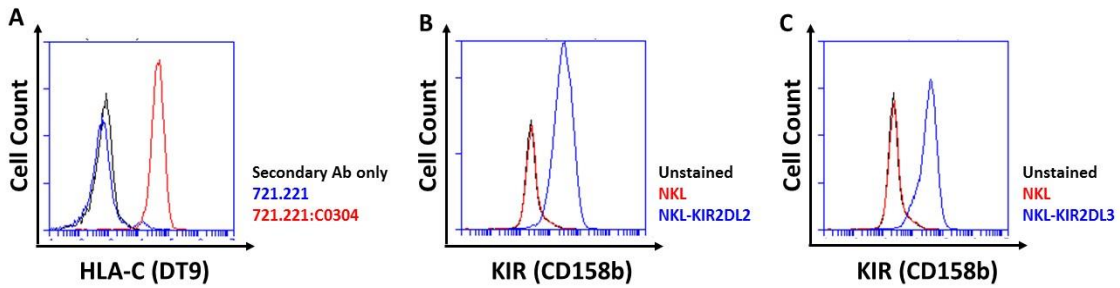

Figure 4-10: HLA-C and KIR expression on cells of interest. (A) HLA-C expression on target cells used as positive (721.221:C*0304) and negative (721.221) controls. (B) KIR staining on NKL2DL2 cells using CD158b antibody which recognise KIR2DL2/L3/S2. (C) KIR staining on NKL2DL2 cells.

C3P digestion was assessed for 24, 48, 72 and 95hrs after incubation at 37°C with the cell culture supernatant (**Figure 4-11 and Figure 4-12**).

Firstly, NKL-2DL2 cells alone did not produce GzmB. We noticed that co-culture of NKL-2DL2 cells with 721.221 cells induced GzmB production that efficiently digested the C3P to completion after 95hrs of incubation. Secondly, we observed that co-culture of NKL-2DL2 cells with 721.221:C*0304 cells induced GzmB production as well. However, digestion of the C3P was not as efficient as the digestion when we used supernatant from NKL-2DL2:721.221 co-cultures. Finally, we noticed that the NKL line alone didn't produce residual GzmB which will facilitate peptide screening for NK activation. Thus our preliminary results showed that NKL-2DL2 cells can be activated in presence of target cells put at 26°C. Furthermore, we noticed that targets cells alone can induce some C3P digestion which means that these cells alone in culture can produce substances that have the same enzymatic activity as GzmB.

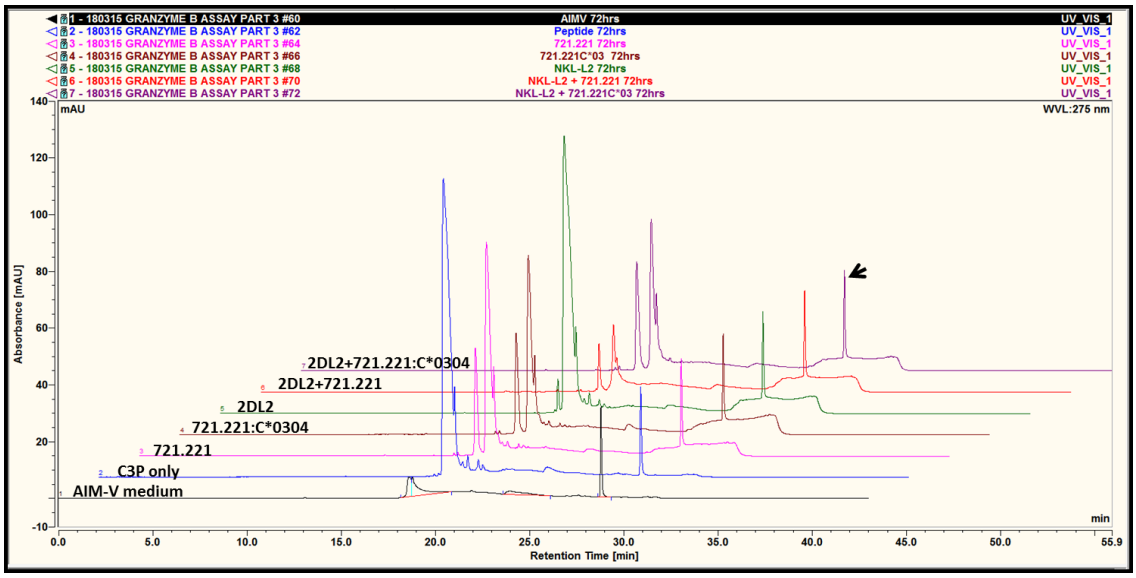

Figure 4-11: Chromatogram of C3P after 95hrs of incubation in supernatants obtained from co-culture between NKL2DL2 with or without 721.221 or 721.221:C*0304 cells. HPLC sample were analysed on a gradient from 4% to 60% solvent B (organic solvent). Arrow indicates peptide present in the AIM-V medium, which allowed us to verify that the same amount of sample have loaded into the HPLC from one condition to another.

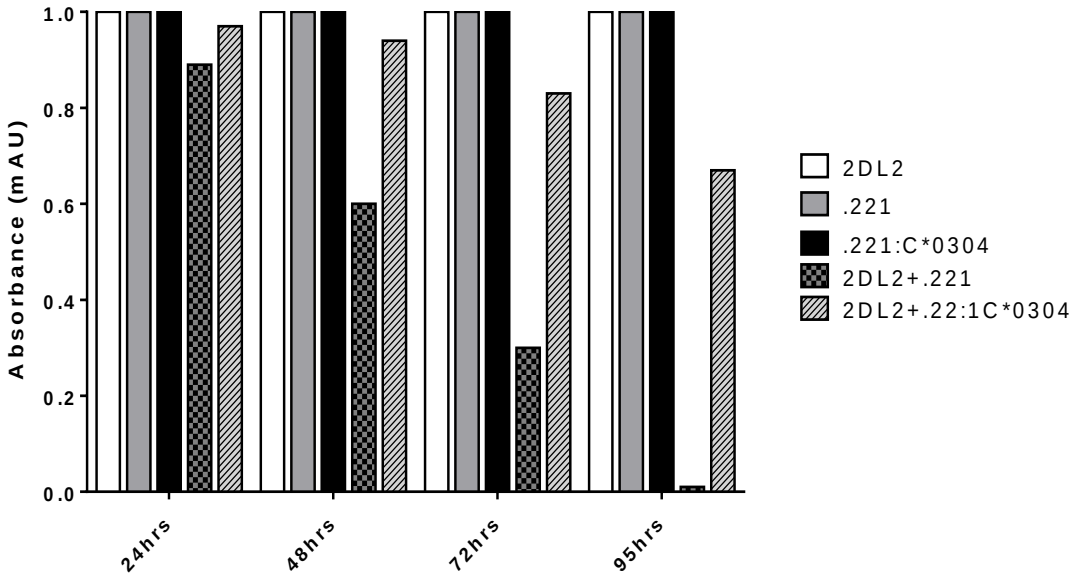

Figure 4-12: Absorbance of C3P after digestion using supernatant from co-culture between NKL2DL2 with or without 721.221 or 721.221C*0304 cells. Representation of absorbance in miliAbsorbance unit (mAU) of C3P obtained under a gradient from 4% to 60% solvent B (organic solvent). Peptide digestion was assessed for 24, 48, 72 and 95hrs. Data were normalised to 721.221 or 721.221:C*0304 depending on whether effector cells have been in co-culture with 721.221 or 721.221:C*0304. 2DL2 values have been normalised to themselves. Representative experiment from two repeat.

4.5 Analysis of Granzyme B (GzmB) produced after peptide pulsed Targets and Effector cell co-culture: comparison between HPLC and GzmB activity assay

We used 721.221 and 721.21C*0304 cells as control, respectively negative and positive. Target cells were pulsed with peptide and co-cultured with KIR2DL3 expressing NKL cell line. Cells were incubated for 5hrs at 26°C (which is the temperature suitable for peptide loading). Supernatants were harvested the same way as done above and the incubation with the C3P was also carried the same way as mentioned above. For this comparative experiments, half of the supernatant was used for the Granzyme B activity assay and the other half was reserved for the HPLC experiment.

GzmB activity assay (**Figure 4-13A**) showed that although the controls presented differences: GzmB production and activity from 721.221 supernatant and low level of GzmB production and activity from 721.221:C*0304 supernatant. Unfortunately, there were no differences observed between samples coming from co-cultures with target cells pulsed with peptides. Indeed, data from functional assays (CD107a) clearly showed that GAV series peptides strongly inhibited (AL, L8S and L7R), mildly inhibited (L7F) or did not inhibit (L8Y, L8V, L8K, L7D) NK cells. We used these peptides to test NK cells activation or inhibition. We found that there were no differences between the different peptides used. Furthermore, the results from the HPLC assay showed the same results pattern (**Figure 4-13B-C**) where the positive and the negative control gave the expected results: C3P digestion when effector cells were incubated with 721.221 cells and less digestion of the C3P when effectors were incubated with 721.221:C*0304 cells. Here again, we can see that there were no differences when between supernatant coming from co culture of target cells incubated with peptides. Therefore neither the HPLC assay nor the GzmB activity assay were able to distinguish between strong inhibitory, weak inhibitory or non-inhibitory/antagonistic peptides.

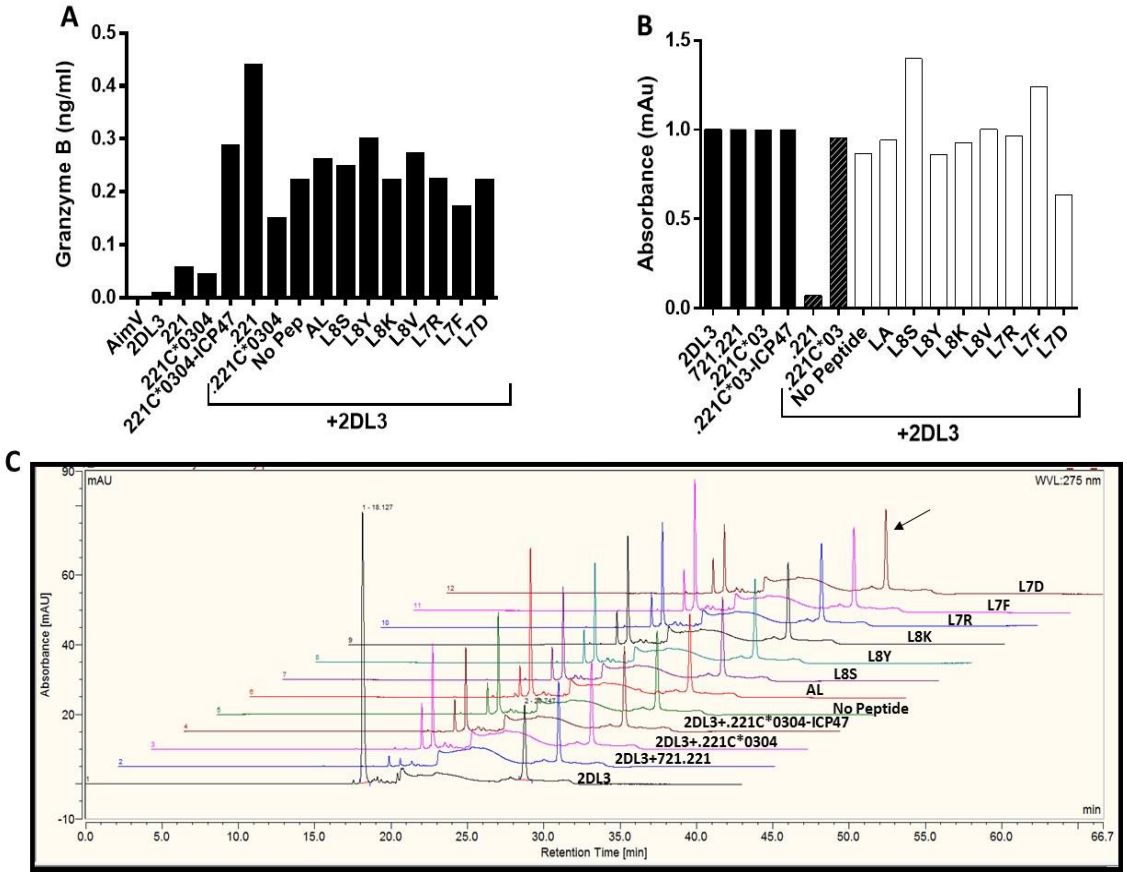

Figure 4-13: Comparison between a commercial GzmB Assay and HPLC based GzmB assay. (A) GzmB activity in supernatants obtained after co-culture between NKL2DL3 (2DL3) and target cells with or without peptides. (B) Absorbance of C3P after digestion using supernatant from co-culture between NKL2DL3 cells with or without target cells. Representation of absorbance in miliAbsorbance unit (mAU) of C3P obtained under a gradient from 4% to 60% solvent B (organic solvent). Peptide digestion was assessed for 95hrs. Data were normalised to Absorbance of C3P peptide obtained with target cells alone. Black bars represent effectors and target cells alone, stripped bars represent control cell lines and white bars represent co-culture of target cells of interest with or without loaded peptide. (C) Representation of C3P HPLC profile in different conditions. Arrow indicates the peptide present in the AIM-V medium and which allowed us to verify that the same amount of sample have loaded into the HPLC from one condition to another. Representative experiment from three repeats.

4.6 Discussion

This experiment with GzmB is a novel way to test peptide cleavage and hence test NK cell activation. I determined the incubation time for an optimal cleavage of C3P into its two products (YYGI**ETD** and **SG**VDDYY). In the beginning, our work has demonstrated that our designed peptide (C3P) can be optimally detected by our HPLC system at a specific wavelength of 275nm and we showed that the designed peptide can be cleaved by the rhGzmB which led us to assume that GzmB produced by cells could as well cleave the peptide sequence in two peptide sequences.

The majority of C3P digestion can be achieved within 24hrs when we used a high enzyme activity for the digestion. At low enzyme activity, maximum digestion was only achieved after 95hrs of incubation. This meant that for our cellular assay, 95hrs was an optimal readout. In fact, we noticed that there was some cleavage with 721.221 as well as with 721.221:C*0304 alone or in combination with NL2DL2 but the large difference in term of C3P digestion were visible at 95hrs of incubation.

We showed that NKL2DL2 line did not produce GzmB when in culture alone but in co-culture with 721.221 cells, they induced production of GzmB. The digestion was time dependent as after 95hrs of incubation C3P was undetectable when we combined NKL2DL2 with 721.221 cells. 721.221 cells in culture alone produced GzmB or another serine protease protein that was able to digest C3P. These results informed us that we will have to incubate supernatant from co-culture and C3P for at least 95hrs for an optimal readout.

Lastly, using cells loaded with our characterised GAV peptides series, we noticed that neither the HPLC Assay nor the GzmB activity Assay were able to distinguish between strong inhibitory, weak inhibitory or non-inhibitory/antagonistic peptides. Nevertheless, HPLC data and GzmB activity assay clearly distinguished sensitivity of NK cells toward cells having or missing MHC-I molecule.

5. Replicon expressing cells modulate the MHC-I peptide repertoire

Viral infections are known to change the peptide repertoire which can render infected cells susceptible to elimination by cytotoxic T lymphocytes (CTL) cells (294–296). Down regulation of HLA-I molecules to escape CTL responses may lead to NK cell activation. Therefore, viral infected cells present peptides that may affect the NK cell response. Findings in our group have demonstrated that genes encoding the inhibitory NK cell receptor KIR2DL3 and its human leukocyte antigen C group1 (HLA-C1) ligand directly influence resolution of hepatitis C virus (HCV) infection (297). To investigate how viral infection can affect the peptide repertoire, I have established a study model which includes three different cells lines. The cell model is based on HuH-7 cells which is a well differentiated hepatocyte derived cellular carcinoma cell line that was initially derived from a liver tumour in a 57-year-old Japanese male in 1982. Furthermore this cell line is one of the few to support hepatitis C virus replication. Additionally, Huh7 cells are known to express HLA I at their surface but it appears that this is predominantly HLA-A*1101 and not HLA-B or HLA-C (298–300). The level of class I expression at the cell surface regulates NK cell activity, and modulation of these NK cells ligands by viral proteins could have consequences for recognition by NK cells (301,302). In this chapter I have investigated the involvement of HLA-C peptide repertoire modulation.

5.1 Study model, work flow and cell lines integrity

Three different cell lines (**Figure 5-1**) were used for this study in order to assess the impact of HLA-C on changing the whole endogenous peptide repertoire of Huh-7 cell lines and further the presence of a pathogen on HLA-C peptide repertoire. Huh7 cells were transfected with a GFP tagged HLA-C*0102 allele (Huh7:C*0102 cells). Further introduction of HCV replication system (replicon) in Huh7:C*0102 led to the establishment of the Huh7:C*0102-replicon cells (Rep:C*0102). The generation of these the Rep:C*0102 cells was performed in Dr Arvind Patel's group (MRC Virology Unit, Galsgow) (303,304).

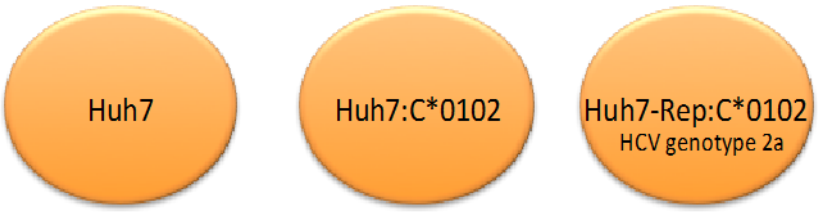

Table 5-1: schematic representing cell line used to study changes in peptide repertoire. Huh7 cells are parental cells. Huh7:C*0102 cell have an extra HLA-C allele compared to the parental cell line and Huh7-Rep:C*0102 cells have an extra HLA-C*0102 as well as a replicon construct which will mimic HCV infection. 5-1

Cell lines were regularly tested for HLA-C*0102 expression by flow cytometry by measuring GFP expression (**Figure 5-2 A**). To evaluate the presence of the replicon system in Rep:C*0102 cells, luciferase activity was measured using a luminometer and signals were compared amongst the three cell lines (**Figure 5-2 B**). All cells were expressing GFP when transfected with HLA-C and the Luciferase was only detected in the cell line that carried the Replicon system.

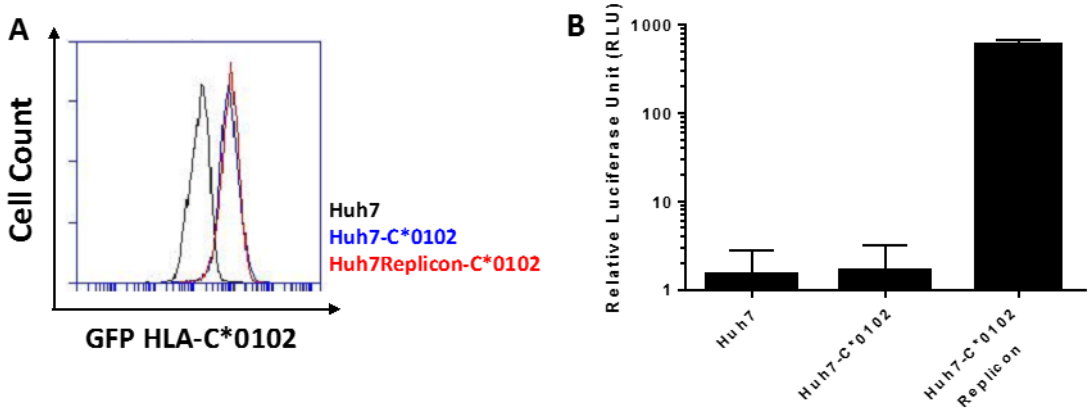

Figure 5-2: GFP expression and Luciferase activity on the cell lines. (A) To ensure the presence of HLA-C*0102, cells were analysed for GFP expression. (B) To ensure the presence of the Replicon in our cell system, a luciferase assay was performed by Dr Mumtaz Naiyer (Southampton University, UK)

5.2 Peptide identification and quantification

To study the influence of presented peptides on NK cells reactivity, a total of $3x10^9$ cells were grown in selection and harvested for MHC-I peptide elution. Before and during expansion, cell lines were regularly tested for HLA-C*0102 and luciferase activity, where relevant. Peptidome analysis was performed in two steps (by Ralf Schittenhelm, Monash University, Australia):

- The first step consisted of peptide identification in order to identify as many peptides as possible and generate a spectral library for subsequent quantification (**Figure 5-3 A**).

- In the second step a peptide quantification strategy was applied by using a Data Independent Acquisition (DIA) method which globally quantifies peptide across many samples (**Figure 5-3 B**). Among the 6000 quantified peptides, it was possible to identify peptides which were specific to Huh7 cells, Huh7:C*0102 cells and Rep:C*0102. Our collaborators used a p value cut-off of 1% which evaluates how accurate the software can choose the correct peak corresponding to the peptide. Within the library of quantified peptide, they were able to quantify 3100 peptides across the three samples which then allowed comparison in term of expression between the three samples. At the, end, by excluding specific and shared peptides from the parental cell lines, we were able generate a library which consisted of hundred that were specific to HLA-C*0102.

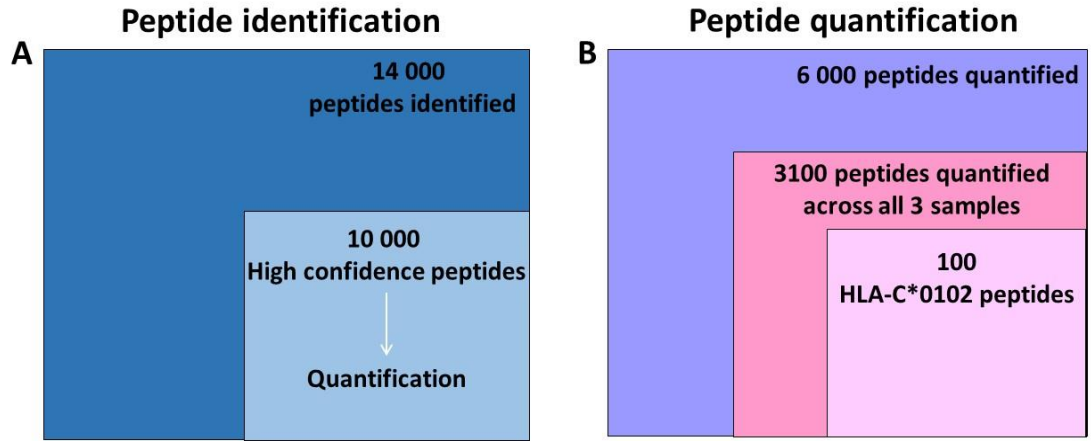

Figure 5-3: Peptidome analysis strategies. (A) Identification many peptides as possible for subsequent quantification. (B) Data Independent acquisition (DIA) method which globally quantify peptide across many samples.

5.3 Eluted peptides displayed features of HLA-A*11 and HLA-C*0102 peptide sequence

14 000 peptides were identified and included 10,000 high confidence peptides which were then used for quantification. During the quantification process, 6,000 peptides were quantified and 3100 peptide quantified across the all three samples. The remaining peptide were either unique to each cell lines or shared between Huh7 and Huh7:C*0102 or Huh7:C0102 and Rep:C*0102 or Huh7:C*01020. Furthermore, after filtering out the peptides of the Huh7 parental cell line, almost 100 peptides were identified that were specific to HLA-C*0102.

Peptide Libraries were first analysed by GibbsCluster which is an online program that identifies multiple specificities in peptide data by simultaneously aligning and clustering the peptide data (http://www.cbs.dtu.dk/services/GibbsCluster/).

Unique peptide sequences to each cell lines were characterized (**Figure 5-4**). This analysis revealed that peptides from Huh7 cells have characteristics of HLA-A*11 peptides with specify amino acid at its anchor residue: P2 (Valine (V)/ Tyrosine (T)/Serine (S)), P3 (Methionine (M)/ Leucine (L)/Phenylalanine (F), P7 (Leucine (L)/ Valine (V)/ Phenylalanine (F)) and P9 Lysine (K)/ Arginine (R)) (**Figure 5-4 A**). Further, I analyzed unique peptides eluted from Huh7:C*0102 cells and we noticed that peptides from this cell line would fit the HLA-A*11 pocket. Moreover, some of the peptides also fit the HLA-C*0102 pocket having the specific anchor residues of HLA-C*0102 (Proline (P) at P3 Leucine (L) at P6 and P9 (**Figure 5-4 B**). Finally, looking into the unique peptidome of Rep:C*0102 cells, the peptides from this cell line only fit the HLA-A*11 pocket based on the residues at P2, P3, P7 and P9 (**Figure 5-4 C**).

Each cluster group was displayed using the SeqLogo program. In this representation each logo consists of stacks of symbols, one stack for each position in the sequence. The overall height of the stack indicates the sequence conservation at that position, while the height of symbols within the stack indicates the relative frequency of each amino acid at that position. In general, a sequence logo provides general Data from the sequence alignments showed that the majority of peptides have a Lysine (K) or Arginine (R) at the C terminus. However there was a subgroup of peptides with Proline (P) at P3 and Leucine (L) at P9 that identified them as HLA-C*0102 specific.

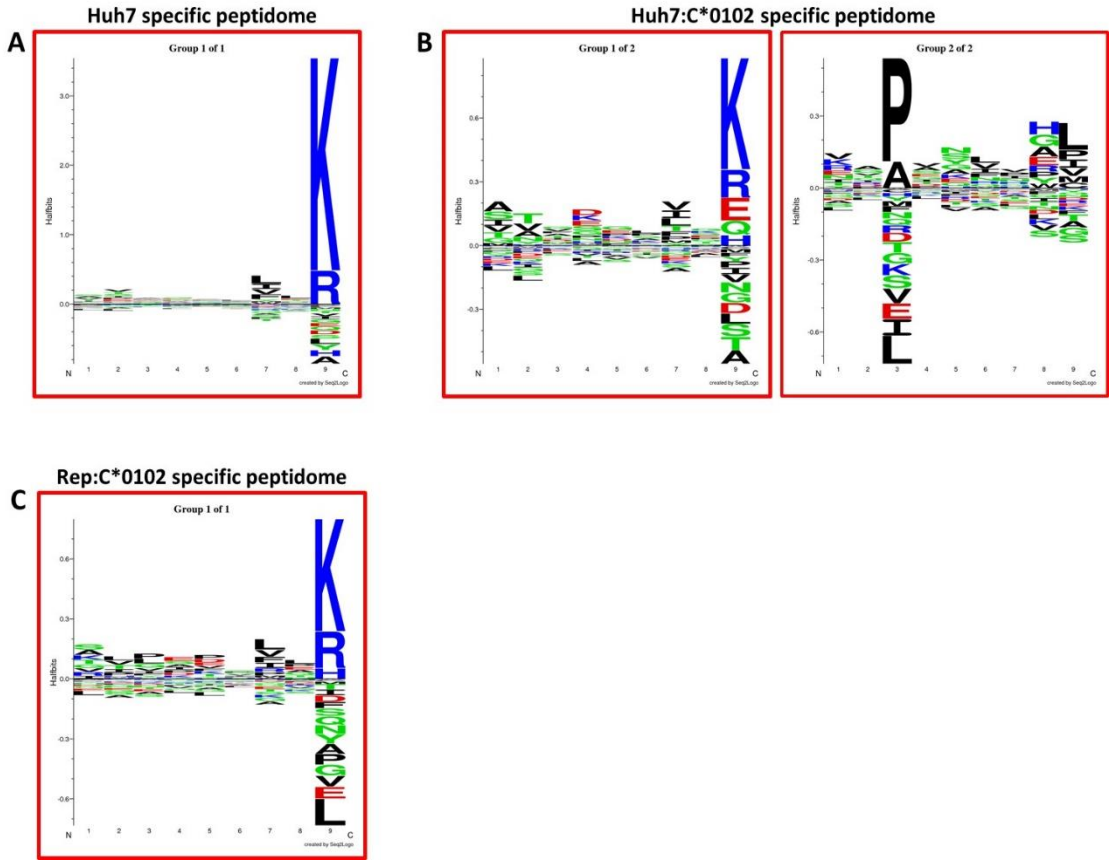

Figure 5-4: SeqLogo representations of the unique peptidome of Huh7, Huh7:C*0102 and Rep:C*0102. (A and C) Identification of one sequence motif for Huh7 and Rep:C*0102 depicting a HLA-A*11 motif. (B) Sequence motifs for Huh7:C*0102 depicting a HLA-A*11 motif as well as a HLA-C*0102 motif.

5.4 HLA-C*0102 sequence motif can be identified after excluding peptides from the parental cell line Huh7

As a "quality control" analysis, I have used the group of 92 peptides which, based on their anchor residues, indicated them to be specific to HLA-C*0102. This peptide library was generated after removing peptides belonging to the parental cell line Huh7 from the Huh7:C*0102 and Rep:C*0102 peptidomes. The GibbsCluster analysis identified 80 unique sequences and has removed twelve sequences that were shorter than a ninemer (ten sequences) and longer than a ninemer (two sequences). The identified sequences motifs showed that peptides selected in this library present anchor residues that fit the HLA-C*0102 peptide groove (**Figure 5-5**).

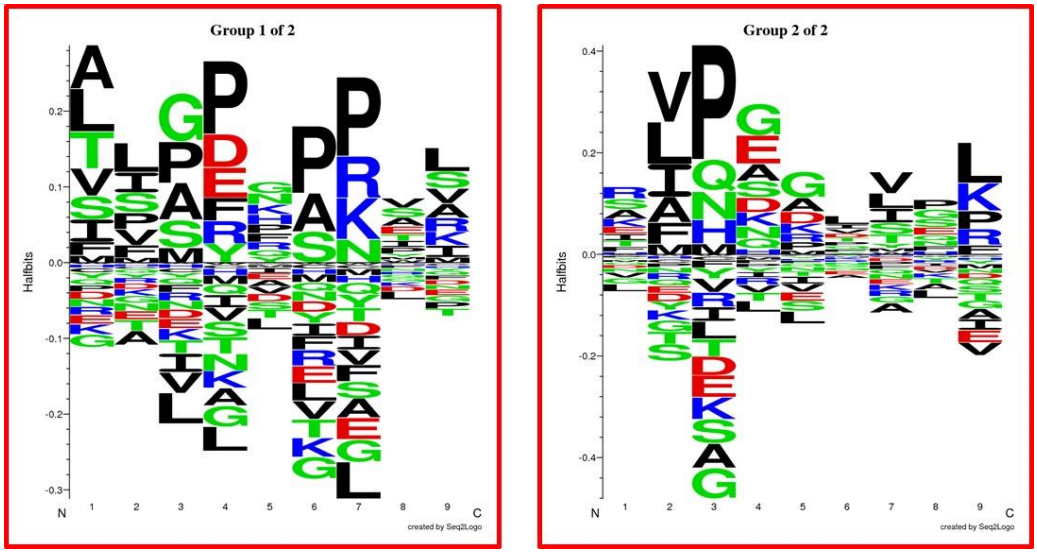

Figure 5-5: SeqLogo representation of the peptidome from HLA-C*0102 expressing cells (Huh7:C*0102 and Rep:C*0102). Two motif sequences identified after the removal of Huh7 peptidome.

5.5 Rep:C*0102 cells peptide repertoire cluster with Huh7 peptide repertoire

We observed differences in peptide repertoire across the three samples. The heat map showed that Huh7 and Rep:C*0102 cells peptide profiles do cluster together. Which means that by introducing the HCV genome in the cell, we changed the peptide repertoire of Huh7:C*0102 in favour of a peptide repertoire which is similar to the peptide repertoire of the parental cell line Huh7 (**Figure 5-6**).

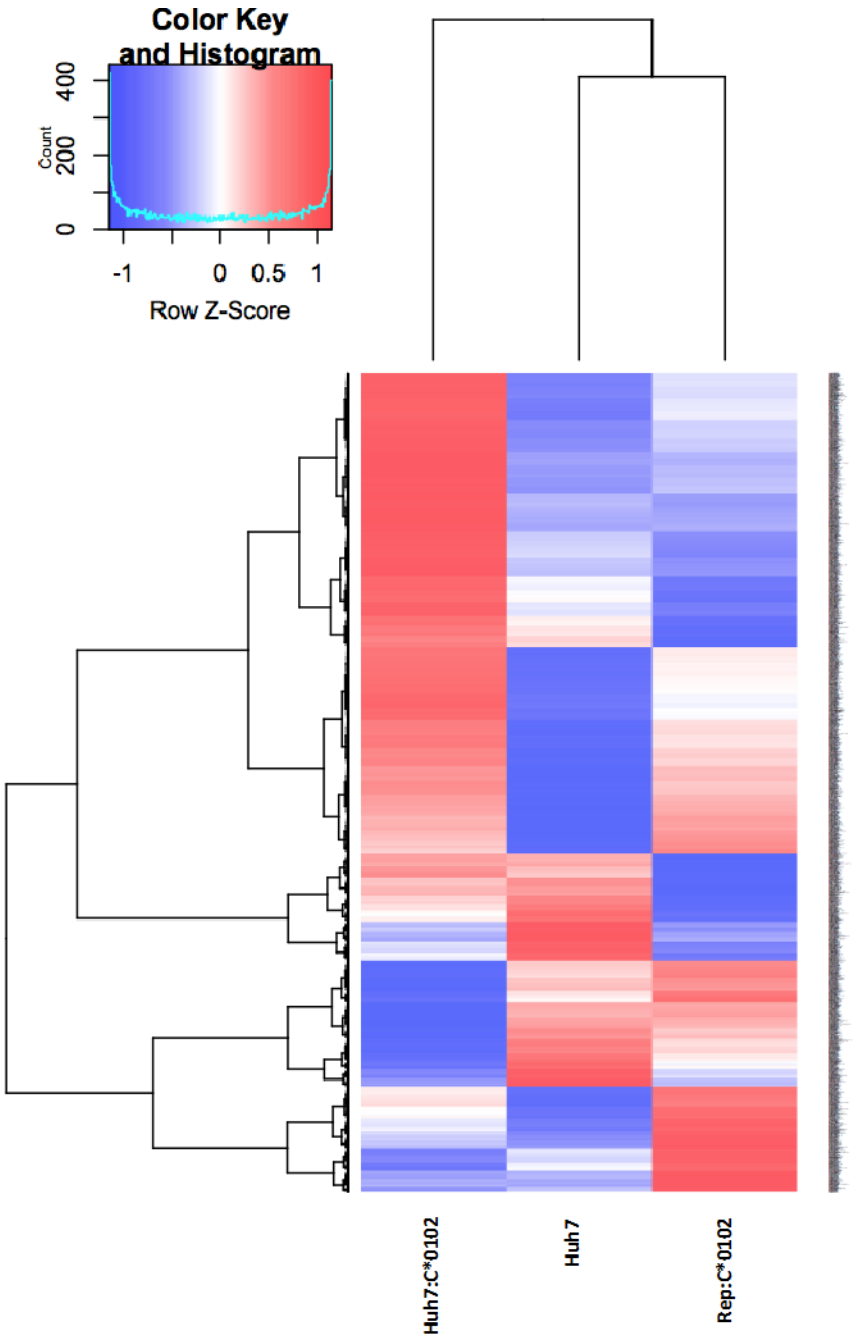

Figure 5-6 Heat map representing peptide expression at the cell surface of each cell line. Log 2 values for each peptide fond in each cell line were graphically represented in a Heat map. Expression values of peptides are depicted as log2 and scaled across each row to indicate the number of standard deviations above (red) or below (blue) the mean, denoted as row Z-score.

I further studied the library of shared peptides using GibbsCluster. The program identified 2,677 unique sequences and removed 134 shorter than ninemers.

Identified sequences depicted a sequence motif consistent with HLA-A*11-binding peptides (**Figure 5-7**).

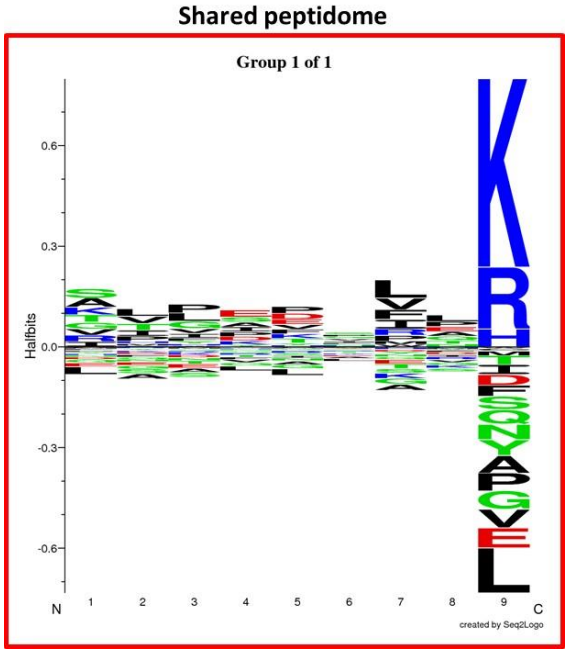

Figure 5-7: SeqLogo representation of the peptidome shared between Huh7, Huh7:C*0102 and Rep:C*0102. Motif sequence identified from the shared peptide library.

5.6 Rep:C*0102 cells have a down-regulated peptide repertoire compared to the parental cell Huh7:C*0102 cells

To evaluate the modulatory effect of the virus on the peptide repertoire, I compared expression of peptides in Huh7:C*0102 cells with peptides from the Rep:C*0102 system. The heat-map of fold change between the three cell lines, revealed a majority of down-regulated peptides in Rep:C*0102 cells compared to Huh7:C*0102, and relatively few up-regulated peptides (**Figure 5-8**). Fold changes observed were subtle (from -6 to +5). I analysed peptides with fold changes of less than -2 for the down-regulated pool and with fold changes greater than +2 for the up-regulated pool.

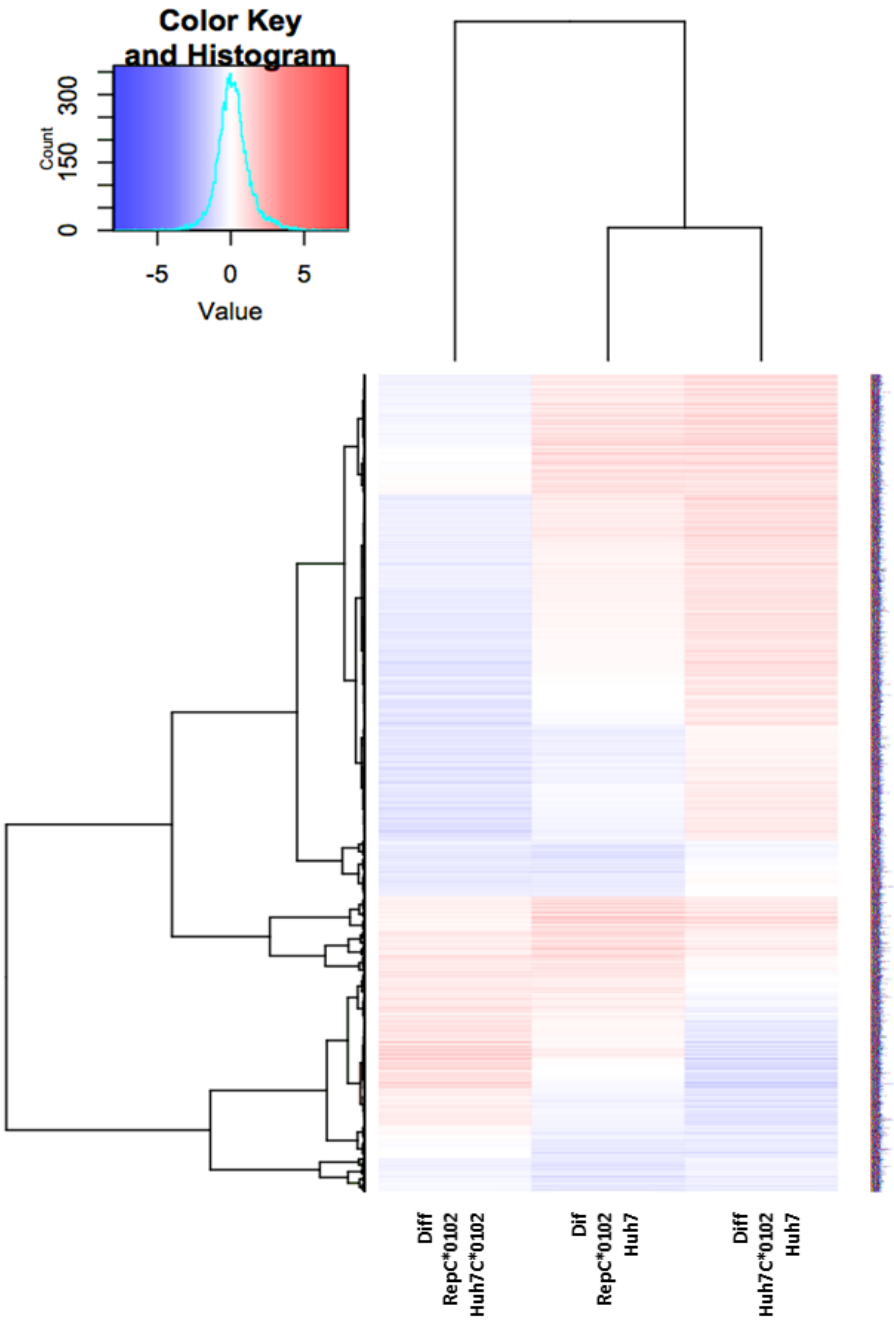

Figure 5-8: Heat map representing fold changes of peptides expression. Fold changes were calculated comparing difference of expression between Huh7 and Huh7C*0102, between Huh7 and Rep: C*0102 and between Huh7C*0102 and Huh7Replicon C*0102. Hierarchical clustering was performed using Pearson correlation metric to calculate distances and clustered using Ward's linkage. Red and blue indicate up- and down regulated peptides, respectively.

I performed an in depth study of the origin of each peptides using PepServe (http://bioserver-1.bioacademy.gr/Bioserver/PepServe/Peptide_index.php) (305) as

well as UniProt (http://www.uniprot.org) which are both online programs that allow protein identification. Results demonstrated that in the replicon expressing cells there was an up-regulation of peptides from the translation machinery in the cells, reflected by upregulation of peptides derived from ribosomes (**Table 5-1**). Down-regulated peptide included apolipoprotein B100 (ApoB-100) (**Table 5-2**). This was consistent with reports have shown that chronic infection with HCV leads to a deficiency in liver ApoB-100 (306,307)

Peptide	Unique	UniProt ID	Protein
GSFGKVFLV	No	Q15418	Ribosomal protein S6 kinase alpha-1.
		P51812	Ribosomal protein S6 kinase alpha-3.
		Q9UK32	Ribosomal protein S6 kinase alpha-6.
RVMTVSFHKY	No	Q13547	Histone deacetylase 1.
		Q92769	Histone deacetylase 2.
		O15379	Histone deacetylase 3.
PHPPPPPPP	No	P13378	Homeobox protein Hox-D8.
		Q15390	Mitochondrial fission regulator 1.
		Q15032	R3H domain-containing protein 1.
RVFNIMREK	No	P20042	Eukaryotic translation initiation factor
QLYWSHPRK	No	P62273	40S ribosomal protein S29.
RIFDLGRKK	No	Q96L21	60S ribosomal protein L10-like.
		P27635	60S ribosomal protein L10.
RVAEALHKLK	No	Q96A73	Putative monooxygenase p33MONOX.
KAFNQGKIFK	No	P26641	Elongation factor 1-gamma.
RTIATALEYVYK	No	P78537	Biogenesis of lysosome-related organelles
RILPKPTRK	Yes	P62081	40S ribosomal protein S7.
RTDERIKQHPK	Yes	Q9ULW0	Targeting protein for Xklp2.
RTPAFSPFVR	Yes	Q7Z5J4	Retinoic acid-induced protein 1.
VIFINTRRK	Yes	P60842	Eukaryotic initiation factor 4A-I.
EEYKKEQAINRAGIVQE	Yes	Q8N5G0	Small integral membrane protein 20.
AVGDIPGVRFK	Yes	P62266	40S ribosomal protein S23.
RIHGVGFKK	Yes	P62899	60S ribosomal protein L31.
FLITQLKML	Yes	P03928	ATP synthase protein 8.
RIIDLIKEK	Yes	Q9NU02	Ankyrin repeat and EF-hand domain-
SIMKWNRER	Yes	Q9P0J0	NADH dehydrogenase [ubiquinone] 1 alpha
ELMPPPPPK	Yes	O60942	mRNA-capping enzyme.
KLISEEDLLRK	Yes	P01106	Myc proto-oncogene protein.
GLAVHLEVLNAR	Yes	Q8N587	Zinc finger protein 561.
SVYDHQGIFKR	Yes	Q96E22	Dehydrodolichyl diphosphate synthase
KIYPGHGRR	Yes	P83731	60S ribosomal protein L24.
KFLPPVLLK	Yes	Q5VYK3	Proteasome-associated protein ECM29
GIKSLSPFA	Yes	Q6NUQ4	Transmembrane protein 214.
YIKSTMGKPQRLY	Yes	P62906	60S ribosomal protein L10a.
SVFTNERFPLR	Yes	O43709	Probable 18S rRNA (guanine-N(7))-
EEYKKEQAINRAG	Yes	Q8N5G0	Small integral membrane protein 20.
AGLSSPLSFPSQ	Yes	Q8TEK3	Histone-lysine N-methyltransferase, H3
RIFAPNHVVAK	Yes	Q02543	60S ribosomal protein L18a.
RTMPLLSLHSR	Yes	P54368	Ornithine decarboxylase antizyme 1.
RILFFNTPK	Yes	P48556	26S proteasome non-ATPase regulatory
GHQQLYW	Yes	P62273	40S ribosomal protein S29.
RTAHVILRY	Yes	Q9UKV5	E3 ubiquitin-protein ligase AMFR.
SSFLIKRNK	Yes	P46779	60S ribosomal protein L28.
AVHLEVLNAR	Yes	Q8N587	Zinc finger protein 561.
LYQSLR	Yes	Q5SNT2	Transmembrane protein 201.
SINFAKVLH	Yes	P51659	Peroxisomal multifunctional enzyme type
KVHGSLARAGK	Yes	P62861	40S ribosomal protein S30.
ASSGASGGKIDNSVLVL	Yes	O95831	Mitochondrion.
AVASFPKKQE	Yes	P14406	Cytochrome c oxidase subunit 7A2,
SSGVPNPPK	Yes	Q8WUA4	General transcription factor 3C

Table 5-2: Representative list of Rep:C*0102 down regulated peptide.

Peptide	Unique	UniProt ID	Protein
LSSFWQLIV	Yes	Q92616	eIF-2-alpha kinase activator GCN1.
TVVNPKYEGK	Yes	P05556	Integrin beta-1.
TTLPPPLFSK	Yes	Q5H8A4	GPI ethanolamine phosphate transferase 2.
TVLGGVYILGK	Yes	P56589	Peroxisomal biogenesis factor 3.
AIYELAVASFPK	Yes	P14406	Cytochrome c oxidase subunit 7A2,
ATAYGSTVSK	Yes	P04114	Apolipoprotein B-100.
ATLDVGGLVFK	Yes	P10074	Zinc finger and BTB domain-containing
GTYSLVPKK	Yes	Q9H9B1	Histone-lysine N-methyltransferase EHMT1.
TIPIFEPL	Yes	Q8N3C0	Activating signal cointegrator 1 complex
GVAVSGPTK	Yes	Q9BR77	Coiled-coil domain-containing protein 77.
GGAGGARISL	Yes	Q9C075	Keratin, type I cytoskeletal 23.
STAPAQLGK	Yes	Q9Y5M8	Signal recognition particle receptor
IGSQRYKL	Yes	P06400	Retinoblastoma-associated protein.
GSQGGNFEGPNK	Yes	Q8WXF1	Paraspeckle component 1.
TATDVFWAK	Yes	P00734	Prothrombin.
SIFSEALLK	Yes	Q08426	Peroxisomal bifunctional enzyme.
TAYGSTVSK	Yes	P04114	Apolipoprotein B-100.
QVEEIFNLK	Yes	P78347	General transcription factor II-I.
VFLPKDVAL	Yes	P15924	Desmoplakin.
SVSPVKATQK	Yes	Q86XJ1	GAS2-like protein 3.
VVFPFPVNK	Yes	P04198	N-myc proto-oncogene protein.
SSPITLQAL	Yes	P04114	Apolipoprotein B-100.
VLQAADILLYK	Yes	Q9UGM6	Tryptophan--tRNA ligase, mitochondrial.
GIIIVGDEILK	Yes	Q8NFF5	FAD synthase.
TSLPPLPFK	Yes	P46013	Antigen KI-67.
TAFDPFLGGK	Yes	Q92598	Heat shock protein 105 kDa.
PLPPPMKI	Yes	O60229	Kalirin.
ASVHLDSKK	Yes	P04114	Apolipoprotein B-100.
SVYAGAGGSGSR	Yes	P05783	Keratin, type I cytoskeletal 18.
TVAPFLYR	Yes	Q8IVL1	Neuron navigator 2.
YVHDAPVRSL	Yes	P01584	Interleukin-1 beta.

Table 5-3: Representative list of Rep:C*0102 up regulated peptide.

As the peptidome analysis have shown that the peptide sequences may fit either HLA-A*11 or HLA-C*0102 peptide grooves, I inputted these sequences into the NetMHCpan (http://www.cbs.dtu.dk/services/NetMHCpan/) online program in order to evaluate their ability to bind to HLA-A*11 (**Figure 5-9**). The majority of the peptides had measurable affinity for HLA-A*11 according to the prediction program. This observation reflects the fact that the shared peptidome mainly have an HLA-A*11 binding motif.

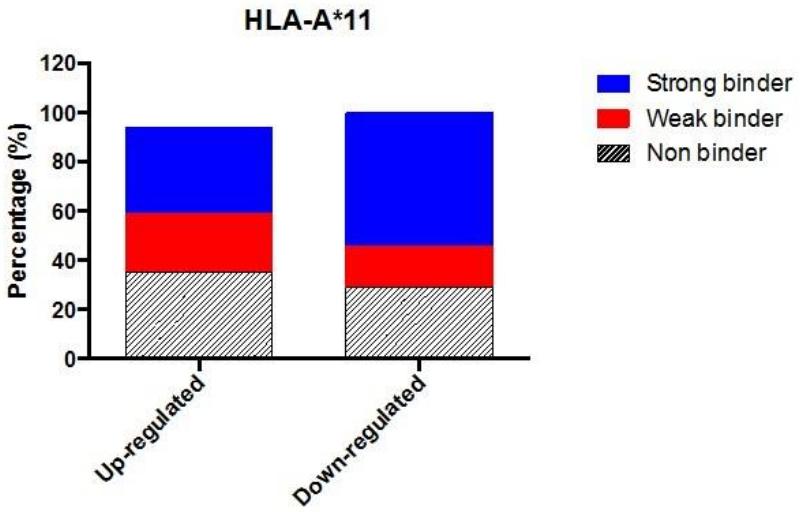

Figure 5-9: HLA-A*11 stabilibilty of up and down regulated peptide from Huh7:C*0102 and Rep:C*0102. Proportion of down- and up- regulated peptides identified which bind to HLA-A*11. Strong (in blue), weak (in red) and non HLA-A*11 binders (in dashed) were represented for both down and up regulated pool.

Although most of the eluted peptides have motifs consistent with HLA-A*11 binding groove, I was able to extract a substantial list of peptides which have the ability to bind HLA-C*0102 with different affinities (**Table 5-4**). These peptide have various cellular origins including two peptides which are known to be linked to cancer: RLPPLLSPL (Podocalyxin-like protein 2) and MAPARLFAL (Syndecan4).

Peptide	Unique	UniProt ID	Origin	HLA-C*0102 binding	Status
VFLPKDVAL	yes	P15924	Desmoplakin.	weak binders	Down regulated
FLVNHDFSPL	yes	P33947	ER lumen protein-retaining receptor 2.		
VVPPFLQPEV	/	/	Not found		
FFMPGFAPL	No	Q9H4B7	Tubulin beta-1 chain.	strong binders	
		Q13885	Tubulin beta-2A chain.		
		Q9BVA1	Tubulin beta-2B chain.		
		P68371	Tubulin beta-4B chain.		
		Q13509	Tubulin beta-3 chain.		
		P04350	Tubulin beta-4A chain.		
		P07437	Tubulin beta chain		
		Q9BUF5	Tubulin beta-6 chain.		
		A6NNZ2	Tubulin beta-8 chain-like protein		
		Q3ZCM7	Tubulin beta-8 chain.		
SSPITLQAL	Yes	P04114	Apolipoprotein B-100.		
YVHDAPVRSL	Yes	P01584	Interleukin-1 beta.		
RLPPLLSPL	Yes	Q9NZ53	Podocalyxin-like protein 2		
FLITQLKML	Yes	P03928	ATP synthase protein 8.	weak binder	Up regulated
MAPARLFAL	Yes	P31431	Syndecan 4	strong binder	

Table 5-4: List of HLA-C*0102 peptides. Peptides identified from the NetMHCpan *in silico* analysis.

Sequence Logo representation confirms that sequences that were identified by the NetMHCPan program, displayed an HLA-C*0102 peptide binding sequence with predominantly Proline (P) at P3, Leucine (L) at P9 (**Figure 5-10**).

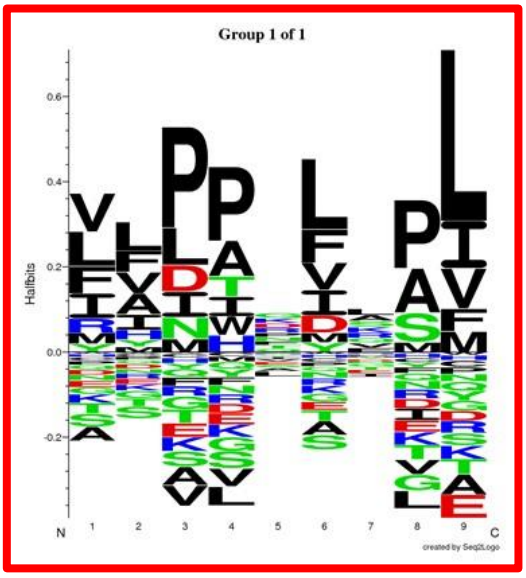

Figure 5-10: SeqLogo representation of HLA-C*0102 identified peptide. Sequences were input into GibbsCluster online program which generated one identified sequence motif.

5.7 HLA-C*0102 eluted peptides bind to HLA-C and can stabilise its cell surface expression

To study these peptides in more depth, I measured their ability to bind HLA-C, by performing an HLA-C stabilisation assay. Each individual peptide was incubated with the TAP deficient 721.174 cells which naturally express HLA-C*0102. Different concentrations of peptide were tested and DT9 staining was performed (**Figure 5-11**). Selected peptides from the immunopeptidome analysis were: VFLPKDVAL (VFL), FLVNHDFSPL (FLV), VVPPFLQPEV (VVP), FFMPGFAPL (FFM), SSPITLQAL (SSP), YVHDAPVRSL (YVH), RLPPLLSPL (RLP), FLITQLKML (FLI) and MAPARLFAL (MAP).

Results showed that all peptide, to some extent stabilise HLA-C. Peptides that were assigned as being a strong binder by the NetMHCpan online program clustered in two groups with strong binders giving high MFI at 200μM and weak binders giving lower MFI at the same concentration.

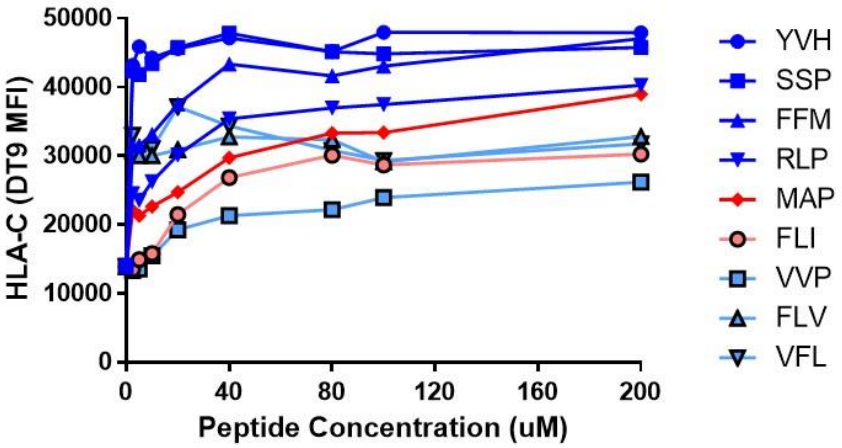

Figure 5-11: HLA-C expression at the surface of 721.174 cells after peptide loading with HLA-C *0102 selected peptides. Series selected of peptides stabilize HLA-C expression on the surface of 721.174 cells. DT9 staining of 721.174 after peptides loading with various and increasing concentrations of peptide. Peptides in in blue are down regulated peptide and red are up regulated peptides. Predicted affinities were colour coded where: Peptides in darker colour are HLA-C*0102 strong binders and peptides in lighter colour weak binders.

In order to more precisely determine the staibility of HLA-C complexed with each peptide I performed a Brefeldin A (BFA) decay assay. This experiment was aimed to correlate with *in silico* data obtained by using NetMHCpan program. Results are summarised in **Table 5-5**. The results obtained using the prediction program are shown **Figure 5-12 A**. This program did classify these series of peptide as strong or weak binders. BFA decay results did correlate with the NetMHCpan classification (**Figure 5-12**). VAPWNSLSL (VAP-LS) which is known as a HLA-C*0102 endogenous was also included as a control. The MFI obtained for each peptide was plotted in **Figure 5-12 B** and was normalised to to the initial surface level in **Figure 5-12 C** in order to determine the peptide off-rate. Results showed that peptides clustered in two distincts groups. Strong binders have the same off-rate with a half-time ($t_{1/2}$) around 4hrs while weak binders peptides had a $t_{1/2}$ around 1hr. VFL peptide which was characterised as a HLA-C*0102 weak binder by NetMHCpan did behave as the strong binders with a $t_{1/2}$ around 4hrs. Thus in summary the *in silico* data using NetNHCpan were verified *in vitro* at the exception of one peptide (VFL).

Peptide	NetMHCpan prediction program	BFA Decay result
VAP-LS	Strong binder	Strong binder
YVH	Strong binder	Strong binder
SSP	Strong binder	Strong binder
FFM	Strong binder	Strong binder
RLP	Strong binder	Strong binder
MAP	Strong binder	Strong binder
FLI	Weak binder	Weak binder
VVP	Weak binder	Weak binder
FLV	Weak binder	Weak binder
VFL	Weak binder	Strong binder

Table 5-5: Comparison of *in silico* results and in vitro results of HLA-C*0102 peptide stability in the peptide groove. Eluted peptide identified as HLA-C*0102 peptides were assessed for their stability by BFA decay assay. *In vitro* results were compared to *in silico* results. VAP-LS peptide was used as a peptide control.

A

```
# Rank Threshold for Strong binding peptides   0.500
# Rank Threshold for Weak binding peptides    2.000
-----------------------------------------------------------------------------------------------------------
  Pos          HLA        Peptide       Core Of Gp Gl Ip Il        Icore        Identity     Score Aff(nM)   %Rank  BindLevel
-----------------------------------------------------------------------------------------------------------
    1  HLA-C*01:02      VFLPKDVAL   VFLPKDVAL  0  0  0  0  0   VFLPKDVAL      PEPLIST 0.18273   6923.2    0.80 <= WB
    1  HLA-C*01:02     FLVNHDFSPL  FLVNHFSPL  0  5  1  0  0  FLVNHDFSPL      PEPLIST 0.19136   6306.5    0.70 <= WB
    1  HLA-C*01:02     VVPPFLQPEV  VVPPFLQPV  0  8  1  0  0  VVPPFLQPEV      PEPLIST 0.13581  11503.2    1.80 <= WB
    1  HLA-C*01:02      FLITQLKHL   FLITQLKHL  0  0  0  0  0   FLITQLKHL      PEPLIST 0.16947   7992.0    1.00 <= WB
    1  HLA-C*01:02      MAPARLFAL   MAPARLFAL  0  0  0  0  0   MAPARLFAL      PEPLIST 0.45520    363.1    0.01 <= SB
    1  HLA-C*01:02      RLPPLLSPL   RLPPLLSPL  0  0  0  0  0   RLPPLLSPL      PEPLIST 0.40275    640.4    0.01 <= SB
    1  HLA-C*01:02      FFMPGFAPL   FFMPGFAPL  0  0  0  0  0   FFMPGFAPL      PEPLIST 0.36013   1015.6    0.03 <= SB
    1  HLA-C*01:02      SSPITLQAL   SSPITLQAL  0  0  0  0  0   SSPITLQAL      PEPLIST 0.31428   1667.9    0.06 <= SB
    1  HLA-C*01:02     YVHDAPVRSL  YVDAPVRSL  0  2  1  0  0  YVHDAPVRSL      PEPLIST 0.22217   4518.4    0.40 <= SB
    1  HLA-C*01:02      VAPWNSLSL   VAPWNSLSL  0  0  0  0  0   VAPWNSLSL      PEPLIST 0.47201    302.7    0.01 <= SB
-----------------------------------------------------------------------------------------------------------

Protein PEPLIST. Allele HLA-C*01:02. Number of high binders 6. Number of weak binders 4. Number of peptides 10
```

B

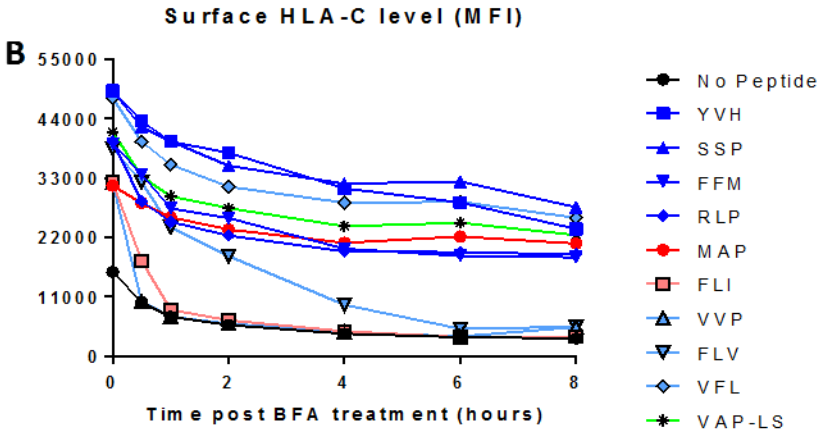

C

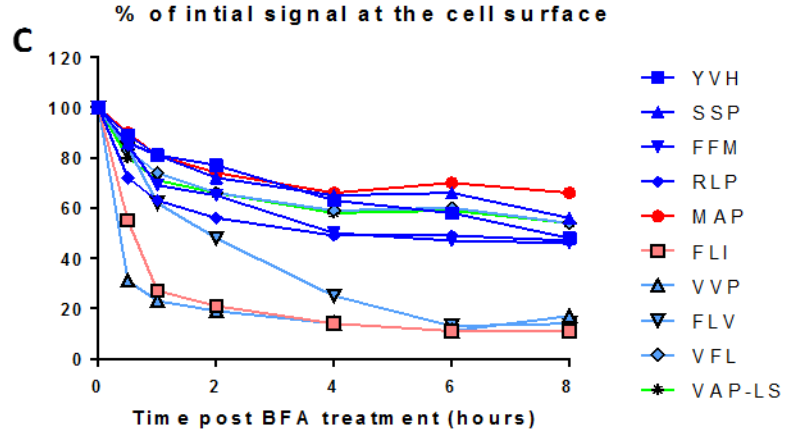

Figure 5-12: Stability of HLA-C*0102 identified peptides on the peptide groove. (A) Original *in silico* estimation of peptide stability using NetMHCpan online program. (B) 721.174 cells were loaded with 100μM of peptide overnight and then treated with Brefeldin A, harvested after 0, 1, 2, 4, 6 and 8hrs, and then stained with HLA-C antibody (DT9). Level of HLA-C at the surface as determined by DT9 staining. (C) The data in panel A is presented as MFI values normalized to the initial HLA-C surface level (MFI at t=0hr). Similar rates of decay were observed in two separate experiments.

To test NK cell reactivity toward each peptide, CD107a assays were performed using seven different donors. 721.174 cells were loaded with 40μM of the down- and up-regulated peptides and NK cells degranulation was measured (**Figure 5-13**). In absence of peptide, 721.174 cells induced NK cells degranulation. The strong inhibitory peptide VAP-FA peptide (in grey) was used as control for inhibition. KIR2DL3^{+} NK cells reacted differently in the presence of the different peptides (**Figure 5-13 A**). FFM, RLP and MAP peptides were inhibitory leading to ≤55% of maximal degranulation by CD158b-positive NK cells. Inhibition driven by all of these peptides was highly statistically significant ($p<0.0001$). MAPARLFAL which was up-regulated in Rep:C*0102 had a phenylalanine at P7 of the peptide sequence and alanine at P8 This combination of residues has been already shown to be strongly inhibitory in the context of HLA-C*0102 (218,219). Regarding FFMPGFAPL and RLPPLLSPL which also inhibited NK cell degranulation, they have small residues at P7 and P8 that are also known to be associated with inhibitory KIR recognition and lead to NK cell inhibition. Additionally, all HLA-C*0102 weak binder peptides did not inhibit NK cell from degranulation. This may be due to the fact that these peptide have non permissive residues at P7 and P8 which prevent KIR binding to the MHC-I:peptide complex. Finally, as all peptide are ligands for receptor KIR2DL2/L3 consequently none of these peptides affected KIR2DL3-negative NK cells (**Figure 5-13 B**).

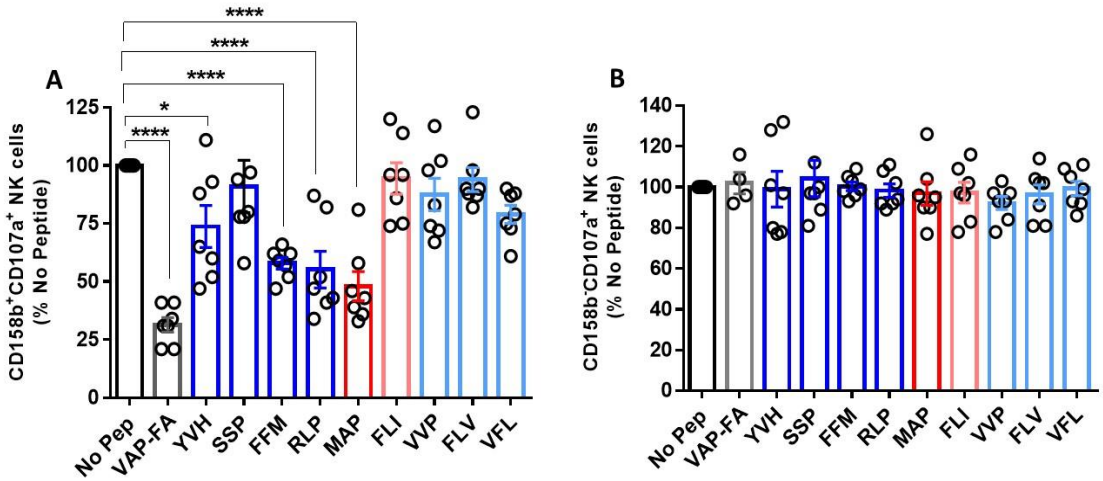

Figure 5-13: Comparison of NK cell degranulation toward target cells loaded with HLA-C*0102 identified peptide. (A) Degranulation assays of KIR2DL2/L3^{+} NK cells. Down-regulated peptides (in blue) and up-regulated peptides (in red) were individually tested using 721.174 cells. VAP-FA peptide in grey was used as peptide control. All values have been normalised to "No Peptide". Representation of n=7 experiments. *****p<0.0001*, and **p<0.05* (One-way Anova) which compares each condition to "No peptide". (B) Degranulation assays of KIR2DL2/L3^{-} NK cells.

I next tested the effect of up-regulated and down-regulated peptides separately or in combination for their ability to influence NK cell reactivity. For combination of peptides, quantification data from mass spectrometry analysis were used to scale peptide quantity used in this functional assay. As MAP and SSP peptide behaved as strong inhibitory and non-inhibitory peptides respectively, they were also included as one of the combinations (**Figure 5-14 A**). In order to test whether the SSP peptide could potentially "antagonise" inhibition due to MAP peptide. The previously described VAP-FA+VAP-DA (VAPWNSFAL and VAPWNSDAL) combination was also incorporated as a control for peptide antagonism. In the absence of peptide, I observed strong degranulation from KIR2DL2/L3+ NK cells. In the presence of the up-regulated peptides, strong degranulation was also observed (>80% of no peptide). The mix of down-regulated peptides gave a lower level degranulation (<70%). Combination of both the up and down regulated peptides strongly inhibited KIR2DL2/L3^{+} NK cells. Combination of MAP+SSP did result in a release of NK cells from their inhibition by MAP, suggesting that SSP peptide can antagonise the inhibition driven by the MAP peptide. As control, FA+DA peptides from the VAP series did induce NK cell antagonism. Furthermore, none of these combinations affected KIR2DL2/L3-negative cells (**Figure 5-14 B**).

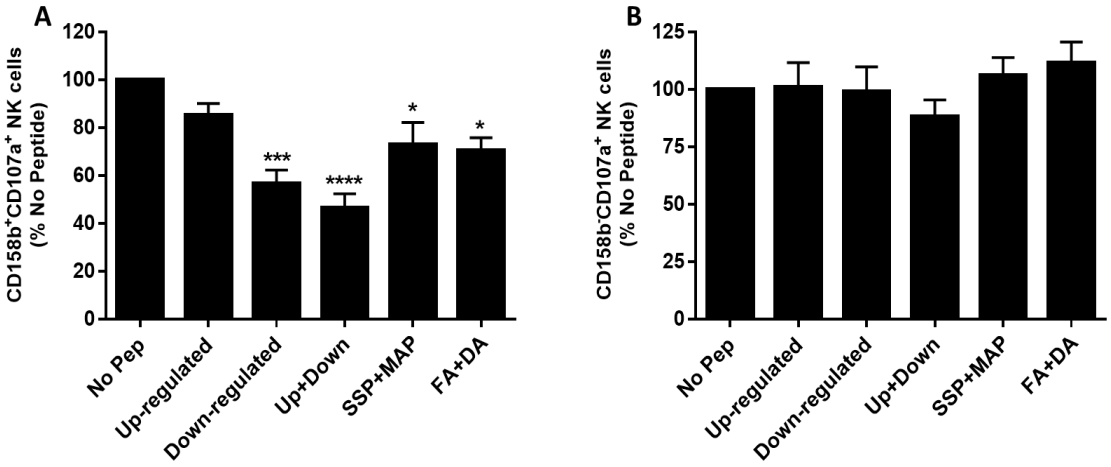

Figure 5-14: Degranulation assay comparing of NK cell reactivity to HLA-C*0102 selected peptide. (A) Degranulation assays of KIR2DL2/L3^{+} NK cells. Up- and down-regulated peptides were loaded into 721.174 cells and tested separately or in combination. All values have been normalised to "No Peptide". Representation of n=5 experiments. *****p<0.0001, ***p<0.001, *p<0.05* (One-way Anova) which compares each condition to "No peptide". (B) Degranulation assays of KIR2DL2/L3^{-} NK cells.

5.8 Replicon expressing cells down regulate MHC-I expression at the cell surface

Reports have shown that introducing a replicon system in hepatic cell lines induces down-regulation of class I surface expression. This phenomenon was related to an intracellular accumulation of unfolded MHC-I molecule (299). As the peptidome analysis revealed a loss of HLAC*0102 peptide at the surface, I decide to investigate the Class I expression of these cell lines. I assessed their Class I expression: for total MHC-I, HLA-A*11 and HLA-C expression. W6.32 staining showed that Huh7 cells expressed HLA-I molecule at the surface (MFI= 6,496) but Huh7:C*0102 (MFI= 14,288) and Rep:C*0201 (MFI= 9,131) did express more HLA-1 overall (**Figure 5-15 A**). This higher expression of total HLA-I in Huh7:C*0102 and Rep:C*0102 cells is most likely related to the HLA-C*0102 over-expressed in these cells. As peptidome analysis revealed an enrichment of HLA-A*11 peptides, I stained cells for this specific HLA allele using the 4i93 antibody (**Figure 5-15 B**). Results showed that all cells did express HLA-A*11 at their surface (MFI= 6,496 for Huh7 cells, 14,288.65 for Huh7:C*0102 and 9,131.13 for Rep:C*0102 cells). HLA-C staining using DT9 revealed that Huh7 cells have lower levels of HLA-C expression at the cell surface (MFI=2,446.45) compared to Huh7:C*0102 (MFI=13,460.46) and Rep:C*0102 (MFI=8,031.71) (**Figure 5-15 C**). But it was noticeable that Rep:C*0102 did express less HLA-C at the cell surface than Huh7:C*0102 cells. I then verified the presence of GFP expression as our HLA-C*0102 construct has a GFP tag attached. It was interesting to observe that the GFP expression was almost the same between Huh:C*0102 (MFI= 104,627.32) and Rep:C*0102 (MFI= 98,239.49) and was not detectable in Huh7 cells (**Figure 5-15 D**). This results suggested that replicon expressing cells were retaining HLA-C molecules in the cytoplasm, hence the lower level of expression at the surface. As controls I used W6.32 (**Figure 5-15 E**), HLA-A*A11 (**Figure 5-15 F**) and DT9 (**Figure 5-15 G**) staining on 721.221 cells and 721.221:C*0304 cells.

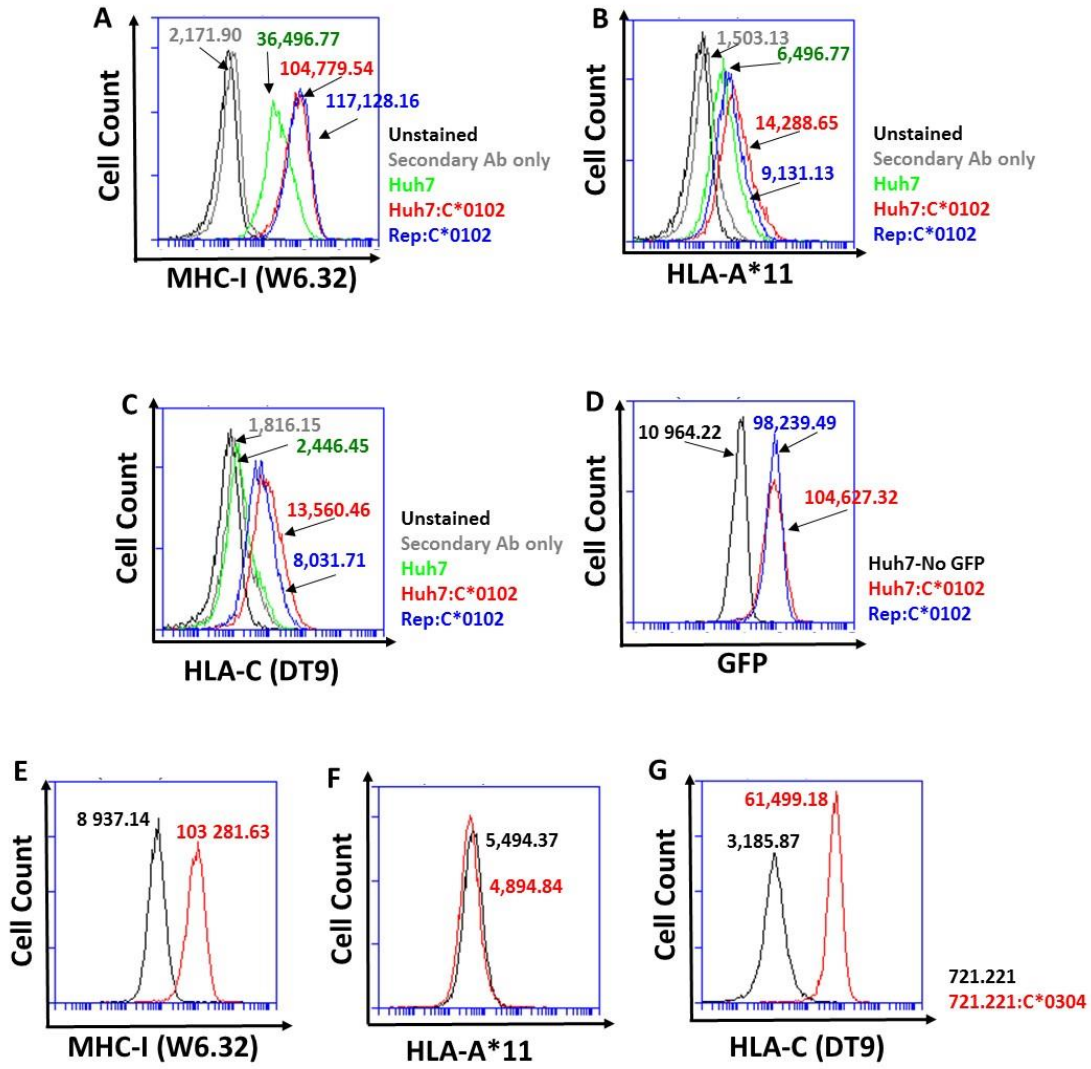

Figure 5-15: Comparison of Class I expression at the cell surface of Huh7, Huh7:C*0102 and Rep:C*0102. Cell lines were stained for total MHC-I (A), HLA-A*11 (B), HLA-C (C) and verify for their GFP expression (D). (E-G) 721.221 and 721.221:C*0304 cells were used as controls.

The summary of HLA staining of three independents experiments is shown in **Figure 5-16 A**. The ratio of HLA-A*11/total HLA I (**Figure 5-16 B**), ratio of HLA-C/total HLA I (**Figure 5-16 C**) have confirmed the observed down-regulation and correlate with data plotted in the heat-map showing how Rep:C*0102 peptide repertoire clustered with Huh7 peptide repertoire. The ratio of HLA-A*C/HLA-A*11 revealed that there were no differences between Huh7:C*0102 and Rep:C*0102 (**Figure 5-16 D)**. This observation confirms the high level of both molecules on Huh7:C*0102 compared to Rep:C*0102.

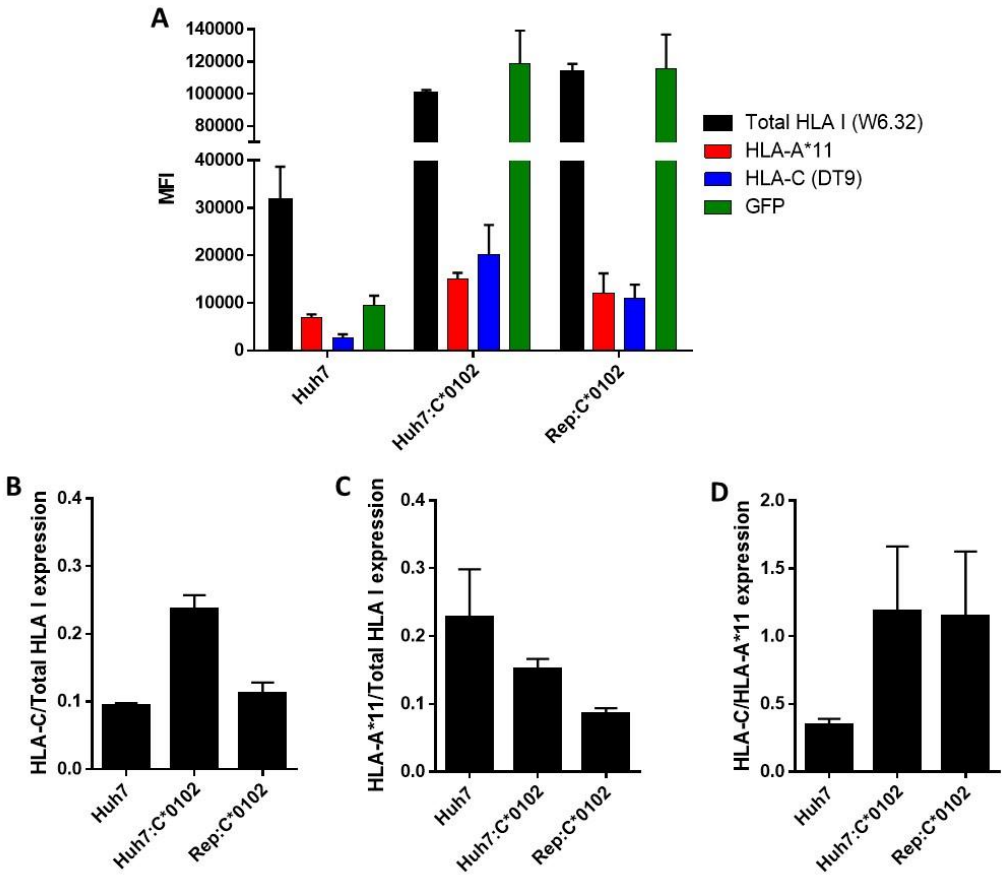

Figure 5-16: Class I molecule expression at the surface of Huh7 cells and its derivatives. (A) Staining was total HLA I, HLA-A*11 HLA-C and GFP measurements from three independent experiments were summarized. (B) Ratio of surface expression of HLA-C/Total HLA I. (C) Ratio of surface expression of HLA-A*11/Total HLA I. (D) Ratio of surface expression of HLA-C/ HLA-A*11.

5.9 Huh7 and Rep:C*0102 cells do not induce NK cell degranulation

Functional assays using CD107a were carried out using the different cell lines as targets for NK cells in degranulation assays (**Figure 5-17**). Analysis of total NK cell populations have shown that Huh7, Huh7:C*0102 as well as Rep:C*0102 were lysed by all NK cells at similar low levels (**Figure 5-17 B-D**)

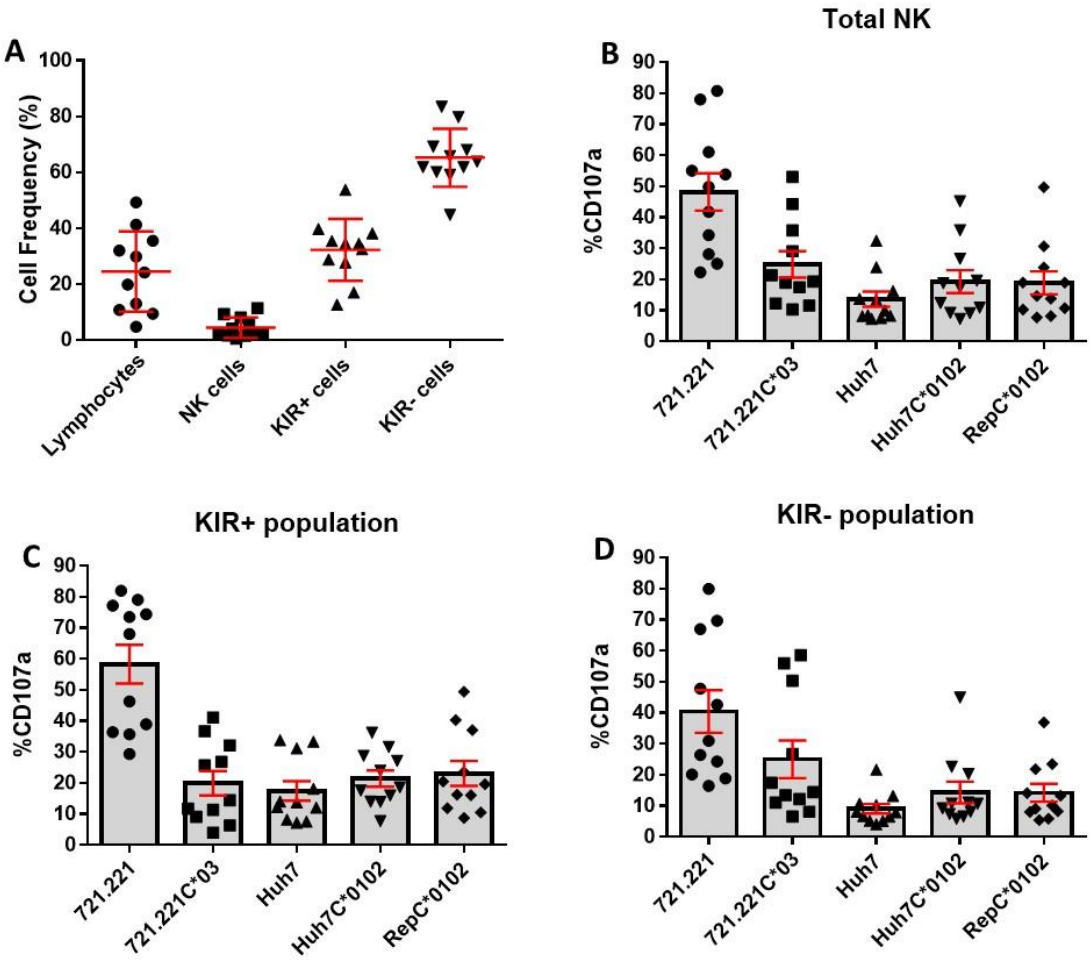

Figure 5-17: Comparison of NK cell degranulation after co-culture with Huh7 cell lines and its derivatives. (A) NK Cell frequency for each donor used in the functional assay: Lymphocyte, NK cells, KIR2DL2/L3/S2 (CD158b) positive and negative NK cells frequencies. (B) Degranulation of total NK cell population. (C) Degranulation of KIR2DL2/L3^{+} NK cells. (D) Degranulation of KIR2DL2/L3^{-} NK cells. 721.221 and 721.221 cells were used as respectively positive and negative controls. Representation of n=11 experiments.

5.10 Discussion

The role of peptides in KIR and HLA interactions has started to be taken into consideration in studies focusing on NK cell reactivity. Reports have shown that failing to recognize the peptide in the MHC-I groove results in activation of KIR-positive NK cells. This has been demonstrated for HLA-C peptides as well (207,209).

I decided to carry out an immunopeptidome analysis in order to investigate the influence of HLAC*0102 allele during viral replication and how the latter modulate peptide repertoire. Using a pan MHC-I antibody (W6.32), we have eluted HLA-A, -B and -C peptides. These peptides were quantified. Although no viral peptide was identified in the unique peptidome of Rep:C*0102 cells, the data has shown that introduction of a viral replicating system into a cell induces a subtle down-regulation of MHC-I molecules (HLA-A11 and HLA-C) at the surface. This phenomenon may be related to an accumulation of unfolded MHC-I molecules in the endoplasmic reticulum as reported by Tardif et al (299).

Additional analysis of the protein of origin of up- and down regulated peptide pool showed that replicon expressing cell have a higher metabolism and have a deficiency in ApoB-100 (306,307). Furthermore, eluted peptides reflected the cell origin, as I was able to detect peptide from liver protein such as Fatty Acid Synthetase, Fatty Acid binding protein, ApoB-100, Fatty Acid Desaturase 2.

This down-regulation of certain peptides was reflected in the immunopeptidome analysis of the difference between Huh7:C*0102 and Rep:C*0102. Peptide elution has demonstrated that there is a modulation of the peptide repertoire in favour of down regulation of a certain class of peptide associated with an up regulation of strong inhibitory peptide. Our elution strategy used the pan-MHC class I antibody W6.32 . Nevertheless we have identified a few key peptides which are presented by HLA-C*0102 and which may be involved in the sensitisation of NK cells after co-culture with Rep:C*0102 cells. Data have suggested that Rep:C*0102 tended to down regulate the surface expression of HLA-C but preserve the expression of strong inhibitory peptides such as MAPARLFAL which can prevent NK cell activation. Using a reductionist model to evaluate the reactivity of individual HLA-C*0102 binding peptides, our results have shown that the majority of down regulated peptides are involved in the prevention of KIR2DL2/L3 expressing NK cell inhibition. This NK cell reactivity was due to the fact that they have a short half-life on the MHC-I groove (VVP,

FLV and VFL) or because they have P7 and P8 residues that prevent KIR recognition (SSP and YVH). Nevertheless two of the down-regulated peptides were inhibitory (FFM and RLP). The combination of MAP (up-regulated) and SSP (down-regulated) peptide did result in a release of NK from the inhibition due to MAP peptide. This observation designated SSP peptide as a potential antagonist peptide and needs to be investigated further.

The W6.32 immunoprecipitation identified two up-regulated peptides: MAPARLFAL and FLITQLKML. The first one was an HLA-C*0102 strong binder and also a strong NK cell inhibitory peptide. The second one was a HLA-C*0102 weak binder and was non-inhibitory, most likely to having a short half-life within the MHC-I groove. This prevents the recognition of the ligand and leads to an activating NK reactivity toward target cells pulsed with this peptide. Moreover, its P7 and P8 residues in this peptide sequence are not predicted to be permissive for inhibitory KIR binding (114,207). Testing up- and down-regulated peptides separately resulted respectively in NK cells activation and inhibition. However the combination of both peptide pools resulted in inhibition.

6. General discussion

NK cells are innate immune lymphocytes that play an important role during infections and cancer. In contrast to T cells, NK cells do not require receptor rearrangement to respond to infections but their function is based on a balance between the activating and inhibitory signals that they receive. The NK cell response is tightly regulated as they express a wide range of various receptors. NK cell reactivity is in part regulated by inhibitory receptors that recognise MHC-I ligands. The MHC-I and KIR receptors are highly polymorphic. Susceptibility to disease is strongly influenced by the host genetics and several studies have reported that viral infection outcome can be influence by HLA-KIR gene interaction on disease. In the case of HCV infection, homozygosity for *KIR2DL3* and *HLA-C1* is associated with resolution of infection (297). These findings reinforce the fact that KIR gene evolution is likely to be pathogen driven.

To date peptide antagonism has been defined only for HLA-C*0102 using peptide variants of VAPWNSLSL and the 721.174 cell line which is TAP-negative and endogenously expresses HLA-C*0102. We investigated this mechanism further by studying HLA-C*0304 allele expressed in the class I-negative cell line 721.221. A series of peptides [GAVDPLL**A**L (**LA**), GAVDPLL**S**L (**L8S**), GAVDPLL**V**L (**L8V**), GAVDPLL**K**L (**L8K**) and GAVDPLL**Y**L (**L8Y**)] with previously described affinities for KIR2DL2 and a modification of the amino acid at position 8 (P8) were first used. All these peptides had similarly bound to HLA-C molecule as described by the original report and this observation was also confirmed by a Brefeldin A decay assay. Equal stabilization of HLA-C on the cell surface due to loaded peptides was an expected result as the P8 modification does not affect the anchor residue recognise by HLA-C*0304 for the peptide binding. Results from the functional assay showed a hierarchy in inhibition that can be correlated with peptide affinities for KIR2DL2. However, there was no convincing antagonism observed when strong and weak inhibitory peptides were mixed together. These results suggested that tested P8 modifications result in null peptides instead of antagonistic peptides. The results was also observed in HLA-C*0102 context where combination of VAP-LS and VAP-LY did not induce a released of NK cells from their inhibition. It has been previously described, that KIR binding and hence NK cell inhibition are particularly sensitive to the residue at P8 (207,221,308). Here, our peptides with low affinity for KIR have Tyrosine (Y), Lysine (K) or Valine (V) at P8.

It has been shown that in terms of KIR recognition of the peptide:MCH-I complex, KIR receptors accommodate complexes with peptide containing small amino acid residue at P8. Characteristics of the P8 residue may explain these aspects of our results: firstly, they can be the reason why we observed NK cell degranulation in presence of these peptides, secondly, they can explain why we did not observe any antagonism and lastly they can be an explanation for describing these peptides as null peptides. In contrast with our new finding, in our unpublished work, we described VAPWNSDYL as a NK cell antagonist peptide for HLAC*0102 alongside with VAPWNSDAL.

As amino acids at position 8 (P8) and position 7 (P7) are critical for KIR recognition, we designed a second series of peptides with modifications at p7 [GAVDPL7**R**AL (**L7R**), GAVDPL7**F**AL (**L7F**) and GAVDPL7**D**AL (**L7D**)]. Stabilisation assays showed that all these peptides had similar affinity for the HLA-C molecule as B_{max} and K_d values were almost similar. These results were predictable as the anchor residue for binding to HLA-C*0304 were not changed. This stabilisation data was confirmed by Brefeldin A decay assay. Using the CD107a as functional assay, I was able to distinguish three different types of peptide: strong inhibitory (L7R), intermediate inhibitory (L7F) and antagonist peptides (L7D). We identified L7D as an antagonist peptide as it did not inhibit NK cells but antagonised the inhibition drove by L7R. Alongside our previous study in the context of HLA-C*0102, results showed that aspartic acid at p7 in the peptide sequence resulted in an antagonist peptide. In contrast to HLA-C*0102, for HLA-C*0304 L7R triggered stronger inhibition compared to an L7F peptide. Indeed, in our previous published studies on the HLA-C*0102 allele, we described VAP-FA (with a F at P7) as a strong inhibitory peptide and VAP-RA (with a R at P7) as intermediate inhibitory peptide (218,219). These observations tend to raise new questions on the impact of the role of these amino acids in term of peptide:MHC-I complex binding to KIR2DL2/L3 in the context of HLA-C*0102 and HLA-C*0304 and allelic diversity for HLA-C. Furthermore this phenomenon implied that allelic diversity plays a role in determining the fine inhibitory specificity of the bound peptide.
Segregation analysis and gene positioning studies within the KIR haplotypes suggests that KIR2DL2 and KIR2DL3 behave as alleles at a single locus (KIR2DL2/3) (309). As expected, based on the homology in their ligand-binding domains, KIR2DL2 and KIR2DL3 bind a similar set of HLA-C ligands. Although KIR2DL2 does bind HLA-C with a higher affinity than KIR2DL3. The lower affinity of KIR2DL3 has been ascribed to arginine 16 of the N-terminal D1 extracellular domain and cysteine 148 of the D2 domain, which decrease its avidity for HLA-C through a more acute inter-domain

hinge angle between D1 and D2 (310). I used KIR2DL2-Fc conjugated with protein A in order to assay the KIR affinity of our P7 modified peptides and we found a hierarchy in term of KIR binding and this hierarchy was then observed in the CD107a assay.

As described in our previous work, we were also able to show that a small amount of a strong inhibitory peptide (L7R here) induced inhibition and this inhibition fitted a one-phase decay curve. Moreover, for all concentration of the antagonist peptide (L7D) tested, we observed a release of NK cells from inhibition due to L7R, our strong inhibitory peptide.

Combination of KIR-Fc binding and CD107a showed a correlation between the binging and the killing. According to my results, it seemed the antagonistic peptide disrupt the distribution of the inhibitory peptide at the immune synapse. This prevent the binding of the KIR-Fc as its avidity and affinity for the peptide:MHC-I complex are altered (**Figure 6-1 A-C**). Further, I have demonstrated that peptide antagonism is not restricted to one HLA-C allele, but is likely to be a more generalizable phenomenon for KIR2DL2/3. Moreover, the P7 residue appears important in defining an antagonist peptide in HLA-C*0304 context and peptide displacement is not involved in this mechanism. Additionally, results suggest a conformational aspect of the KIR-MHC-I:peptide complex recognition that will need to be explored. It may be that this phenomenon also involves the conformation adopted by the ligand and the receptor in the recognition of the MHC-I:peptide complex. As described by Zappacosta et al, the ability of individual peptides to induce NK activation differed widely so the ability to distinguish between subsets of peptides may be a general feature of MHC-I recognition by NK cells (114).

Preliminary data using minigene constructs gave encouraging insight on the ability of endogenously presented peptides to be antagonistic and its effect was noticeable in a reductionist model using KIR2DL3 expressing NKL cell lines. These preliminary results showed that experiments involving minigenes constructs needed to be refined and improved to provide a definitive answer as to the potential for antagonist peptides to be endogenously presented. Further investigation of this topic will be to understand how small changes in a peptide repertoire lead to NK cell activation.

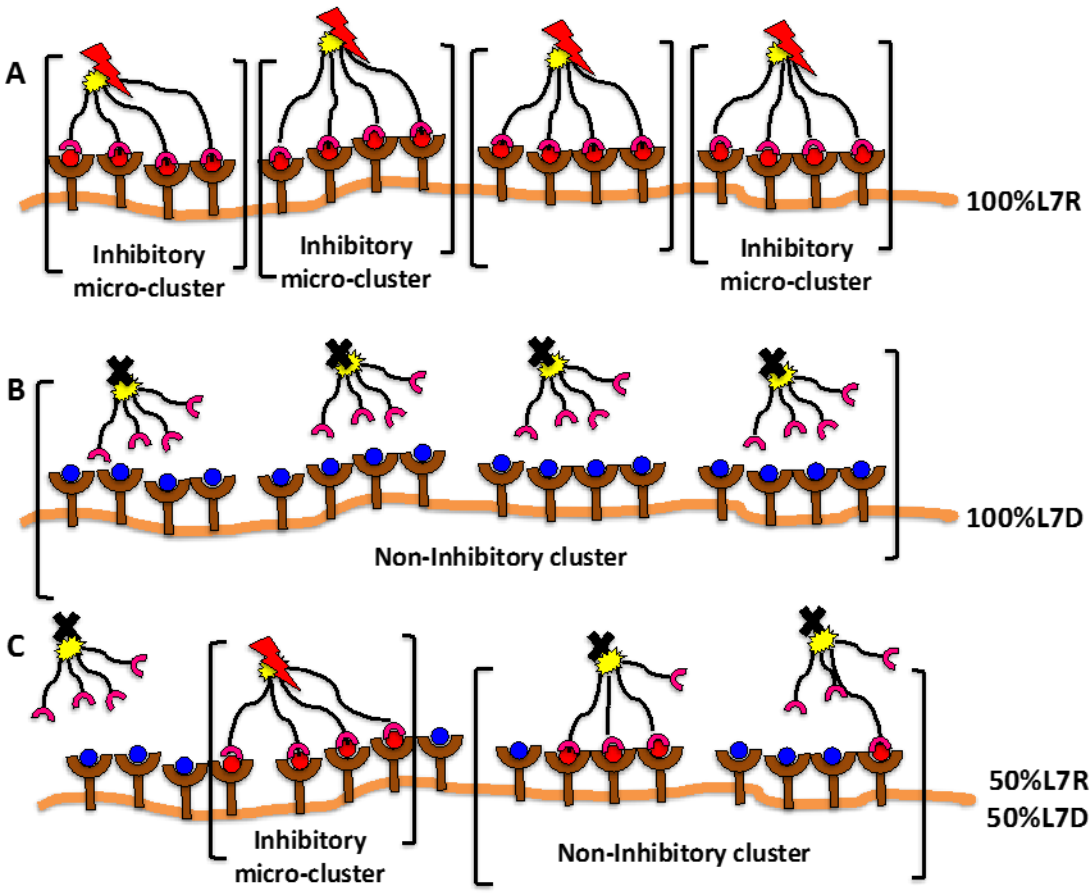

Figure 6-1: Suggested model for antagonism mechanism. (A) Strong KIR-Fc signal presence of strong inhibitory peptide L7R, in red. (B) No KIR-Fc binding in presence of non-inhibitory peptide L7D, in blue. (C) Loss of KIR binding in presence of both L7R and L7D.

The immunopeptidome experiment gave me an opportunity to uncover biologically relevant peptides involved in immune system reactivity. I decided to carry out an immunopeptidome analysis in order to investigate the influence of HLA-C*0102 allele during viral replication and how the latter modulates peptide repertoire by using a HCV replicon system. The immunoprecipitation used a pan MHC-I antibody (W6.32), have resulted in the elution HLA-A and -C peptides. Peptide identification and quantification did not reveal the presence of viral peptide.

The HCV replicon expressing cell presented an HLA-A*11 binding peptidome, with its peptidome being marked by the loss of HLA-C*0102 peptidome, compared to the parental cell, Huh7:C*0102. Furthermore, the data has shown that the introduction of a viral replicating system into a cell induces a subtle down-regulation of MHC-I

molecules (HLA-A11 and HLA-C) at the surface, a phenomenon previously reported by Tardif et al (299).

Overall, quantification analysis showed that Rep:C*0102 cells did down regulate the peptide repertoire compared to the cells without the replicon system (**Figure 6-2 A-C**). Nevertheless, expressed HLA-C*0102 at the surface tended to present strong inhibitory peptides such as MAPARLFAL (MAP). On the other hand within identified down regulated peptide, SSPITLQAL (SSP) was a NK cell non-inhibitory peptide. Residues at P7 and P8 within their amino acid sequence can help to predict their affinity for KIR2DL2/L3 (114,207). The combination of MAP (up-regulated) and SSP (down-regulated) peptide did result in a release of NK from the inhibition due to MAP peptide.

Although the Huh7 cell line allows HCV replication using a Replicon system, it seemed to be a limiting target cell line for NK cell degranulation. Nevertheless, these cells have been used in several studies that aimed to understand HCV replication and physiopathology (311–314). Here, they have allowed me to highlight how HCV replication did modulate the peptide repertoire.

Overall, it is possible that HLA-C*0102 can present peptides that mediate weak interaction with KIR receptors leading to resulting in NK cell activation during viral infection. W6.32 elution will need to be completed with a DT9 elution in order to enriched the HLA-C*0102 peptide library.

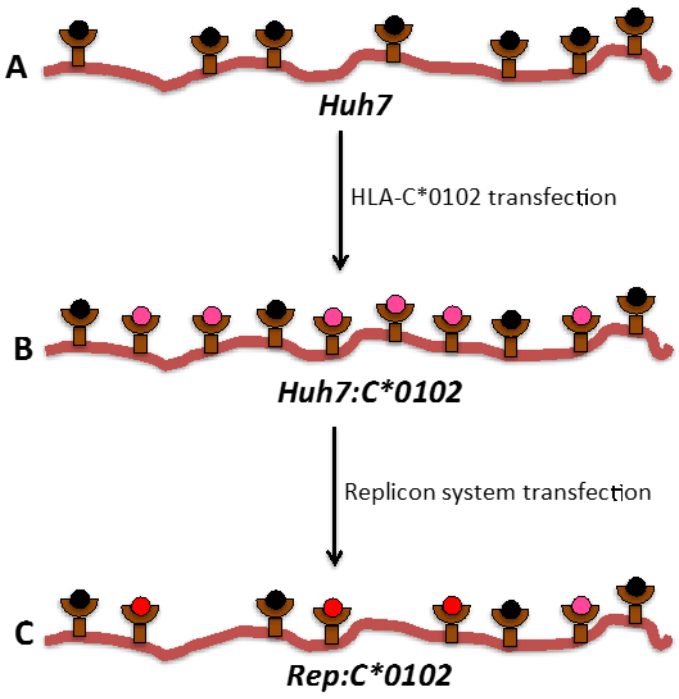

Figure 6-2: Suggested model of Huh7 cells peptide repertoire modulation. (A) Peptide repertoire of Huh7 cells. In black are shown peptides that rare naturally present. (B) Up regulation of HLA-C*0102 expression on Huh7 cells after transfection with HLA-C*0102. In pink are presented HLA-C*0102 peptides and in black peptides which are naturally present. (C) Down regulation of total HLA molecules after transfection with Replicon. In pink are presented HLA-C*0102 peptides, in red HLA-C*0102 strong inhibitory peptides and in black peptide which are naturally present.

In this study, we were able to elute peptides which are cancer related. RLPPLLSPL and MAPARLFAL are sequences found respectively in Podocalyxin-like protein 2 and Syndecan-4 proteins (315–321). In our experiments, the first one is down regulated and the second one up regulated. Both bind strongly to HLA-C and strongly inhibit NK cells via KIR2DL2/L3 receptor.

The study of the immunopeptidome gives an opportunity to understand the influence of peptide repertoire changes and its impact on the immune response. Usually identification of a peptide library is obtained and needs to be screened in vitro for their influence on NK cells reactivity. Such experiment requires improved and high-throughput methods. Functional assays for NK cell study follow a trend that tends to replace radioactive assays with calorimetric procedures. Unfortunately, these assays mainly suit primary NK cells and previously unpublished work in our group has shown that they can be difficult to adapt when using NK cell lines. I therefore decided to design a new cellular and HPLC based assay to study NK cell function and activation. During the setting-up of this assay, I have demonstrated that the Caspase 3 peptide YYGI**ETDSG**VDDYY (C3P) can be optimally detected by UHPLC system at a specific wavelength of 275nm. We expected the C3P detection to happen between 270 and 280nm as we placed a total of four tyrosines at the beginning and at the end of the C3P sequence. I have demonstrated that recombinant human Granzyme B (rhGzmB) was able to cleave C3P into two peptides of seven amino acids each (YYGI**ETD** and **SG**VDDYY). As expected, at high enzyme concentrations the majority of C3P digestion was achieved within 24hrs whereas maximum digestion at low enzyme concentration was achieved only after 95hrs of incubation. This meant that for our cellular assay, 95hrs might be a reasonable readout of NK cell activity. However I also needed to take into account the fact that during this period of time, 721.221 (MHC-I negative cells) as well as C*0304 cells alone in culture produce substances that, after 95hrs induce a considerable digestion of the C3P. These substances have a serine protease

like activity which may be responsible of the digestion of the C3P (322). Biró et al identified and reported that this substance have a molecular weight within the range of 85 to 90kDa and is expressed by activated human B cells and BL41/95 Burkitt's lymphoma cell line. This protease can be detected on the cell surface as well as in the supernatant as a secreted protein. However, complete digestion of the C3P was observed after 95hrs of incubation when we used supernatant coming from co-culture between NKL-2DL2 cells and 721.221 cells. Similar results were obtained using KIR2DL3 expressing NKL cells, indicating that this assay can detect NK cell activation in this system. Conversely, using cells loaded with previously studied peptides (GAV peptide series), I observed that neither the HPLC Assay nor the GzmB activity Assay were able to distinguish between strong inhibitory, weak inhibitory or non-inhibitory/antagonistic peptides. Nevertheless, HPLC data and GzmB activity assay clearly distinguished sensitivity of NK cells toward cells expressing or lacking MHC-I molecule. The HPLC method establishes as a novel technique to assess killing ability of NK cells. The protocol may be applied to test primary NK cells.

In summary, we have identified two antagonistic systems. These findings give new insights that lead to new opportunities to understand the peptide antagonism mechanism. Future experiments are required to understand how small changes in a peptide repertoire lead to NK cell activation. As we found that small down regulation of HLA-C*0102 goes along with up-regulation of strong inhibitory peptide, we can perceive the importance and the sensitivity of HLA-C binding peptides for NK cells reactivity during viral infections or cancer

7. Future Directions

7.1 Peptide Antagonism

I have demonstrated that peptide antagonism can be a generalizable phenomenon for HLA-C group 1 bound peptides. Still, these findings raised new questions and challenges. In depth investigation will allow us to understand how an antagonistic peptide reorganises the distribution of inhibitory peptides at the cell surface during KIR recognition. Indeed we have the possibility of generating a cell line that expresses both HLA-C*0102 and HLA-C*0304 (tagged with two distinct fluorochromes) and visualise their distribution in presence of inhibitory or antagonistic peptide by analysing micro-cluster by confocal microscopy.
Another question to answer will concern other HLA-C alleles. Is it possible to describe more antagonistic peptides? We can test for HLA-C*0801 or HLA-C*0702 which belong to the HLA-C group 1 (HLA-C1) for example.

Finally, understanding why P8 variants do result in null peptide when mixed with strong inhibitory peptides can be one key in describing what is an antagonistic peptide. This can be done by peptides elution after peptide loading to confirm the presence or absence of both peptides at the surface. This experiment may help to confirm that these P8 variants do not have any effect despite being present. Additionally, modelling and crystalisation of HLA-C*0304 and its receptor may give more insight in this phenomenon.

7.2 Immunopeptidome study

Analysis of peptidome modulation of Huh7:C*0102 in presence of a HCV replicating system have raised new questions. Is the Rep:C*0102 peptide repertoire more inhibitory than its parental cell line (Huh7:C*0102) peptide repertoire? This question can be answered by evaluating un-changed peptides between Huh7:C*0102 and Rep:C*0102. Furthermore, we can investigate the effect of the replicon system on other HLA-C alleles. Does it have the same effect as the one observed with HLA-C*0102? We can test the effect of the replicon on the peptidomes of HLA-C*0304 and HLA-C*0702 for example. In completion of our first study, it will be interesting to investigate the antagonistic potential of SSPITLQAL peptide.

Finally, an in-depth investigation of HLA-A*11 peptides will be important, focussing on the study of up- and down-regulated peptides, especially as HLA-A*11 is recognised to be an allele which can bind to activating and inhibitory KIR. Are up-regulated peptides more likely to bind inhibitory KIR and down regulated peptide susceptible to bind activating KIR and what are the implications of this for viral infections and cancer?

Appendices

A.1 Material and Reagents used

A.1.1 Equipment

- Flow cytometer Accuri C6 Flow, cat.#: 2775, BD bioscience
- UHPLC UltiMate 3000, cat.#: 8076932 (Pump, NCS-3500RS), ThermoScientific
- DNA Engine Tetrad 2, Peltier Thermal Cycler, MJ Research, cat.#: ALS1296 (unit block)
- UV transilluminator, UVP
- Bench centrifuge Heraeus Fresco 17 centrifuge, Thermo Scientific
- CR4i Centrifuge, cat.#: 30402276, Jouan
- DHD autoflow CO_2 air Jacketed incubator, Nuaire
- Purcell TC direct heat CO_2 incubator, Nuaire
- Axiovert 40 CFL, Zeiss (inverted microscope)
- Vortex Genius 3, Ika
- Sub Aqua 12 water bath, Grant
- pH 210 Microprocessor pH meter, Hanna Instruments
- Spectrophotometer,Nanodrop, ND-1000
- Confocal microscopy SP8, Leica

A.1.2 Reagents

- AIM-V + AlbuMAX (BSA) (1X), cat.#: 31035-025, Gibco Life Technologies
- Citric Acid monohydrate, cat.#: C/6200/53, Fisher Scientific
- Dimethyl sulfoxide (DMSO), cat.#: D8418, Sigma-Aldrich
- Glycerol
- Human AB serum, cat.#: H6914, Sigma-Aldrich
- PBS 1X, filtred and sterile, cat.#: BE17-516F, Lonza
- PBS tablets, cat.#: P4417-100TAB, Sigma-Aldrich
- PFA (4%) in PBS, cat.#: sc-281692, Santa Cruz
- Proteine A Alexa Fluor 488, Invitrogen, cat #: P11047, lot #: 16118347
- RPMI medium 1640 (1X) + GlutaMAX-I, cat.#: 61870-010, Gibco Life Technologies

- rhIL2: from NIH services
- rhIL15, cat.#: 247-IL-025, R&D systems
- rhKIR2DL2-Fc chimera, R&D systems, cat. #: 3015-KR, lot#: NHI0114091
- Hygromycin (HygroGold), cat.#: ant-hg-5, Invivogen
- Pen Strep Glutamine (100X), cat.#: 10378-016, Gibco Life Technologies
- FBS, cat.#: SV30180.03, lot#: SYJ20004, Hyclone
- BSA, cat.#: A2153-100G, Sigma-Aldrich
- Sodium Azide (NaN_3), cat.#: S2002-100G, Sigma-Aldrich
- Sodium Phosphate Dibasic solution, cat.#: 94046-100ML-F, Sigma-Aldrich

A.1.3 Antibodies

Antigen	Clone	Fluorochr.	Dil.	Cat. #	Compagny
CD107a (LAMP-1)	eBioH4A3	eFluor 660	1/400	50-1079-42	eBioscience
CD3	UCHT1	PerCP	1/100	300428	BioLegend
CD56	HCD56	PE	1/50	318306	BioLegend
CD56	B159	PE	1/2.5	555516	BD Bioscience
CD158b (KIR2DL2/L3/S2)	CH-L	FITC	1/5	559784	BD Bioscience
Goat F(ab')2 IgG H&L	polyclonal	PE	1/50	ab7002	Abcam
Goat F(ab')2 IgG H&L	polyclonal	AF647	1/6000		Abcam
HLA-A*11	4i93	-	1/10	ab33641	Abcam

A.1.4 Software

- BD Accuri C6, version 1.0.264.21
- Chromeleon, version 6.80, ThermoScientific
- WinTV2000
- GraphPad Prism, version 6.05

A.2 Buffers

- Non-sterile PBS 1X (1L):
- 1L H_2O
- 5 PBS tablets

- FACS wash buffer (1L):
- 1L non-sterile PBS 1X
- 10g BSA (1% final concentration)
- 1g NaN_3 (0.1% final concentration)

- FACS blocking buffer (50ml):
- 45ml FACS wash buffer
- 5ml human AB serum (10% final concentration)

- Fixing buffer (50ml):
- 37.5ml non-sterile PBS 1X
- 12.5ml 4% PFA (1% final concentration)

- Citrate buffer (50ml):
- 1.37g Citric Acid (M final concentration)
- 6.6ml Sodium Phosphate Dibasic solution (M final concentration)
- 43.4ml H_2O (filtrated)

A.3 HPLC Programs

A.3.1 GAV Peptides elution

ColumnOven.TempCtrl =	On
ColumnOven.Temperature.Nominal =	35.0 [°C]
ColumnOven.Temperature.LowerLimit =	35.0 [°C]
ColumnOven.Temperature.UpperLimit =	45.0 [°C]
EquilibrationTime =	0.5 [min]
ColumnOven.ReadyTempDelta =	1.0 [°C]

```
LoadingPump.Pressure.LowerLimit =           0 [bar]
LoadingPump.Pressure.UpperLimit =           620 [bar]
LoadingPump.MaximumFlowRampDown =           10 [µl/min²]
LoadingPump.MaximumFlowRampUp =             10 [µl/min²]
LoadingPump.%A.Equate                                          =
          "98%H2O/2%ACN+0.05%TFA"
LoadingPump.%B.Equate =                     "%B"
%C.Equate =                                 "%C"
NC_Pump.Pressure.LowerLimit =               0 [bar]
NC_Pump.Pressure.UpperLimit =               400 [bar]
NC_Pump.MaximumFlowRampDown =               0.300 [µl/min²]
NC_Pump.MaximumFlowRampUp =                 0.300 [µl/min²]
NC_Pump.%A.Equate =                         "100%H2O+0.05%TFA"
NC_Pump.%B.Equate                                              =
          "20%H2O/80%ACN+0.05%TFA"
DrawSpeed =                                 350 [nl/s]
DrawDelay =                                 3000 [ms]
DispSpeed =                                 2500 [nl/s]
DispenseDelay =                             0 [ms]
WasteSpeed =                                6000 [nl/s]
WashSpeed =                                 8333 [nl/s]
LoopWashFactor =                            1.000
SampleHeight =                              2.000 [mm]
PunctureDepth =                             10.000 [mm]
WashVolume =                                50.000 [µl]
SyncWithPump =                              Off
LowDispersionMode =                         Off
InjectMode =                                ulPickUp
FirstTransportVial =                        R1
LastTransportVial =                         R1
TransportVialCapacity =                     Unlimited
TransLiquidHeight =                         5.000 [mm]
```

```
TransVialPunctureDepth =                        7.000 [mm]

FlushVolume =                                   3.500 [µl]

LoadingPump_Pressure.Step =                     0.01
[s]LoadingPump_Pressure.Average =               Off

NC_Pump_Pressure.Step =                         0.01 [s]

NC_Pump_Pressure.Average =                      Off

UV.Data_Collection_Rate =                       2.5 [Hz]

TimeConstant =                                  0.60 [s]

UV_VIS_1.Wavelength =                           220 [nm]

LoadingPump.Flow =                              15.000 [µl/min]

LoadingPump.%B =                                0.0 [%]

%C =                                            0.0 [%]

LoadingPump.Curve =                             5

ValveLeft =                                     1_2

ValveRight =                                    1_2

Sampler.TempCtrl =                              On

Sampler.Temperature.Nominal =                   8.0 [°C]

Sampler.Temperature.LowerLimit =                4.0 [°C]

Sampler.Temperature.UpperLimit =                10.0 [°C]

Sampler.ReadyTempDelta =                        2.0 [°C]


 0.000     Autozero

           NC_Pump.Flow =                       0.350 [µl/min]

           NC_Pump.%B =                         4.0 [%]

           Wait                                 UV.Ready            and
LoadingPump.Ready   and   NC_Pump.Ready   and   ColumnOven.Ready   and
Sampler.Ready and PumpModule.Ready

           Inject

           LoadingPump_Pressure.AcqOn

           NC_Pump_Pressure.AcqOn

           CollectFractions =                   No

           UV_VIS_1.AcqOn
```

```
          NC_Pump.Flow =                    0.350 [µl/min]
          NC_Pump.%B =                      4.0 [%]
 3.000    NC_Pump.Flow =                    0.350 [µl/min]
          NC_Pump.%B =                      4.0 [%]
          ValveLeft =                       10_1
          ValveRight =                      1_2

33.000    NC_Pump.Flow =                    0.350 [µl/min]
          NC_Pump.%B =                      60.0 [%]

33.100    NC_Pump.Flow =                    0.350 [µl/min]
          NC_Pump.%B =                      90.0 [%]

38.000    NC_Pump.Flow =                    0.350 [µl/min]
          NC_Pump.%B =                      90.0 [%]

38.100    NC_Pump.Flow =                    0.350 [µl/min]
          NC_Pump.%B =                      4.0 [%]

53.000    NC_Pump.Flow =                    0.350 [µl/min]
          UV_VIS_1.AcqOff
          NC_Pump.%B =                      4.0 [%]
          ValveLeft =                       1_2
          ValveRight =                      1_2

          LoadingPump_Pressure.AcqOff
          NC_Pump_Pressure.AcqOff
          End
```

A.3.2 Granzyme B Assay: initial program

```
Sampler.Temperature.LowerLimit =                4.0 [°C]

Sampler.Temperature.UpperLimit =                10.0 [°C]

Sampler.ReadyTempDelta =                        2.0 [°C]

ColumnOven.TempCtrl =                           On

ColumnOven.Temperature.Nominal =                35.0 [°C]

ColumnOven.Temperature.LowerLimit =             35.0 [°C]

ColumnOven.Temperature.UpperLimit =             45.0 [°C]

EquilibrationTime =                             0.5 [min]

ColumnOven.ReadyTempDelta =                     1.0 [°C]

LoadingPump.Pressure.LowerLimit =               0 [bar]

LoadingPump.Pressure.UpperLimit =               620 [bar]

LoadingPump.MaximumFlowRampDown =               10 [µl/min²]

LoadingPump.MaximumFlowRampUp =                 10 [µl/min²]

LoadingPump.%A.Equate                                                   =
          "98%H2O/2%ACN+0.05%TFA"

LoadingPump.%B.Equate =                         "%B"

%C.Equate =                                     "%C"

NC_Pump.Pressure.LowerLimit =                   0 [bar]

NC_Pump.Pressure.UpperLimit =                   400 [bar]

NC_Pump.MaximumFlowRampDown =                   0.300 [µl/min²]

NC_Pump.MaximumFlowRampUp =                     0.300 [µl/min²]

NC_Pump.%A.Equate =                             "100%H2O+0.05%TFA"

NC_Pump.%B.Equate                                                       =
          "20%H2O/80%ACN+0.05%TFA"

DrawSpeed =                                     350 [nl/s]

DrawDelay =                                     3000 [ms]

DispSpeed =                                     2500 [nl/s]

DispenseDelay =                                 0 [ms]

WasteSpeed =                                    6000 [nl/s]

WashSpeed =                                     8333 [nl/s]

LoopWashFactor =                                1.000
```

```
SampleHeight =                          2.000 [mm]
PunctureDepth =                         10.000 [mm]
WashVolume =                            50.000 [µl]
SyncWithPump =                          Off
LowDispersionMode =                     Off
InjectMode =                            ulPickUp
FirstTransportVial =                    R1
LastTransportVial =                     R1
TransportVialCapacity =                 Unlimited
TransLiquidHeight =                     5.000 [mm]
TransVialPunctureDepth =                7.000 [mm]
FlushVolume =                           3.500 [µl]
LoadingPump_Pressure.Step =             0.01 [s]
LoadingPump_Pressure.Average =          Off
NC_Pump_Pressure.Step =                 0.01 [s]
NC_Pump_Pressure.Average =              Off
UV.Data_Collection_Rate =               2.5 [Hz]
TimeConstant =                          0.60 [s]
UV_VIS_1.Wavelength =                   270 [nm]
LoadingPump.Flow =                      15.000 [µl/min]
LoadingPump.%B =                        0.0 [%]
%C =                                    0.0 [%]
LoadingPump.Curve =                     5
ValveLeft =                             1_2
ValveRight =                            1_2
Sampler.TempCtrl =                      On
Sampler.Temperature.Nominal =           4.0 [°C]
UV_VIS_2.Wavelength =                   275 [nm]
UV_VIS_3.Wavelength =                   280 [nm]
UV_VIS_4.Wavelength =                   290 [nm]
UV.Data_Collection_Rate =               2.5 [Hz]
```

```
TimeConstant =                                  0.60 [s]

UV_VIS_1.Wavelength =                           270 [nm]

UV_VIS_2.Wavelength =                           275 [nm]

UV_VIS_3.Wavelength =                           280 [nm]

UV_VIS_4.Wavelength =                           290 [nm]

LoadingPump.Flow =                              15.000 [µl/min]

LoadingPump.%B =                                0.0 [%]

%C =                                            0.0 [%]

LoadingPump.Curve =                             5

ValveLeft =                                     1_2

ValveRight =                                    1_2


 0.000     Autozero

           NC_Pump.Flow =                       0.350 [µl/min]

           NC_Pump.%B =                         4.0 [%]

           Autozero

           NC_Pump.Flow =                       0.350 [µl/min]

           NC_Pump.%B =                         4.0 [%]

           Wait                                 UV.Ready            and
LoadingPump.Ready   and   NC_Pump.Ready   and   ColumnOven.Ready   and
Sampler.Ready and PumpModule.Ready

           Inject

           LoadingPump_Pressure.AcqOn

           NC_Pump_Pressure.AcqOn

           CollectFractions =                   No

           UV_VIS_1.AcqOn

           UV_VIS_2.AcqOn

           UV_VIS_3.AcqOn

           UV_VIS_4.AcqOn

           NC_Pump.Flow =                       0.350 [µl/min]

           NC_Pump.%B =                         4.0 [%]

           NC_Pump.Flow =                       0.350 [µl/min]
```

```
          NC_Pump.%B =                    4.0 [%]

 3.000    NC_Pump.Flow =                  0.350 [µl/min]
          NC_Pump.%B =                    4.0 [%]
          ValveLeft =                     10_1
          ValveRight =                    1_2
          NC_Pump.Flow =                  0.350 [µl/min]
          NC_Pump.%B =                    4.0 [%]
          ValveLeft =                     10_1
          ValveRight =                    1_2

23.000    NC_Pump.Flow =                  0.350 [µl/min]
          NC_Pump.%B =                    60.0 [%]
          NC_Pump.Flow =                  0.350 [µl/min]
          NC_Pump.%B =                    90.0 [%]
          NC_Pump.Flow =                  0.350 [µl/min]
          NC_Pump.%B =                    60.0 [%]
          NC_Pump.Flow =                  0.350 [µl/min]
          NC_Pump.%B =                    90.0 [%]

28.000    NC_Pump.Flow =                  0.350 [µl/min]
          NC_Pump.%B =                    90.0 [%]
          NC_Pump.Flow =                  0.350 [µl/min]
          NC_Pump.%B =                    4.0 [%]
          NC_Pump.Flow =                  0.350 [µl/min]
          NC_Pump.%B =                    90.0 [%]
          NC_Pump.Flow =                  0.350 [µl/min]
          NC_Pump.%B =                    4.0 [%]

43.000    LoadingPump_Pressure.AcqOff
          NC_Pump_Pressure.AcqOff
```

```
UV_VIS_1.AcqOff
NC_Pump.Flow =                          0.350 [µl/min]
NC_Pump.%B =                            4.0 [%]
ValveLeft =                             1_2
ValveRight =                            1_2
UV_VIS_2.AcqOff
UV_VIS_3.AcqOff
UV_VIS_4.AcqOff
End
```

A.3.3 Granzyme B Assay

```
ColumnOven.TempCtrl =                   On
ColumnOven.Temperature.Nominal =        35.0 [°C]
ColumnOven.Temperature.LowerLimit =     35.0 [°C]
ColumnOven.Temperature.UpperLimit =     45.0 [°C]
EquilibrationTime =                     0.5 [min]
ColumnOven.ReadyTempDelta =             1.0 [°C]
LoadingPump.Pressure.LowerLimit =       0 [bar]
LoadingPump.Pressure.UpperLimit =       620 [bar]
LoadingPump.MaximumFlowRampDown =       10 [µl/min²]
LoadingPump.MaximumFlowRampUp =         10 [µl/min²]
LoadingPump.%A.Equate                                    =
          "98%H2O/2%ACN+0.05%TFA"
LoadingPump.%B.Equate =                 "%B"
%C.Equate =                             "%C"
NC_Pump.Pressure.LowerLimit =           0 [bar]
NC_Pump.Pressure.UpperLimit =           400 [bar]
NC_Pump.MaximumFlowRampDown =           0.300 [µl/min²]
NC_Pump.MaximumFlowRampUp =             0.300 [µl/min²]
NC_Pump.%A.Equate =                     "100%H2O+0.05%TFA"
```

```
NC_Pump.%B.Equate                                                    =
          "20%H2O/80%ACN+0.05%TFA"
DrawSpeed =                                    350 [nl/s]
DrawDelay =                                    3000 [ms]
DispSpeed =                                    2500 [nl/s]
DispenseDelay =                                0 [ms]
WasteSpeed =                                   6000 [nl/s]
WashSpeed =                                    8333 [nl/s]
LoopWashFactor =                               1.000
SampleHeight =                                 2.000 [mm]
PunctureDepth =                                10.000 [mm]
WashVolume =                                   50.000 [µl]
SyncWithPump =                                 Off
LowDispersionMode =                            Off
InjectMode =                                   ulPickUp
FirstTransportVial =                           R1
LastTransportVial =                            R1
TransportVialCapacity =                        Unlimited
TransLiquidHeight =                            5.000 [mm]
TransVialPunctureDepth =                       7.000 [mm]
FlushVolume =                                  3.500 [µl]
LoadingPump_Pressure.Step =                    0.01 [s]
LoadingPump_Pressure.Average =                 Off
NC_Pump_Pressure.Step =                        0.01 [s]
NC_Pump_Pressure.Average =                     Off
UV.Data_Collection_Rate =                      2.5 [Hz]
TimeConstant =                                 0.60 [s]
UV_VIS_1.Wavelength =                          275 [nm]
LoadingPump.Flow =                             15.000 [µl/min]
LoadingPump.%B =                               0.0 [%]
%C =                                           0.0 [%]
```

```
LoadingPump.Curve =                          5

ValveLeft =                                  1_2

ValveRight =                                 1_2

Sampler.TempCtrl =                           On

Sampler.Temperature.Nominal =                4.0 [°C]

Sampler.Temperature.LowerLimit =             4.0 [°C]

Sampler.Temperature.UpperLimit =             10.0 [°C]

Sampler.ReadyTempDelta =                     2.0 [°C]


 0.000     Autozero

           NC_Pump.Flow =                    0.350 [µl/min]

           NC_Pump.%B =                      4.0 [%]

           Wait                              UV.Ready             and
LoadingPump.Ready   and   NC_Pump.Ready   and   ColumnOven.Ready   and
Sampler.Ready and PumpModule.Ready

           Inject

           LoadingPump_Pressure.AcqOn

           NC_Pump_Pressure.AcqOn

           CollectFractions =                No

           UV_VIS_1.AcqOn

           NC_Pump.Flow =                    0.350 [µl/min]

           NC_Pump.%B =                      4.0 [%]


 3.000     NC_Pump.Flow =                    0.350 [µl/min]

           NC_Pump.%B =                      4.0 [%]

           ValveLeft =                       10_1

           ValveRight =                      1_2


23.000     NC_Pump.Flow =                    0.350 [µl/min]

           NC_Pump.%B =                      60.0 [%]

           NC_Pump.Flow =                    0.350 [µl/min]

           NC_Pump.%B =                      90.0 [%]
```

```
28.000     NC_Pump.Flow =                    0.350 [µl/min]
           NC_Pump.%B =                      90.0 [%]
           NC_Pump.Flow =                    0.350 [µl/min]
           NC_Pump.%B =                      4.0 [%]

43.000     LoadingPump_Pressure.AcqOff
           NC_Pump_Pressure.AcqOff
           UV_VIS_1.AcqOff
           NC_Pump.Flow =                    0.350 [µl/min]
           NC_Pump.%B =                      4.0 [%]
           ValveLeft =                       1_2
           ValveRight =                      1_2
           End
```

A.4 Immunopeptidome study: Origin

A.4.1 List of HLA-C*0102 peptide (“quality control”)

peptide	Unique	UniProt ID	Orginated from
LPPPPPPPP	No	Q7Z5R6	Amyloid beta A4 precursor protein-binding
		P10323	Acrosin.
		P55196	Afadin.
		Q9C0F0	Putative Polycomb group protein ASXL3.
		Q7Z7K6	Centromere protein V.
		C9JLR9	Uncharacterized protein C11orf95.
		Q8N144	Gap junction delta-3 protein.
		Q96MA1	Doublesex- and mab-3-related
		B1AK53	Espin.
		Q8WUP2	Filamin-binding LIM protein 1.
		Q68DA7	Formin-1.
		O95466	Formin-like protein 1.
		P55316	Forkhead box protein G1.
		P52951	Homeobox protein GBX-2.
		O15054	Lysine-specific demethylase 6B.
		Q6P5Q4	Leiomodin-2.
		Q8ND23	Capping protein, Arp2/3 and myosin-I
		Q86VE0	Myb-related transcription factor, partner
		Q96HR8	H/ACA ribonucleoprotein complex non-core
		Q8IZL8	Proline-, glutamic acid- and leucine-rich
		Q86XR5	Proline-rich membrane anchor 1.
		Q7Z7A4	PX domain-containing protein kinase-like
		Q70E73	Ras-associated and pleckstrin homology
		Q7L0R7	RING finger protein 44.
		Q9UPS6	Histone-lysine N-methyltransferase
		Q99590	Protein SCAF11.
		Q8TF72	Protein Shroom3.
		Q6BEB4	Transcription factor Sp5.
		O14669	Transmembrane gamma-carboxyglutamic acid
		P48023	Tumor necrosis factor ligand superfamily
		Q96PN7	Transcriptional-regulating factor 1.
		Q92558	Wiskott-Aldrich syndrome protein family
		Q8TF30	WASP homolog-associated protein with
		O15156	Zinc finger and BTB domain-containing
		Q96T25	Zinc finger protein ZIC 5.
		Q5VUA4	Zinc finger protein 318.

EVQLVESGGGLVQPG	No	P01766	Ig-like.
		P01777	Ig-like.
		P80419	Ig-like.
KLHEEEIQEL	No	P08670	Vimentin.
PQQARSL	No	Q15406	Nuclear receptor subfamily 6 group A
RFPDGTNGL	Yes	Q99967	Cbp/p300-interacting transactivator 2.
SSFVQNGSTFVK	Yes	P35573	Glycogen debranching enzyme.
TSPEAFLAL	Yes	P78527	DNA-dependent protein kinase catalytic
SLQEEIAFLK	Yes	P08670	Vimentin.
SVDERLIYK	Yes	Q9Y3B1	PRELI domain containing protein 3B.
FRDGPPL	Yes	Q15056	Eukaryotic translation initiation factor
ASALPALVMSK	Yes	P36578	60S ribosomal protein L4.
NQEVNKGVKEE	Yes	Q8WXH0	Nesprin-2.
LLHQSFQPL	Yes	Q9NU22	Midasin.
FSPNRVIGL	Yes	O00303	Eukaryotic translation initiation factor
LFPRHTNASA	Yes	O15144	Actin-related protein 2/3 complex subunit
SYTSGPGSRISSSS	Yes	P05787	Keratin, type II cytoskeletal 8.
VNLAELFK	Yes	P30044	Peroxiredoxin-5, mitochondrial.
LESEHPKVM	Yes	Q9NUA8	Zinc finger and BTB domain-containing
GAPGRDLPL	Yes	Q9NUP1	Biogenesis of lysosome-related organelles
IIHVDPVSQL	Yes	Q8IVL1	Neuron navigator 2.
RSFSDKNGLTSK	Yes	P22466	Galanin.
TSGPRAFSS	Yes	P05787	Keratin, type II cytoskeletal 8.
STSGPRAFSS	Yes	P05787	Keratin, type II cytoskeletal 8.
SIQHPLIKK	Yes	Q9NZJ4	Sacsin.
ISPKLLSHF	Yes	Q9H4H8	Protein FAM83D.
VFHPRQEL	Yes	P53621	Coatomer subunit alpha.
AVPEAIPTPR	Yes	P57086	SCAN domain-containing protein 1.

VEGGQVLK	Yes	P06756	Integrin alpha-V.
RVPSAGSSL	Yes	Q8IX21	SMC5-SMC6 complex localization factor
LLPPPMKEL	Yes	O60841	Eukaryotic translation initiation factor
RNVSTGDVNVE	Yes	P13645	Keratin, type I cytoskeletal 10.
RINEILSNAL	Yes	P52272	Heterogeneous nuclear ribonucleoprotein
SVPLPISHK	Yes	P51784	Ubiquitin carboxyl-terminal hydrolase 11.
SVQSSERPL	Yes	P49327	Fatty acid synthase.
FSGVYKK	Yes	P62081	40S ribosomal protein S7.
SSLPTFKTA	Yes	Q6PIW4	Fidgetin-like protein 1.
GTIAYLPPER	Yes	P57078	Receptor-interacting serine/threonine-
AVSDTVPERK	Yes	O00472	RNA polymerase II elongation factor ELL2.
AVYEDQVGK	Yes	Q8N766	ER membrane protein complex subunit 1.
RVMKALVNR	Yes	Q08945	FACT complex subunit SSRP1.
TIIDKSKSV	Yes	Q01581	Hydroxymethylglutaryl-CoA synthase,
SAFKPSSAITK	Yes	P13611	Versican core protein.
RSIPYDQSPGPK	Yes	Q9H3K2	Growth hormone-inducible transmembrane
RVPDGMVGL	Yes	Q92945	Far upstream element-binding protein 2.
IFHEKTSEF	Yes	P52569	Cationic amino acid transporter 2.
SYNAIRTGL	Yes	P53992	Protein transport protein Sec24C.
EVQLKNYGKFLE	Yes	Q2M389	WASH complex subunit 7.
TAAHFGGGGGLL	Yes	P78316	Nucleolar protein 14.
LAPRQVLD	Yes	O75643	U5 small nuclear ribonucleoprotein 200
TVNQSLLSPL	Yes	P05787	Keratin, type II cytoskeletal 8.
RVTELQQQPL	Yes	Q96AG4	Leucine-rich repeat-containing protein
AIAEFARSL	Yes	P17987	T-complex protein 1 subunit alpha.
TPVLMNQPPQI	Yes	Q04637	Eukaryotic translation initiation factor
KAPEMTNEL	Yes	Q5QJE6	Deoxynucleotidyltransferase terminal-
RLPDGIGQL	Yes	Q14160	Protein scribble homolog.
RPSSLPVGPVL	Yes	Q96SU4	Oxysterol-binding protein-related protein
TAIGMPVEK	Yes	Q14728	Major facilitator superfamily domain-
LTPGLYEFK	Yes	Q8IZA0	Dyslexia-associated protein KIAA0319-like
YTSGPGSRISSS	Yes	P05787	Keratin, type II cytoskeletal 8.
LLMPLPGTK	Yes	Q9UMZ2	Synergin gamma.
ASVLNPYVK	Yes	P48047	ATP synthase subunit O, mitochondrial.
STFSTNYRSL	Yes	P05783	Keratin, type I cytoskeletal 18.
ISGFYKLLS	Yes	P78527	DNA-dependent protein kinase catalytic
ATAFSSLDR	Yes	Q8N766	ER membrane protein complex subunit 1.
EFGGPEVLK	Yes	Q08257	Quinone oxidoreductase.
VSTSGPRAFSS	Yes	P05787	Keratin, type II cytoskeletal 8.
FLPRQPPMSL	Yes	Q13045	Protein flightless-1 homolog.
MLPEKLRPL	Yes	O95563	Mitochondrial pyruvate carrier 2.
MGPGTVNGGHPPSAL	Yes	Q99967	Cbp/p300-interacting transactivator 2.
RLPDGFTQL	Yes	Q14160	Protein scribble homolog.
VQPQVTVPL	Yes	Q96TA2	ATP-dependent zinc metalloprotease
KVQAGNSSL	Yes	Q9Y617	Phosphoserine aminotransferase.
QAPSYGARPV	Yes	P05783	Keratin, type I cytoskeletal 18.
YVTTSTRT	Yes	P08670	Vimentin.
IGPRGNTL	Yes	Q15637	Splicing factor 1.
SASSVTVTR	Yes	P02545	Prelamin-A/C.
RLPSKPYSTL	Yes	Q08AE8	Protein spire homolog 1.
RVPLGSVI	Yes	P27338	Amine oxidase [flavin-containing] B.
KIQGDDWEPRPL	Yes	O95817	BAG family molecular chaperone regulator
AAPPKRPAV	Yes	P27816	Microtubule-associated protein 4.
AIMENANVL	Yes	P04075	Fructose-bisphosphate aldolase A.
RAMGEQLLPGK	Yes	Q14671	Pumilio homolog 1.
RMPDGPVAL	Yes	Q14204	Cytoplasmic dynein 1 heavy chain 1.

A.4.2 List of down-regulated peptide

peptide	Unique	UniProt ID	Orginated from
PPPPLPPPP	No	A6NF34	Anthrax toxin receptor-like.
		O60885	Bromodomain-containing protein 4.
		Q9Y613	FH1/FH2 domain-containing protein 1.
		O15054	Lysine-specific demethylase 6B.
		Q96Q04	Serine/threonine-protein kinase LMTK3.
		Q96HR8	H/ACA ribonucleoprotein complex non-core
		O75376	Nuclear receptor corepressor 1.
		Q8N8D1	Programmed cell death protein 7.
		Q08499	cAMP-specific 3',5'-cyclic
		Q86XR5	Proline-rich membrane anchor 1.
		Q96HE9	Proline-rich protein 11.
		Q9ULL5	Proline-rich protein 12.
		Q9Y6X0	SET-binding protein.
		A0MZ66	Shootin-1.
		P48023	Tumor necrosis factor ligand superfamily
		O15016	Tripartite motif-containing protein 66.
		Q96JH7	Deubiquitinating protein VCIP135.
		A6NGB9	WAS/WASL-interacting protein family
		P49750	YLP motif-containing protein 1.
		Q9BYN7	Zinc finger protein 341.
AVSEGTKAVTK	No	Q96A08	Histone H2B type 1-A.
		P33778	Histone H2B type 1-B.
		P62807	Histone H2B type 1-C/E/F/G/I.
		P58876	Histone H2B type 1-D.
		Q93079	Histone H2B type 1-H.
		P06899	Histone H2B type 1-J.
		O60814	Histone H2B type 1-K.
		Q99880	Histone H2B type 1-L.
		Q99879	Histone H2B type 1-M.
		Q99877	Histone H2B type 1-N.
		P23527	Histone H2B type 1-O.
		Q16778	Histone H2B type 2-E.
		Q5QNW6	Histone H2B type 2-F.
		Q8N257	Histone H2B type 3-B.
		P57053	Histone H2B type F-S.

FFMPGFAPL	No	Q9H4B7	Tubulin beta-1 chain.
		Q13885	Tubulin beta-2A chain.
		Q9BVA1	Tubulin beta-2B chain.
		P68371	Tubulin beta-4B chain.
		Q13509	Tubulin beta-3 chain.
		P04350	Tubulin beta-4A chain.
		P07437	Tubulin beta chain.
		Q9BUF5	Tubulin beta-6 chain.
		A6NNZ2	Tubulin beta-8 chain-like protein
		Q3ZCM7	Tubulin beta-8 chain.
SYELPDGQVITIGNER	No	P62736	Actin, aortic smooth muscle.
		Q562R1	Beta-actin-like protein 2.
		Q9BYX7	Putative beta-actin-like protein 3.
		P60709	Actin, cytoplasmic 1.
		P68032	Actin, alpha cardiac muscle 1.
		P63261	Actin, cytoplasmic 2.
		P63267	Actin, gamma-enteric smooth muscle.
		P68133	Actin, alpha skeletal muscle.
		Q6S8J3	POTE ankyrin domain family member E.
		A5A3E0	POTE ankyrin domain family member F.
LYAMKVLKK	No	Q15418	Ribosomal protein S6 kinase alpha-1.
		Q15349	Ribosomal protein S6 kinase alpha-2.
		P51812	Ribosomal protein S6 kinase alpha-3.
		O75582	Ribosomal protein S6 kinase alpha-5.
		Q9UK32	Ribosomal protein S6 kinase alpha-6.
AVQKKTFTK	No	Q01082	Spectrin beta chain, non-erythrocytic 1.
		O15020	Spectrin beta chain, non-erythrocytic 2.
		Q9H254	Spectrin beta chain, non-erythrocytic 4.
FTFDNVLPGK	No	Q15155	Nodal modulator 1.
		Q5JPE7	Nodal modulator 2.
		P69849	Nodal modulator 3.
EVQLVESGGGLVQPGG	No	P01766	Ig-like.
		P01777	Ig-like.
STEPPYSQK	No	P68104	Elongation factor 1-alpha 1.
		Q5VTE0	Putative elongation factor 1-alpha-like
AVFPSLLTNPK	No	P52292	Importin subunit alpha-1.
SVYDGEEHGR	No	Q9Y2D4	Exocyst complex component 6B.
ATIEDILFK	No	Q6P1K8	General transcription factor IIH subunit
		Q13888	General transcription factor IIH subunit
SVMSTVEWNK	No	Q7L1Q6	Basic leucine zipper and W2 domain-
GNPTVEVDLFTSK	Yes	P06733	Alpha-enolase.
SVVSLLDGVVEK	Yes	Q7L5Y9	Macrophage erythroblast attacher.
SVQENIQQK	Yes	P52732	Kinesin-like protein KIF11.
SSFGGLGGGSVR	Yes	P08727	Keratin, type I cytoskeletal 19.
NTMTLGDIVFK	Yes	P07148	Fatty acid-binding protein, liver.
AIEDFFLEH	Yes	Q13144	Translation initiation factor eIF-2B
ATLEVSSIIKK	Yes	Q9NP61	ADP-ribosylation factor GTPase-activating
SVLPVLDNPLSK	Yes	P53992	Protein transport protein Sec24C.
SGYEFDEGSIIFNK	Yes	P36542	ATP synthase subunit gamma,
KTIDASVSK	Yes	Q6VMQ6	Activating transcription factor 7-
AVMDDFAAFVEK	Yes	P02768	Serum albumin.
LALFQAIGK	Yes	P58107	Epiplakin.
ASDPNVSKKLK	Yes	Q9P2Q2	FERM domain-containing protein 4A.
SSSRAVVVKK	Yes	P05787	Keratin, type II cytoskeletal 8.
ATFSTGERK	Yes	Q9NPD3	Exosome complex component RRP41.
STAVVVAELLK	Yes	Q9Y2D2	UDP-N-acetylglucosamine transporter.
IVGDPSTAK	Yes	Q14566	DNA replication licensing factor MCM6.
VVFVIDPGFAK	Yes	O43143	Pre-mRNA-splicing factor ATP-dependent
AVTYTEHAK	Yes	P62805	Histone H4.
TVAEISQFLK	Yes	Q9Y689	ADP-ribosylation factor-like protein 5A.
TVQGDIDAIFK	Yes	Q15056	Eukaryotic translation initiation factor

SIHGRPVTK	Yes	O94988	Protein FAM13A.
LQGSPLPPR	Yes	Q9H2D6	TRIO and F-actin-binding protein.
AILDYLITK	Yes	Q9UPY3	Endoribonuclease Dicer.
ATFVSELEAAK	Yes	Q96BN2	Transcriptional adapter 1.
AAPLLNLPPK	Yes	Q9NR48	Histone-lysine N-methyltransferase ASH1L.
SSFREMLQK	Yes	Q96FQ6	Protein S100-A16.
ATYPMPTAK	Yes	O75179	Ankyrin repeat domain-containing protein
SVFVDSLTK	Yes	P21333	Filamin-A.
FLVNHDFSPL	Yes	P33947	ER lumen protein-retaining receptor 2.
LSQVPMSALK	Yes	Q7Z417	Nuclear fragile X mental retardation-
ATYSEDGLLK	Yes	Q2TAY7	WD40 repeat-containing protein SMU1.
GSDPYQEPK	Yes	Q99447	Ethanolamine-phosphate
KTLSALLLPA	Yes	Q86VI3	Ras GTPase-activating-like protein
SSSRAVVVK	Yes	P05787	Keratin, type II cytoskeletal 8.
VSLWLPVSK	Yes	Q9HBT8	Zinc finger protein 286A.
STATDVFWAK	Yes	P00734	Prothrombin.
GTLSPLDIYPK	Yes	P18074	TFIIH basal transcription factor complex
AIIEGADASSLQK	Yes	Q6E0U4	Dermokine.
AVYLLPVPK	Yes	P42694	Probable helicase with zinc finger
ATLLPDLIQK	Yes	P55786	Puromycin-sensitive aminopeptidase.
AVLYQPLFDK	Yes	P55209	Nucleosome assembly protein 1-like 1.
SSNSYAIKK	Yes	P46782	40S ribosomal protein S5.
GTFYQIGDSWEK	Yes	P02751	Fibronectin.
ITVGDIGPK	Yes	Q15067	Peroxisomal acyl-coenzyme A oxidase 1.
VLLKAFIAN	Yes	P42858	Huntingtin.
VVFPFPVNK	Yes	P04198	N-myc proto-oncogene protein.
SSPITLQAL	Yes	P04114	Apolipoprotein B-100.
VLQAADILLYK	Yes	Q9UGM6	Tryptophan--tRNA ligase, mitochondrial.
GIIIVGDEILK	Yes	Q8NFF5	FAD synthase.
TSLPPLPFK	Yes	P46013	Antigen KI-67.
TAFDPFLGGK	Yes	Q92598	Heat shock protein 105 kDa.
PLPPPMKI	Yes	O60229	Kalirin.
ASVHLDSKK	Yes	P04114	Apolipoprotein B-100.
SVYAGAGGSGSR	Yes	P05783	Keratin, type I cytoskeletal 18.
TVAPFLYR	Yes	Q8IVL1	Neuron navigator 2.
YVHDAPVRSL	Yes	P01584	Interleukin-1 beta.
KVGENVLPPK	Yes	Q9Y520	Protein PRRC2C.
STLPPVKSK	Yes	Q9Y6D6	Brefeldin A-inhibited guanine nucleotide-
TIITDTELPPLK	Yes	P10646	Tissue factor pathway inhibitor.
GTLPHPLQR	Yes	P37088	Amiloride-sensitive sodium channel
LSPALSVALS	Yes	Q99973	Telomerase protein component 1.
TTVPPNLRK	Yes	Q12905	Interleukin enhancer-binding factor 2.
ATARNLLGK	Yes	O94876	Transmembrane and coiled-coil domains
SVLDYFSER	Yes	O75586	Mediator of RNA polymerase II
VVNSPHRQYK	Yes	Q9H2D1	Mitochondrial folate transporter/carrier.
SVYEQHESTPLR	Yes	P02751	Fibronectin.
MTLGDIVFK	Yes	P07148	Fatty acid-binding protein, liver.
QAQEVFFLK	Yes	Q8WUM4	Programmed cell death 6-interacting
AIFFLPDSSK	Yes	P33908	Mannosyl-oligosaccharide 1,2-alpha-
ATIIDILTK	Yes	P04083	Annexin A1.
AVLTALDVLQK	Yes	Q7Z3U7	Protein MON2 homolog.
VIVLVENFYK	Yes	Q96FQ6	Protein S100-A16.
LSSFWQLIV	Yes	Q92616	eIF-2-alpha kinase activator GCN1.
TVVNPKYEGK	Yes	P05556	Integrin beta-1.
TTLPPPLFSK	Yes	Q5H8A4	GPI ethanolamine phosphate transferase 2.
TVLGGVYILGK	Yes	P56589	Peroxisomal biogenesis factor 3.
AIYELAVASFPK	Yes	P14406	Cytochrome c oxidase subunit 7A2,
ATAYGSTVSK	Yes	P04114	Apolipoprotein B-100.
ATLDVGGLVFK	Yes	P10074	Zinc finger and BTB domain-containing
GTYSLVPKK	Yes	Q9H9B1	Histone-lysine N-methyltransferase EHMT1.
TIPIFEPL	Yes	Q8N3C0	Activating signal cointegrator 1 complex
GVAVSGPTK	Yes	Q9BR77	Coiled-coil domain-containing protein 77.
GGAGGARISL	Yes	Q9C075	Keratin, type I cytoskeletal 23.
STAPAQLGK	Yes	Q9Y5M8	Signal recognition particle receptor
IGSQRYKL	Yes	P06400	Retinoblastoma-associated protein.
GSQGGNFEGPNK	Yes	Q8WXF1	Paraspeckle component 1.
TATDVFWAK	Yes	P00734	Prothrombin.
SIFSEALLK	Yes	Q08426	Peroxisomal bifunctional enzyme.
TAYGSTVSK	Yes	P04114	Apolipoprotein B-100.
QVEEIFNLK	Yes	P78347	General transcription factor II-I.
VFLPKDVAL	Yes	P15924	Desmoplakin.
SVSPVKATQK	Yes	Q86XJ1	GAS2-like protein 3.

A.4.3 List of up-regulated peptides

peptide	Unique	UniProt ID	Orginated from
PPQPPPPPP	No	Q99626	Homeobox protein CDX-2.
		Q16760	Diacylglycerol kinase delta.
		Q9H7P6	Multivesicular body subunit 12B.
		Q5VYV0	Forkhead box protein B2.
		P31249	Homeobox protein Hox-D3.
		A6NNE9	E3 ubiquitin-protein ligase MARCH11.
		Q86TG7	Retrotransposon-derived protein PEG10.
		P20264	POU domain, class 3, transcription factor
		Q8N5S1	Solute carrier family 25 member 41.
		Q9UPS6	Histone-lysine N-methyltransferase
		Q9BYN7	Zinc finger protein 341.
		Q96JM2	Zinc finger protein 462.
GSFGKVFLV	No	Q15418	Ribosomal protein S6 kinase alpha-1.
		P51812	Ribosomal protein S6 kinase alpha-3.
		Q9UK32	Ribosomal protein S6 kinase alpha-6.
RVMTVSFHKY	No	Q13547	Histone deacetylase 1.
		Q92769	Histone deacetylase 2.
		O15379	Histone deacetylase 3.
PHPPPPPPP	No	P13378	Homeobox protein Hox-D8.
		Q15390	Mitochondrial fission regulator 1.
		Q15032	R3H domain-containing protein 1.
RVFNIMREK	No	P20042	Eukaryotic translation initiation factor
QLYWSHPRK	No	P62273	40S ribosomal protein S29.
RIFDLGRKK	No	Q96L21	60S ribosomal protein L10-like.
		P27635	60S ribosomal protein L10.
RVAEALHKLK	No	Q96A73	Putative monooxygenase p33MONOX.
KAFNQGKIFK	No	P26641	Elongation factor 1-gamma.
RTIATALEYVYK	No	P78537	Biogenesis of lysosome-related organelles
RILPKPTRK	Yes	P62081	40S ribosomal protein S7.
RTDERIKQHPK	Yes	Q9ULW0	Targeting protein for Xklp2.
RTPAFSPFVR	Yes	Q7Z5J4	Retinoic acid-induced protein 1.
VIFINTRRK	Yes	P60842	Eukaryotic initiation factor 4A-I.
EEYKKEQAINRAGIVQE	Yes	Q8N5G0	Small integral membrane protein 20.
AVGDIPGVRFK	Yes	P62266	40S ribosomal protein S23.
RIHGVGFKK	Yes	P62899	60S ribosomal protein L31.
FLITQLKML	Yes	P03928	ATP synthase protein 8.
RIIDLIKEK	Yes	Q9NU02	Ankyrin repeat and EF-hand domain-
SIMKWNRER	Yes	Q9P0J0	NADH dehydrogenase [ubiquinone] 1 alpha
ELMPPPPPK	Yes	O60942	mRNA-capping enzyme.
KLISEEDLLRK	Yes	P01106	Myc proto-oncogene protein.
GLAVHLEVLNAR	Yes	Q8N587	Zinc finger protein 561.
SVYDHQGIFKR	Yes	Q96E22	Dehydrodolichyl diphosphate synthase
TVQEHLIEK	Yes	O14980	Exportin-1.
RAFHPDLEFVGK	Yes	O95864	Fatty acid desaturase 2.
SVVGLFLRH	Yes	Q9UJX4	Anaphase-promoting complex subunit 5.
RTINVYPNFRPTPK	Yes	O95168	NADH dehydrogenase [ubiquinone] 1 beta
ARNLSDIDL	Yes	Q96B49	Mitochondrial import receptor subunit
FVELGTQPATQ	Yes	P02652	Proapolipoprotein A-II.
IQRTPKIQVYS	Yes	P61769	Beta-2-microglobulin.
VVRHQLLKT	Yes	P15954	Cytochrome c oxidase subunit 7C,
AQNPSGETAFK	Yes	Q8TB40	Protein ABHD4.
SSLPKKLALLK	Yes	Q9UNZ5	Leydig cell tumor 10 kDa protein homolog.
ATLIGLSIKVK	Yes	Q9Y3D0	Mitotic spindle-associated MMXD complex
LARNLSDID	Yes	Q96B49	Mitochondrial import receptor subunit
KSIEERQLLK	Yes	O15164	Transcription intermediary factor 1-
PAPPLAEHG	Yes	Q5VT52	Regulation of nuclear pre-mRNA domain-
ASLGNLFAR	Yes	Q92520	Protein FAM3C.
AQLSTIRSFLK	Yes	Q9Y262	Eukaryotic translation initiation factor
GLAVHLEVLNARQ	Yes	Q8N587	Zinc finger protein 561.
ALIVLYFK	Yes	Q96IX5	Up-regulated during skeletal muscle
TLFIPENSFRK	Yes	Q9NR48	Histone-lysine N-methyltransferase ASH1L.

MLQSIIKN	Yes	P56378	6.8 kDa mitochondrial proteolipid.
RTFISPEELIK	Yes	Q13905	Rap guanine nucleotide exchange factor 1.
RVYGEPHRR	Yes	O95486	Protein transport protein Sec24A.
VELGTQPATQ	Yes	P02652	Proapolipoprotein A-II.
AVAHILGIRDLA	Yes	P49327	Fatty acid synthase.
SHLETYRRPE	Yes	P10176	Cytochrome c oxidase subunit 8A,
KTFPYQHRY	Yes	Q8NI27	THO complex subunit 2.
LRVTPFIL	Yes	Q8N4H5	Mitochondrial import receptor subunit
RLNHYVLYK	Yes	O43242	26S proteasome non-ATPase regulatory
RTIVTTLQDSIRK	Yes	P07996	Thrombospondin-1.
RVLPSITTEILK	Yes	P35232	Prohibitin.
SSIRHMIRK	Yes	P46779	60S ribosomal protein L28.
LARNLSDIDL	Yes	Q96B49	Mitochondrial import receptor subunit
SVIRPPFKK	Yes	Q9BTE1	Dynactin subunit 5.
YTESISVAK	Yes	Q99519	Sialidase-1.
FDRAFSYI	Yes	P49757	Protein numb homolog.
DVQPPGLKVWSDPFGRK	Yes	Q8N5G0	Small integral membrane protein 20.
YSISQERF	Yes	Q9Y2R0	Cytochrome c oxidase assembly factor 3
SIFSPEGKFKTK	Yes	O75382	Tripartite motif-containing protein 3.
YKKEQAINRAG	Yes	Q8N5G0	Small integral membrane protein 20.
KLFNGEFTK	Yes	O75845	Lathosterol oxidase.
RSSFVFVRK	Yes	Q9ULT8	E3 ubiquitin-protein ligase HECTD1.
RAYPHVFTK	Yes	O14949	Cytochrome b-c1 complex subunit 8.
KIYPGHGRR	Yes	P83731	60S ribosomal protein L24.
KFLPPVLLK	Yes	Q5VYK3	Proteasome-associated protein ECM29
GIKSLSPFA	Yes	Q6NUQ4	Transmembrane protein 214.
YIKSTMGKPQRLY	Yes	P62906	60S ribosomal protein L10a.
SVFTNERFPLR	Yes	O43709	Probable 18S rRNA (guanine-N(7))-
EEYKKEQAINRAG	Yes	Q8N5G0	Small integral membrane protein 20.
AGLSSPLSFPSQ	Yes	Q8TEK3	Histone-lysine N-methyltransferase, H3
RIFAPNHVVAK	Yes	Q02543	60S ribosomal protein L18a.
RTMPLLSLHSR	Yes	P54368	Ornithine decarboxylase antizyme 1.
RILFFNTPK	Yes	P48556	26S proteasome non-ATPase regulatory
GHQQLYW	Yes	P62273	40S ribosomal protein S29.
RTAHVILRY	Yes	Q9UKV5	E3 ubiquitin-protein ligase AMFR.
SSFLIKRNK	Yes	P46779	60S ribosomal protein L28.
AVHLEVLNAR	Yes	Q8N587	Zinc finger protein 561.
LYQSLR	Yes	Q5SNT2	Transmembrane protein 201.
SINFAKVLH	Yes	P51659	Peroxisomal multifunctional enzyme type
KVHGSLARAGK	Yes	P62861	40S ribosomal protein S30.
ASSGASGGKIDNSVLVL	Yes	O95831	Mitochondrion.
AVASFPKKQE	Yes	P14406	Cytochrome c oxidase subunit 7A2,
SSGVPNPPK	Yes	Q8WUA4	General transcription factor 3C

List of References

1. Kiessling R, Klein E, Wigzell H. “Natural” killer cells in the mouse. I. Cytotoxic cells with specificity for mouse Moloney leukemia cells. Specificity and distribution according to genotype. Eur J Immunol. WILEY- VCH Verlag GmbH; 1975 Feb 1;5(2):112–7.

2. Kiessling R, Klein E, Pross H, Wigzell H. “Natural” killer cells in the mouse. II. Cytotoxic cells with specificity for mouse Moloney leukemia cells. Characteristics of the killer cell. Eur J Immunol. WILEY- VCH Verlag GmbH; 1975 Feb 1;5(2):117–21.

3. Vasold J, Wagner M, Drolle H, Deniffel C, Kütt A, Oostendorp R, et al. The bone marrow microenvironment is a critical player in the NK cell response against acute myeloid leukaemia in vitro. Leuk Res. Elsevier Ltd; 2015;39(2):257–62.

4. Comans-Bitter WM, De Groot R, Van den Beemd R, Neijens HJ, Hop WCJ, Groeneveld K, et al. Immunophenotyping of blood lymphocytes in childhood: Reference values for lymphocyte subpopulations. J Pediatr. 1997;130(3):388–93.

5. Shearer WT, Rosenblatt HM, Gelman RS, Oymopito R, Plaeger S, Stiehm ER, et al. Lymphocyte subsets in healthy children from birth through 18 years of age: The pediatric AIDS clinical trials group P1009 study. J Allergy Clin Immunol. 2003;112(5):973–80.

6. Fox RI, Fong S, Tsoukas C, Vaughan JH. Characterization of recirculating lymphocytes in rheumatoid arthritis patients: selective deficiency of natural killer cells in thoracic duct lymph. J Immunol. 1984;132(6):2883–7.

7. Perussia B, Chen Y, Loza MJ. Peripheral NK cell phenotypes: Multiple changing of faces of an adapting, developing cell. Mol Immunol. 2005;42(4 SPEC. ISS.):385–95.

8. Vitale C, Chiossone L, Morreale G, Lanino E, Cottalasso F, Moretti S, et al. Human natural killer cells undergoing in vivo differentiation after allogeneic bone marrow transplantation: Analysis of the surface expression and function of activating NK receptors. Mol Immunol. 2005;42(4 SPEC. ISS.):405–11.

9. Cichocki F, Miller JS, Anderson SK, Bryceson YT. Epigenetic regulation of NK cell

differentiation and effector functions. Front Immunol. 2013;4(FRB).

10. Puel a, Ziegler SF, Buckley RH, Leonard WJ. Defective IL7R expression in T(-)B(+)NK(+) severe combined immunodeficiency. Nat Genet. 1998;20(4):394–7.

11. Notarangelo LD, Giliani S, Mazza C, Mella P, Savoldi G, Rodriguez-Pérez C, et al. Of genes and phenotypes: the immunological and molecular spectrum of combined immune deficiency. Defects of the gamma(c)-JAK3 signaling pathway as a model. Immunol Rev. 2000;178:39–48.

12. Kumaki S, Ishii N, Minegishi M, Tsuchiya S, Cosman D, Sugamura K, et al. Functional role of interleukin-4 (IL-4) and IL-7 in the development of X-linked severe combined immunodeficiency. Blood. 1999;93(2):607–12.

13. Lodolce JP, Boone DL, Chai S, Swain RE, Dassopoulos T, Trettin S, et al. IL-15 receptor maintains lymphoid homeostasis by supporting lymphocyte homing and proliferation. Immunity. 1998;9(5):669–76.

14. Gilmour KC, Fujii H, Cranston T, Davies EG, Kinnon C, Gaspar HB. Defective expression of the interleukin-2 / interleukin-15 receptor ᴺL subunit leads to a natural killer cell – deficient form of severe combined immunodeficiency. Blood. 2001;98(3):2000–2.

15. Yu J, Freud AG, Caligiuri MA. Location and cellular stages of natural killer cell development. Trends Immunol. Elsevier Ltd; 2013;34(12):573–82.

16. Cerwenka A, Baron JL, Lanier LL. Ectopic expression of retinoic acid early inducible-1 gene (RAE-1) permits natural killer cell-mediated rejection of a MHC class I-bearing tumor in vivo. Proc Natl Acad Sci U S A. 2001;98(20):11521–6.

17. Champsaur, M. and Lanier LL. Effects of NKG2D ligand expression on host immune responses. Immunol Rev. 2010;235(1):267–85.

18. Diefenbach A, Jensen ER, Jamieson AM, Raulet DH. Rae1 and H60 ligands of the NKG2D receptor stimulate tumour immunity. Nature. 2001;413:165–71.

19. Lodoen M, Ogasawara K, Hamerman J a, Arase H, Houchins JP, Mocarski ES, et al. NKG2D-mediated natural killer cell protection against cytomegalovirus is impaired by viral gp40 modulation of retinoic acid early inducible 1 gene

molecules. J Exp Med. 2003;197(10):1245–53.

20. Lodoen MB, Abenes G, Umamoto S, Houchins JP, Liu F, Lanier LL. The cytomegalovirus m155 gene product subverts natural killer cell antiviral protection by disruption of H60-NKG2D interactions. J Exp Med. 2004;200(8):1075–81.

21. Ogasawara K, Benjamin J, Takaki R, Phillips JH, Lanier LL. Function of NKG2D in natural killer cell–mediated rejection of mouse bone marrow grafts. Nat Immunol. 2005;6(9):938–45.

22. Oppenheim DE, Roberts SJ, Clarke SL, Filler R, Lewis JM, Tigelaar RE, et al. Sustained localized expression of ligand for the activating NKG2D receptor impairs natural cytotoxicity in vivo and reduces tumor immunosurveillance. Nat Immunol. 2005;6(9):928–37.

23. Champsaur M, Beilke JN, Ogasawara K, Koszinowski UH, Jonjic S, Lanier LL. Intact NKG2D-independent function of NK cells chronically stimulated with the NKG2D ligand Rae-1. J Immunol. 2010;185(1):157–65.

24. Wiemann K, Mittrücker H-W, Feger U, Welte S a, Yokoyama WM, Spies T, et al. Systemic NKG2D down-regulation impairs NK and CD8 T cell responses in vivo. J Immunol. 2005;175(2):720–9.

25. Coudert JD, Scarpellino L, Gros F, Vivier E, Held W. Sustained NKG2D engagement induces cross-tolerance of multiple distinct NK cell activation pathways Sustained NKG2D engagement induces cross-tolerance of multiple distinct NK cell activation pathways. Hematology. 2008;111(7):3571–8.

26. Sun JC, Lanier LL. Tolerance of NK cells encountering their viral ligand during development. J Exp Med. 2008;205(8):1819–28.

27. Tripathy SK, Keyel P a., Yang L, Pingel JT, Cheng TP, Schneeberger A, et al. Continuous engagement of a self-specific activation receptor induces NK cell tolerance. J Exp Med. 2008;205(8):1829–41.

28. George TC, Ortaldo JR, Lemieux S, Kumar V, Bennett M. Tolerance and alloreactivity of the Ly49D subset of murine NK cells. J Immunol. 1999;163(4):1859–67.

29. Kulkarni S, Martin MP, Carrington M. The Yin and Yang of HLA and KIR in human

disease. Semin Immunol. 2008;20(6):343–52.

30. Fauriat C, Ivarsson MA, Ljunggren H, Malmberg K, Michae J. Education of human natural killer cells by activating killer cell immunoglobulin-like receptors. Blood. 2010;115(6):1166–75.

31. Arase H, Mocarski ES, Campbell AE, Hill AB, Lanier LL. Direct recognition of cytomegalovirus by activating and inhibitory NK cell receptors. Science. 2002;296(5571):1323–6.

32. Smith HRC, Heusel JW, Mehta IK, Kim S, Dorner BG, Naidenko O V, et al. Recognition of a virus-encoded ligand by a natural killer cell activation receptor. Proc Natl Acad Sci U S A. 2002;99(13):8826–31.

33. Carlyle JR, Mesci A, Fine JH, Chen P, Bélanger S, Tai LH, et al. Evolution of the Ly49 and Nkrp1 recognition systems. Semin Immunol. 2008;20(6):321–30.

34. Hanke T, Takizawa H, McMahon CW, Busch DH, Pamer EG, Miller JD, et al. Direct assessment of MHC class I binding by seven Ly49 inhibitory NK cell receptors. Immunity. 1999;11(1):67–77.

35. Parham P. The genetic and evolutionary balances in human NK cell receptor diversity. Semin Immunol. 2008;20(6):311–6.

36. Fernandez NC, Treiner E, Vance RE, Jamieson a M, Lemieux S, Raulet DH. A subset of natural killer cells achieve self-tolerance without expressing inhibitory receptors specific for self MHC molecules. Blood. 2005;105(0006-497):4416–24.

37. Yawata M, Yawata N, Draghi M, Partheniou F, Little A-MM, Parham P. MHC class I-specific inhibitory receptors and their ligands structure diverse human NK cell repertoires towards a balance of missing-self response. Blood. 2008;112(6):blood – 2008.

38. Raulet DH, Held W, Correa I, Dorfman JR, Wu MF, Corral L. Specificity, tolerance and developmental regulation of natural killer cells defined by expression of class I-specific Ly49 receptors. Immunol Rev. 1997;155(I):41–52.

39. Valiante NM, Phillips JH, Lanier LL, Parham P. Killer cell inhibitory receptor recognition of human leukocyte antigen (HLA) class I blocks formation of a pp36/PLC-gamma signaling complex in human natural killer (NK) cells. J Exp

Med. 1996;184(6):2243–50.

40. Held W, Dorfman JR, Wu M-F, Raulet DH. Major histocompatibility complex class I-dependent skewing of the natural killer cell Ly49 receptor repertoire. EurJImmunol. 1996;26:2286–92.

41. Salcedo M, Diehl a D, Olsson-Alheim MY, Sundback J, Van Kaer L, Karre K, et al. Altered expression of Ly49 inhibitory receptors on natural killer cells from MHC class I-deficient mice. JImmunol. 1997;158(7):3174–80.

42. Roth C, Carlyle J, Takizawa H, Raulet D. Clonal acquisition of inhibitory Ly49 receptors on developing NK cells is successively restricted and regulated by stromal class I MHC. Immunity. 2000;13(1):143–53.

43. Sykes M, Harty MW, Karlhofer FM, Pearson D a, Szot G, Yokoyama WM. Hematopoietic cells and radioresistant host elements influence natural killer cell differentiation. JExpMed. 1993;178(July):223–9.

44. Held W, Raulet DH. Ly49A transgenic mice provide evidence for a major histocompatibility complex-dependent education process in natural killer cell development. J Exp Med. 1997;185(12):2079–88.

45. Hanke T, Takizawa H, Raulet DH. MHC-dependent shaping of the inhibitory Ly49 receptor repertoire on NK cells: Evidence for a regulated sequential model. Eur J Immunol. 2001;31(11):3370–9.

46. Shilling HG, Young N, Guethlein L a, Cheng NW, Gardiner CM, Tyan D, et al. Genetic control of human NK cell repertoire. J Immunol. 2002;169(1):239–47.

47. Yawata M, Yawata N, Draghi M, Little A-M, Partheniou F, Parham P. Roles for HLA and KIR polymorphisms in natural killer cell repertoire selection and modulation of effector function. J Exp Med. 2006;203(3):633–45.

48. Boudreau JE, Liu X-R, Zhao Z, Zhang A, Shultz LD, Greiner DL, et al. Cell-Extrinsic MHC Class I Molecule Engagement Augments Human NK Cell Education Programmed by Cell-Intrinsic MHC Class I. Immunity. Elsevier Inc.; 2016;45(2):280–91.

49. Valiante M. N, Lienert K, Shilling HG, Smits BJ, Parham P. Killer cell receptors: keeping pace with MHC class I evolution. Immunoiogical Rev. 1997;155:155–64.

50. Bix M, Liao NS, Zijlstra M, Loring J, Jaenisch R, Raulet D. Rejection of class I MHC-deficient haemopoietic cells by irradiated MHC-matched mice. Nature. 1991;349(6307):329–31.

51. Liao NS, Bix M, Zijlstra M, Jaenisch R, Raulet D. MHC class I deficiency: susceptibility to natural killer (NK) cells and impaired NK activity. Science. 1991;253(5016):199–202.

52. Anfossi N, André P, Guia S, Falk CS, Roetynck S, Stewart CA, et al. Human NK cell education by inhibitory receptors for MHC class I. Immunity. 2006 Aug;25(2):331–42.

53. Kim S, Poursine-Laurent J, Truscott SM, Lybarger L, Song Y-J, Yang L, et al. Licensing of natural killer cells by host major histocompatibility complex class I molecules. Nature. 2005;436(7051):709–13.

54. Orr MT, Murphy WJ, Lanier LL. "Unlicensed" natural killer cells dominate the response to cytomegalovirus infection. Nat Immunol. 2010;11(4):321–7.

55. Tarek N, Luduec JB Le, Gallagher MM, Zheng J, Venstrom JM, Chamberlain E, et al. Unlicensed NK cells target neuroblastoma following anti-GD2 antibody treatment. J Clin Invest. 2012;122(9):3260–70.

56. Bryceson YT, March ME, Ljunggren HG, Long EO. Synergy among receptors on resting NK cells for the activation of natural cytotoxicity and cytokine secretion. Blood. 2006;107(1):159–66.

57. Guia S, Jaeger BN, Piatek S, Mailfert S, Fenis A, Chevrier N, et al. Confinement of activating receptors at the plasma membrane controls natural killer cell tolerance. Sci Signal. 2011;4(167):ra21.

58. Viant C, Fenis A, Chicanne G, Payrastre B, Ugolini S, Vivier E. SHP-1-mediated inhibitory signals promote responsiveness and anti-tumour functions of natural killer cells. Nat Commun. 2014;5:5108.

59. Raulet DH. Missing self recognition and self tolerance of natural killer (NK) cells. Semin Immunol. 2006 Jun;18(3):145–50.

60. Goodnow CC. Transgenic mice and analysis of B-cell tolerance. Annu Rev Immunol. 1992;10:489–518.

61. Schwartz RH. T cell anergy. Annu Rev Immunol [Internet]. 2003;21(1):305–34.

62. Johansson MH, Bieberich C, Jay G, Kärre K, Höglund P. Natural killer cell tolerance in mice with mosaic expression of major histocompatibility complex class I transgene. J Exp Med. 1997;186(3):353–64.

63. Wu M-F, Raulet DH. Class I-Deficient Hemopoietic Cells and Nonhemopoietic Cells Dominantly Induce Unresponsiveness of Natural Killer Cells to Class I-Deficient Bone Marrow Cell Grafts. J Immunol. 1997;158(4):1628–33.

64. Salcedo M, Andersson M, Lemieux S, Van Kaer L, Chambers BJ, Ljunggren HG. Fine tuning of natural killer cell specificity and maintenance of self tolerance in MHC class I-deficient mice. Eur J Immunol. 1998;28(4):1315–21.

65. Sun JC, Lanier LL. Cutting edge: viral infection breaks NK cell tolerance to "missing self". J Immunol. 2008;181(11):7453–7.

66. Orr MT, Murphy WJ, Lanier LL. "Unlicensed" natural killer cells dominate the response to cytomegalovirus infection. Nat Immunol. 2010;11(4):321–7.

67. Daniels K a, Devora G, Lai WC, O'Donnell CL, Bennett M, Welsh RM. Murine cytomegalovirus is regulated by a discrete subset of natural killer cells reactive with monoclonal antibody to Ly49H. J Exp Med. 2001;194(1):29–44.

68. Shifrin N, Raulet DH, Ardolino M. NK cell self tolerance, responsiveness and missing self recognition. Semin Immunol. Elsevier Ltd; 2014;26(2):138–44.

69. Street SE a, Hayakawa Y, Zhan Y, Lew AM, MacGregor D, Jamieson AM, et al. Innate immune surveillance of spontaneous B cell lymphomas by natural killer cells and gammadelta T cells. J Exp Med. 2004;199(6):879–84.

70. Dendy PP. Mobile phones and the illusory pursuit of safety. Lancet. 2000;356:1782–3.

71. Ghiringhelli F, Ménard C, Terme M, Flament C, Taieb J, Chaput N, et al. CD4+CD25+ regulatory T cells inhibit natural killer cell functions in a transforming growth factor-beta-dependent manner. J Exp Med. 2005;202(8):1075–85.

72. Doubrovina ES, Doubrovin MM, Vider E, Sisson RB, O'Reilly RJ, Dupont B, et al. Evasion from NK cell immunity by MHC class I chain-related molecules

expressing colon adenocarcinoma. J Immunol. 2003;171(12):6891–9.

73. Nedvetzki S, Sowinski S, Eagle R a, Harris J, Pende D, Trowsdale J, et al. Reciprocal regulation of human natural killer cells and macrophages associated with distinct immune synapses. Interactions. 2007;109(9):3776–85.

74. Moffett A, Loke C. Immunology of placentation in eutherian mammals. Nat Rev Immunol. 2006;6(8):584–94.

75. Hiby SE, Walker JJ, O'shaughnessy KM, Redman CWG, Carrington M, Trowsdale J, et al. Combinations of maternal KIR and fetal HLA-C genes influence the risk of preeclampsia and reproductive success. J Exp Med. 2004;200(8):957–65.

76. Hiby SE, Apps R, Sharkey AM, Farrell LE, Gardner L, Mulder A, et al. Maternal activating KIRs protect against human reproductive failure mediated by fetal HLA-C2. J Clin Invest. 2010;120(11):4102–10.

77. Chazara O, Xiong S, Moffett A. Maternal KIR and fetal HLA-C: a fine balance. J Leukoc Biol. 2011;90(4):703–16.

78. Colucci F, Boulenouar S, Kieckbusch J, Moffett A. How does variability of immune system genes affect placentation? Placenta. 2011. p. 539–45.

79. Hiby SE, Apps R, Chazara O, Farrell LE, Magnus P, Trogstad L, et al. Maternal KIR in combination with paternal HLA-C2 regulate human birth weight. J Immunol. 2014;192(11):5069–73. l

80. Kieckbusch J, Gaynor LM, Colucci F. Assessment of Maternal Vascular Remodeling During Pregnancy in the Mouse Uterus. J Vis Exp. 2015;(106):1–7.

81. Biron CA, Byron KS, Sullivan JL. Severe Herpesvirus Infections in an Adolescent without Natural Killer Cells. N Engl J Med. 1989;320(26):1731–5.

82. Fitzgerald PA, Mendelsohn M, Lopez C. Human natural killer cells limit replication of herpes simplex virus type 1 in vitro. J Immunol. 1985;134(4):2666–72.

83. Orange JS, Fassett MS, Koopman L a, Boyson JE, Strominger JL. Viral evasion of natural killer cells. Nat Immunol. 2002;3(11):1006–12.

84. Coscoy L. Immune evasion by Kaposi's sarcoma-associated herpesvirus. Nat Rev Immunol . 2007;7(5):391–401.

85. Jackson SE, Mason GM, Wills MR. Human cytomegalovirus immunity and immune evasion. Virus Res. 2011;157(2):151–60.

86. Lunemann S, Malone DFG, Hengst J, Port K, Grabowski J, Deterding K, et al. Compromised function of natural killer cells in acute and chronic viral hepatitis. J Infect Dis. 2014;209(9):1362–73.

87. Guo H, Kumar P, Moran TM, Garcia-Sastre A, Zhou Y, Malarkannan S. The functional impairment of natural killer cells during influenza virus infection. Immunol Cell Biol. Nature Publishing Group; 2009;87(8):579–89.

88. Alter G, Martin MP, Teigen N, Carr WH, Suscovich TJ, Schneidewind A, et al. Differential natural killer cell-mediated inhibition of HIV-1 replication based on distinct KIR/HLA subtypes. J Exp Med. 2007;204(12):3027–36.

89. Iannello A, Debbeche O, Samarani S, Ahmad A. Antiviral NK cell responses in HIV infection: I. NK cell receptor genes as determinants of HIV resistance and progression to AIDS. J Leukoc Biol. 2008;84(1):1–26.

90. Martin MP, Gao X, Lee J-H, Nelson GW, Detels R, Goedert JJ, et al. Epistatic interaction between KIR3DS1 and HLA-B delays the progression to AIDS. Nat Genet. 2002;31(4):429–34.

91. Stein-Streilein J, Bennett M, Mann D, Kumar V. Natural killer cells in mouse lung: surface phenotype, target preference, and response to local influenza virus infection. J Immunol. 1983;131(6):2699–704.

92. Stein-Streilein J, Guffee J. In vivo treatment of mice and hamsters with antibodies to asialo GM1 increases morbidity and mortality to pulmonary influenza infection. J Immunol. 1986;136(4):1435–41.

93. Nogusa S, Ritz BW, Kassim SH, Jennings SR, Gardner EM. Characterization of age-related changes in natural killer cells during primary influenza infection in mice. Mech Ageing Dev. 2008;129(4):223–30.

94. Wingett D, Nielson CP. Divergence in NK cell and cyclic AMP regulation of T cell CD40L expression in asthmatic subjects Abstract : T cells are central in the pathogenesis of asthma , and the associated ligand , CD40L , plays. J Leukoc Biol. 2003;74(October):531–41.

95. Ple C, Barrier M, Amniai L, Marquillies P, Bertout J, Tsicopoulos a., et al. Natural

killer cells accumulate in lung-draining lymph nodes and regulate airway eosinophilia in a murine model of asthma. Scand J Immunol. 2010;72(2):118–27.

96. Haworth O, Cernadas M, Levy BD. NK Cells Are Effectors for Resolvin E1 in the Timely Resolution of Allergic Airway Inflammation. J Immunol [Internet]. 2011;186(11):6129–35.

97. Culley FJ. Natural killer cells in infection and inflammation of the lung. Immunology. 2009;128(2):151–63.

98. Wehner R, Dietze K, Bachmann M, Schmitz M. The bidirectional crosstalk between human dendritic cells and Natural killer cells. J Innate Immun. 2011;3(3):258–63.

99. Mavilio D, Benjamin J, Daucher M, Lombardo G, Kottilil S, Planta M a, et al. Natural killer cells in HIV-1 infection: dichotomous effects of viremia on inhibitory and activating receptors and their functional correlates. Proc Natl Acad Sci U S A. 2003;100(25):15011–6.

100. Garcia-Beltran WF, Hölzemer A, Martrus G, Chung AW, Pacheco Y, Simoneau CR, et al. Open conformers of HLA-F are high-affinity ligands of the activating NK-cell receptor KIR3DS1. Nat Immunol. 2016;17(July).

101. Cerboni C, Neri F, Casartelli N, Zingoni A, Cosman D, Rossi P, et al. Human immunodeficiency virus 1 Nef protein downmodulates the ligands of the activating receptor NKG2D and inhibits natural killer cell-mediated cytotoxicity. J Gen Virol. 2007;88(1):242–50.

102. Carroll IR, Wang J, Howcroft TK, Singer D. HIV Tat represses transcription of the b2-microglobulin promoter. Mol Immunol. 1998;35:1171–8.

103. Altfeld M, Fadda L, Frleta D, Bhardwaj N. DCs and NK cells: critical effectors in the immune response to HIV-1. Nat Publ Gr. Nature Publishing Group; 2011;11(3):176–86.

104. Gur C, Porgador A, Elboim M, Gazit R, Mizrahi S, Stern-Ginossar N, et al. The activating receptor NKp46 is essential for the development of type 1 diabetes. Nat Immunol. Nature Publishing Group; 2010;11(11):121–8.

105. Gur C, Enk J, Kassem S a, Suissa Y, Magenheim J, Stolovich-Rain M, et al.

Recognition and killing of human and murine pancreatic beta cells by the NK receptor NKp46. J Immunol. 2011;187(6):3096–103.

106. Brauner H, Elemans M, Lemos S, Broberger C, Holmberg D, Flodström-Tullberg M, et al. Distinct phenotype and function of NK cells in the pancreas of nonobese diabetic mice. J Immunol. 2010;184(5):2272–80.

107. Poulton LD, Smyth MJ, Hawke CG, Silveira P, Shepherd D, Naidenko O V, et al. Cytometric and functional analyses of NK and NKT cell deficiencies in NOD mice. Int Immunol. 2001;13(7):887–96.

108. Rodacki M, Svoren B, Butty V, Besse W, Laffel L, Benoist C, et al. Altered natural killer cells in type 1 diabetic patients. Diabetes. 2007;56(1):177–85.

109. Pazmany L. Do NK cells regulate human autoimmunity? Cytokine. 2005;32(2):76–80.

110. Schepis D, Gunnarsson I, Eloranta ML, Lampa J, Jacobson SH, Kärre K, et al. Increased proportion of CD56bright natural killer cells in active and inactive systemic lupus erythematosus. Immunology. 2009;126(1):140–6.

111. Deniz G, Erten G, Kucuksezer UC, Kocacik D, Karagiannidis C, Aktas E, et al. Regulatory NK Cells Suppress Antigen-Specific T Cell Responses. J Immunol. 2008;180:850–7.

112. Arase N, Arase H, Hirano S, Yokosuka T, Sakurai D, Saito T. IgE-Mediated Activation of NK Cells Through Fc RIII. J Immunol. 2003;170(6):3054–8.

113. Lapaque N, Walzer T, Méresse S, Vivier E, Trowsdale J. Interactions between human NK cells and macrophages in response to Salmonella infection. J Immunol. 2009;182(7):4339–48.

114. Zappacosta F, Borrego F, Brooks a G, Parker KC, Coligan JE. Peptides isolated from HLA-Cw*0304 confer different degrees of protection from natural killer cell-mediated lysis. Proc Natl Acad Sci U S A. 1997 Jun 10;94(12):6313–8.

115. Liu R, Kaer L V., Cava a. L, Price M, Campagnolo DI, Collins M, et al. Autoreactive T Cells Mediate NK Cell Degeneration in Autoimmune Disease. J Immunol. 2006;176(9):5247–54.

116. Hayes RL, Koslow M, Hiesiger EM, Hymes KB, Hochster HS, Moore EJ, et al.

Improved long term survival after intracavitary interleukin-2 and lymphokine-activated killer cells for adults with recurrent malignant glioma. Cancer. 1995;76(5):840–52.

117. Ruggeri L, Capanni M, Urbani E, Perruccio K, Shlomchik WD, Tosti A, et al. Effectiveness of donor natural killer cell alloreactivity in mismatched hematopoietic transplants. Science. 2002;295(5562):2097–100.

118. Miller JS, Soignier Y, Panoskaltsis-mortari A, Mcnearney S a, Yun GH, Fautsch SK, et al. Successful adoptive transfer and in vivo expansion of human haploidentical NK cells in patients with cancer. Cancer. 2005;105(8):3051–7.

119. Castriconi R, Dondero A, Corrias MV, Lanino E, Pende D, Moretta L, et al. Natural killer cell-mediated killing of freshly isolated neuroblastoma cells: Critical role of DNAX accessory molecule-1-poliovirus receptor interaction. Cancer Res. 2004;64(24):9180–4.

120. Carlsten M, Björkström NK, Norell H, Bryceson Y, Van Hall T, Baumann BC, et al. DNAX accessory molecule-1 mediated recognition of freshly isolated ovarian carcinoma by resting natural killer cells. Cancer Res. 2007;67(3):1317–25.

121. Geller M a, Cooley S, Judson PL, Ghebre R, Carson LF, Argenta P a, et al. Patients With Recurrent Ovarian and Breast Cancer. Cytotherapy. 2013;13(1):98–107.

122. Söderström K, Stein E, Colmenero P, Purath U, Müller-Ladner U, de Matos CT, et al. Natural killer cells trigger osteoclastogenesis and bone destruction in arthritis. Proc Natl Acad Sci U S A. 2010;107(29):13028–33.

123. Fasth AER, Björkström NK, Anthoni M, Malmberg KJ, Malmström V. Activating NK-cell receptors co-stimulate CD4+CD28- T cells in patients with rheumatoid arthritis. Eur J Immunol. 2010;40(2):378–87.

124. Ahern DJ, Brennan FM. The role of Natural Killer cells in the pathogenesis of rheumatoid arthritis: Major contributors or essential homeostatic modulators? Immunol Lett. 2011;136(2):115–21.

125. Woll PS, Martin CH, Miller JS, Kaufman DS. Human Embryonic Stem Cell-Derived NK Cells Acquire Functional Receptors and Cytolytic Activity. J Immunol. 2005;175(8):5095–103.

126. Woll P, Grzywacz B, Tian X. Human embryonic stem cells differentiate into a

homogeneous population of natural killer cells with potent in vivo antitumor activity. Blood. 2009;113(24):6094–101.

127. Ni Z, Knorr D a, Clouser CL, Hexum MK, Southern P, Mansky LM, et al. Human pluripotent stem cells produce natural killer cells that mediate anti-HIV-1 activity by utilizing diverse cellular mechanisms. J Virol. 2011;85(1):43–50.

128. Trinchieri G, Matsumo-Kobayashi M, Clark SC, Seehra J, London L, Perussia B. Response of resting Human peripheral blood Natural Killer cells to Interleukin 2. J Exp Med. 1984;160(October):1147–69.

129. Carson WE, Fehniger T a, Haldar S, Eckhert K, Lindemann MJ, Lai CF, et al. A potential role for interleukin-15 in the regulation of human natural killer cell survival. J Clin Invest. 1997;99(5):937–43.

130. Berg M, Lundqvist A, Jr PM, Samsel L, Fan Y, Childs R. Clinical Grade Ex Vivo-Expanded Human Natural Killer Cells Upregulate Activating Receptors and Death Receptor Ligands and Have Enhanced Cytolytic Activity against Tumor Cells. Cytotherapy. 2009;11(3):341–55.

131. Harada H, Watanabe S, Saijo K, Ishiwata I, Ohno T. A Wilms tumor cell line, HFWT, can greatly stimulate proliferation of CD56+ human natural killer cells and their novel precursors in blood mononuclear cells. Exp Hematol. 2004;32(7):614–21.

132. Boyiadzis M, Memon S, Carson J, Allen K, Szczepanski MJ, Vance B a., et al. Up-regulation of NK Cell Activating Receptors Following Allogeneic Hematopoietic Stem Cell Transplantation under a Lymphodepleting Reduced Intensity Regimen is Associated with Elevated IL-15 Levels. Biol Blood Marrow Transplant. 2008;14(3):290–300.

133. Fujisaki H, Kakuda H, Shimasaki N, Imai C, Ma J, Lockey T, et al. Expansion of highly cytotoxic human natural killer cells for cancer cell therapy. Cancer Res. 2009;69(9):4010–7.

134. Schirrmann T, Pecher G. Specific targeting of CD33+ leukemia cells by a natural killer cell line modified with a chimeric receptor. Leuk Res. 2005;29(3):301–6.

135. Müller T, Uherek C, Maki G, Chow KU, Schimpf A, Klingemann HG, et al. Expression of a CD20-specific chimeric antigen receptor enhances cytotoxic

activity of NK cells and overcomes NK-resistance of lymphoma and leukemia cells. Cancer Immunol Immunother. 2008;57(3):411–23.

136. Kruschinski A, Moosmann A, Poschke I, Norell H, Chmielewski M, Seliger B, et al. Engineering antigen-specific primary human NK cells against HER-2 positive carcinomas. Proc Natl Acad Sci U S A. 2008;105(45):17481–6.

137. Biron C a, Nguyen KB, Pien GC, Cousens LP, Salazar-Mather TP. Natural killer cells in antiviral defense: function and regulation by innate cytokines. Annu Rev Immunol. 1999;17:189–220.

138. Cosman D, Fanger N, Borges L, Kubin M, Chin W, Peterson L, et al. A novel immunoglobulin superfamily receptor for cellular and viral MHC class I molecules. Immunity. 1997;7(2):273–82.

139. Reyburn HT, Mandelboim O, Vales Gomez M, Davis DM, Pazmany L, Strominger JL. The class I MHC homologue of human cytomegalovirus inhibits attack by natural killer cells. Nature. 1997. p. 514–7.

140. Subleski JJ, Hall VL, Back TC, Ortaldo JR, Wiltrout RH. Enhanced antitumor response by divergent modulation of natural killer and natural killer T cells in the liver. Cancer Res. 2006;66(22):11005–12.

141. Chang CJ, Chen YH, Huang KW, Cheng HW, Chan SF, Tai KF, et al. Combined GM-CSF and IL-12 gene therapy synergistically suppresses the growth of orthotopic liver tumors. Hepatology. 2007;45(3):746–54.

142. Houot R, Kohrt HE, Marabelle A, Levy R. Targeting immune effector cells to promote antibody-induced cytotoxicity in cancer immunotherapy. Trends Immunol. 2011;32(11):510–6.

143. Kohrt HE, Houot R, Goldstein MJ, Weiskopf K, Alizadeh A a., Brody J, et al. CD137 stimulation enhances the antilymphoma activity of anti-CD20 antibodies. Blood. 2011;117(8):2423–32.

144. Koh CY, Blazar BR, George T, Welniak L a, Capitini CM, Raziuddin a, et al. Augmentation of antitumor effects by NK cell inhibitory receptor blockade in vitro and in vivo. Blood. 2001;97(10):3132–7.

145. Benson DM, Bakan CE, Zhang S, Collins SM, Liang J, Srivastava S, et al. IPH2101, a novel anti-inhibitory KIR antibody, and lenalidomide combine to enhance the

natural killer cell versus multiple myeloma effect. Blood. 2011;118(24):6387–91.

146. Vivier E, Raulet DH, Moretta A, Caligiuri MA, Zitvogel L, Lanier LL, et al. Innate or Adaptive Immunity? The Example of Natural Killer Cells. Science. 2011;331(January):44–9.

147. McQueen KL, Parham P. Variable receptors controlling activation and inhibition of NK cells Karina L McQueen * and Peter Parham †. Curr Opin Immunol. 2002;1:615–21.

148. Ljunggren HG, Kärre K. In search of the "missing self": MHC molecules and NK cell recognition. Immunol Today. 1990;11(7):237–44.

149. Watzl C. The NKG2D receptor and its ligands – recognition beyond the " missing self "? Microbes Infect. 2003;5:31–7.

150. Lanier LL, Corliss B, Phillips JH. Arousal and inhibition of human NK cells. Immunol Rev. 1997;155:145–54.

151. Kärre K. Natural killer cell recognition of missing self. Nat Immunol. 2008;9(5):477–80.

152. Groh V, Rhinehart R, Randolph-habecker J, Topp MS, Riddell SR, Spies T. Costimulation of CD8 αβ T cells by NKG2D via engagement by MIC induced on virus-infected cells. Nat Immunol. 2001;2(3):255–60.

153. Tomasello E, Blery M, Vely F, Vivier E. Signaling pathways engaged by NK cell receptors : double concerto for activating receptors , inhibitory receptors and NK cells. Semin Immunol. 2000;12:139–47.

154. Yu M, Su L, Zou L, Liu Y, Wu N, Kong L, et al. An essential function for b -arrestin 2 in the inhibitory signaling of natural killer cells. Nat Immunol. 2008;9(8):898–907.

155. Bryceson YT, Ljunggren H, Long EO. Minimal requirement for induction of natural cytotoxicity and intersection of activation signals by inhibitory receptors. Bloo. 2009;114(13):2657–66.

156. Peterson ME, Long EO. Inhibitory Receptor Signaling via Tyrosine Phosphorylation of the Adaptor Crk. Immunity. Elsevier Inc.; 2008;29(4):578–

88.

157. Tassi I, Cella M, Presti R, Colucci A, Gilfillan S, Littman DR, et al. NK cell-activating receptors require PKC-_ for sustained signaling, transcriptional activation, and IFN-_ secretion. Blood. 2008;112(10):4109-17.

158. Bryceson YT, March ME, Ljunggren H, Long EO. Synergy among receptors on resting NK cells for the activation of natural cytotoxicity and cytokine secretion. Blood. 2006;107(1):159-67.

159. Lanier LL, Corliss BC, Wu J, Leong C, Phillips JH. Immunoreceptor DAP12 bearing a tyrosine-based activa- tion motif is involved in activating NK cells. Nature. 1998;391:703-7.

160. Wu J, Song Y, Bakker ABH, Bauer S, Spies T, Lanier LL, et al. An Activating Immunoreceptor Complex Formed by NKG2D and. Science (80-). 1999;285:28-31.

161. Sutherland CL, Chalupny NJ, Schooley K, Vandenbos T, Kubin M, Cosman D, et al. UL16-Binding Proteins, Novel MHC Class I-Related Proteins, Bind to NKG2D and Activate Multiple Signaling Pathways in Primary NK Cells. J Immunol. 2002;168(2):671-9.

162. Zompi S, Hamerman JA, Ogasawara K, Schweighoffer E, Tybulewicz VLJ, Santo JP Di, et al. NKG2D triggers cytotoxicity in mouse NK cells lacking DAP12 or Syk family kinases. Nat Immunol. 2003;4(6):25-8.

163. Billadeau DD, Upshaw JL, Schoon RA, Dick CJ, Leibson PJ. NKG2D-DAP10 triggers human NK cell - mediated killing via a Syk-independent regulatory pathway. Nat Immunol. 2003;4(6):557-64.

164. Veillette A. NK cell regulation by SLAM family receptors and SAP-related adapters. Immunol Rev. 2006;214:22-34.

165. Faure M, Long EO. KIR2DL4 (CD158d), an NK Cell-Activating Receptor with Inhibitory Potential. J Immunol. 2002;168:6208-14.

166. Bottino C, Biassoni R, Millo R, Moretta L, Moretta a. The human natural cytotoxicity receptors (NCR) that induce HLA class I-independent NK cell triggering. Hum Immunol. 2000;61(1):1-6.

167. Arnon TI, Achdout H, Lieberman N, Gazit R, Gonen-Gross T, Katz G, et al. The mechanisms controlling the recognition of tumor- and virus-infected cells by NKp46. Blood. 2004;103(2):664–72.

168. Nolte ENM, Almeida CR, Cohen NR, Nedvetzki S, Davis DM, Yarwood H. Increased surveillance of cells in mitosis by human NK cells suggests a novel strategy for limiting tumor growth and viral replication Brief report Increased surveillance of cells in mitosis by human NK cells suggests a novel strategy for limiting tumor g. Blood. 2008;109(2):670–3.

169. Moretta L, Ferlazzo G, Bottino C, Vitale M, Pende D, Mingari MC, et al. Effector and regulatory events during natural killer-dendritic cell interactions. Immunol Rev. 2006;214(1):219–28.

170. Pogge von Strandmann E, Simhadri VR, von Tresckow B, Sasse S, Reiners KS, Hansen HP, et al. Human Leukocyte Antigen-B-Associated Transcript 3 Is Released from Tumor Cells and Engages the NKp30 Receptor on Natural Killer Cells. Immunity. 2007;27(6):965–74.

171. Byrd A, Hoffman SC, Jarahian M, Momburg F, Watzl C. Expression analysis of the ligands for the natural killer cell receptors NKp30 and NKp44. PLoS One. 2007;2(12).

172. Arnon TI, Achdout H, Levi O, Markel G, Saleh N, Katz G, et al. Inhibition of the NKp30 activating receptor by pp65 of human cytomegalovirus. Nat Immunol. 2005;6(5):515–23.

173. Mistry AR, O'Callaghan C a. Regulation of ligands for the activating receptor NKG2D. Immunology. 2007;121(4):439–47.

174. Gasser S, Orsulic S, Brown EJ, Raulet DH. The DNA damage pathway regulates innate immune system ligands of the NKG2D receptor. Nature. 2005;436(7054):1186–90.

175. Kaiser BK, Yim D, Chow I-T, Gonzalez S, Dai Z, Mann HH, et al. Disulphide-isomerase-enabled shedding of tumour-associated NKG2D ligands. Nature. 2007;447(7143):482–6.

176. Smyth MJ, Swann J, Cretney E, Zerafa N, Yokoyama WM, Hayakawa Y. NKG2D function protects the host from tumor initiation. J Exp Med. 2005;202(5):583–

8.

177. Ogasawara K, Hamerman J a., Ehrlich LR, Bour-Jordan H, Santamaria P, Bluestone J a., et al. NKG2D blockade prevents autoimmune diabetes in NOD mice. Immunity. 2004;20(6):757–67.

178. Meresse B, Chen Z, Ciszewski C, Tretiakova M, Bhagat G, Krausz TN, et al. Coordinated induction by IL15 of a TCR-independent NKG2D signaling pathway converts CTL into lymphokine-activated killer cells in celiac disease. Immunity. 2004;21(3):357–66.

179. Fuchs A, Colonna M. The role of NK cell recognition of nectin and nectin-like proteins in tumor immunosurveillance. Semin Cancer Biol. 2006;16(5):359–66.

180. Reymond N, Imbert A-M, Devilard E, Fabre S, Chabannon C, Xerri L, et al. DNAM-1 and PVR regulate monocyte migration through endothelial junctions. J Exp Med. 2004;199(10):1331–41.

181. Cao E, Ramagopal U a., Fedorov A, Fedorov E, Yan Q, Lary JW, et al. NTB-A Receptor Crystal Structure: Insights into Homophilic Interactions in the Signaling Lymphocytic Activation Molecule Receptor Family. Immunity. 2006;25(4):559–70.

182. Velikovsky CA, Deng L, Chlewicki LK, Fernández MM, Kumar V, Mariuzza R a. Structure of Natural Killer Receptor 2B4 Bound to CD48 Reveals Basis for Heterophilic Recognition in Signaling Lymphocyte Activation Molecule Family. Immunity. 2007;27(4):572–84.

183. Welte S, Kuttruff S, Waldhauer I, Steinle A. Mutual activation of natural killer cells and monocytes mediated by NKp80-AICL interaction. Nat Immunol. 2006;7(12):1334–42.

184. Rajalingam R. Human diversity of killer cell immunoglobulin-like receptors and disease. Korean J Hematol. 2011;46(4):216.

185. Sullivan LC, Clements CS, Beddoe T, Johnson D, Hoare HL, Lin J, et al. The Heterodimeric Assembly of the CD94-NKG2 Receptor Family and Implications for Human Leukocyte Antigen-E Recognition. Immunity. 2007;27(6):900–11.

186. Gründemann C, Bauer M, Schweier O, von Oppen N, Lässing U, Saudan P, et al. Cutting edge: identification of E-cadherin as a ligand for the murine killer cell

lectin-like receptor G1. J Immunol. 2006;176(3):1311–5.

187. Ito M, Maruyama T, Saito N, Koganei S, Yamamoto K, Matsumoto N. Killer cell lectin-like receptor G1 binds three members of the classical cadherin family to inhibit NK cell cytotoxicity. J Exp Med. 2006;203(2):289–95.

188. Lebbink RJ, de Ruiter T, Adelmeijer J, Brenkman AB, van Helvoort JM, Koch M, et al. Collagens are functional, high affinity ligands for the inhibitory immune receptor LAIR-1. J Exp Med. 2006;203(6):1419–25.

189. Wilson MJ, Torkar M, Haude a, Milne S, Jones T, Sheer D, et al. Plasticity in the organization and sequences of human KIR/ILT gene families. Proc Natl Acad Sci U S A. 2000;97(9):4778–83.

190. Trowsdale J. Genetic and Functional Relationships between MHC and NK Receptor Genes. Immunity. 2001;15:363–74.

191. Wilson MJ, Torkar M, Trowsdale J. Genomic organization of a human killer cell inhibitory receptor gene. Tissue Antigens. 1997;49(6):574–9.

192. Vilches C, Pando MJ, Parham P. Genes encoding human killer-cell Ig-like receptors with D1 and D2 extracellular domains all contain untranslated pseudoexons encoding a third Ig-like domain. Immunogenetics. 2000;51(8-9):639–46.

193. Vilches C, Gardiner CM, Parham P. Gene structure and promoter variation of expressed and nonexpressed variants of the KIR2DL5 gene. J Immunol. 2000;165(11):6416–21.

194. Moretta a, Biassoni R, Bottino C, Pende D, Vitale M, Poggi a, et al. Major histocompatibility complex class I-specific receptors on human natural killer and T lymphocytes. Immunol Rev. 1997;155:105–17.

195. Colonna M. Specificity and function of immunoglobulin superfamily NK cell inhibitory and stimulatory receptors. Immunol Rev. 1997;155:127–33.

196. Long EO, Burshtyn DN, Rojo S, Winter CC. Killer cell inliibitory receptors : diversity , specificity , and function. Immunol Rev. 1997;155:135–45.

197. Wagtmann N, Rajagopalan S, Winter CC, Peruzzi M, Long EO. Killer cell inhibitory receptors specific for HLA-C and HLA-B identified by direct binding

and by functional transfer. Immunity. 1995;3(6):801–9.

198. Rajagopalan S, Long EO. Zinc bound to the killer cell-inhibitory receptor modulates the negative signal in human NK cells. J Immunol. 1998;161(3):1299–305.

199. Richardson J, Reyburn HT, Luque I, Valés-Gómez M, Strominger JL. Definition of polymorphic residues on killer Ig-like receptor proteins which contribute to the HLA-C binding site. Eur J Immunol. 2000;30(5):1480–5.

200. Döhring C, Colonna M. Human natural killer cell inhibitory receptors bind to HLA class I molecules. Eur J Immunol. 1996;26(2):365–9.

201. Biassoni R, Pessino A, Malaspina A, Cantoni C, Bottino C, Sivori S, et al. The molecular basis of the binding affinity of p50.l/pS8.1 NK receptors 3095 Role of amino acid position 70 in the binding affinity of p50.1 and p58.1 receptors for HLA-Cw4 molecules. Eur J Immunol. 1997;27:3095–9.

202. Fan QR, Garboczi DN, Winter CC, Wagtmann N, Long EO, Wiley DC. Direct binding of a soluble natural killer cell inhibitory receptor to a soluble human leukocyte antigen-Cw4 class I major histocompatibility complex molecule. Proc Natl Acad Sci U S A. 1996;93(14):7178–83.

203. Fan QR, Long EO, Wiley DC. A disulfide-linked natural killer cell receptor dimer has higher affinity for HLA-C than wild-type monomer. Eur J Immunol. 2000;30(9):2692–7.

204. Fan QR, Long EO, Wiley DC. Cobalt-mediated dimerization of the human natural killer cell inhibitory receptor. J Biol Chem. 2000;275(31):23700–6.

205. Vales-Gomez M, Reyburn HT, Mandelboim M, Strominger JL. Kinetics of interaction of HLA-C ligands with natural killer cell inhibitory receptors (published erratum appears in Immunity 9, 892). Immunity. 1998;9(3):337–44.

206. Maenaka K, Juji T, Nakayama T, Wyer JR, Gao GF, Maenaka T, et al. Killer cell immunoglobulin receptors and T cell receptors bind peptide-major histocompatibility complex class I with distinct thermodynamic and kinetic properties. J Biol Chem. 1999;274(40):28329–34.

207. Boyington JC, Motyka S a, Schuck P, Brooks a G, Sun PD. Crystal structure of an NK cell immunoglobulin-like receptor in complex with its class I MHC ligand.

Nature. 2000 Jun 1;405(6786):537–43.

208. Valés-Gómez M, Reyburn H, Strominger J. Molecular analyses of the interactions between human NK receptors and their HLA ligands. Hum Immunol. 2000;61(1):28–38.

209. Fan QR, Long EO, Wiley DC. Crystal structure of the human natural killer cell inhibitory receptor KIR2DL1-HLA-Cw4 complex. Nat Immunol. 2001 May;2(5):452–60.

210. Snyder G a, Brooks a G, Sun PD. Crystal structure of the HLA-Cw3 allotype-specific killer cell inhibitory receptor KIR2DL2. Proc Natl Acad Sci U S A. 1999 Mar 30;96(7):3864–9.

211. Fan QR, Mosyak L, Winter CC, Wagtmann N, Long EO, Wiley DC. Structure of the inhibitory receptor for human natural killer cells resembles haematopoietic receptors. Nature. 1997;389:96–100.

212. Maenaka K, Juji T, Stuart DI, Jones EY. Crystal structure of the human p58 killer cell inhibitory receptor (KIR2DL3) specific for HLA-Cw3-related MHC class I. Structure. 1999;7(4):391–8.

213. Malnati MS, Peruzzi M, Parker KC, Biddison WE, Ciccone E, Moretta a, et al. Peptide specificity in the recognition of MHC class I by natural killer cell clones. Science. 1995;267(5200):1016–8.

214. Rajagopalan S, Eric OL. The Direct Binding of a p58 Killer Cell Inhibitory Receptor to Human Histocompatibility Leukocyte Antigen (HLA)-Cw4 Exhibits Peptide Selectivity. J Exp Med. 1997;185(8):1523–8.

215. Hansasuta P, Dong T, Thananchai H, Weekes M, Willberg C, Aldemir H, et al. Recognition of HLA-A3 and HLA-A11 by KIR3DL2 is peptide-specific. Eur J Immunol. 2004 Jun [cited 2014 Jan 16];34(6):1673–9.

216. Colantonio AD, Bimber BN, Neidermyer WJ, Reeves RK, Alter G, Altfeld M, et al. KIR polymorphisms modulate peptide-dependent binding to an MHC class I ligand with a Bw6 motif. PLoS Pathog. 2011;7(3).

217. Saulquin X, Gastinel LN, Vivier E. Crystal structure of the human natural killer cell activating receptor KIR2DS2 (CD158j). J Exp Med. 2003;197(7):933–8.

218. Fadda L, Borhis G, Ahmed P, Cheent K, Pageon S V, Cazaly A, et al. Peptide antagonism as a mechanism for NK cell activation. Proc Natl Acad Sci U S A. 2010 Jun 1;107(22):10160–5.

219. Borhis G, Ahmed PS, Mbiribindi B, Naiyer MM, Davis DM, Purbhoo M a, et al. A peptide antagonist disrupts NK cell inhibitory synapse formation. J Immunol. 2013 Mar 15;190(6):2924–30.

220. Winter CC, Long E. A single amino acid in the p58 killer cell inhibitory receptor controls the ability of natural killer cells to discriminate between the two groups of HLA-C allotypes. J Immunol. 1997;142:142–4.

221. Winter CC, Gumperz JE, Parham P, Long EO, Wagtmann N. Direct binding and functional transfer of NK cell inhibitory receptors reveal novel patterns of HLA-C allotype recognition. J Immunol. 1998 Jul 15;161(2):571–7.

222. Mandelboim O, Reyburn HT, Pazmany L, Colonna M, Borsellino G, Strominger JL. Protection from Lysis by Natural Killer Cells of Group 1 and 2 Specificity Is Mediated by Residue 80 in Human Histocompatibility Leukocyte Antigen C Alleles and Also Occurs with Empty Major Histocompatibility Complex Molecules. Cell. 1996;184.

223. Mandelboim O, Reyburn HT, Sheu EG, Valés-Gómez M, Davis DM, Pazmany L, et al. The binding site of NK receptors on HLA-C molecules. Immunity. 1997;6(3):341–50.

224. Pamer E, Cresswell P. Mechanisms of MHC Class I -restricted antigen processing. Annu Rev Immunol. 1998;

225. Hoof I, van Baarle D, Hildebrand WH, Keşmir C. Proteome sampling by the HLA class I antigen processing pathway. PLoS Comput Biol. 2012 Jan;8(5):e1002517.

226. Yewdell JW. Class I Antigen Processing. 2012;32(11):548–58.

227. Croft NP, Smith S a, Wong YC, Tan CT, Dudek NL, Flesch IE a, et al. Kinetics of antigen expression and epitope presentation during virus infection. PLoS Pathog. 2013 Jan;9(1):e1003129.

228. Mandelboim O, Wilson SB, Valés-Gómez M, Reyburn HT, Strominger JL. Self and viral peptides can initiate lysis by autologous natural killer cells. Proc Natl Acad Sci U S A. 1997 Apr 29;94(9):4604–9.

229. Peruzzi M, Wagtmann N, Long EO. A p70 killer cell inhibitory receptor specific for several HLA-B allotypes discriminates among peptides bound to HLA-B*2705. J Exp Med. 1996;184(4):1585–90.

230. Peruzzi M, Parker KC, Long EO, Malnati MS. Peptide sequence requirements for the recognition of HLA-B*2705 by specific natural killer cells. J Immunol. 1996;157(8):3350–6.

231. Liberatore C, Capanni M, Albi N, Volpi I, Urbani E, Ruggeri L, et al. Natural killer cell-mediated lysis of autologous cells modified by gene therapy. J Exp Med. 1999;189(12):1855–62.

232. Kim J, Chwae YJ, Hong I, Han J, Jong S. Molecular Basis of HLA-C Recognition by p58 Natural Killer Cell Inhibitory Receptors. J Immunol. 1997;159(22):3875–82.

233. McCutcheon J a, Gumperz J, Smith KD, Lutz CT, Parham P. Low HLA-C expression at cell surfaces correlates with increased turnover of heavy chain mRNA. J Exp Med. 1995;181(6):2085–95.

234. Neisig A, Melief CJM, Neefjes J. Reduced Cell Surface Expression of HLA-C Molecules Correlates with Restricted Peptide Binding and Stable TAP Interaction. J Immunol. 1998;160:171–9.

235. Valés-Gómez M, Reyburn HT, Erskine R a, Strominger J. Differential binding to HLA-C of p50-activating and p58-inhibitory natural killer cell receptors. Proc Natl Acad Sci U S A. 1998 Nov 24;95(24):14326–31.

236. Braud VM, Allan DS, O'Callaghan C a, Söderström K, D'Andrea a, Ogg GS, et al. HLA-E binds to natural killer cell receptors CD94/NKG2A, B and C. Nature. 1998 Feb 19;391(6669):795–9.

237. Lee N, Llano M, Carretero M, Ishitani A, Navarro F, López-Botet M, et al. HLA-E is a major ligand for the natural killer inhibitory receptor CD94/NKG2A. Proc Natl Acad Sci U S A. 1998;95(9):5199–204.

238. Carretero M, Cantoni C, Bellh T, Bottino C, Biassoni R, Rodriguez A, et al. The CD94 and NKG2-A C-type lectins covalently assemble to form a natural killer cell inhibitory receptor for HLA class I molecules. Eur J Immunol. 1997;563–7.

239. Brooks AG, Posch PE, Scorzelli CJ, Borrego F, Coligan JE. NKG2A complexed with CD94 defines a novel inhibitory natural killer cell receptor. J Exp Med.

1997;185(4):795–800.

240. Borrego F, Ulbrecht M, Weiss ES, Coligan JE, Brooks AG. Recognition of Human Histocompatibility Leukocyte Antigen (HLA)-E Complexed with HLA Class I Signal Sequence–derived Peptides by CD94/NKG2 Confers Protection from Natural Killer Cell–mediated Lysis. J Exp Med. 1998;187(5):813–8.

241. Braud V, Jones EY, McMichael A. The human major histocompatibility complex class Ib molecule HLA-E binds signal sequence-derived peptides with primary anchor residues at positions 2 and 9. Eur J Immunol. 1997;27(5):1164–9.

242. Valés-Gómez M, Reyburn HT, Erskine RA, López-Botet M, Strominger JL. Kinetics and peptide dependency of the binding of the inhibitory NK receptor CD94/NIKG2-A and the activating receptor CD94/NKG2-C to HLA-E. EMBO J. 1999;18(15):4250–60.

243. Hoare HL, Sullivan LC, Clements CS, Ely LK, Beddoe T, Henderson KN, et al. Subtle Changes in Peptide Conformation Profoundly Affect Recognition of the Non-Classical MHC Class I Molecule HLA-E by the CD94-NKG2 Natural Killer Cell Receptors. J Mol Biol. 2008;377(5):1297–303.

244. Kaiser BK, Pizarro JC, Kerns J, Strong RK. Structural basis for NKG2A/CD94 recognition of HLA-E. Proc Natl Acad Sci U S A. 2008;105(18):6696–701.

245. Petrie EJ, Clements CS, Lin J, Sullivan LC, Johnson D, Huyton T, et al. CD94-NKG2A recognition of human leukocyte antigen (HLA)-E bound to an HLA class I leader sequence. J Exp Med. 2008;205(3):725–35.

246. Kaiser BK, Barahmand-Pour F, Paulsene W, Medley S, Geraghty DE, Strong RK. Interactions between NKG2x immunoreceptors and HLA-E ligands display overlapping affinities and thermodynamics. J Immunol. 2005;174(5):2878–84.

247. Maloveste SM, Chen D, Gostick E, Vivian JP, Plishka RJ, Iyengar R, et al. Degenerate recognition of MHC class I molecules with Bw4 and Bw6 motifs by a killer cell Ig-like receptor 3DL expressed by macaque NK cells. J Immunol. 2012;189(9):4338–48.

248. Barber LD, Percival L, Valiante NM, Chen L, Lee C, Gumperz JE, et al. The Inter-Locus Recombinant HLA-B*4601 Has High Selectivity in Peptide Binding and Functions Characteristic of HLA-C. J Exp Med. 1996;184:735–40.

249. Cassidy S, Mukherjee S, Myint TM, Mbribindi B, North H. Peptide selectivity discriminates NK cells from KIR2DL2- and KIR2DL3-positive individuals. Eur J Immunol. :1–29.

250. Rajagopalan S, Long EO. Antagonizing inhibition gets NK cells going. Proc Natl Acad Sci U S A. 2010;107(23):10333–4.

251. Hansen TH, Bouvier M. MHC class I antigen presentation: learning from viral evasion strategies. Nat Rev Immunol. Nature Publishing Group; 2009;9(7):503–13.

252. Yewdell JW, Nicchitta C V. The DRiP hypothesis decennial: support, controversy, refinement and extension. Trends Immunol. 2006;27(8):368–73.

253. de Verteuil D, Granados DP, Thibault P, Perreault C. Origin and plasticity of MHC I-associated self peptides. Autoimmun Rev. Elsevier B.V.; 2012;11(9):627–35.

254. Dalet A, Robbins PF, Stroobant V, Vigneron N, Li YF, El-Gamil M, et al. An antigenic peptide produced by reverse splicing and double asparagine deamidation. Proc Natl Acad Sci U S A. 2011;108(29):E323–31.

255. Khan S, Giuli R De, Schmidtke G, Bruns M, Buchmeier M, Broek M Van Den. Cutting Edge: Neosynthesis Is Required for the Presentation of a T Cell Epitope from a Long-Lived Viral Protein. J Immunol. 2001;167:4801–4084.

256. Dolan BP, Sharma a. a., Gibbs JS, Cunningham TJ, Bennink JR, Yewdell JW. MHC class I antigen processing distinguishes endogenous antigens based on their translation from cellular vs. viral mRNA. Proc Natl Acad Sci. 2012;109(18):7025–30.

257. Dolan BP, Knowlton JJ, David A, Bennink JR, Yewdell JW. RNA Polymerase II Inhibitors Dissociate Antigenic Peptide Generation from Normal Viral Protein Synthesis: A Role for Nuclear Translation in Defective Ribosomal Product Synthesis? J Immunol. 2010;185(11):6728–33.

258. Alter G, Heckerman D, Schneidewind A, Fadda L, Kadie CM, Carlson JM, et al. HIV-1 adaptation to NK-cell-mediated immune pressure. Nature. Nature Publishing Group; 2011 Aug 4;476(7358):96–100.

259. Berglund P, Finzi D, Bennink JR, Yewdell JW. Viral alteration of cellular translational machinery increases defective ribosomal products. J Virol.

2007;81(13):7220–9.

260. Mohr I, Sonenberg N. Host translation at the nexus of infection and immunity. Cell Host Microbe. Elsevier Inc.; 2012;12(4):470–83.

261. Fadda L, Körner C, Kumar S, van Teijlingen NH, Piechocka-Trocha A, Carrington M, et al. HLA-Cw*0102-restricted HIV-1 p24 epitope variants can modulate the binding of the inhibitory KIR2DL2 receptor and primary NK cell function. PLoS Pathog. 2012;8(7):40.

262. Bottino C, Sivori S, Vitale M, Cantoni C, Falcol M, Pende D, et al. A novel surface molecule homologous to the p58/ p50 family of receptors is selectively expressed on a subset of human natural killer cells and induces both triggering of cell functions and proliferation. Eur J Immunol. 1996;26(8):1816–24.

263. Mandelboim O, Davis DM, Reyburn HT, Valés-Gómez M, Sheu EG, Pazmany L, et al. Enhancement of class II-restricted T cell responses by costimulatory NK receptors for class I MHC proteins. Science. 1996;274(5295):2097–100.

264. Campbell KS, Cella M, Carretero M, López-Botet M, Colonna M. Signaling through human killer cell activating receptors triggers tyrosine phosphorylation of an associated protein complex. Eur J Immunol. 1998;28(2):599–609.

265. Katz G, Markel G, Mizrahi S, Arnon TI, Mandelboim O. Recognition of HLA-Cw4 but not HLA-Cw6 by the NK cell receptor killer cell Ig-like receptor two-domain short tail number 4. J Immunol. 2001;166(12):7260–7.

266. Kägi D, Ledermann B, Bürki K, Seiler P, Odermatt B, Olsen KJ, et al. Cytotoxicity mediated by T cells and natural killer cells is greatly impaired in perforin-deficient mice. Nature. 1994;369(6475):31–7.

267. Trapani J a., Davis J, Sutton VR, Smyth MJ. Proapoptotic functions of cytotoxic lymphocyte granule constituents in vitro and in vivo. Curr Opin Immunol. 2000;12(3):323–9.

268. Bradley M, Zeytun a, Rafi-Janajreh a, Nagarkatti PS, Nagarkatti M. Role of spontaneous and interleukin-2-induced natural killer cell activity in the cytotoxicity and rejection of Fas+ and Fas- tumor cells. Blood. 1998;92(11):4248–55.

269. Screpanti V, Wallin RP, Ljunggren HG, Grandien a. A central role for death

receptor-mediated apoptosis in the rejection of tumors by NK cells. J Immunol. 2001;167(4):2068–73.

270. Kayagaki N, Yamaguchi N, Nakayama M, Takeda K, Akiba H, Tsutsui H, et al. Expression and function of TNF-related apoptosis-inducing ligand on murine activated NK cells. J Immunol. 1999;163(4):1906–13.

271. Takeda K, Hayakawa Y, Smyth MJ, Kayagaki N, Yamaguchi N, Kakuta S, et al. Involvement of tumor necrosis factor-related apoptosis-inducing ligand in surveillance of tumor metastasis by liver natural killer cells. Nat Med. 2001;7(1):94–100.

272. Cretney E, Takeda K, Yagita H, Glaccum M, Peschon JJ, Smyth MJ. Increased susceptibility to tumor initiation and metastasis in TNF-related apoptosis-inducing ligand-deficient mice. J Immunol. 2002;168(3):1356–61.

273. Alici E, Sutlu T. Natural killer cell-based immunotherapy in cancer: Current insights and future prospects. J Intern Med. 2009;266(2):154–81.

274. Street SE a, Cretney E, Smyth MJ. Perforin and interferon-γ activities independently control tumor initiation, growth, and metastasis. Blood. 2001;97(1):192–7.

275. Smyth MJ, Crowe NY, Pellicci DG, Kyparissoudis K, Kelly JM, Takeda K, et al. Sequential production of interferon-gamma by NK1.1(+) T cells and natural killer cells is essential for the antimetastatic effect of alpha-galactosylceramide. Blood. 2002;99(4):1259–66.

276. Cifone MG, D'Alò S, Parroni R, Millimaggi D, Biordi L, Martinotti S, et al. Interleukin-2-activated rat natural killer cells express inducible nitric oxide synthase that contributes to cytotoxic function and interferon-gamma production. Blood. 1999;93(11):3876–84.

277. Furuke K, Burd PR, Horvath-Arcidiacono J a, Hori K, Mostowski H, Bloom ET. Human NK cells express endothelial nitric oxide synthase, and nitric oxide protects them from activation-induced cell death by regulating expression of TNF-alpha. J Immunol. 1999;163(3):1473–80.

278. Smyth MJ, Hayakawa Y, Takeda K, Yagita H. New aspects of natural killer cell surveillance and therapy of cancer. Nat Rev Cancer. 2002;2:850–61.

279. Talmadge JE, Phillips H, Schindler J, Tribble H, Pennington R. Systematic Preclinical Study on the Therapeutic Properties of Recombinant Human Interleukin 2 for the Treatment of Metastatic Disease Systematic Preclinical Study on the Therapeutic Properties of Recombinant Human Interleukin 2 for the Treatment of Metast. Cancer Res. 1987;5725–32.

280. Wiltrout RH, Herberman RB, Zhang SR, Chirigos M a, Ortaldo JR, Green KM, et al. Role of organ-associated NK cells in decreased formation of experimental metastases in lung and liver. J Immunol. 1985;134(6):4267–75.

281. Smyth MJ, Cretney E, Takeda K, Wiltrout RH, Sedger LM, Kayagaki N, et al. Tumor necrosis factor-related apoptosis-inducing ligand (TRAIL) contributes to interferon gamma-dependent natural killer cell protection from tumor metastasis. J Exp Med. 2001;193(6):661–70.

282. Yao L, Sgadari C, Furuke K, Bloom ET, Teruya-Feldstein J, Tosato G. Contribution of natural killer cells to inhibition of angiogenesis by interleukin-12. Blood. 1999;93(5):1612–21.

283. Shimizu Y, Geraghty DE, Koller BH, Orr HT, DeMars R. Transfer and expression of three cloned human non-HLA-A,B,C class I major histocompatibility complex genes in mutant lymphoblastoid cells. Proc Natl Acad Sci U S A. 1988;85(1):227–31.

284. Braud VM, Allan DS, Wilson D, McMichael a J. TAP- and tapasin-dependent HLA-E surface expression correlates with the binding of an MHC class I leader peptide. Curr Biol. 1998;8(1):1–10.

285. Alter G, Malenfant JM, Altfeld M. CD107a as a functional marker for the identification of natural killer cell activity. J Immunol Methods. 2004 Nov;294(1-2):15–22.

286. Storkus WJ, Ill JZ, Maeurer MJ, Salter RD, Lotze MT. Identification of Human Melanoma Peptides Recognized by Class I Restricted Tumor Infiltrating T Lymphocytes. J Immunol. 1993;151(7):3719–27.

287. Gómez-Lozano N, Vilches C. Genotyping of human killer-cell immunoglobulin-like receptor genes by polymerase chain reaction with sequence-specific primers: an update. Tissue Antigens. 2002 Mar;59(3):184–93.

288. Andreatta M, Lund O, Nielsen M. Simultaneous alignment and clustering of peptide data using a Gibbs sampling approach. Bioinformatics. 2013;29(1):8–14.

289. Thomsen MCF, Nielsen M. Seq2Logo: A method for construction and visualization of amino acid binding motifs and sequence profiles including sequence weighting, pseudo counts and two-sided representation of amino acid enrichment and depletion. Nucleic Acids Res. 2012;40(W1):281–7.

290. Früh K, Ahn K, Djaballah H, Sempé P, van Endert PM, Tampé R, Peterson PA YY. A viral inhibitor of peptide transporters for antigen presentation.pdf. Nature. 1995;375.

291. Hill A, Jugovic P, York I, Russ G, Bennink J, Yewdell J, Ploegh H JD. Herpes simplex virus turns off TAP to evade host immunity.pdf. Nature. 1995;375:411–5.

292. Kurokohchi K, Carrington M, Mann DL, Simonis TB, Alexander-Miller M a, Feinstone SM, et al. Expression of HLA class I molecules and the transporter associated with antigen processing in hepatocellular carcinoma. Hepatology. 1996 May;23(5):1181–8.

293. Frazier WR, Steiner N, Hou L, Dakshanamurthy S, Hurley CK. Allelic variation in KIR2DL3 generates a KIR2DL2-like receptor with increased binding to its HLA-C ligand. J Immunol. 2013;190(12):6198–208.

294. Hermann E, Yu DT, Meyer zum Büschenfelde KH, Fleischer B. HLA-B27-restricted CD8 T cells derived from synovial fluids of patients with reactive arthritis and ankylosing spondylitis. Lancet. 1993;342:646–50.

295. Goulder PJ, Brander C, Tang Y, Tremblay C, Colbert R a, Addo MM, et al. Evolution and transmission of stable CTL escape mutations in HIV infection. Nature. 2001;412(6844):334–8.

296. Timm J, Lauer GM, Kavanagh DG, Sheridan I, Kim AY, Lucas M, et al. CD8 epitope escape and reversion in acute HCV infection. J Exp Med. 2004;200(12):1593–604.

297. Khakoo SI, Thio CL, Martin MP, Brooks CR, Gao X, Astemborski J, et al. HLA and NK cell inhibitory receptor genes in resolving hepatitis C virus infection.

Science. 2004 Aug 6;305(5685):872–4.

298. Benz C, Reusch U, Muranyi W, Brune W, Atalay R, Hengel H. Efficient downregulation of major histocompatibility complex class I molecules in human epithelial cells infected with cytomegalovirus. J Gen Virol. 2001;82(9):2061–70.

299. Tardif KD, Siddiqui A. Cell surface expression of major histocompatibility complex class I molecules is reduced in hepatitis C virus subgenomic replicon-expressing cells. J Virol. 2003;77(21):11644–50.

300. Herzer K, Falk CS, Encke J, Eichhorst ST, Ulsenheimer A, Seliger B, et al. Upregulation of major histocompatibility complex class I on liver cells by hepatitis C virus core protein via p53 and TAP1 impairs natural killer cell cytotoxicity. J Virol. 2003;77(15):8299–309.

301. Raulet DH, Vance RE, McMahon CW. Regulation of the natural killer cell receptor repertoire. Annu.Rev.Immunol. 2001. p. 291–330.

302. Moretta A, Biassoni R, Bottino C, Mingari MC, Moretta L. Natural cytotoxicity receptors that trigger human NK-cell-mediated cytolysis. Immunol Today. 2000;21(5):228–34.

303. Magri A, Ozerov AA, Tunitskaya VL, Valuev-Elliston VT, Wahid A, Pirisi M, et al. Exploration of acetanilide derivatives of 1-(ω-phenoxyalkyl)uracils as novel inhibitors of Hepatitis C Virus replication. Scientific Reports. 2016. p. 29487.

304. Angus AGN, Loquet A, Stack SJ, Dalrymple D, Gatherer D, Penin F, et al. Conserved glycine 33 residue in flexible domain I of hepatitis C virus core protein is critical for virus infectivity. J Virol. 2012;86(2):679–90.

305. Alexandridou A, Dovrolis N, Tsangaris GT, Nikita K, Spyrou G. PepServe: A web server for peptide analysis, clustering and visualization. Nucleic Acids Res. 2011;39(SUPPL. 2).

306. Gupte P, Dudhade A, Desai HG. Acquired apolipoprotein B deficiency with chronic hepatitis C virus infection. Indian J Gastroenterol. 2006;25(6):311–2.

307. Mancone C, Montaldo C, Santangelo L, Di Giacomo C, Costa V, Amicone L, et al. Ferritin heavy chain is the host factor responsible for HCV-induced inhibition of apoB-100 production and is required for efficient viral infection. J Proteome

Res. 2012;11(5):2786–97.

308. Moesta AK, Parham P. Diverse functionality among human NK cell receptors for the C1 epitope of HLA-C: KIR2DS2, KIR2DL2, and KIR2DL3. Front Immunol. 2012 Jan;3(November):336.

309. Hsu KC, Chida S, Geraghty DE, Dupont B. The killer cell immunoglobulin-like receptor (KIR) genomic region: gene-order, haplotypes and allelic polymorphism. Immunol Rev. 2002 Dec;190(1):40–52.

310. Moesta AK, Norman PJ, Yawata M, Yawata N, Gleimer M, Parham P. Synergistic polymorphism at two positions distal to the ligand-binding site makes KIR2DL2 a stronger receptor for HLA-C than KIR2DL3. J Immunol. 2008;180(6):3969–79.

311. Lohmann V, Körner F, Koch J, Herian U, Theilmann L, Bartenschlager R. Replication of subgenomic hepatitis C virus RNAs in a hepatoma cell line. Science. 1999;285(5424):110–3.

312. Bartenschlager R, Kaul A, Sparacio S. Replication of the hepatitis C virus in cell culture. Antiviral Research. 2003. p. 91–102.

313. Bartenschlager R, Pietschmann T. Efficient hepatitis C virus cell culture system: what a difference the host cell makes. Proc Natl Acad Sci U S A. 2005;102(28):9739–40.

314. Ploss A, Evans MJ. Hepatitis C virus host cell entry. Curr Opin Virol. 2012;2(1):14–9.

315. Larsson A, Johansson ME, Wangefjord S, Gaber A, Nodin B, Kucharzewska P, et al. Overexpression of podocalyxin-like protein is an independent factor of poor prognosis in colorectal cancer. Br J Cancer. 2011;105(5):666–72.

316. Boman K, Larsson AH, Segersten U, Kuteeva E, Johannesson H, Nodin B, et al. Membranous expression of podocalyxin-like protein is an independent factor of poor prognosis in urothelial bladder cancer. Br J Cancer. 2013;108(11):2321–8.

317. Nielsen JS, McNagny KM. The role of podocalyxin in health and disease. J Am Soc Nephrol. 2009;20(8):1669–76.

318. Larsson A, Fridberg M, Gaber A, Nodin B, Levéen P, Jönsson G, et al. Validation

of podocalyxin-like protein as a biomarker of poor prognosis in colorectal cancer. BMC Cancer. 2012;12:282.

319. Beauvais DM, Rapraeger AC, Brooks P, Montgomery A, Rosenfeld M, Reisfeld R, et al. Syndecans in tumor cell adhesion and signaling. Reprod Biol Endocrinol. 2004;2(1):3.

320. Labropoulou VT, Skandalis SS, Ravazoula P, Perimenis P, Karamanos NK, Kalofonos HP, et al. Expression of syndecan-4 and correlation with metastatic potential in testicular germ cell tumours. Biomed Res Int. 2013;2013.

321. Couchman JR, Woods a. Syndecan-4 and integrins: combinatorial signaling in cell adhesion. J Cell Sci. 1999;112 Pt 2:3415–20.

322. Biró A, Hérincs Z, Fellinger E, Szilágyi L, Barad Z, Gergely J, et al. Characterization of a trypsin-like serine protease of activated B cells mediating the cleavage of surface proteins. Biochim Biophys Acta - Gen Subj. 2003;1624(1-3):60–9.

323. Blais M-E, Dong T, Rowland-Jones S. HLA-C as a mediator of natural killer and T-cell activation: spectator or key player? Immunology. 2011 May;133(1):1–7.

324. Orange JS, Ballas ZK. Natural killer cells in human health and disease. Clin Immunol. 2006 Jan;118(1):1–10.